SECONDARY NATURAL GAS RECOVERY: TARGETED TECHNOLOGY APPLICATIONS FOR INFIELD RESERVE GROWTH IN FLUVIAL RESERVOIRS, STRATTON FIELD, SOUTH TEXAS

TOPICAL REPORT

(January 1, 1990–April 30, 1993)

Prepared by

Raymond A. Levey, Bob A. Hardage, Richard P. Langford, Andrew R. Scott, and Robert J. Finley
Bureau of Economic Geology
W. L. Fisher, Director
The University of Texas at Austin
Austin, Texas 78713-7508

Mark A. Sippel and R. E. Collins
Research and Engineering Consultants, Inc.

José M. Vidal and W. E. Howard
ResTech, Inc.

James R. Ballard
Envirocorp Services & Technology, Inc.

Jeffry D. Grigsby
Department of Geology, Ball State University
Muncie, Indiana 47036

Dennis R. Kerr
Department of Geosciences, University of Tulsa
Tulsa, Oklahoma 74104

for

April 1993

QAe7711

DISCLAIMER

50272-101

REPORT DOCUMENTATION PAGE	1. REPORT NO. GRI-93/0187	2.	3. Recipient's Accession No.

4. Title and Subtitle

Secondary Natural Gas Recovery: Targeted Technology Applications for Infield Reserve Growth in Fluvial Reservoirs, Stratton Field, South Texas

5. Report Date
April 30, 1993

6.

7. Author(s) R. A. Levey, B. A. Hardage, R. P. Langford, A. R. Scott, R. J. Finley, M. A. Sippel, R. E. Collins, J. M. Vidal, W. E. Howard, J. R. Ballard, J. D. Grigsby, and D. R. Kerr

8. Performing Organization Rept. No.

9. Performing Organization Name and Address

Bureau of Economic Geology
The University of Texas at Austin
University Station, Box X
Austin, Texas 78713-7508

10. Project/Task/Work Unit No.

11. Contract(C) or Grant(G) No.

(C) 5088-212-1718(GRI)

(G) DE-FG21-88MC25031(DOE)

12. Sponsoring Organization Name and Address

Gas Research Institute
8600 West Bryn Mawr Avenue
Chicago, IL 60631

Project Manager: Raymond W. Owens

13. Type of Report & Period Covered
Topical Report
1/1/90–4/30/93

14.

15. Supplementary Notes

16. Abstract (Limit: 200 words)

Integrated geologic, geophysical, reservoir engineering, and petrophysical evaluations in mid-Oligocene-age fluvial reservoirs of Stratton field were conducted for this study. Stratton field is a mature gas field in the Frio Fluvial-Deltaic Sandstone along the Vicksburg Fault Zone play (FR-4) in South Texas. Significant natural gas reserve appreciation opportunities exist here in heterogeneous fluvial reservoirs that commonly contain multiple compartments. A reserve appreciation potential of 100 percent is documented for a large contiguous area in Stratton field that has undergone 40 years of prior development. Remaining natural gas can be contacted either by recompleting existing wells that have bypassed these reservoir compartments or by drilling infield wells to contact compartments not effectively drained at the current well spacing. Exploration for new reservoirs, incompletely drained compartments, or bypassed gas zones in old fields can be improved using detailed geologic studies that integrate engineering, petrophysical, and geophysical methods. Currently available geophysical techniques, including 3-D surface seismic, vertical seismic profiling, amplitude versus offset, and 2-D seismic inversion, were used to image subtle changes in reservoir topology and compartment boundaries at depths as low as 6,800 ft. Three classes of compartment sizes were delineated from 10 groups of Frio reservoirs. Forward stochastic modeling of maximum gas recovery indicates that well spacings of 340, 200, and 60 acres (or less) provide the maximum gas-contact efficiency in large, medium, and small compartment size reservoirs, respectively.

17. Document Analysis a. Descriptors

compartment size, depositional facies, fluvial reservoirs, Frio Formation, Gas-Wizard, secondary natural gas recovery, South Texas, stochastic modeling, 3-D seismic, vertical seismic profile

b. Identifiers/Open-Ended Terms

Integrated geologic, engineering, petrophysical, and geophysical evaluation of fluvial reservoirs; identification of secondary natural gas resources

c. COSATI Field/Group

18. Availability Statement

Release unlimited

19. Security Class (This Report)
Unclassified

20. Security Class (This Page)
Unclassified

21. No. of Pages
244

22. Price

(See ANSI—Z39.18)

See Instructions on Reverse

OPTIONAL FORM 272 (4–77)
(Formerly NTIS–35)
Department of Commerce

RESEARCH SUMMARY

Title	Secondary Natural Gas Recovery: Targeted Technology Applications for Infield Reserve Growth in Fluvial Reservoirs, Stratton Field, South Texas
Contractor	Bureau of Economic Geology, The University of Texas at Austin, GRI Contract No. 5088-212-1718, titled "Secondary Natural Gas Recovery: Targeted Technology Applications for Infield Reserve Growth"
Principal Investigators	Robert J. Finley and Raymond A. Levey
Report Period	January 1990–April 1993

Objectives

The primary objective of this report is to better enable natural gas producers to develop additional natural gas resources in fields with conventional permeability and porosity. Integrated geologic, geophysical, reservoir engineering, and petrophysical evaluations in mid-Oligocene-age fluvial reservoirs are evaluated from Stratton field, a mature gas field located in the Frio Fluvial-Deltaic Sandstone along the Vicksburg Fault Zone play (FR-4) in South Texas. This multidisciplinary field study serves as a testing area and model in its approach to incremental resource development for other gas fields.

Technical Perspective

A major goal of the Infield Natural Gas Reserve Growth Joint Venture project is to assess the potential for maximizing economic recovery of natural gas, mainly in reservoirs with conventional porosity and permeability. Secondary or incremental gas may be contained in reservoirs that are untapped or bypassed or have incompletely drained compartments that are primarily a function of depositional facies and diagenetic heterogeneity and secondarily are dependent upon structural heterogeneity. Multiple stacked reservoirs deposited in thick stratigraphic intervals such as the FR-4 play and other fluvially dominated units can be affected by variations in sandstone stacking patterns and contain opportunities for identifying reserve appreciation in existing fields. Remaining natural gas in these fields can be contacted either by recompletion of existing wells that have bypassed these reservoir compartments or by infield wells that contact compartments not effectively drained at the current well spacing. Exploration for new reservoirs, incompletely drained compartments, or bypassed gas zones in old fields can be improved using detailed geologic studies that integrate engineering, petrophysical, and geophysical methods.

Results

This report summarizes the results of research designed to evaluate the effectiveness of extensive infield development accomplished by drilling new wells or by recompleting in previous wells for secondary gas recovery in fluvial reservoirs in the middle Frio Formation in Stratton field. These reservoirs consist of channel-fill and splay deposits that are bounded by nonreservoir floodplain, levee, and abandoned channel-fill siltstones and mudstones.

Significant natural gas reserve appreciation opportunities exist in heterogeneous fluvial reservoirs that are prone to multiple compartments. Reserve appreciation potential of 100 percent is documented for a large contiguous area in Stratton field after 40 years of prior development.

Project analysis indicates that an additional technically recoverable gas resource of 48 Bcf is present in the Wardner lease study area. However, part of that gas resource is found in the middle Frio interval, where reservoir permeability is often affected by diagenetic alteration and may need hydraulic stimulation.

Using the Gas-Wizard (G-WIZ) compartmented gas reservoir simulator, 3 classes of compartment sizes were delineated from 10 groups of Frio reservoirs. Forward stochastic modeling of maximum gas recovery indicates that well spacings of 340, 200, and 60 acres (or less) provide the maximum gas-contact efficiency in large, medium, and small compartment size reservoirs, respectively.

Application of currently available geophysical techniques, including 3-D surface seismic, vertical seismic profiling, amplitude-versus-offset, and 2-D seismic inversion, were used to image subtle changes in reservoir topology and compartment boundaries at depths as deep as 6,800 ft.

Technical Approach

The research integrated geologic subsurface mapping, engineering analysis of project-designed well tests, open- and cased-hole petrophysical techniques, and both surface and downhole geophysical methods to evaluate the impact of both depositional and diagenetic reservoir heterogeneities on the recovery of incremental gas. The technical approach included:

(1) Subsurface mapping of lithostratigraphic units corresponding to operator-designated regulatory gas reservoirs in the middle Frio stratigraphic interval.

(2) Calibration of core and rock properties to well logs to determine genetic depositional units, reservoir variability, and stacking patterns.

(3) Determining the statistics of primary pore volume and transmissibility for each of 10 reservoir groups and then defining 3 classes of reservoir compartment sizes (large, medium, and small) delineated from a spectrum of fluvial reservoirs.

(4) Forward stochastic modeling of abundant Stratton field data to analyze gas recovery versus well spacing for infill development of different types of meandering fluvial systems.

(5) Acquisition and interpretation of 3-D surface seismic and high-resolution vertical seismic profiles to image seismic thin beds corresponding to high reserve growth gas reservoirs.

Implications

This report summarizes the results of the integrated geological, geophysical, petrophysical, and engineering research as part of a broader

project to investigate technology applications for infield reserve growth in fluvial-deltaic reservoirs. Analysis of gas reservoirs in stratigraphically complex Tertiary fluvial deposits in Stratton field indicates that significant reserve appreciation potential exists in heterogeneous and compartmentalized fluvial reservoirs.

Continued operator access to reserve appreciation in the FR-4 play and other similar gas plays in the lower 48 states will require application of SGR technologies and concepts. The Secondary Natural Gas Recovery project is continuing to transfer technology and reporting results from this research to the gas industry through publications, short courses, and workshops.

CONTENTS

FIGURES

TABLES

EXECUTIVE SUMMARY

This research is part of a broader multiyear, multifield research program designed to investigate targeted technology applications for infield reserve growth. Stratton field, in the Frio Fluvial-Deltaic Sandstone along the Vicksburg Fault Zone play (FR-4) in South Texas, is used as a natural laboratory to identify and measure the resource potential within fluvial reservoirs and to focus on the results of various technical approaches enhancing incremental gas recovery. Stratton field is an ideal natural laboratory because the field is more than 50 years old and is one of the largest onshore Gulf Coast gas fields (greater than 2 Tcf cumulative gas production) that has undergone extensive infield development.

Results from the 1992 National Petroleum Council study (1992) indicate that a total of 1,295 Tcf of technically recoverable resources at a wellhead price of $2.50/MMBtu or less are available in the lower 48 states. A large part of these total resources (an estimated 216 Tcf of nonassociated reserve appreciation resources) will come from infield reserve growth within existing gas fields like Stratton. Technology advancement will probably be crucial both to developing this incremental resource and to reducing costs of this gas production.

Results from operator-initiated infield drilling and recompletions in Stratton field indicate that reserve replacement of 100 percent was achieved when adjusted for reserves projected in 1979, after more than 40 years of prior development history from 1937 to 1979. Fifty percent of this reserve appreciation occurred in reservoirs less than 7,000 ft with more than 80 percent of original reservoir pressure. The reserve replacement occurred primarily among 37 operational reservoirs in the middle Frio. The replaced reserves were achieved primarily from reservoirs in the lower part of the middle Frio that had often been penetrated by prior development during the 1937 to 1939 period, in contrast to the reserve appreciation in the deeper pool reservoirs of the lower Frio and Vicksburg Formations. In 1979 the completion spacing among the 37 reservoir intervals that were less than 7,000 ft ranged from a maximum of

1

343 to a minimum of 91 acres. In 1990, before the implementation of fieldwide commingling rules, the completion spacing ranged from a maximum of 249 to a minimum of 65 acres.

Examining reservoir flow units across a spectrum of fluvial depositional channels indicates that even in reservoirs with moderate to high (10 to 100 md) permeabilities, depositional facies boundaries associated with crosscutting channels are more likely to be effective baffles to gas flow in thin (5 to 20 ft), narrow (200 to 1,000 ft), high sinuosity (>1.3) fluvial channel systems that are typical of small compartment size class reservoirs.

The personal-computer-based Gas-Wizard (G-WIZ) compartmented gas reservoir simulator is a product of the infield gas reserve growth project. The G-WIZ simulator was used to determine the distribution and variation of primary pore volume compartment size and transmissibility from 256 separate gas completions in fluvially dominated reservoirs in Stratton and Agua Dulce fields. Three compartment sizes were characterized from 10 reservoir groups across a spectrum of fluvial reservoirs in multiple stacked reservoir intervals. Reservoir compartment size distributions were delineated from a spectrum of fluvial reservoirs. Three classes characterized as large, medium, or small reservoir compartment sizes were delineated from 10 groups of Frio reservoirs stacked over a 2,000-ft interval in Stratton–Agua Dulce field. Producing rate and static pressure data were used to determine three fundamental reservoir parameters: primary drained pore volume, supporting pore volume, and barrier transmissibility. Statistical distributions of the primary pore volume and transmissibility were found to be closely approximated by a log-normal distribution in each of the 10 reservoir groups. Forward stochastic modeling of gas recovery from the three compartment size classes indicates that well spacing of 340, 200, and 60 acres (or less) provides maximum gas contact efficiency. The correlations developed should be transferable to other fields with similar fluvial facies architecture. Two reservoir simulation examples are presented in which the G-WIZ compartmented gas reservoir simulator has been used to identify incompletely drained resources. The G-WIZ simulator was capable of hindsight prediction of incremental resources that resulted in 2.0 to 5.7 Bcf incremental resource volumes. These incompletely drained resources represent 40 percent of the 100 percent

2

reserve appreciation in the Wardner lease study area and are considered illustrative of the potential for reserve growth in other fields of similar geological character.

Analysis of 3-D seismic imagery in a 7.5-mi^2 grid, coincident with multiple well tests in Stratton field, was used to investigate reservoir compartment boundaries identified by geologic, engineering, and formation evaluation techniques. Data volume flattening and seiscrop slicing above and below reference horizons were used to reveal depositional topography and to determine the extent of structural influence on reservoir horizons. Seiscrop imagery has revealed fluvial channels as narrow as 200 ft and as thin as 10 ft at depths as deep as 6,750 ft. Some reservoir compartment boundaries were seismically imaged within individual channel systems. Because many Stratton reservoirs are only 10 to 15 ft thick and occur within seismic time windows as thin as 2 to 4 milliseconds (ms), careful calibration of subsurface stratigraphy with the surface seismic response is required to accurately locate these narrow time windows in the reflection waveforms. The Stratton field study has demonstrated that a properly calibrated 3-D seismic data volume provides a cost-effective tool for imaging fluvial reservoir topology in the interwell space.

On the basis of the character of pressure buildup test data in middle Frio fluvial reservoirs, project-designed well tests identified long and narrow drainage shapes in 10 of 26 wells. These channel-like drainage shapes have an average width of 220 ft and range from a minimum of 50 ft to a maximum of 600 ft, matching the dimensions and morphology of seismic narrow thin-bed reservoirs imaged on seiscrop slice maps. These well tests have confirmed geologic-based reservoir characterization models and indicate that significant incremental gas resources are trapped by reservoir compartments in fluvial-channel systems. Close completion spacing (40 to 80 acres per well) is required to access these reserve additions in selective fluvial depositional systems characterized by small compartment size classes.

Results from the SGR project analysis of Stratton field should be applicable for maximizing the recovery of gas from fluvial reservoirs in other gas fields in the FR-4 gas play and in other gas plays with similar depositional settings.

3

OBJECTIVES

The primary objective of the research by the Secondary Gas Recovery project is to develop, test, and verify tools and techniques for maximizing the recovery of natural gas resources from conventional reservoirs in existing fields. The supporting detailed objectives addressed in this report include the following:

(1) To verify that incremental gas resources exist and to document reserve appreciation in normally pressured depletion drive reservoirs (in contrast to rate acceleration), from an infield development program in a 50-year-old gas field.

(2) To test the concept of stratigraphic compartmentalization in gas reservoirs resulting from differences in fluvial depositional facies, including channel-channel contacts, intrachannel heterogeneity, and channel-splay contacts that cause reservoir compartmentalization and hence inhibit the recovery of natural gas.

(3) To evaluate the capability of the G-WIZ compartmented gas reservoir simulator, previously developed by this project, in analyzing the variability of a broad spectrum of fluvial reservoirs, and to apply this PC-based tool in evaluating well-documented examples of incremental gas resources.

(4) To design and analyze transient well tests to identify compartment boundaries and determine drainage shapes, confirm pressure variations, and quantify reservoir permeability.

(5) To determine the capability of 3-D surface seismic data, vertical seismic profiling, amplitude versus offset responses, and 2-D seismic inversions for imaging fluvial compartment boundaries and reservoir topology.

INTRODUCTION

A diverse and vast resource base of 1,295 Tcf of technically recoverable natural gas resources is estimated by a recent analysis of domestic petroleum supplies by the National Petroleum Council (1992). Over 200 Tcf of this resource base is expected to be recoverable by reserve appreciation in existing fields in the lower 48 states. The integrated application of cost-effective technologies from the disciplines of geology, engineering, geophysics, and petrophysics will be required for production of these resources. The Secondary Natural Gas Recovery (SGR) project aims to develop and disseminate cost-effective technological applications in each of these disciplines, which will help maximize the economic recovery of this important infield gas resource.

An increasing trend in the lower 48 states during the past five years has been toward reexploration and redevelopment in large known fields with an existing infrastructure. The viability of this trend has important implications for our future domestic gas supply as both major integrated companies and independents seek to recover the substantial remaining gas resources identified in the 1992 resource assessment completed by the National Petroleum Council (1992). Fifty percent of the cumulative natural gas production in Texas is derived from siliciclastic reservoirs in existing fields. Evaluation of gas resources in sandstone reservoirs is part of a continuing research initiative at the Bureau of Economic Geology focusing on strategies to maximize the producibility of the natural gas resource base in the lower 48 states. This topical report focuses on the impact of the reservoir compartmentalization in natural gas reservoirs and the potential for infield reserve growth through reexploration in a mature field. The Secondary Natural Gas Recovery (SGR): Targeted Technology Applications for Infield Reserve Growth is a joint venture research project sponsored by the Gas Research Institute (GRI), the U.S. Department of Energy (DOE), and the State of Texas, with the cofunding and cooperation of the natural gas industry. The SGR project is a field-based program using an integrated multidisciplinary approach that integrates geology, geophysics, engineering, and petrophysics.

A major objective of this research project is to develop, test, and verify those technologies and methodologies that have near- to mid-term potential for maximizing recovery of gas from conventional reservoirs in known fields. Natural gas reservoirs in the Gulf Coast Basin are targeted as data-rich field-based models for evaluating infield development. Fluvial-deltaic strata of the Frio and Vicksburg Formations in the onshore South Texas Gulf Coast Basin are the site of geologic and engineering investigations of multiple stacked reservoir horizons in a mature gas field (fig. 1).

The SGR research program focuses on sandstone-dominated reservoirs in fluvial-deltaic plays within the onshore Gulf Coast Basin of Texas. Geologic and engineering screening of 14 major gas fields in the onshore Gulf Coast Basin indicated that both Stratton and Seeligson fields were potential candidates for detailed investigations within the Frio Fluvial-Deltaic Sandstone along the Vicksburg Fault Zone gas play (FR-4) (Kosters and others, 1989; Finley and others, 1990). Seeligson field was the first SGR research field study site in the Frio Formation. Geologic and engineering evaluation of Seeligson's middle Frio gas reservoirs indicated that well-connected fluvial sandstones have been effectively drained by dense well and completion spacing (Ambrose and others, 1992). Starting in mid-1990, with the cooperation of Union Pacific Resources Corporation, the SGR project focused its research efforts in quantifying secondary gas resources in middle Frio gas reservoirs on Stratton field in Nueces, Kleberg, and Jim Wells Counties, Texas. The emphasis of the SGR project is on studying the influence of depositional systems on reservoir heterogeneity and the resulting degree of nonstructurally induced compartmentalization in sandstone gas reservoirs.

Stratton field is an excellent candidate for detailed analysis because (1) it has a development and production history exceeding 50 years, (2) an aggressive infield drilling and recompletion program during the late 1980's provided a strong basis for using a historical approach to resource assessment, and (3) development of the Stratton field gas cap has provided a densely drilled "natural laboratory" that is not commonly available in other Frio fluvial-deltaic fields. Stratton field natural gas production is presented as an example of the

6
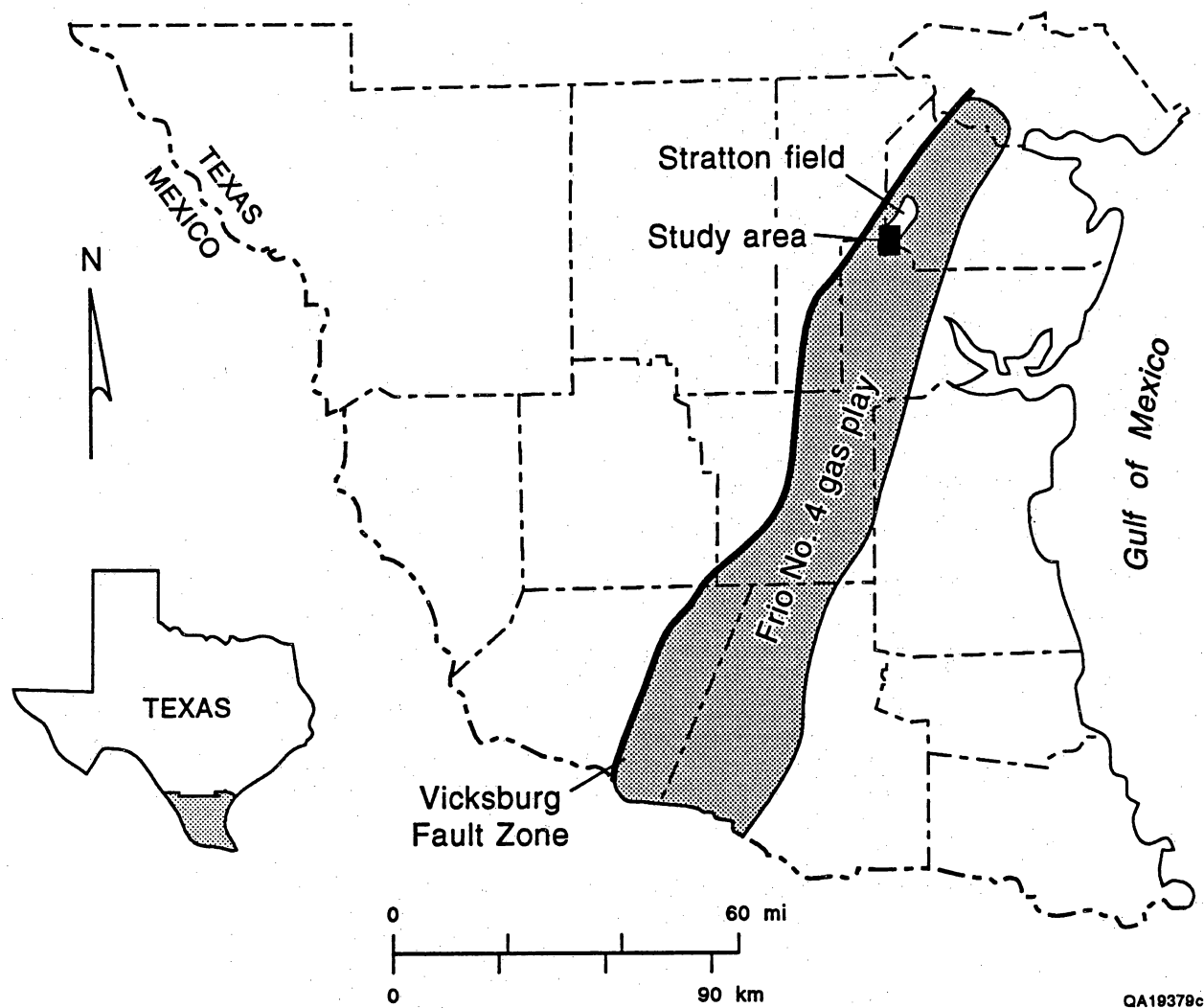
Figure 1. Location map showing Stratton field within the Frio fluvial-deltaic play.

significant additional gas reserves that were achieved through conventional drilling and completion methods using existing technology in a fluvial-deltaic (dominantly fluvial) depositional setting. Stratton is one of several mature South Texas fields with both fluvial and deltaic gas reservoirs. This study documents the effect of depositionally controlled reservoir heterogeneity from that part of the field with fluvially dominated reservoir architecture. Stratigraphic and production analysis of natural gas reservoirs within the fluvial-facies tract of the Oligocene-age middle Frio Formation is used to demonstrate the importance of evaluating gas-well completion spacing in areas with multiple stacked reservoirs.

Regional Structural and Stratigraphic Setting

The Oligocene Frio Formation is one of the major progradational offlapping stratigraphic units in the northwest Gulf of Mexico basin (fig. 2). The Frio Formation is a sediment-supply-dominated depositional sequence characterized by rapid deposition and high subsidence rates (Galloway and others, 1982; Morton and Galloway, 1991). Thickness of the Frio Formation varies from less than 2,000 ft near the Vicksburg Flexure to greater than 9,000 ft downdip toward the central part of the embayment. The structural style in the Rio Grande Embayment is characterized by discontinuous belts of strike parallel to growth faults and deep shale ridges and massifs. Underlying salt is thin or absent (Galloway and others, 1982). The Oligocene Frio Formation of Texas is volumetrically the largest gas-productive interval of eight major depositional episodes of the Cenozoic onshore Gulf Coast Basin (fig. 3). The middle Oligocene section was deposited during the Catahoula-Frio depositional episode described by Galloway (1977). The entire Frio Formation is divided into 10 gas plays on the basis of regional variations in structure and depositional setting (Kosters and others, 1989). Stratton field is within the gas play known as the Frio Fluvial-Deltaic Sandstone along the Vicksburg Fault Zone (FR-4), which had a cumulative gas production of 11.8 Tcf as of January 1, 1987 (Kosters and others, 1989).
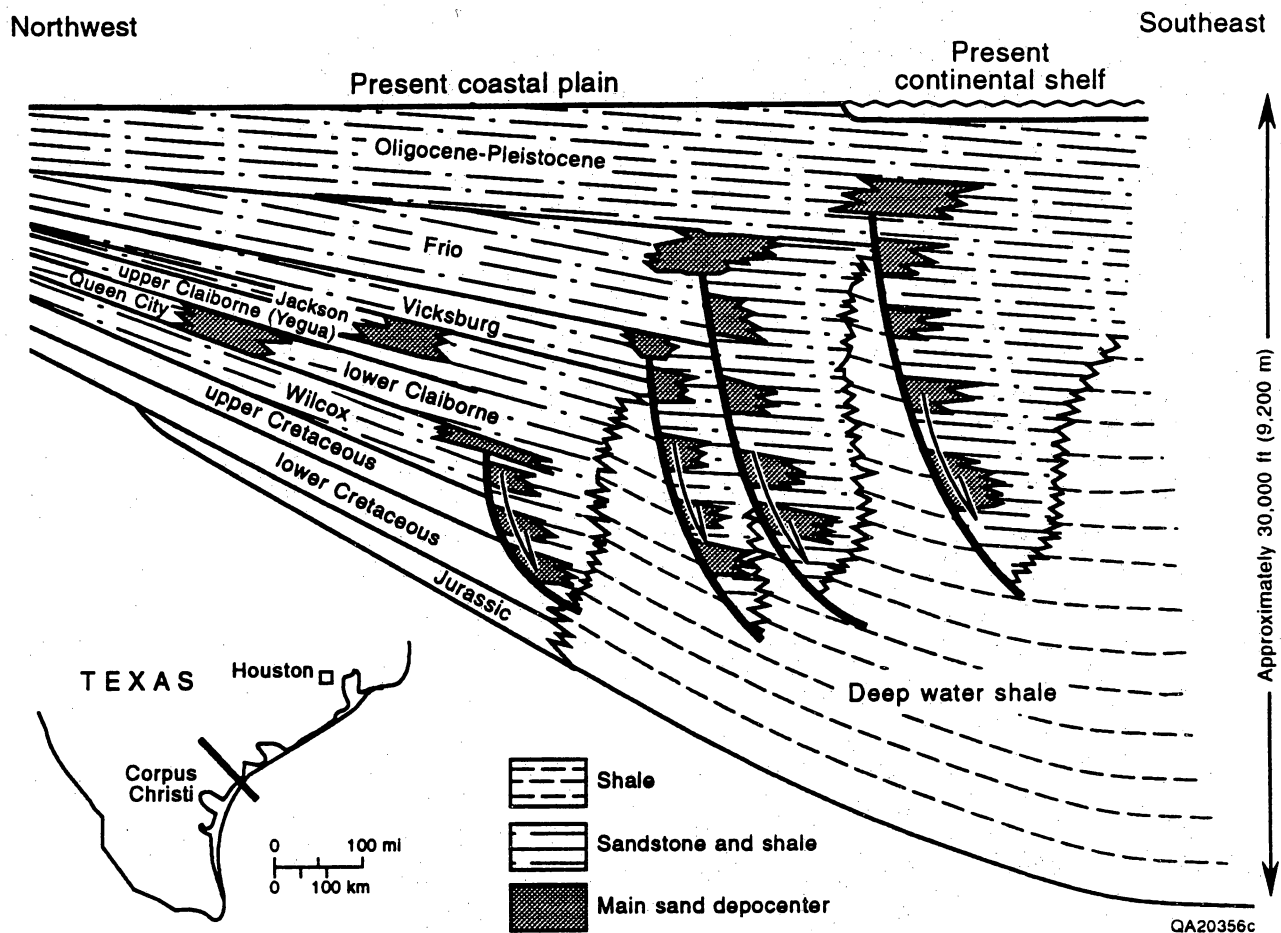
Figure 2. Depositional dip-oriented cross section through the central Texas Gulf Coast Basin illustrating the relative position of major sand depocenters (after Bebout and others, 1982).

9
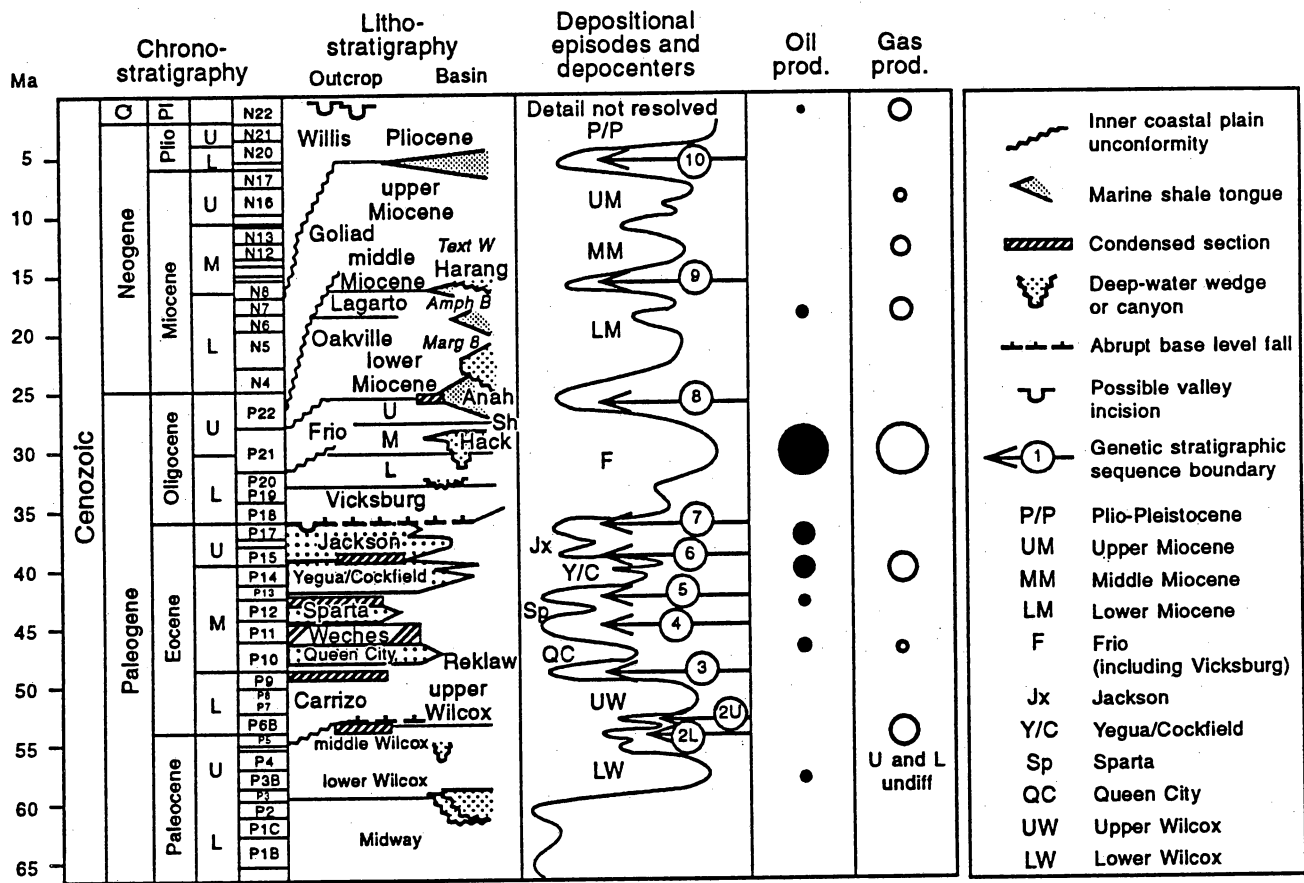
Figure 3. Relative rank of the volume of gas produced in the eight depositional episodes of the onshore Gulf Coast Basin (modified from Galloway, 1989; Xue and Galloway, 1990).

The FR-4 gas play, ranked third largest of all 73 gas plays in Texas, is the largest nonassociated gas play in the Gulf Coast.

Stratton field lies within the Rio Grande Embayment structural province (fig. 4). The Rio Grande Embayment is one of several entry points for major river systems draining the ancestral Gulf of Mexico. Variation in the structural framework of Frio and Vicksburg reservoirs in Stratton field is illustrated by a dip-oriented 2-D cross section based on an analysis of subregional reflection seismic lines crossing the Vicksburg Fault Zone and extending across the study area (figs. 5 and 6). Structural attitude of the gas reservoirs in the Vicksburg and lower Frio Formations is affected by a series of normal faults that sole out into the Vicksburg detachment zone within the Jackson shale. The relatively undeformed and flat-lying stratigraphic interval of the middle and upper Frio Formation is structurally much simpler than the underlying Vicksburg and lower Frio, both of which show the effects of structural rotation into the Vicksburg décollement surface, including antithetic faulting.

The upper and middle Frio is characterized by a relatively gentle north-to-south elongated subsurface domal closure. The structural relief typical of the upper and middle Frio reservoirs is shown by the structure map on one of the fieldwide extensive shale markers in the middle Frio Formation (fig. 5). There is about 200 ft of relief from the crest to the maximum depth along the outer limits of the study area boundary. This structural relief of 200 ft also approximates the maximum height of the gas cap above the oil rim that is present in the E-41 and F-11 reservoirs. Many of the completions in the Wardner lease study area are above the gas-oil contact of these reservoirs. Analysis of both well log correlations and 2-D reflection seismic data indicates that only a few faults extend upward into the middle Frio, and that the amount of fault throw in the middle Frio is usually small and fault block rotation is minimal. A large part of the middle and upper Frio is relatively undeformed across Stratton field. Expansion of the middle Frio section from east to west results in stratigraphic thickening between shale marker horizons separating individual reservoir intervals. This minor expansion is visible on the 2-D seismic reflection lines that are parallel to structural dip across the field (fig. 6).

11

Datum: Marker horizon near base of middle Frio

0   1   2 mi

0   1   2   3 km

Contour interval = 200 ft

——— 2−D sesmic reflection form line cross section

OAaI418
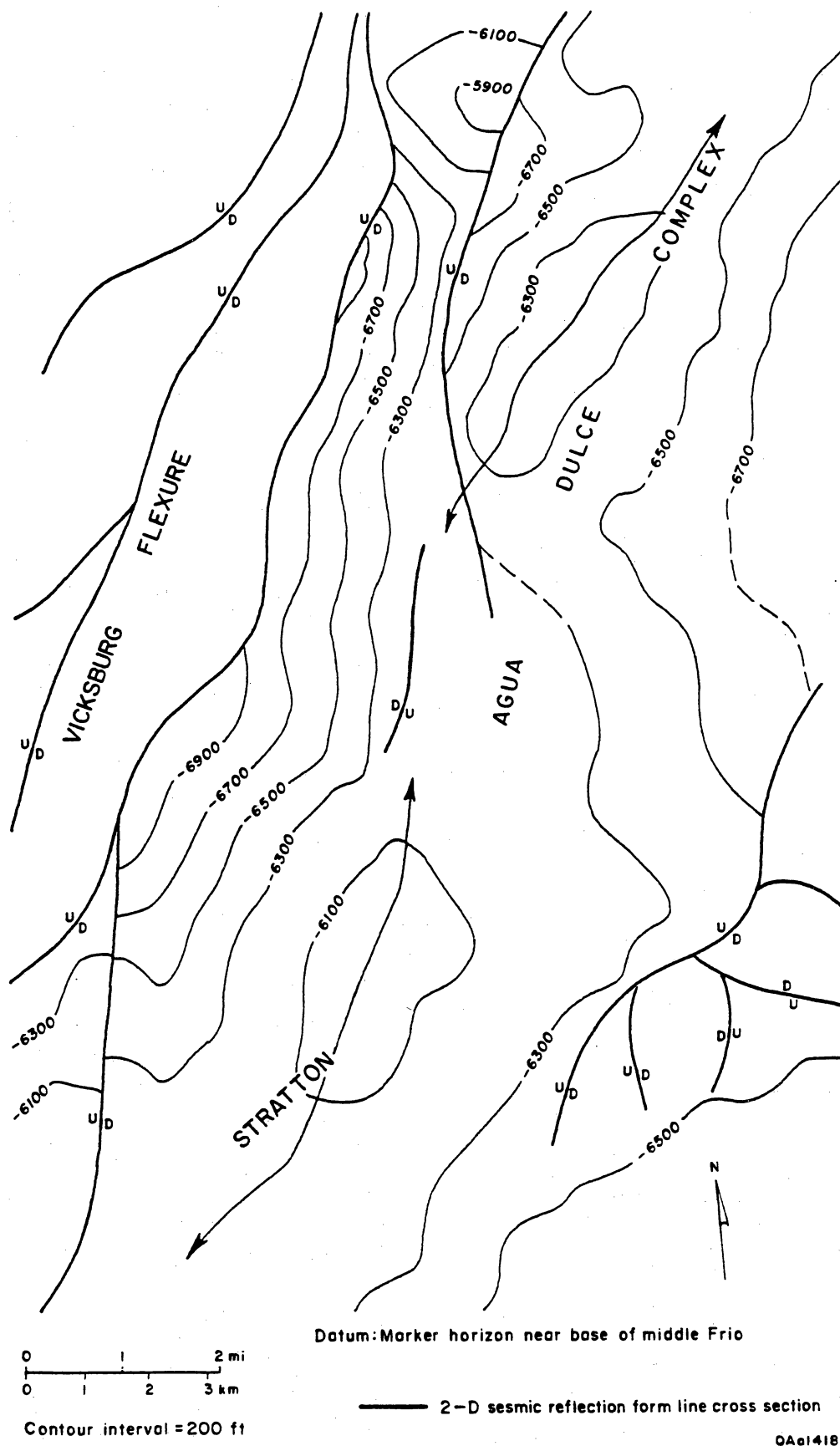
Figure 4. Structural and tectonic setting of Stratton field in the Rio Grande Embayment.

12
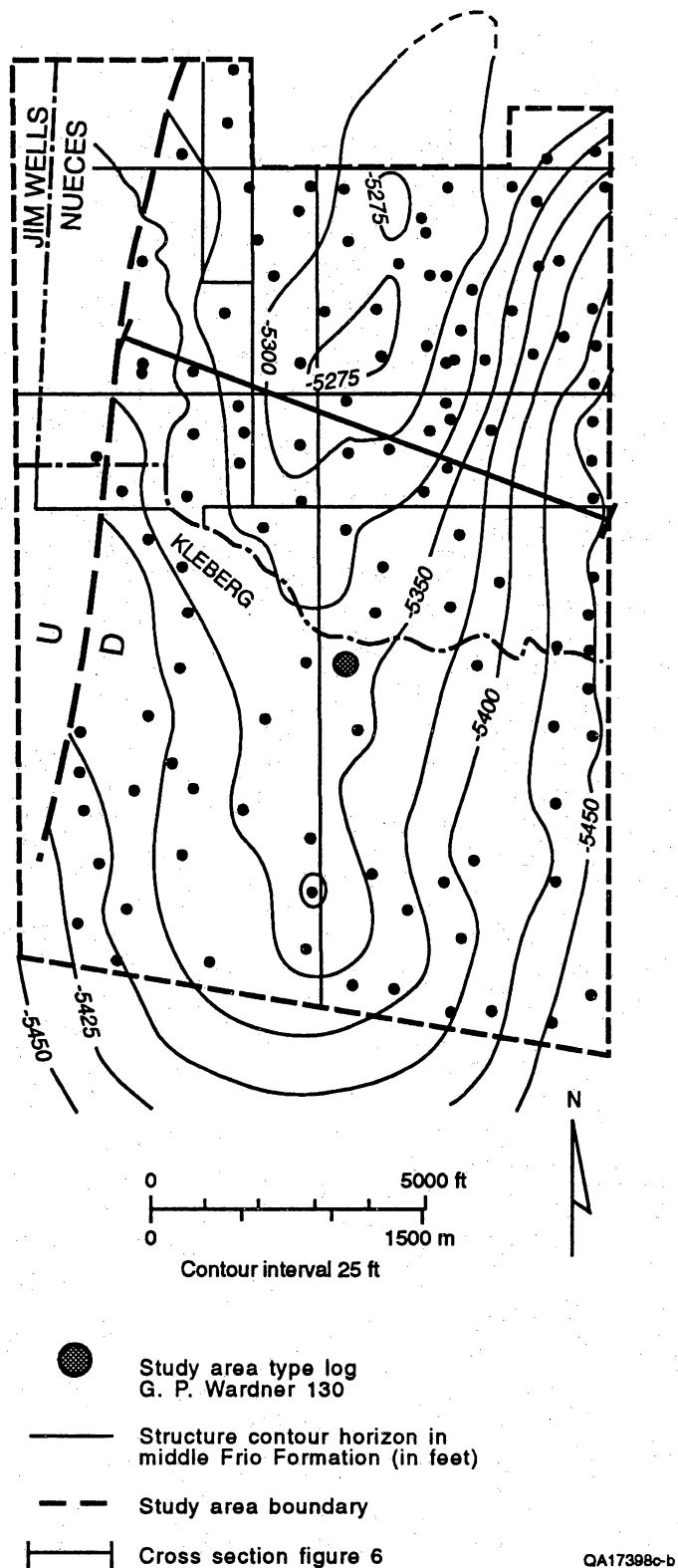
Figure 5. Subsea structural horizon in the middle Frio showing the gentle structural domal closure that is typical of reservoir intervals in the middle Frio Formation.
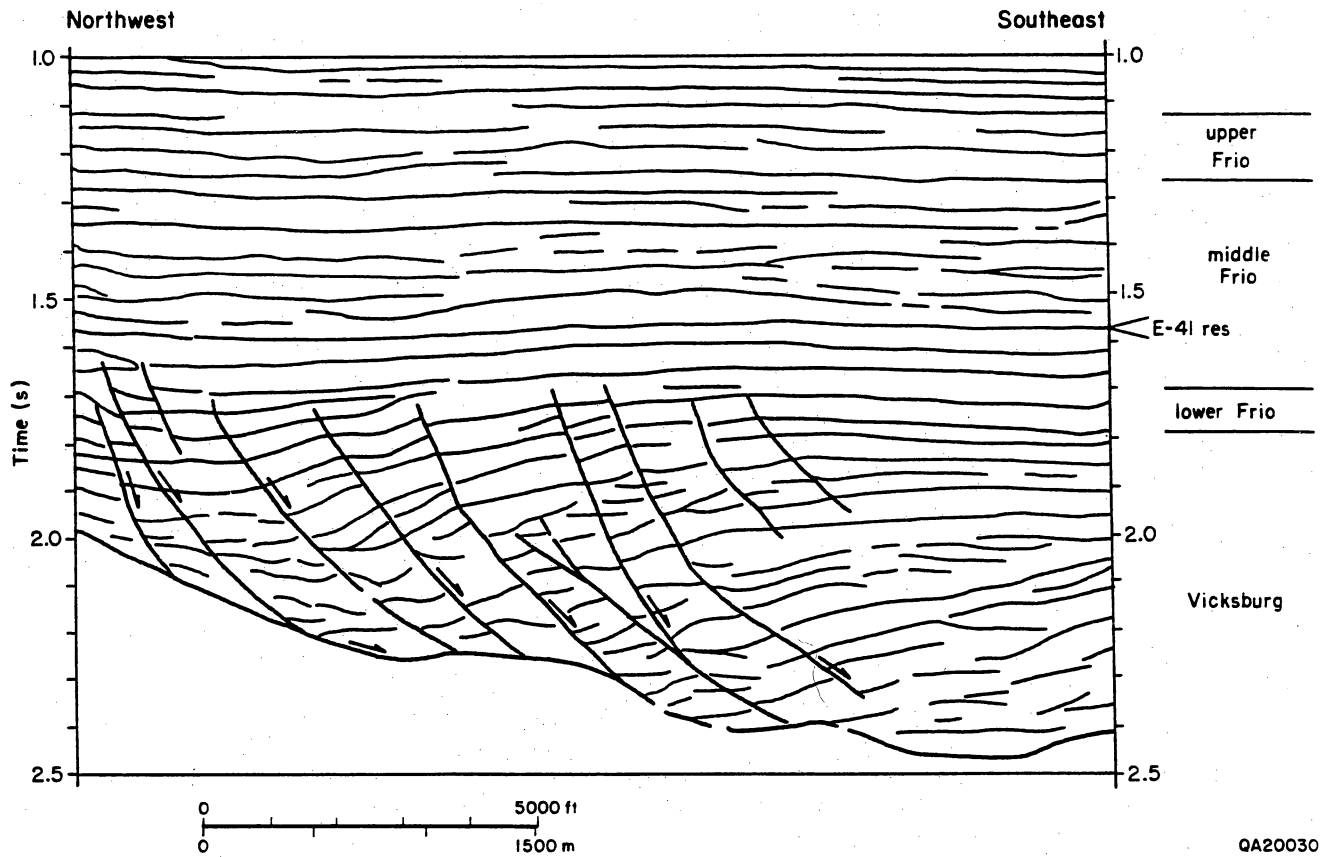
Figure 6. Subregional dip-oriented form line cross section through the Wardner lease study area showing rotation of fault blocks in the lower Frio and Vicksburg Formations compared to the lack of faulting in the upper and middle Frio Formations. Cross section shown in figure 5.

The dominant trapping mechanism for reservoirs in the FR-4 gas play is controlled by a combination of structural and stratigraphic factors, with faulted anticlinal closure, facies change, and reservoir pinch-outs (Kosters and others, 1989). Most of the gas production in the FR-4 play is from middle Frio reservoirs. Middle Frio reservoirs in Stratton field are part of the Gueydan fluvial system (fig. 7), updip from the Norias delta system (Galloway and others, 1982). Middle Frio strata consist of fluvial depositional systems that contain channel-fill and associated crevasse-splay reservoir facies. Criteria for identifying these channel-fill and splay deposits from well logs and core were described by Jirik (1990), Kerr and Jirik (1990), and Kerr (1990). Stratton field is near the northern limit of the FR-4 gas play. Several giant gas fields, including Seeligson and Agua Dulce, are part of this play. Initial geologic analysis of middle Frio reservoirs in these fields reported the composite channel-fill deposits to be as much as 30 ft thick and 2,500 ft wide and probably occur in rather long linear belts (Kerr and Jirik, 1990). Splay deposits in the middle Frio are up to 20 ft thick and are proximal to channel systems (Kerr, 1990). Porosities in these fluvial reservoirs range from 15 to 25 percent, with permeabilities of less than 1 to greater than 4,000 md.

A type log for the study area illustrates the distinct stratigraphic variation between the Vicksburg and Frio Formations (fig. 8). Analysis of conventional electric wireline logs (spontaneous potential [SP] and resistivity) indicates that the middle Frio contains multiple stacked pay sandstones within a series of vertically stacked reservoir sequences referred to as the B-, C-, D-, E-, and F-series reservoirs (descending stratigraphic order). Reservoir lithofacies distributions identified from core and borehole images, calibrated to well logs, support the interpretation of fluvial deposits composed of both single and multiple amalgamated channel-fill and splay sandstones as the dominant reservoir facies of the middle Frio producing reservoir units. Channel-fill deposits range from 10 to 30 ft in thickness and show either a bell-shaped or blocky SP log profile. The bell-shaped curve indicates an upward fining of grain-size distribution, in contrast to the blocky curve that indicates a uniform grain-size distribution. Lateral splay deposits often range from less than 5 ft to as much as 20 ft in thickness. The character of the SP

EXPLANATION

FACIES

Fluvial

Floodplain and Lacustrine

Deltaic

Barrier - strandplain

Shelf and slope

QA 10637
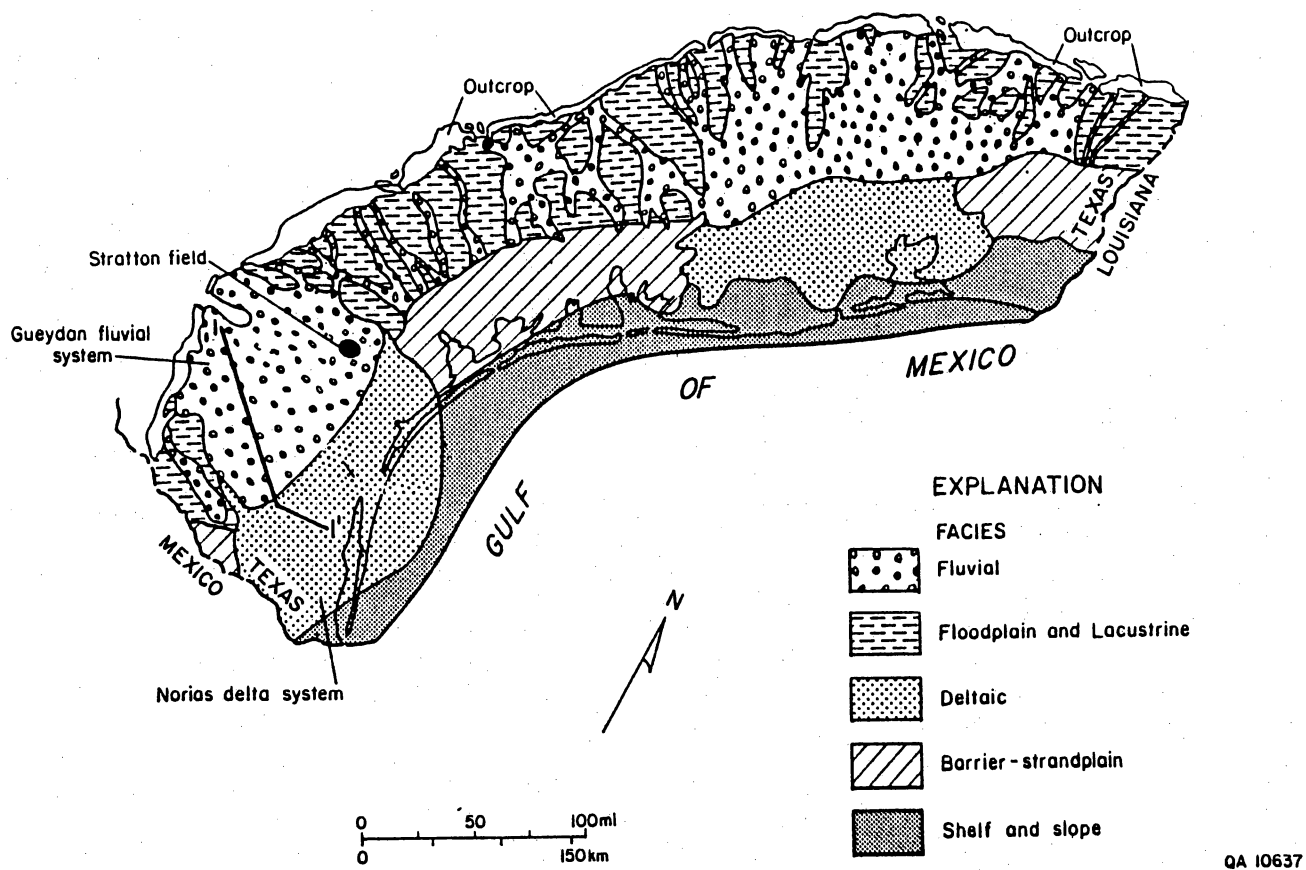
Figure 7. Depositional framework of the Frio Formation (after Galloway and others, 1982).
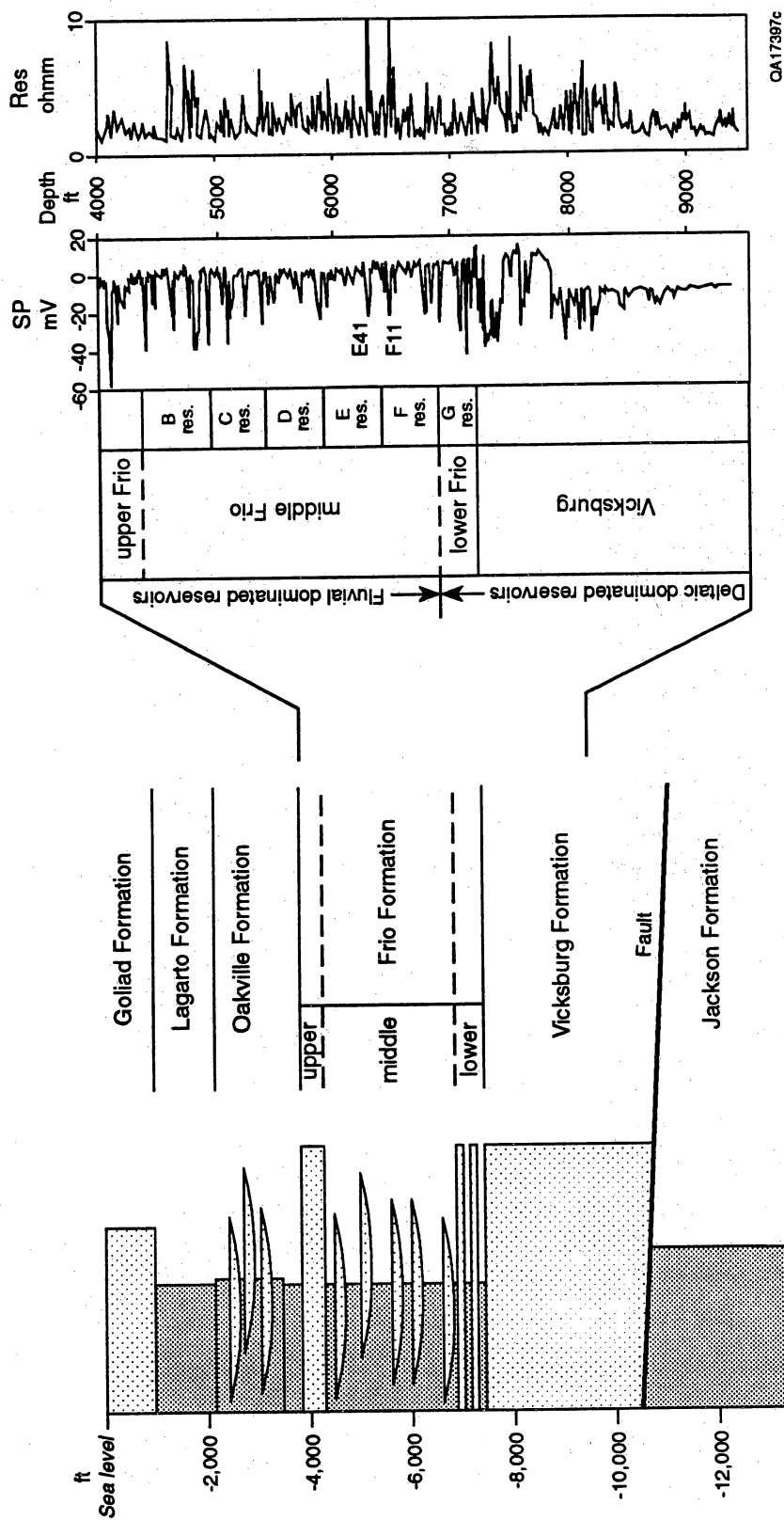
Figure 8. Type well log (spontaneous profile and resistivity) from the Wardner lease study area showing the reservoir nomenclature in the Frio and Vicksburg Formations.

17

profile on electric logs within splay deposits has a classic funnel shape, indicating an upward-coarsening textural profile. The lower Frio Formation in the Wardner lease occurs at depths between approximately 7,000 and 7,400 ft subsea. These sandstones range from 5 to 15 ft in thickness and show a funnel shape on the SP log profile. These lower Frio Formation sandstone packages are interpreted as lower coastal plain deposits to inner shelf deposits (Kerr, 1990) and are probably related to the Norias wave-dominated delta system delineated by Galloway and others (1982). Correlation of fieldwide resistivity and conductivity markers across Stratton field indicates that these sandstone packages are equivalent to the G-series reservoirs (fig. 8).

The Vicksburg Formation contains siliciclastic intervals with SP and gamma-ray logs indicative of upward-coarsening grain-size profiles consistent with deltaic-dominated depositional systems. Genetic stratigraphic analysis by Han (1981), Han and Scott (1981), and Langford and others (1992) identified variations in delta morphology within the middle and upper Vicksburg Formation that are thought to consist of mostly dip-oriented fluvial-dominated deltaic deposits. These sandstones in the upper Vicksburg Formation are often greater than 20 ft in thickness (up to 80 ft thick) and show a distinctive funnel-shaped spontaneous potential (SP) log profile, representative of upward-shoaling deposits that are characteristic of progradational deltaic depositional environments.

Reservoir Compartment Terminology

The term "secondary resources" refers to that segment of in-place gas that is typically not produced during historical approaches to development of a field containing mostly conventional permeability reservoirs. Secondary natural gas is the incremental gas that is recoverable using currently available production methods in mature fields in conventional reservoirs. Reserve growth of the nonassociated gas resources examined in this report consists of gas that has been either uncontacted or incompletely drained at current field spacing.

Development wells can be categorized as either infield or infill wells. Infield wells are commonly exploratory and are often targeted to deeper pool objectives. Infield wells are within the established field boundary but are often irregularly spaced. Infill wells are often spaced at half, or some variant of the established regulatory well pattern. Infill wells are targeted with the objective of increased or accelerated recovery from a previously known productive reservoir. Infield wells may be closer to previous wells than the established spacing either specified by field rules or typically utilized for that class of reservoirs.

Within a mature field, besides currently producing and depleted reservoirs, five additional categories are useful for evaluating infield reserve growth potential (fig. 9): (1) *New infield reservoirs* are reservoirs not contacted during the original development of the field, and they are separated vertically and laterally from adjacent reservoirs. (2) *Untapped reservoir compartments* are produced by completions within a reservoir that are not easily identified as being separated either vertically or laterally from the established production within the same reservoir. New completions within untapped reservoir compartments are usually at or close to original reservoir pressure of the prior productive completions. (3) *Incompletely drained reservoir compartments* are also not easily identified as being separated vertically or laterally from a reservoir that is productive. The term "incompletely drained" refers to the ineffective drainage of the previous completions in the reservoir. Incompletely drained reservoir compartments reach an economic limit, and the recoverable resource without additional operational efforts such as stimulation or perforation in a laterally adjacent well bore will not be effectively drained. (4) *Bypassed reservoirs* are reservoirs contacted by existing well bores that have not been produced during the course of field development. Reservoirs may be bypassed because they were evaluated as nonproductive or uneconomic. These are typically shallower reservoirs that can now be reevaluated by reprocessing of the original logs, acquiring cased-hole logs in existing well bores, or by new open-hole higher resolution logging tools. (5) *Deeper pool reservoirs* are categorized as those reservoirs penetrated by drilling deeper either in existing well bores or in new infield wells adjacent to shallower wells, and below the previously established productive pools.

QA17992c
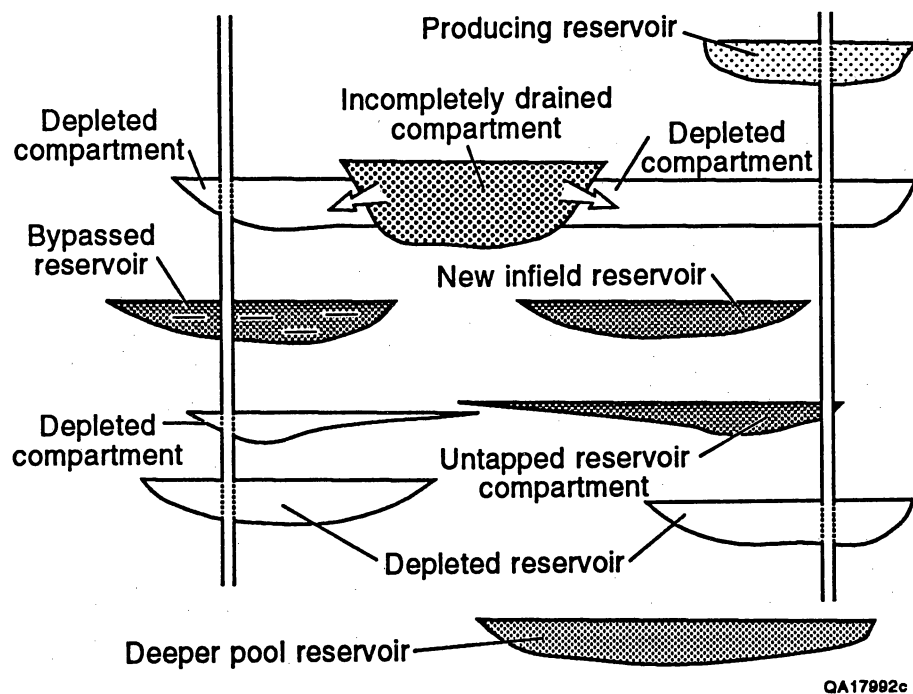
Figure 9. Diagrammatic sketch of reservoir-compartment terminology illustrating the variation in reservoir-compartment position and relation to well bores within a field (after Levey and others, 1992).

20

ANALYSIS OF RESERVE APPRECIATION

Analysis of infield drilling and recompletions in existing wells in a 7,400-acre area

documents total reserve appreciation in the Frio and Vicksburg reservoirs of 48 Bcf of gas

between 1979 and 1990 in a field that is now over 50 years old. For reservoirs less than 7,000 ft

deep, 33 of the 48 Bcf comes primarily from the fluvial-dominated reservoirs in the middle Frio

Formation. This is compared to reservoirs >7,000 ft deep, with 15 of the 48 Bcf coming

primarily from deltaic reservoirs in the lower Frio and Vicksburg Formations.

Historical Framework (1927–1990)

Stratton field is a mature giant gas field that has produced more than 2.0 Tcf of natural gas

since its discovery in 1922 as part of the Stratton–Agua Dulce field complex. This gas-prone

complex is one of the earliest fields discovered in the second phase of giant hydrocarbon fields

discovered in the Gulf of Mexico Basin between 1928 and 1941 (Nehring, 1991). Analysis of

Railroad Commission of Texas gas well production records indicates that between 1937 and

1990, more than 340 regulatory reservoirs were designated within Stratton field; 49 of these

reservoirs are part of the fluvial-dominated sandstones in the middle Frio. Stratigraphic analyses

based on well log correlations indicate that these 49 regulatory reservoirs can be grouped into

37 lithostratigraphic units. These lithostratigraphic units contain individual gas reservoirs that

are bounded by fieldwide stratigraphic markers detectable on standard electric well logs.

Calibration of these well log markers to cores indicates that the markers represent floodplain

shales that are identifiable as resistivity or conductivity markers on conventional electrical

survey and induction logs. A total of 34 of these 37 middle Frio reservoirs have been developed

across Stratton field as of January 1, 1990.

Several phases of field development are identifiable based on the production history

between 1938 and 1990. Fieldwide gas production continuously exceeded 50 Bcf per year

between 1940 and 1977 (fig. 10). The maximum peak in gross gas production occurred during
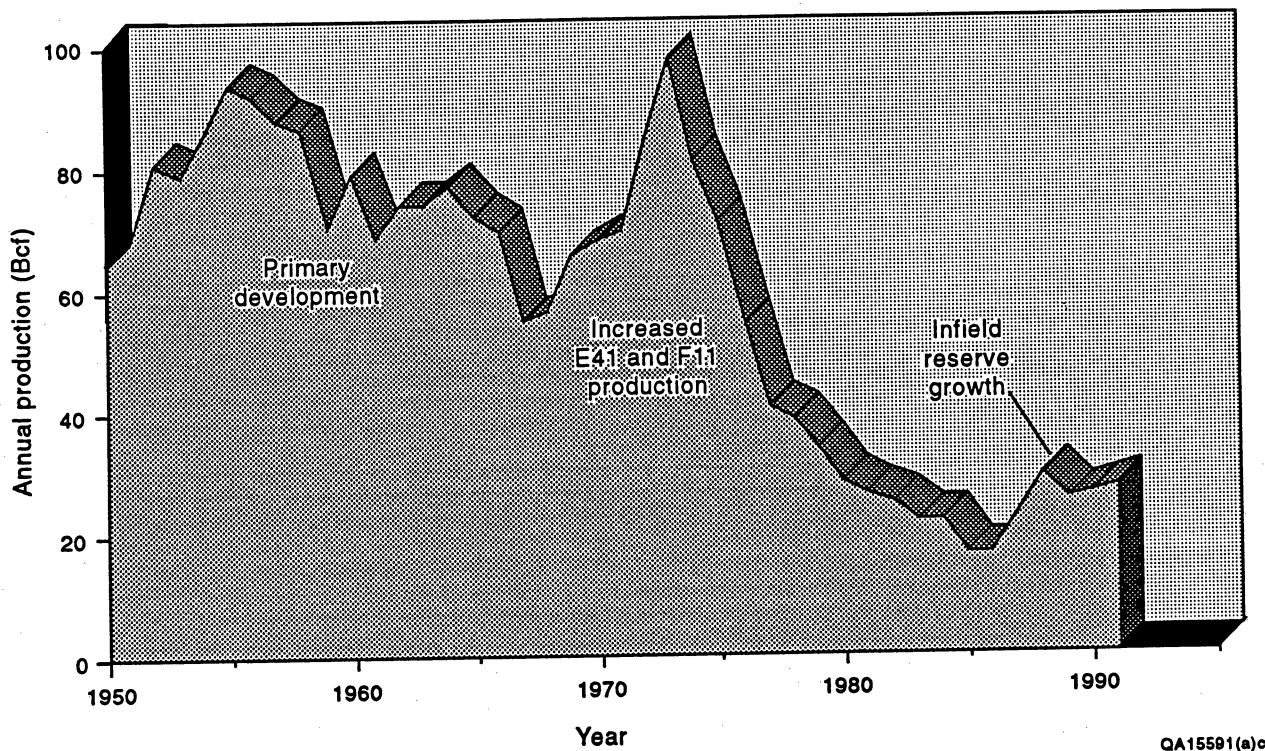
Figure 10. Annual gas production of Stratton field from 1940 to 1990.

1973, when annual production exceeded 95 Bcf. This peak was achieved during a phase of selective reservoir development of the Stratton field gas cap when production was dominated by the two most prolific gas reservoirs, the Bertram (E-41) and Wardner (F-11). The approximate lateral extents of these two fieldwide reservoirs are illustrated in figure 11. During this later phase of development in the 1970's, the reservoir pressure in these two laterally continuous reservoirs (E-41 and F-11) was partly supported by gas cycling to produce associated oil. From 1975 to 1986, gas production declined substantially and reached a low of less than 20 Bcf per year in 1985. The reversal in gas production decline, from 1986 through 1989, is a function of the recent infield drilling and recompletions of existing wells in the field.

In the early stage of development in Stratton field, almost all the natural gas produced was from middle Frio reservoirs. Starting in the early 1950's, production from lower Frio and Vicksburg reservoirs was initiated. Middle Frio reservoirs have always been the dominant productive stratigraphic horizons in Stratton field. The primary development of middle Frio fluvial reservoirs occurred from 1938 to 1960, when more than 90 percent of all active reservoirs were in the middle Frio Formation. A second phase of reservoir development occurred from 1965 through 1975, when development of middle Frio reservoirs represented 80 percent of all active reservoirs. The most recent phase of infield drilling (post 1986) has also increased the percentage of middle Frio productive reservoirs.

The 340 reservoirs reported for Stratton field in the public files of the Railroad Commission of Texas is the largest number of regulatory reservoirs for any of the fields in the FR-4 gas play. Detailed stratigraphic correlations using well logs to identify reservoir intervals across the field indicate that this number of reservoirs is relatively high. This large number of reservoirs is attributed to (1) multiple stacked pay horizons, (2) physical compartmentalization in some reservoirs, and (3) separate reservoir designations as different lease boundaries are crossed within the field. Comparing the discovery year for each reservoir and the depth to the reservoir illustrates the development history in Stratton field (fig. 12). In addition, a trend
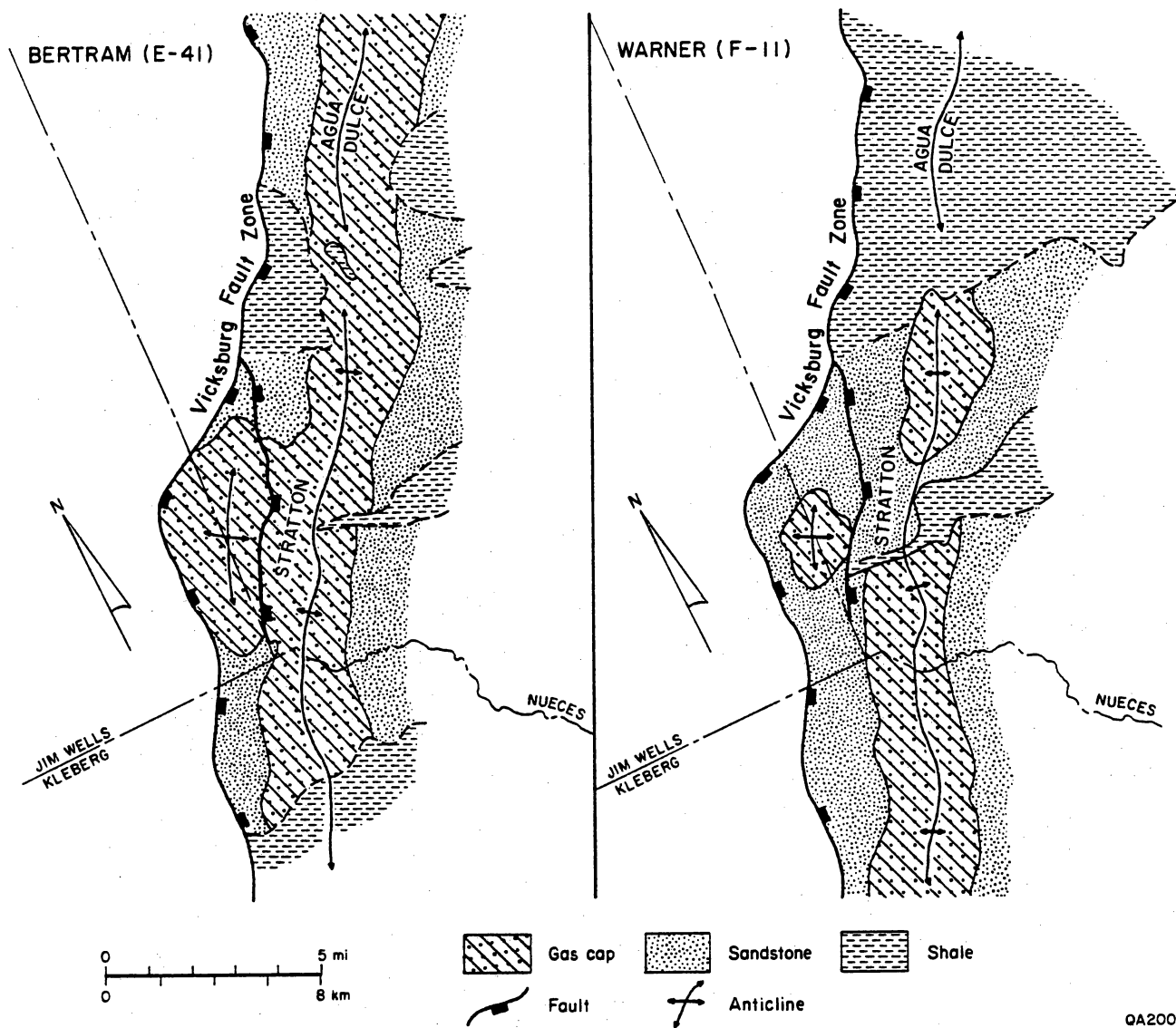
Figure 11. Stratton-Agua Dulce field complex showing the lateral extent of the major productive reservoirs, Bertram (E-41) and Wardner (F-11).
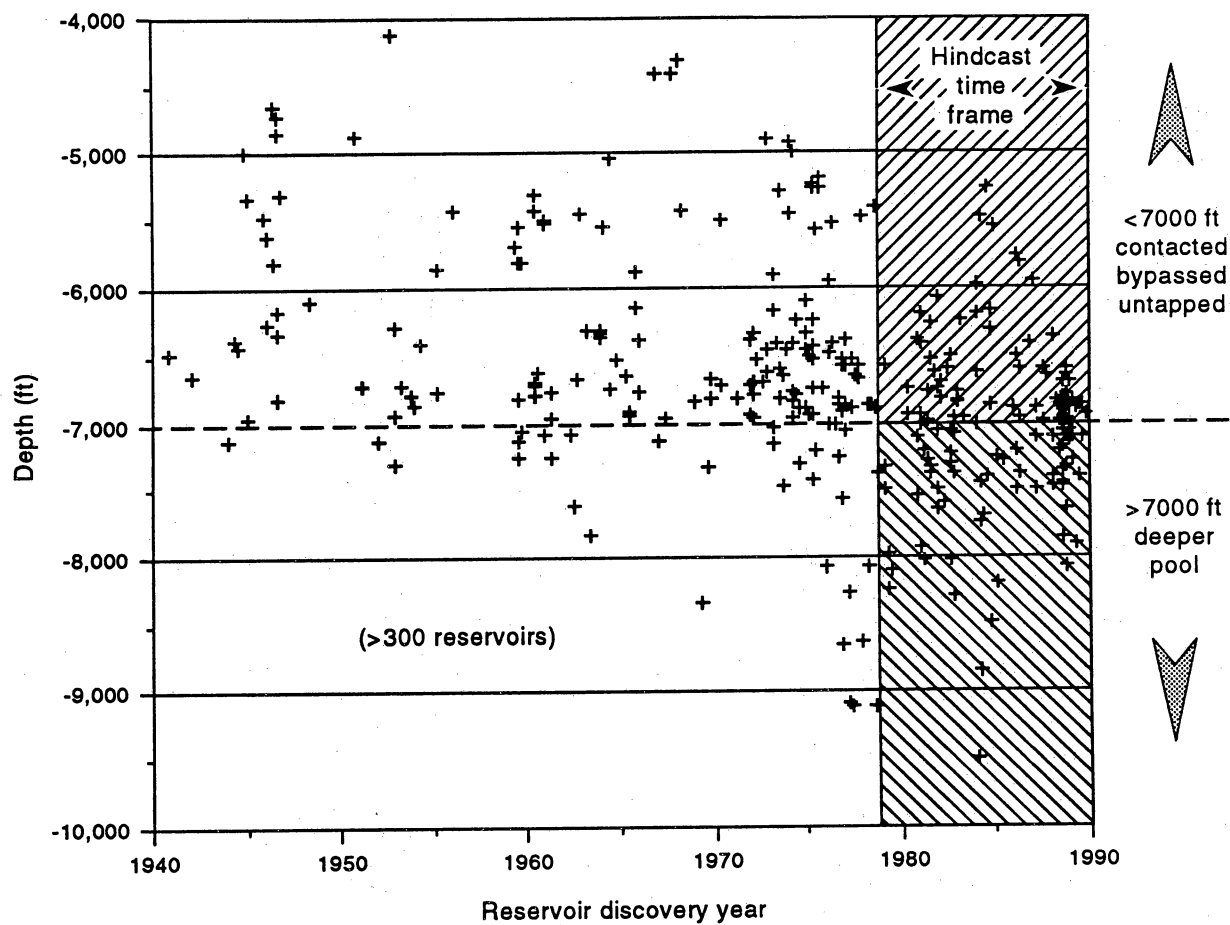
Figure 12. Reservoir discovery year versus reservoir depth in Stratton field. The hindcast time period was used in the historical analysis of infield drilling in the field.

toward deeper pool development is indicated by the number of new reservoirs discovered after 1960 at depths greater than 7,000 ft.

Area of Investigation—Wardner Lease

One major objective of this research is to investigate secondary gas resources in Stratton field and to use these results to predict probable sources of incremental reserves in fields similar to Stratton. As part of this research, a large contiguous area of Stratton field was analyzed to evaluate the impact of additional drilling and recompletions within the established geographic limits of the field. The area of detailed analysis is located in the Wardner lease in the south part of Stratton field (fig. 13). The study area comprises approximately 7,400 acres and is operated by Union Pacific Resources. This study area is on the downthrown side of the Vicksburg flexure. Analyzing the reserve growth for the study area by depth, reservoir type, and spacing has allowed us to arrive at conclusions as to the probable source and amount of future incremental reserves for Stratton and other fields with similar reservoir architecture.

Methods of Gas Reserve Assessment

The purpose of this gas reserve assessment is to compare pre-infield development with the magnitude of reserve growth obtained by recompletions in existing wells and the drilling of new wells in the study area. Incremental gas reserves developed since January 1, 1979, were determined instead of ultimate recovery since discovery because several reservoirs were cycled until the late 1960's. Records of cumulative gas production for each well were obtained from the Dwights Production computer-based data base. Remaining developed reserves were determined from extrapolation of the decline of the producing rate with time for each completion in the study area. A best-fit exponential decline (a straight line on a semilog rate versus time plot) was made to a rate limit of 1,000 Mcf per month. This gas production rate is compatible with production rate cutoff volumes used by operators for gas fields producing from

26
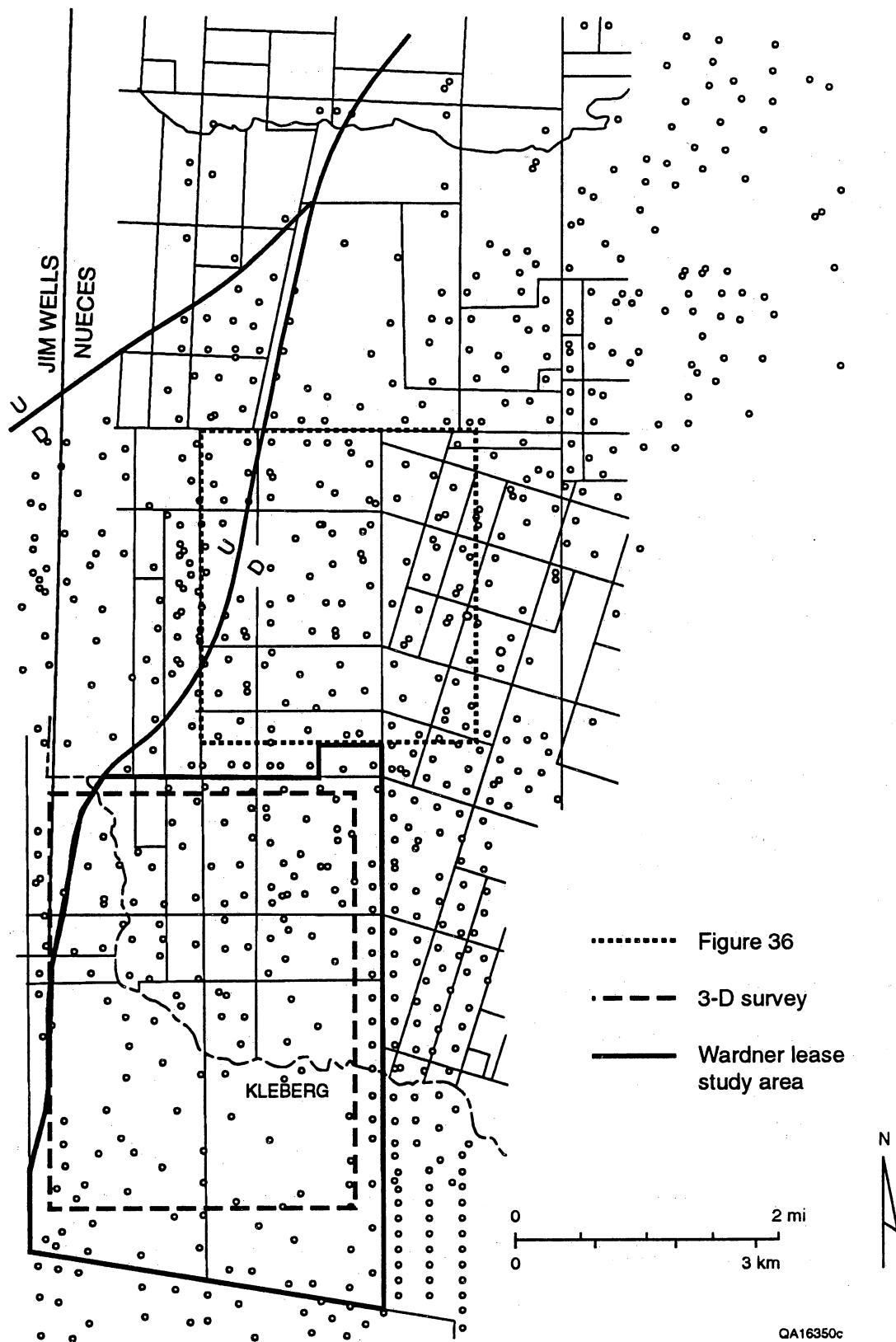
Figure 13. Location of the Wardner lease study area, Stratton field.

No Reserve Revision
Wardner 3 Production History

(b)

Monthly Gas Production (Mcf)

Time (Years)

1990 Evaluation

1979 Evaluation

Reservoir Without
Reserve Revision

Projected

30
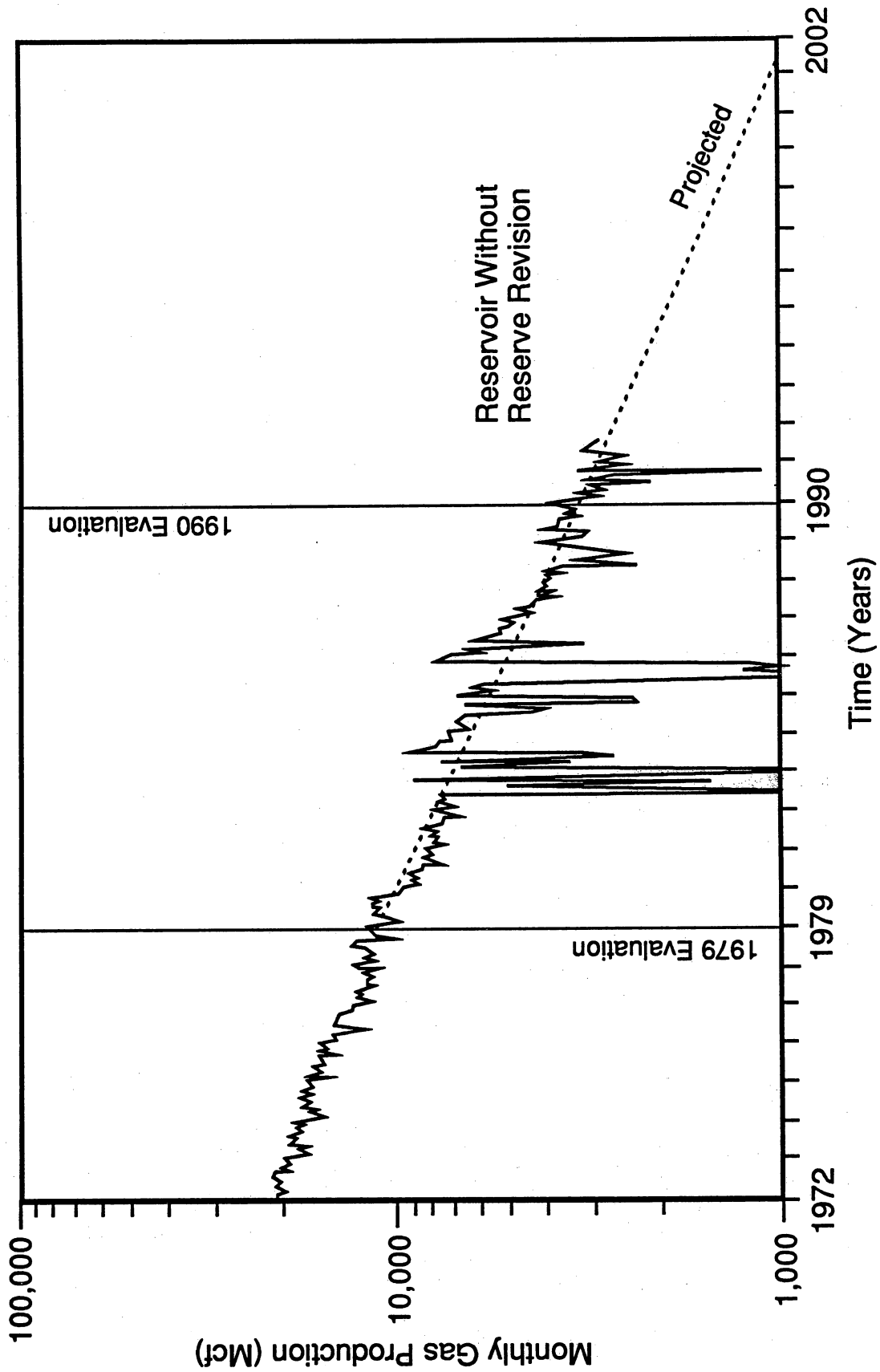
Negative Reserve Revision
Wardner 92 Production History

(c)

Monthly Gas Production (Mcf)

Time (Years)

1990 Evaluation

1979 Evaluation

Well with Negative
Reserve Revision

1/1/79
Projection

100,000

10,000

1,000

1974   1979   1990   2009
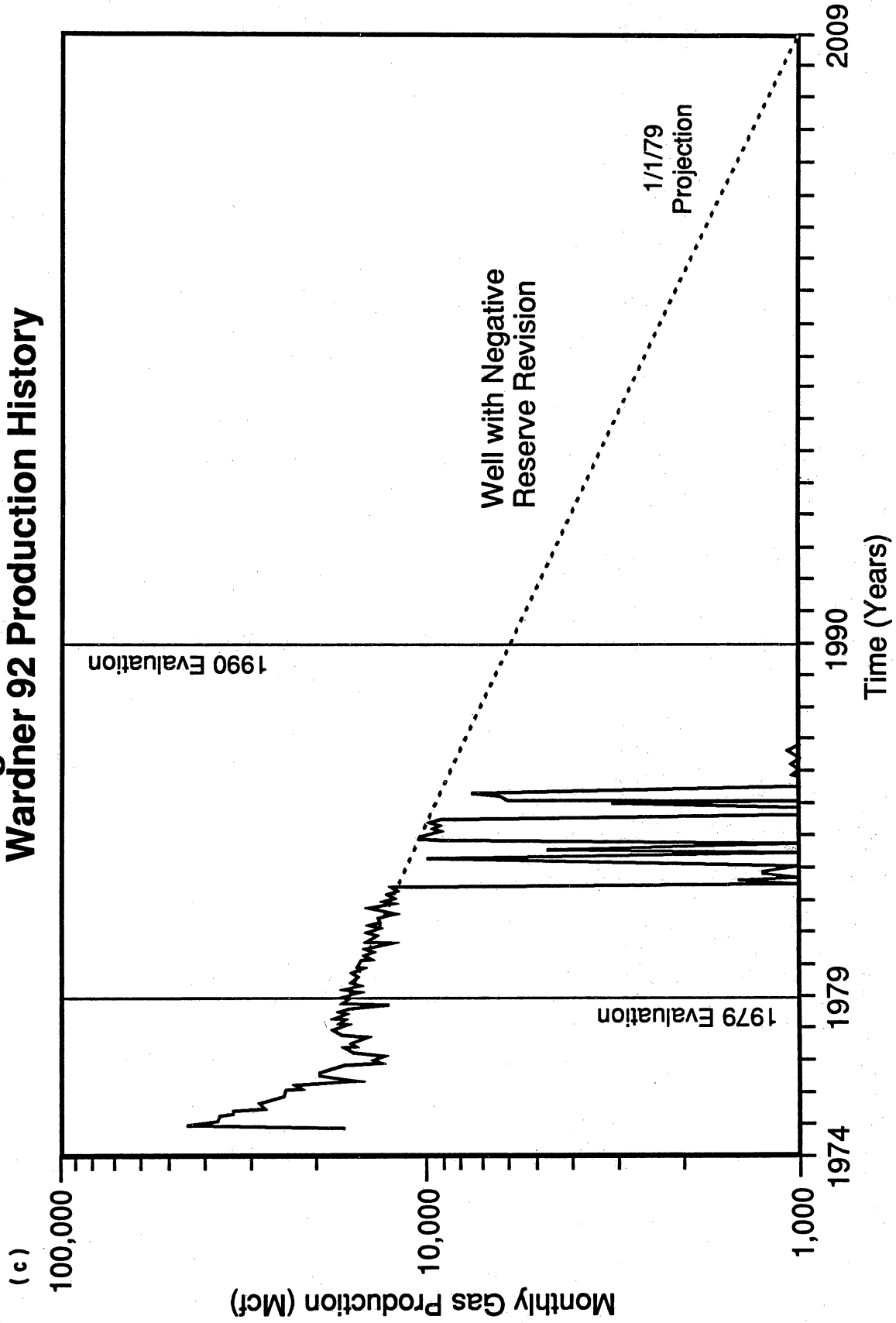
January 1, 1979. This gas reserve assessment is a comparison of incremental remaining reserves as viewed from a historical perspective as of January 1, 1979, and of January 1, 1990.

The reported reservoir pressure at completion was also investigated as an indicator of reserve growth potential. Chronological analysis of the reported reservoir pressures at less than 7,000 ft in the study area indicates that greater than 50 percent of the gas completions from 1979 to 1990 had initial reservoir pressures greater than 60 percent of the expected original reservoir pressure based on a normal Stratton field hydrostatic gradient of 0.45 psi/ft. The cumulative frequency distribution for reported reservoir pressures for all completions less than 7,000 ft for the 1979 to 1990 period shows this pressure attribute (fig. 15). Within the Wardner lease study area it is not uncommon for sequentially later reservoir pressure tests to have higher initial pressure than previous adjacent wells in the same reservoir. This tendency toward higher pressures in new completions in conventional permeability reservoirs is indicative of reservoir compartmentalization.

Results of Reserve Assessment (1979–1990)

In a mature gas field such as Stratton, a hindcast approach to resource assessment is effective because of (1) its extensive period of previous field development history and (2) the large number of recent infield drilling and recompletions. The time period used in this hindcast analysis compares completion history and gas reserves based on all completions in January 1979 with the known performance of the same completions and additional completions from infield drilling after 1978 to January 1990. The discovery years for new reservoirs in Stratton field are illustrated in figure 12. The 1979 to 1990 time period is represented by the shaded area. Reserve additions are considered in two depth categories: those reserves shallower than 7,000 ft and those deeper than 7,000 ft.

Since the peak of gas production in 1973, reserve additions in Stratton field in the past two decades have effectively kept pace with production. The average daily gas producing rate,
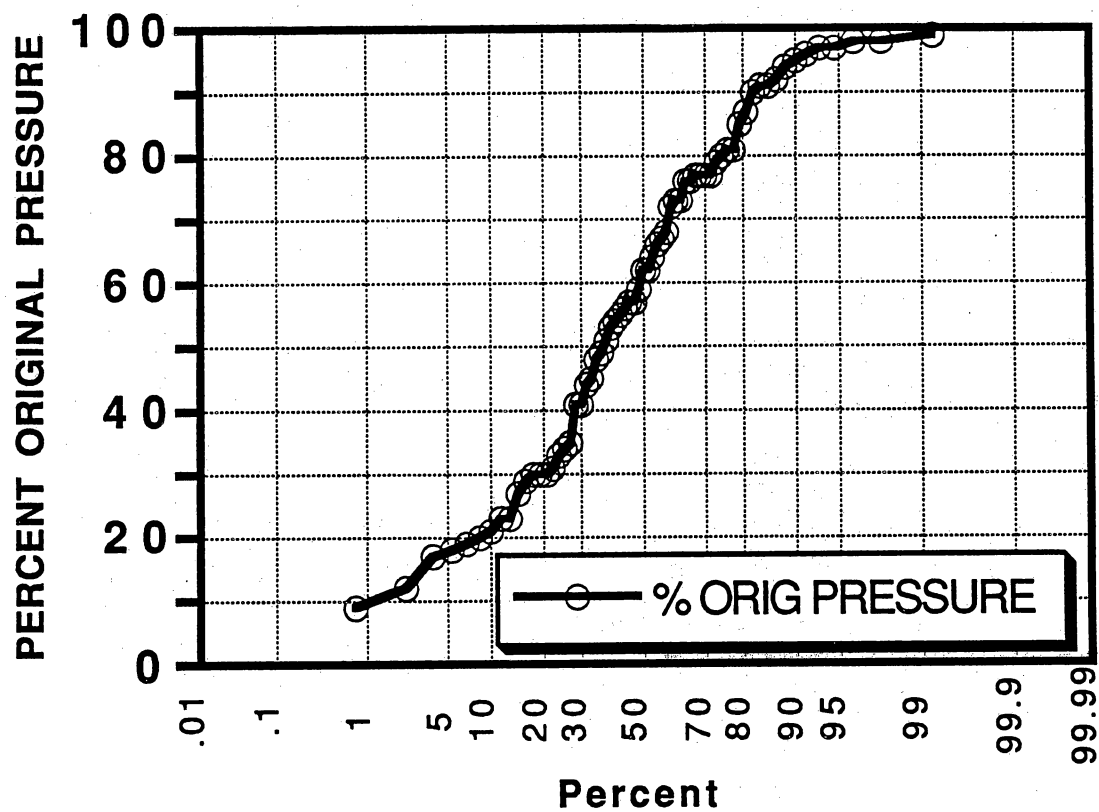
Figure 15. Cumulative frequency plot of reservoir pressure for all completions above 7,000 ft within the time period of 1979 to 1990, Wardner lease study area.

determined from annual production, for completions in the Wardner lease study area is shown in figure 16. The production data are divided into two separate curves that reflect the contributions from reservoir completions made at the two time frames. The lower curve represents the production from completions made prior to 1979. This is the base case for reserve growth assessment. The upper curve represents the production from completions made in the period 1979 through 1989. Before 1979, an increase in rate and reserve additions is noted from 1977 through 1978 as a result of several successful discoveries in deeper pool reservoirs. The upper curve represents the summation of production from all completions. The area between the two curves shows the relative reserve additions that are attributable to post-1978 completions. Annual gas production shows that the decline of producing rate and depletion of reserves has been dramatically slowed by continued drilling and completion activity initiated in 1986 (fig. 10).

By evaluating reserve additions by depth categories we can consider the contribution of deeper pool additions in comparison with that of new wells completed in the existing productive reservoirs and recompletions in the older wells. In the study area, 7,000 ft is the approximate depth of transition from middle Frio to lower Frio and Vicksburg reservoirs. Incremental recovery from reservoirs in the middle Frio has contributed more reserve additions than have reservoirs in the lower Frio and Vicksburg. The next step in evaluating the incremental reserve growth is to identify which group or series of reservoirs in the middle Frio have accounted for the largest contributions to the overall reserve additions.

Using the reservoir nomenclature adapted by gas operators in Nueces and Kleberg Counties (fig. 8), we further subdivided reserve additions into reservoir groups (B-, C-, D-, E-, and F-series reservoirs). The most significant reserve growth occurred in the E-series and F-series reservoirs, and closer examination by specific operational reservoir indicates that the lower F-series reservoirs have contributed the most reserve growth. Many of these reservoirs were penetrated by early development wells that have been producing from major separate reservoirs such as the E-41 and F-11 since the 1950's. Stratigraphic and structural analysis of
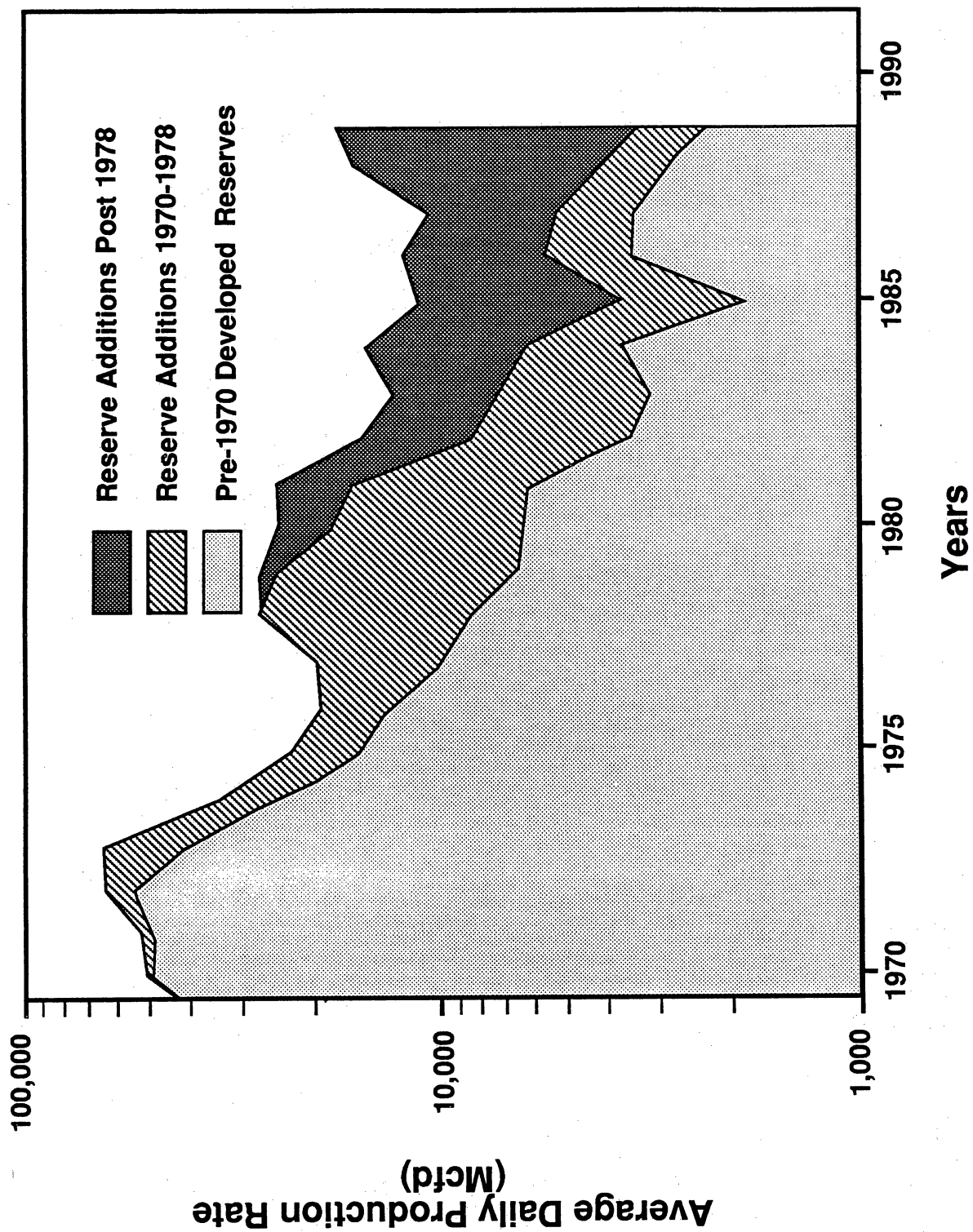
Figure 16. Gas production rate with time from 1970 to 1989, Stratton field.

reservoirs in the Wardner lease study area indicated that stratigraphic variation is one mechanism for the reserve growth realized from 1979 to 1990. Structural complexity caused by faulting is minor at depths above 7,000 ft across the Wardner lease study area (fig. 6). Geologic and engineering analysis indicate that most of the reserve growth has occurred from reservoirs previously contacted in existing well bores. These reservoirs are ineffectively drained by the existing completion spacing, or in untapped reservoir compartments (Levey and others, 1991; Sippel and Levey, 1991; Levey and others, 1992). The magnitude of reserve growth in new infield reservoirs is volumetrically smaller than gas volumes in incompletely drained reservoirs and previously untapped reservoir compartments.

The level of effort required to produce the total combined reserve additions is indicated by the number of completions through time (fig. 17). The successfully producing gas completions for time-segregated completion groups clearly indicate the impact of the infield drilling and recompletions in the late 1980's. Annual producing rates were used to determine the gas well completion status. A completion producing less than an average of 5 Mcf/d for a calendar year was determined to be inactive. The active completion count was nearly constant over time until 1987, when there was a sharp rise in completion activity.

To evaluate the impact of well spacing on reserve additions, completion and well density were determined from the digitized locations of wells in the study area. The relative x-y coordinates were used in a computer program to perform the tedious calculation of the distance to the nearest well. The completions were sorted by reservoir to make spacing calculations at each of the reservoir levels. The allocated area for each completion, or well, was assigned as the square of the distance to its nearest neighbor at the appropriate completion or reservoir level. The mean surface spacing between all well bores has decreased from 48 acres in 1970 to 27 acres in 1990. Quantifying well or completion spacing can be difficult in fields such as Stratton–Agua Dulce, which has stratigraphically complex reservoirs. Sandstones in these reservoirs were deposited in fluvial settings and vary greatly in reservoir quality. Stratton field also presents a problem in quantifying well spacing and reservoir completion because the

36
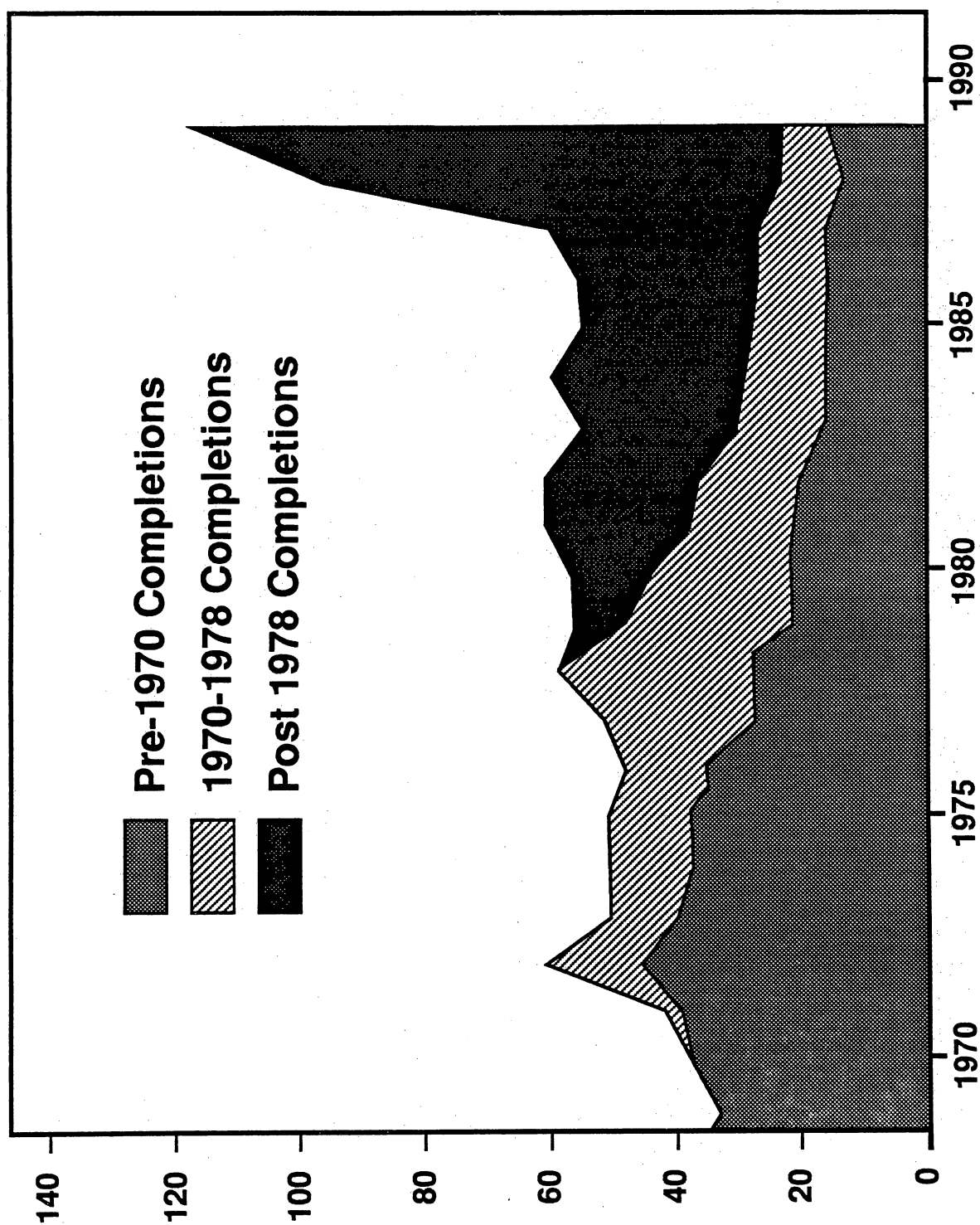
Figure 17. Number of active completions through time in the Wardner lease study area.

structural crest is intensely developed and the flank is poorly developed. Other operational factors can also affect the quantification of spacing in areas where wells have been closely spaced on the periphery to protect the lease line and in the interior of the lease, which has been less developed.

The statistics on well and completion density provide an important perspective on the development that has occurred at Stratton field as well as a means of comparison with other fields. A common problem in assessing spacing and development results from a situation where 4 completions in a 640-acre reservoir area are clustered in a 160-acre group, resulting in 40 acres to the nearest completion: is the average spacing 40 or 160 acres? In the laterally extensive reservoirs like E-41 and F-11 (fig. 11), which cover a large part of the Stratton–Agua Dulce field and have a large number of completions, the completion spacing is approximately 160 acres per completion. Reservoirs in the lower F-series that are present in only certain parts of the field had a completion spacing between approximately 320 to 160 acres in 1979. In 1990, the completion spacing of these reservoirs is between approximately 160 to 80 acres.

Impact of Infield Drilling (1986–1991)

The period from 1986 through 1991 was a time of aggressive infield drilling across a large part of Stratton field, including the Warder lease study area. In January 1979, 53 active completions existed in the study area (fig. 18). Of these original 53 completions, 22 were still active in January 1990. A total of 149 new completions were made between 1979 and 1990. Of the 149 new completions, 82 were still active in January 1990.

A histogram of gas volume for the two time periods illustrates the degree of reserve growth attributed to incremental drilling and completions (fig. 19). As of January 1, 1979, remaining recoverable reserves of 52 Bcf are projected from 53 completions in 43 wells. From 1979 to 1990 a total of 38 Bcf was produced, and 10 Bcf are projected as the reserves remaining of the 52 Bcf projected in 1979. By comparison, 149 completions made in 84 wells between January
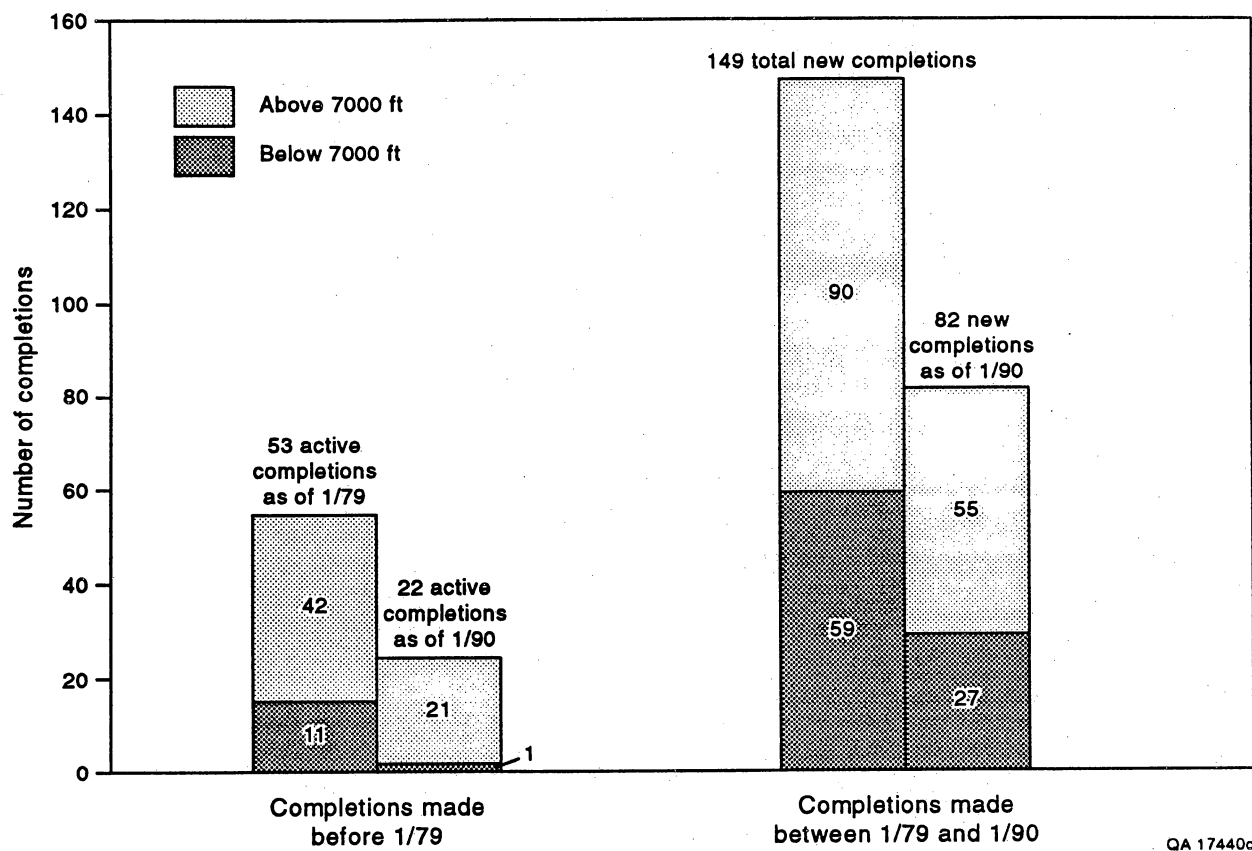
Figure 18. Number of completions by depth category in the Wardner lease study area.
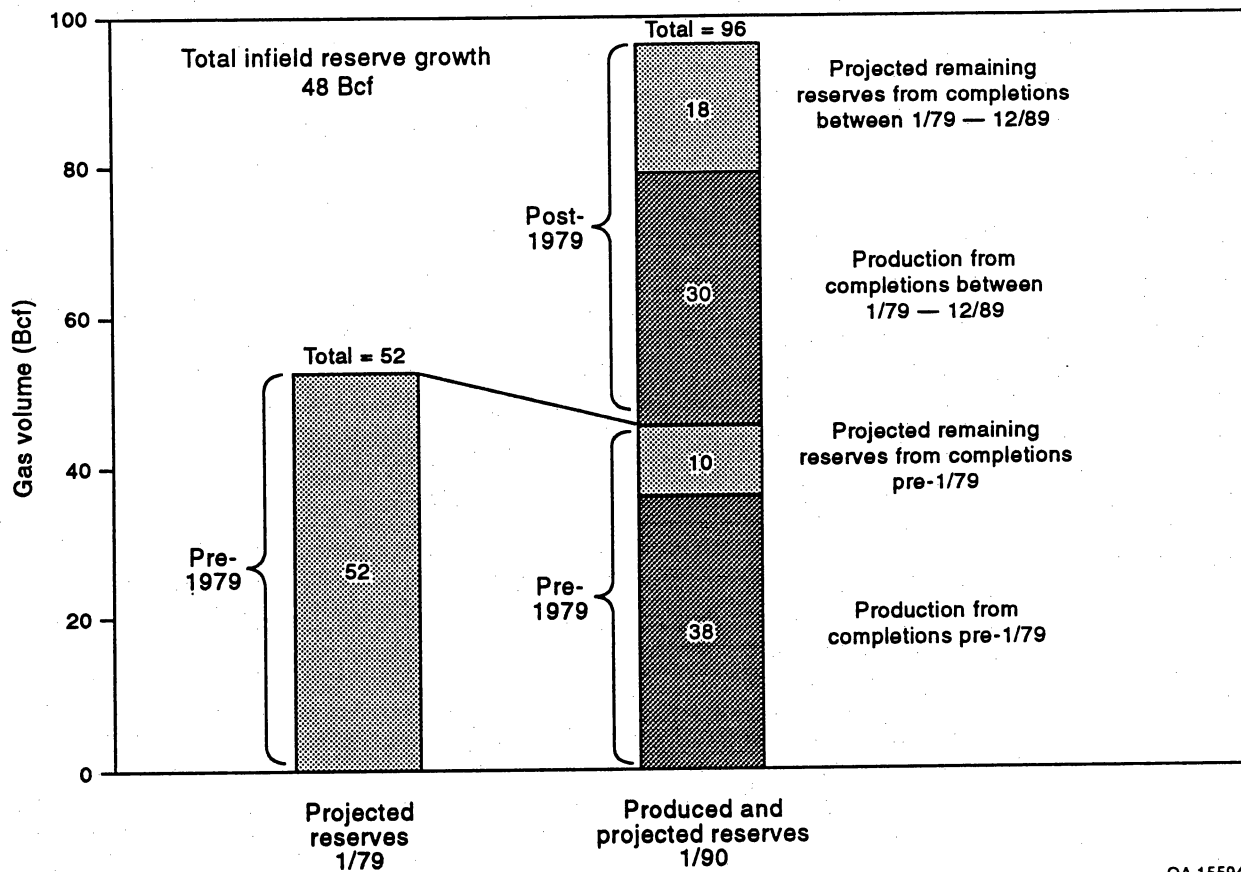
Figure 19. Total gas volume for all completions in the Wardner lease study area.

1979 and January 1990 added 44 Bcf of reserve additions to the projections made for completions active in January 1979. From these new completions a total of 30 Bcf was actually produced between 1979 and 1990, and an additional 18 Bcf was projected as remaining to be produced after January 1990 to an economic producing limit of 30 Mcf/d per completion. The additional completions from January 1979 to January 1990 provided more than 90 percent replacement of reserves beyond the projected remaining developed reserves for all completions active in 1979.

Comparison of reserve estimates using a depth cutoff of 7,000 ft demonstrates the overprint of depositional system on incremental gas reserves. Because of the simple low-relief structure and consistent surface elevation across the study area, the 7,000-ft depth approximates the transition from the middle Frio (<7,000 ft) to the lower Frio and Vicksburg Formations (>7,000 ft). For the completions less than 7,000 ft deep as of January 1979, a total of 39 Bcf is projected as the remaining recovery for the gas reserves, compared with a total of 70 Bcf as actually produced and estimated to be remaining as of January 1990 (fig. 20). Actual production and projected reserves in January 1990 indicate that of the projected 39 Bcf of original reserves, 27 Bcf was produced, and 10 Bcf is projected as remaining for the completions made before January 1979.

For the 11 completions deeper than 7,000 ft made before January 1979 (fig. 21), 13 Bcf of original reserves is indicated. Analysis of the completions deeper than 7,000 ft between January 1979 and January 1990 indicates that an additional incremental 15 Bcf of reserves was developed from 59 post-1978 completions within 35 wells. Of that 15 Bcf, 9 Bcf was actually produced, and an additional 6 Bcf is projected as the recovery remaining from these completions as of January 1, 1990.

Overall reserve growth achieved from the shallower, middle Frio reservoirs is superior to that obtained by completions in the deeper reservoirs in the lower Frio and Vicksburg, both on a total gas volume basis and on a per completion comparison. Analysis of the reserve additions per completion indicates that the gas completions less than 7,000 ft added 379 MMcfg per
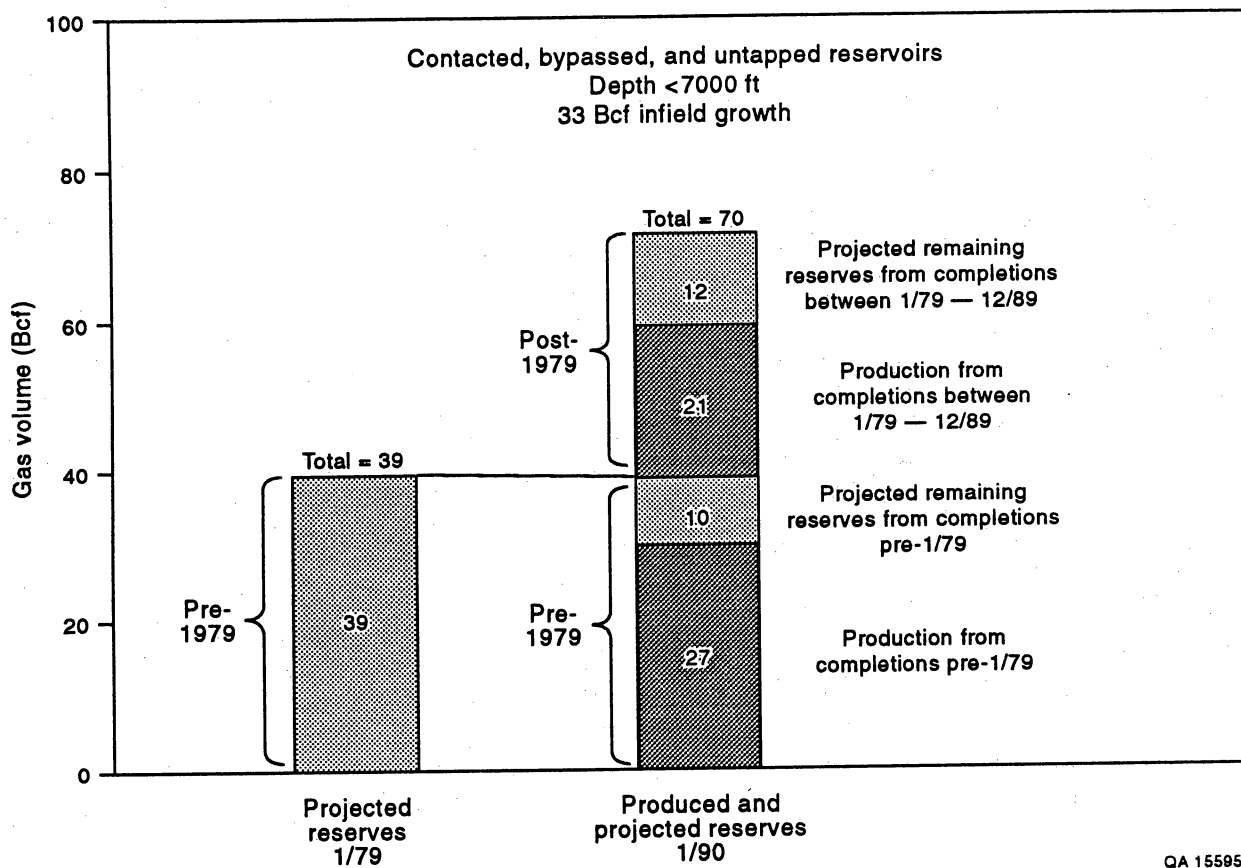
Figure 20. Gas volume for completions above 7,000 ft in the Wardner lease study area.
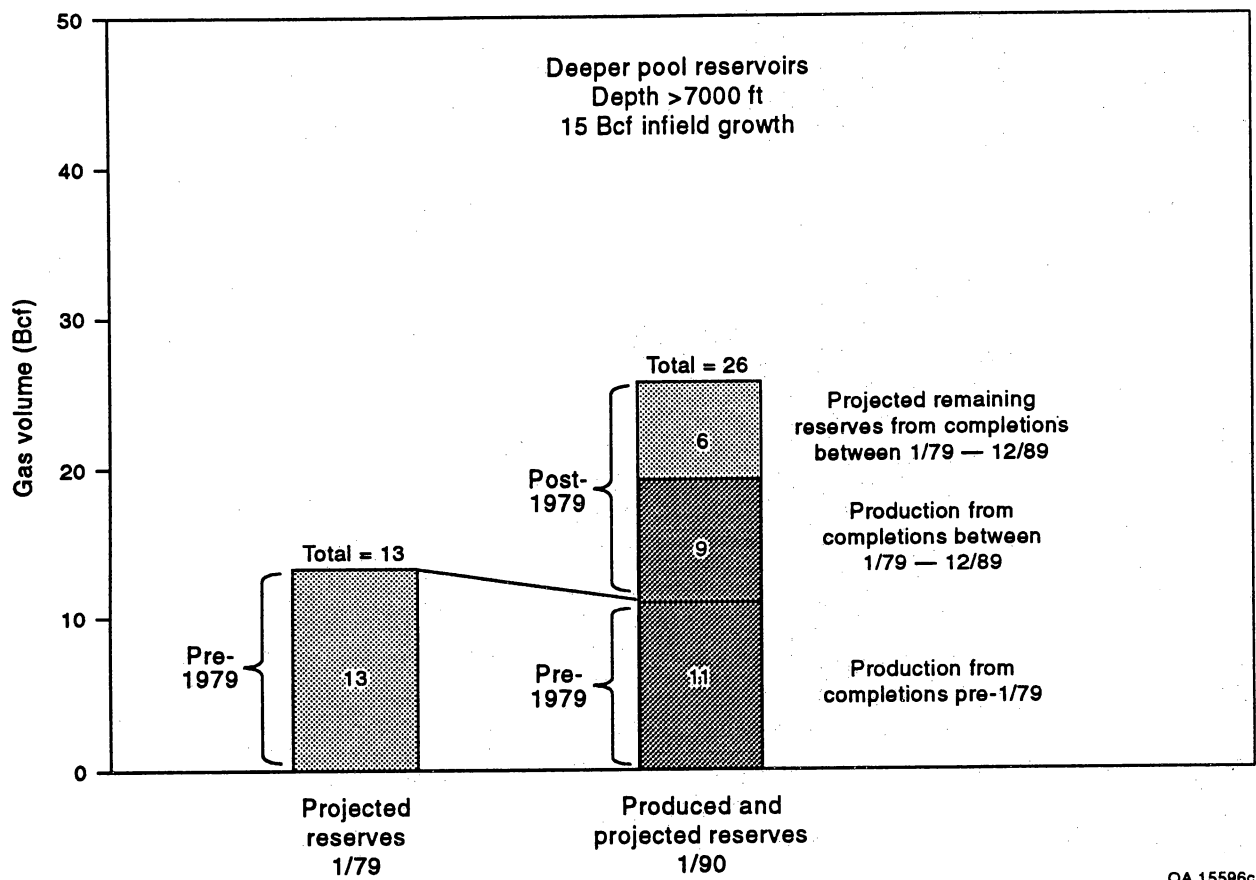
Figure 21. Gas volume for completions below 7,000 ft in the Wardner lease study area.

completion (33 Bcf in 90 completions), compared with 250 MMcfg for completions greater than 7,000 ft (15 Bcf in 59 completions). The contrast in gas production between reserves shallower than 7,000 ft and those deeper than 7,000 ft coincides with a major change in the structural and depositional setting in the study area. The middle Frio Formation reservoirs (<7,000 ft) are in fluvially dominated reservoirs; in contrast, the lower Frio and Vicksburg reservoirs (>7,000 ft) are in a predominantly deltaic setting that approaches the top of geopressure or requires penetration into geopressured intervals (cross section 19–19′, Dodge and Posey, 1981). In addition, structurally rotated fault blocks are encountered in the lower Frio and Vicksburg below 7,000 ft (fig. 6). It is well recognized that drilling costs almost always increase when (1) drilling deeper wells, (2) penetrating geopressured intervals, and (3) drilling in structurally deformed intervals.

Forecast for Gas Reserve Growth (1990–2009)

Potential Remaining Gas Resources

A study was performed to evaluate the volume of the remaining gas resource and to determine which middle Frio reservoirs contain the most potential for future reserve growth. A comparison of volumetric OGIP (from log evaluation) and cumulative production indicates that the D- and upper E-series (D-6 through E-18) sandstones contain the largest potential remaining resource and should be a major source for reserve growth in the future. The D- and upper E-series reservoirs are uphole from the current reserve growth successes in the lower F-series and are also uphole from the major E-41 and F-11 reservoirs. The potential for future reserve growth from the D-series and upper E-series reservoirs is estimated to be 19 Bcf. Although this analysis does not exclude other reservoirs from having additional reserve growth potential, the magnitude of the potential remaining reserves from volumetric OGIP and the cumulative production for the D- and upper E-series reservoirs indicate that these reservoirs have the additional potential for future reserve growth.

44

Method for Volumetric Assessment

Volumetric analysis was performed for the middle Frio reservoirs in the Wardner lease study area. A macro approach was used to estimate OGIP and expected ultimate recovery of past and existing completions. Thirty-five modern logs (consisting of gamma-ray, spontaneous potential, induction, and density and neutron logs) from wells covering most of the Wardner study area were digitized for this volumetric appraisal. The 35 well logs are evenly distributed over the study area and provide a representative sampling of the reservoir distribution. All potential reservoirs in the middle Frio from the B-41 through the F-44 were considered in this evaluation. The cumulative production from these reservoir intervals is 671 Bcf, with 343 Bcf accounted for as injection volumes in the E-41 and F-11 at the Wardner lease. A net cumulative production of 328 Bcf as of 1990 is calculated from the difference between these two quantities. Volumetric analysis of some reservoirs in Stratton field is uncertain because information concerning gas production and injection volumes over the 50-plus years of development are difficult to obtain. In addition, several reservoirs were recycled to extract liquids and to maintain pressure of the downdip oil column. Gas cycling operations ceased in 1968.

The effective hydrocarbon pore volume was determined after applying cutoff parameters for computed porosity greater than 15 percent, water saturation less than 60 percent, bulk volume of water less than 11 percent, and shale volume less than 20 percent. Using these petrophysical cutoffs, the effective hydrocarbon pore volume from log analysis is representative of gas productive intervals with immobile water saturations. Water saturations were calculated using a water resistivity of 0.17 ohm-meters at 75°F, which is equivalent to a formation water salinity (obtained from representative water samples of 23,700 ppm Cl). Although formation water salinity in the middle Frio is considered constant, formation water resistivity changes with temperature. A shaly-sand petrophysical model (explained in

appendix 1) was used to derive the values for lithology, porosity, water saturation, and permeability.

A total of 395 Bcf is estimated as the OGIP for the middle Frio reservoirs B-41 through F-44, with average depths of 4,828 to 6,868 ft in the 7,400-acre Wardner lease study area. This volume compares favorably with the cumulative net production of 328 Bcf. The largest remaining gas reserves after subtracting cumulative production from OGIP are found in the D- and upper E-series. The deeper pool targets in the new wells and the long production history of the cycled reservoirs precluded development of shallower objectives. Analysis of remaining gas potential focused on the D- and upper E-series reservoirs, which are uphole from the recent reserve growth in the F- and G-series reservoirs. Reservoir parameters and resource calculations for these reservoirs are summarized in table 1. The average depth of each group interval (column 2) was used to estimate the original reservoir pressure and temperature using established gradients from known production in the middle Frio. A temperature gradient of 1.7°F per 100 ft and a pressure gradient of 0.45 psi per ft were used for these reservoir parameters. A gas gravity value of 0.65 was used to determine the original gas volume factor at the appropriate temperature and pressure of each interval by standard correlations. The hydrocarbon porosity-feet determined from the average net pay thickness of the 35 logs evaluated in the study area (column 3) and the appropriate gas volume factor were used to determine the OGIP (column 6) based on a 60 percent recovery factor, reported cumulative production (column 7), projected EUR from existing completions (column 8), remaining developed reserves (column 9), and undeveloped reserves (column 10). The undeveloped remaining reserves were determined by subtracting the currently estimated EUR (column 8) from the recoverable gas in place (column 6), if positive. The developed remaining reserves were estimated by decline-curve projection of individual production histories from completions producing as of January 1, 1990. The remaining undeveloped recoverable reserves are estimated by subtracting the EUR from 60 percent of the OGIP.

Table 1. Reservoir parameters for OGIP estimates and remaining reserves in D- and upper E-series, Wardner lease study area, Stratton field.

(1) Reservoir group	(2) Average depth (ft)	(3) Average net pay (ft)	(4) Unit OGIP (Mcf per acre-ft)	(5) Study area OGIP (MMcf)	(6) Recoverable 60% GIP (MMcf)	(7) 1/1/90 cumulative (MMcf)	(8) 1/1/90 EUR (MMcf)	(9) 1/1/90 Developed remaining reserves (MMcf)	(10) 1/1/90 Undeveloped remaining reserves (MMcf)
D6–D34	5,564	4.4	834	26,940	16,164	13,450	14,415	965	1,749
D35–D40	5,728	2.7	736	14,926	8,956	1,327	1,933	606	7,023
D44–E13	5,897	3.7	717	19,391	11,634	1,819	1,867	48	9,767
E29–E35	6,196	2.2	606	12,349	7,409	6,029	6,851	822	558
Total				73,606	44,163	22,625	25,066	2,441	19,098

Note: 7,400 acres used in all volumetric estimates. Average net pay includes all 35 wells. Remaining reserves are 60 percent of OGIP minus the developed EUR. Technically recoverable gas is estimated at 60 percent of the OGIP. Petrophysical cutoff parameters are the following: greater than 15 percent for computed porosity, less than 11 percent for water saturation, less than 60 percent for bulk volume of water, and less than 20 percent for shale volume.

A reservoir unit recovery factor of 60 percent was applied to estimate the technically recoverable gas by pressure depletion for the D- and upper E-series reservoirs from about 5,400 to 6,000 ft. This 600-ft interval contains sandstones that have produced previously at the Wardner lease and elsewhere in the field, but these sandstones are likely to be affected by diagenesis resulting from volcanic ash, as described by Grigsby and Kerr (1991). Close completion spacing (40 acres) and hydraulic stimulation may be required to effectively produce the remaining reserves. The technically and economically recoverable portion of the remaining resource is estimated to be less than the recovery from the other lower E- and F-series reservoirs because of several factors: (1) lower permeability, (2) higher water saturations, and (3) smaller compartment sizes. Unit recovery factors from 80 to 90 percent have been demonstrated in the higher permeability reservoirs, where abandonment pressures have been less than 200 psi.

Future Reserve Growth

Having established that there is a volumetric basis for additional gas resources, it is possible to project future production trends for the Wardner lease study area using the results of the infield drilling and recompletion program. Between 1979 and 1990, the greatest magnitude of infield activity occurred in the period from 1986 to 1990, when 60 new wells were drilled in the Wardner lease study area. Overall, between 1979 to 1990, a total of 143 primary and recompletions accounted for 30 Bcf of reserve growth production. The remaining post-1990 gas reserves from these 143 completions is projected as 18 Bcf; 12 Bcf from shallower than 7,000 ft and 6 Bcf from deeper than 7,000 ft (figs. 20 and 21).

Well histories of the initial development wells within the study area indicate that an average of six shallower pool completions were achieved in the middle Frio reservoirs above a typical 8,000 ft lower Frio to Vicksburg test for wells drilled before 1979. The recent post-1978 wells have two or more completions in the G- and F-series as of 1990. A reasonable projection

for infield development between 1990 and 1999 of the 60 post-1978 infield wells estimates an additional 4 successful recompletions, for a total of 240 future recompletions within the middle Frio stratigraphic interval. Using a conservative EUR of 75 MMcf per completion, an additional 18 Bcf of probable reserve growth is calculated for the Wardner lease study area from 240 projected recompletions from 1990 to 1999.

A composite analysis of reserve growth for the Wardner lease study area, spanning the period from 1970 to 2009, is developed by combining past production and projections of future recoverable resources (fig. 22). Results of this analysis demonstrate that a projection of more than 65 Bcf of gas reserves should be added after 1979 in the study area, where production was previously established over 40 years ago. This projection for reserve growth is in close agreement with a volumetric analysis of the uphole potential for the study area. Using a 60 percent recovery factor for the reservoirs in the E- and D-series above the large E-41 reservoir, a total of 19 Bcf is undeveloped remaining reserves. For the Wardner lease study area, a total reserve growth of 67 Bcf from middle Frio reservoirs is derived from the production of 30 Bcf, proved reserve growth of 18 Bcf, and potential reserve growth from uphole recompletions (undeveloped remaining reserves) of 19 Bcf.

This reserve growth analysis focuses on the gas resources that can be converted to reserves from the uphole completions in the middle Frio reservoirs. Additional reserve growth potential of deeper pool objectives associated with structural complexity or by additional recovery from the currently partially depleted low-pressure reservoirs would also provide a secondary natural gas resource.
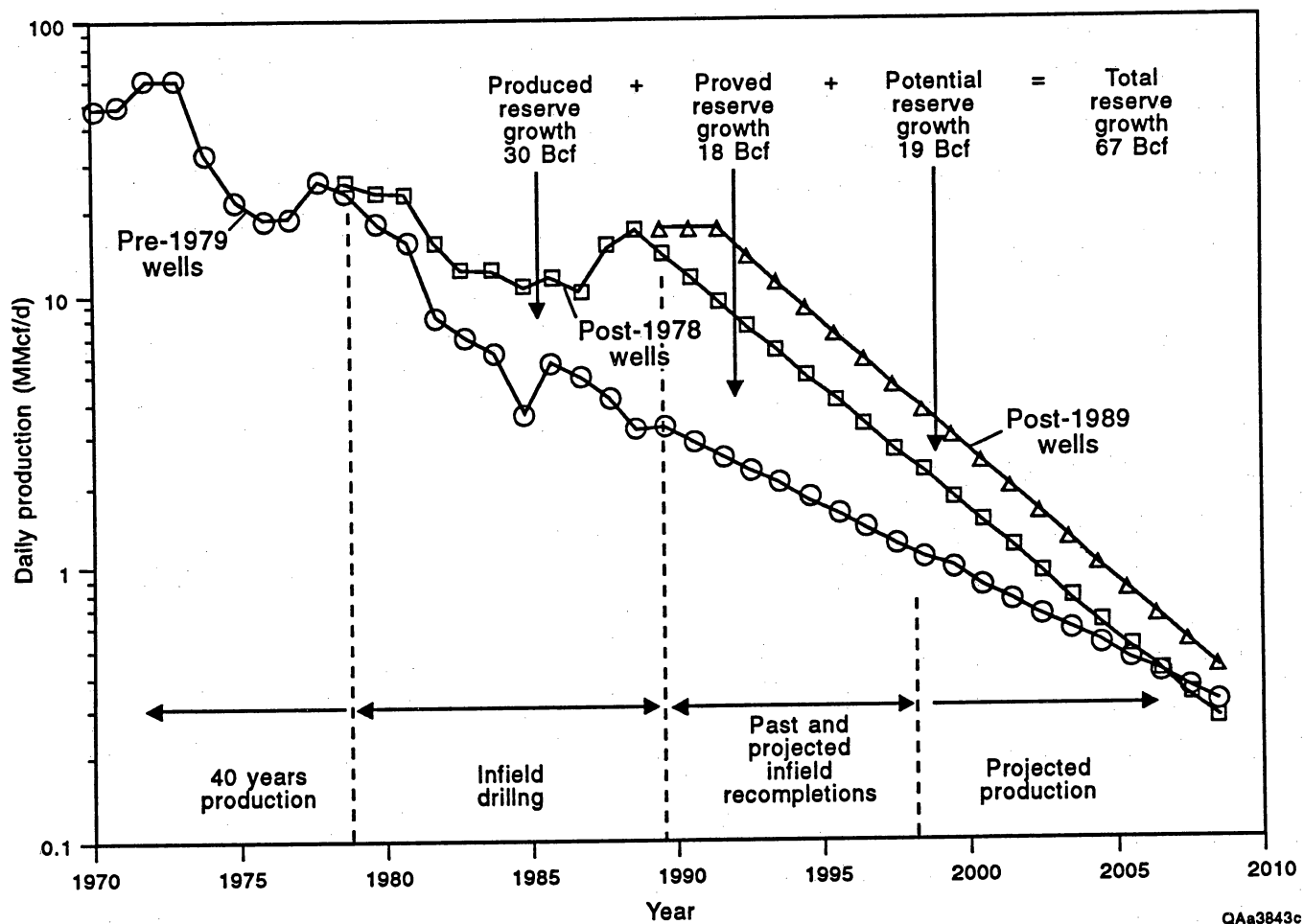
Figure 22. Historical production and projections of rate versus time for the Wardner lease study area.

DELINEATION OF RESERVOIR COMPARTMENT SIZE CLASSES

Compartment Size Distributions in 10 Reservoir Groups

A study of production histories from 256 completions in 10 reservoir groups delineated 3 classes of reservoirs characterized by large, medium, and small mean reservoir compartment size. The statistical distributions of primary compartment pore volume and intercompartment transmissibility were found to be closely approximated by log-normal distributions in each of the 10 reservoir groups. These statistical distributions can serve as a basis to evaluate probable recovery resulting from infill development in conventional permeability compartmented gas reservoirs. These statistics from the Stratton–Agua Dulce middle Frio reservoirs are unique and can provide a quantitative basis for comparison between reservoirs, fields, and plays if similar data are obtained in the manner described here.

The SGR project has clearly demonstrated that it is possible to determine, from individual well production data, functional reservoir parameters of primary drained pore volume, or compartment size, supporting pore volume, and barrier transmissibility in a reservoir by using the G-WIZ compartmented gas reservoir simulator. G-WIZ is a personal-computer-based gas reservoir evaluation tool developed by the SGR project; it was described in a previous topical report (Lord and Collins, 1991).

Production histories were analyzed to quantify functional parameters relating to compartmented behavior in a spectrum of fluvial reservoirs to provide a basis for comparison between reservoirs, fields, and plays if similar data are obtained. The SGR project developed an extensive production data base from the greater Stratton and Agua Dulce field areas for evaluating reserve growth and compartmented reservoir behavior. The pressure and production histories from 584 completions in this data base were reviewed, and from this group 256 completions were selected as having data suitable for evaluation using the G-WIZ simulator. These 256 production histories were divided into 10 reservoir groups that include 2,000 ft of

the middle Frio section and represent the spectrum of fluvial reservoirs at Stratton–Agua Dulce. Stratigraphic positions of the 10 reservoir groups are indicated on a type log shown in figure 23.

The effective permeability to gas in most of the middle Frio reservoirs is 10 to 100 md from analysis of pressure transient and deliverability tests. Some of the reservoirs in the D- and E-series have lower effective permeability, 1 to 10 md. Some completions in these lower permeability reservoirs have been stimulated by hydraulic fracture treatment during completion operations.

Stratigraphic analyses based on well log correlations indicate that 37 unique operational reservoirs are in the middle Frio section over an interval of approximately 2,500 ft. The 10 reservoir groups were selected from these 37 operational reservoirs by the following criteria:

(1) There were a sufficient number of active completions since 1966 to allow a reliable representation of the reservoir group. The number of completions in each group ranged from 7 to 43.

(2) Certain reservoirs were attributed as having a significant portion of reserve appreciation since 1979, documented in the SGR project analysis of reserve growth in the Wardner lease.

(3) Certain reservoirs had produced significant reserves in prior development phases (pre-1979), but were found to have had minimal reserve growth since 1979 in the Wardner lease.

(4) The selected reservoir groups represent the spectrum of fluvial depositional styles of the middle Frio in the Stratton–Agua Dulce field area.

Fluvial Architecture Spectrum

Numerous characterizations of fluvial depositional environments based on morphological form of surface deposits, internal arrangement of bedding or vertical facies and grain-size profile of the sediment, and variations in discharge patterns, slope, or gradient have been proposed to explain the variation in depositional style or facies architecture of sediments deposited by
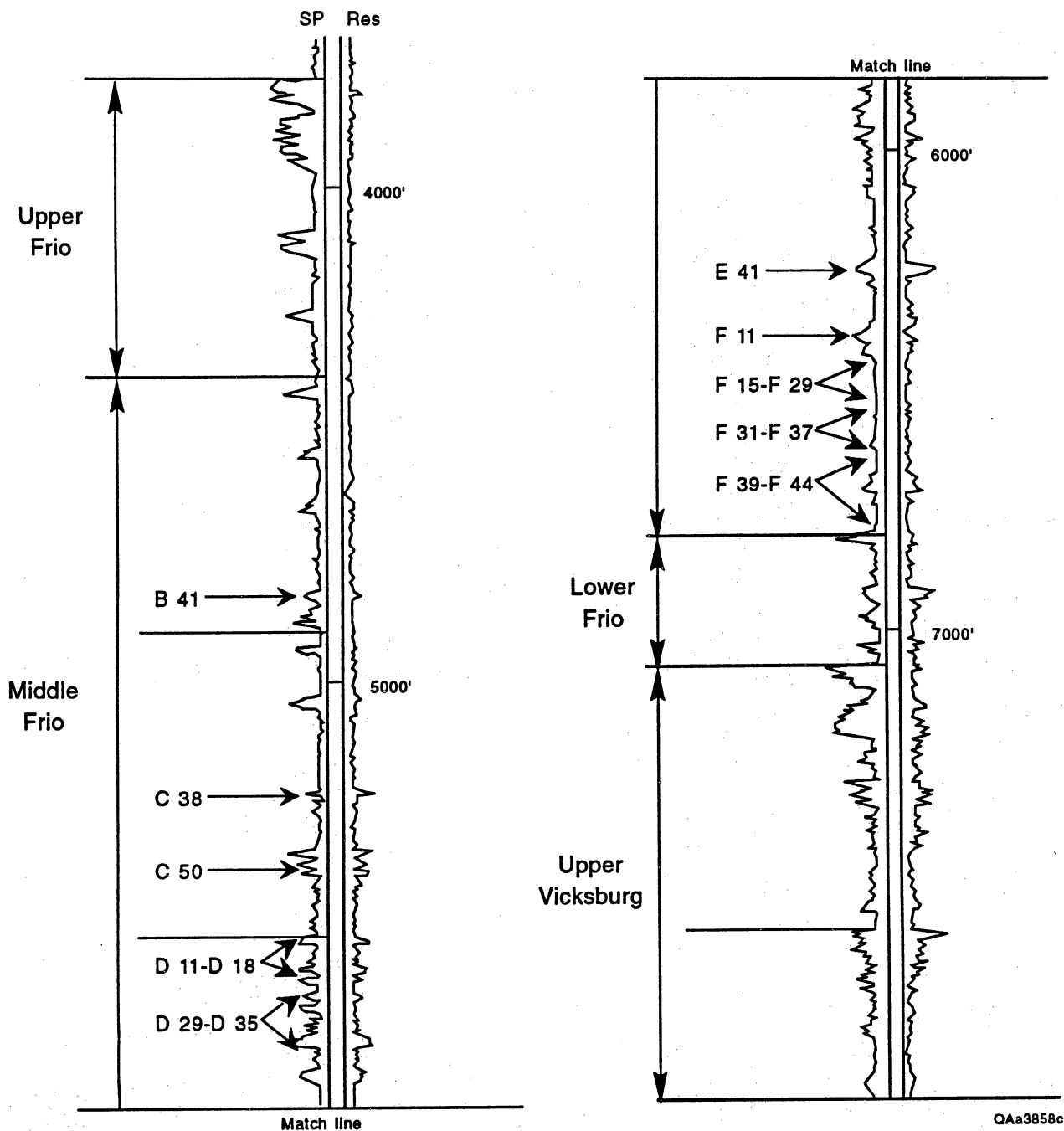
Figure 23. Type log illustrating the stratigraphic position of the 10 reservoir groups. Reservoir nomenclature developed by gas operators in Nueces and Kleberg counties (modified from Kling, 1972; Kerr, 1990). Well is the Union Producing Co. No. 7A Driscoll.

channelized flow. Well log correlations in cross section through the middle Frio stratigraphic interval of the FR-4 gas play in South Texas indicate that the gas reservoirs in Stratton, Seeligson, and Agua Dulce fields are characterized primarily by sandstone bodies of channel-fill and splay deposits. Fluvial reservoirs at Stratton–Agua Dulce (Kerr and Jirik, 1990) are ranked in character from less to more compartmented as (1) thick, broad-channel amalgamated sandstones (laterally stacked), (2) mixed-load channel sandstones, and (3) thin, narrow-channel dispersed sandstones (vertically stacked). Figure 24 diagrammatically shows the progression of compartmented fluvial reservoir development. The most compartmented gas reservoirs are the narrow fluvial channel sandstones. The least compartmented reservoirs are the thick sandstones deposited in broad channel systems.

Each reservoir group exhibits a log-normal distribution of primary drained pore volume, as shown in figure 25. The logarithm of primary drained pore volumes from the compartment model results are plotted with cumulative frequency on a normal probability scale. The straight line through these data defines a normal distribution of the logarithm of volume or a log-normal distribution. Since a log-normal distribution is defined by specifying only two parameters, the geometric mean value and the variance of the log value about this mean, the reservoir statistics are summarized in terms of only a few parameters.

The barrier transmissibility from each of the single well evaluations from this reservoir group is plotted in a similar fashion and is shown in figure 26. A straight line through the log of transmissibility plotted with the cumulative frequency on a normal probability scale also indicates a log-normal distribution.

The pore volume and transmissibility data shown in figures 25 and 26 are from a reservoir group that comprises several reservoirs that are vertically stacked, narrow-channel dispersed sandstones with typical widths of 0.25 mi and net productive thicknesses of 10 ft or less. These sandstones are separated vertically by shales approximately the same thickness as the reservoir sandstone, and lithologic correlations between adjacent well pairs are often difficult. Completions made in these reservoirs have frequently encountered undepleted pressures and
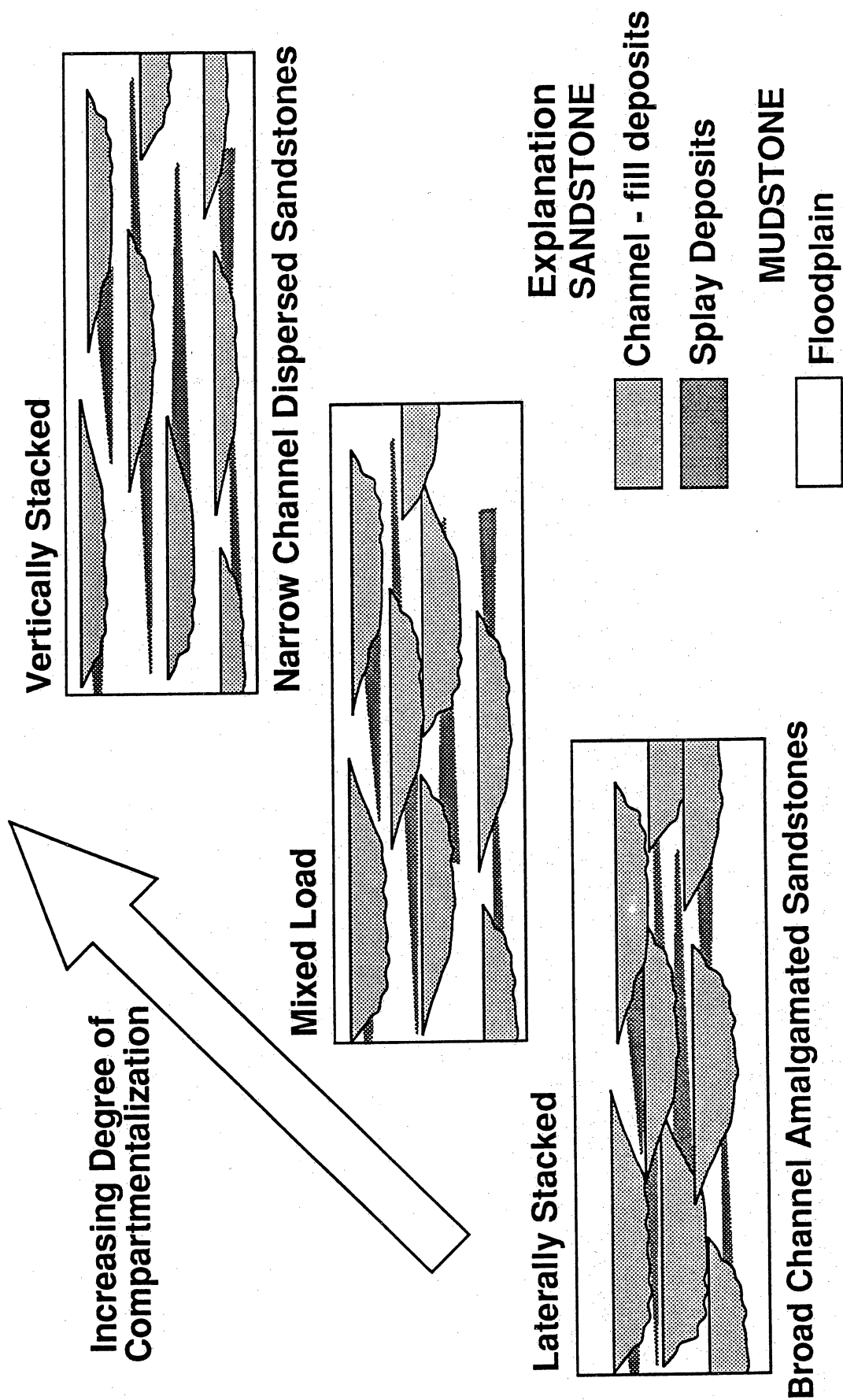
Figure 24. Schematic diagram illustrating the fluvial architectural continuum (modified from Kerr and Jirik, 1990).
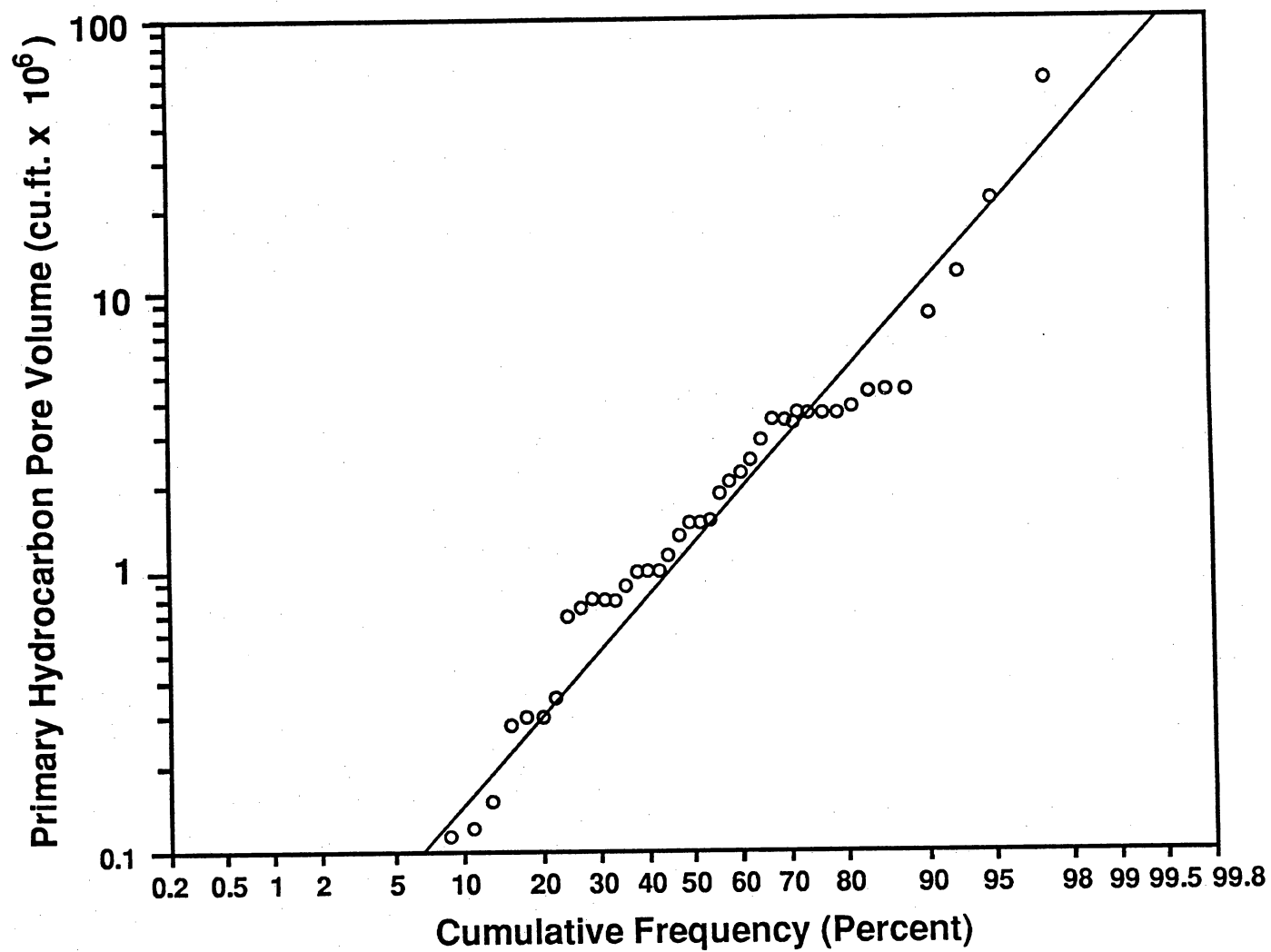
Figure 25. Cumulative frequency distribution of primary compartment volumes for the F-15 to F-29 reservoirs, Stratton field.
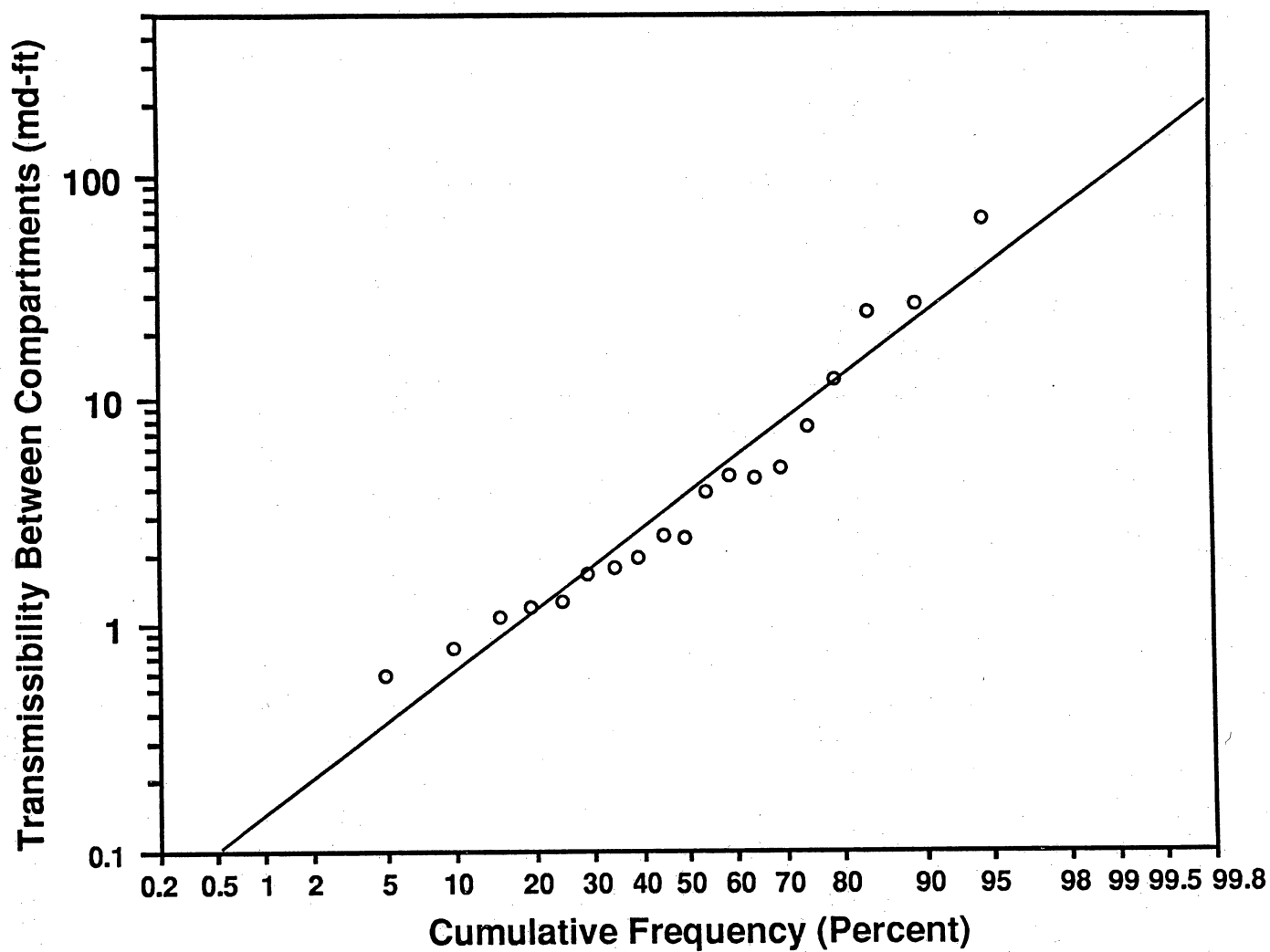
Figure 26. Cumulative frequency distribution of compartment transmissibilities for the F-15 to F-29 reservoirs, Stratton field.

contributed greatly to reserve growth since 1979 in the Wardner lease reserve growth study. The SGR project performed two transient well tests in the F-21 reservoir of this group and found the near-well permeability to range from 30 to 100 md.

Distributions of primary drained pore volume from the 256 completions divided into the 10 reservoir groups are shown in figure 27. The range of distributions represents the variation of mean compartment size in the fluvial reservoirs at Stratton–Agua Dulce. Distributions of transmissibility for the 10 reservoir groups exhibit a similar pattern.

From the single-well analyses of the Stratton–Agua Dulce wells using the G-WIZ model, the 10 reservoir groups were divided into three compartment size classes. These reservoir classes were defined by the frequency distribution of primary compartment size. The cumulative distributions of compartment volumes for reservoir groups representing the large, medium, and small mean volume classes are shown in figure 28, and the corresponding cumulative distributions of barrier transmissibilities are shown in figure 29. The values of the geometric mean of compartment volume and the associated compartment volumes at plus and minus one standard deviation about this mean are shown for each compartment size class in table 2. Similarly, the values for barrier transmissibility at the geometric mean and plus and minus one standard deviation and shown on figure 29 are listed in table 3. Since a log normal distribution is defined by the geometric mean value and the variance of the log value about this mean, the production behavior of the fluvial reservoir at Stratton–Agua Dulce is summarized in terms of these few parameters.

Predictably, there is a strong correlation between the compartment size class and fluvial facies architecture shown in figure 24. The thick, broad-channel amalgamated sandstone reservoirs are associated with the large compartment size class. The vertically dispersed, narrow-channel sandstone reservoirs are associated with the small compartment size class.

The statistics of net perforated thickness were collected from the wells evaluated in this study and were found to range from about 5 to 50 ft. The net perforated thickness of each completion is shown in a log-log plot with the corresponding primary compartment volume in

58
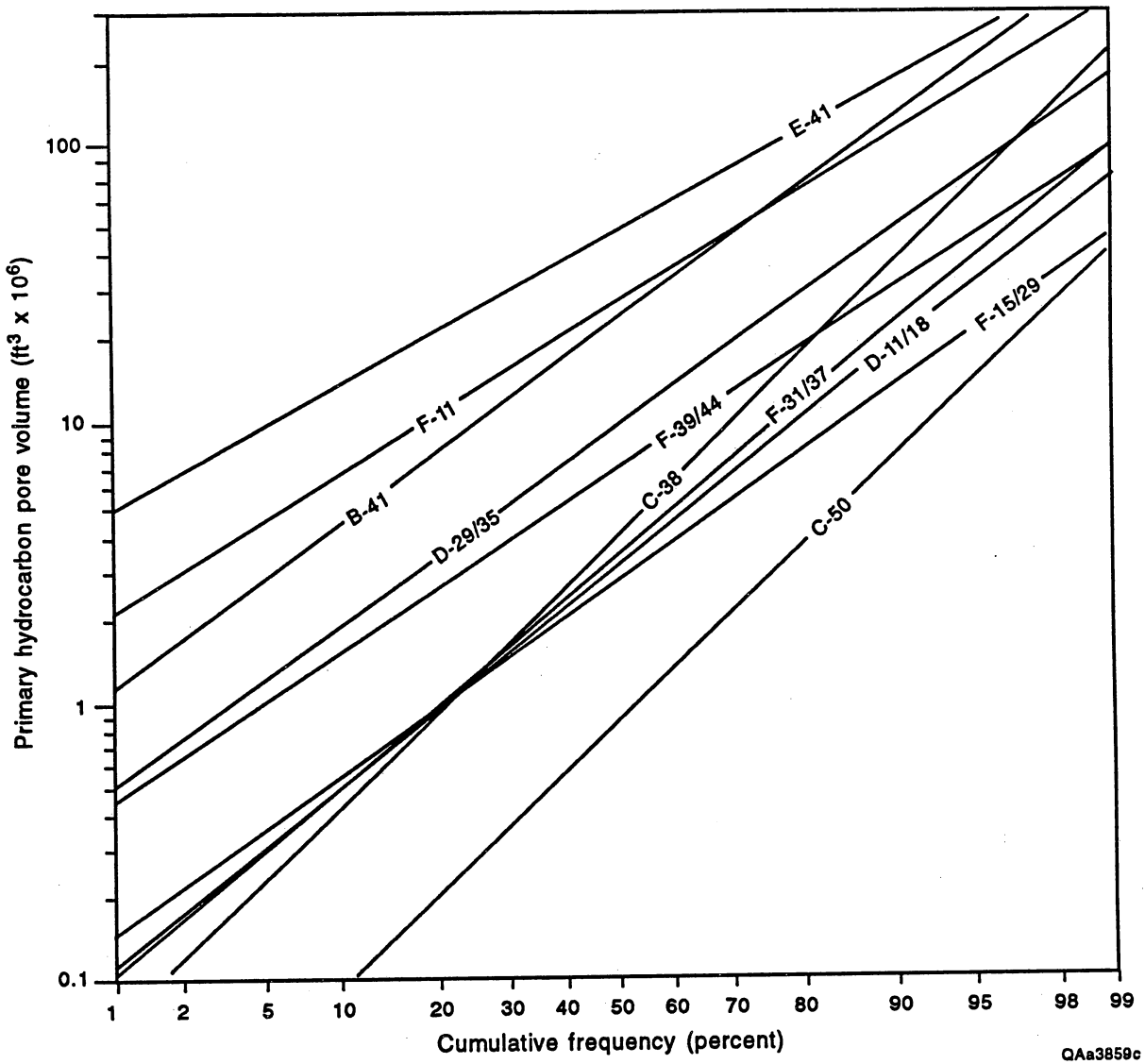
Figure 27. Cumulative frequency distribution of primary pore volume for the 10 reservoir groups in Stratton field.

Table 2. Volume statistics for each compartment size class.

Compartment size class	Geometric mean volume (ft³) E6	Mean plus 1 std. dev. (ft³) E6	Mean minus 1 std. dev. (ft³) E6
Large	33.3	88.8	12.5
Medium	9.7	32.6	2.9
Small	2.9	9.6	0.9

Table 3. Transmissibility statistics for each compartment size class.

Compartment size class	Geometric mean (md-ft)	Mean plus 1 std. dev. (md-ft)	Mean minus 1 std. dev. (md-ft)
Large	44.3	191.0	10.3
Medium	25.3	70.0	9.1
Small	5.7	19.5	1.7

figure 30. There are two trends of increasing thickness with primary drained pore volume. One trend is for the large compartment size class reservoirs and the other is for the small and medium compartment size class reservoirs. The trends indicate that a primary drained pore volume in a large compartment size class reservoir is likely to have a smaller corresponding net thickness for the same compartment volume in a small or medium class reservoir. This is consistent with the geologic model and fluvial architecture shown in figure 24. The broad-channel amalgamated sandstone reservoirs are more likely to have compartments that are large in areal extent. For the same primary drained pore volume in each compartment size class, the large class compartment has a larger area and therefore would have a smaller average thickness.

Fluvial reservoirs at Stratton–Agua Dulce are described and quantified with only a few functional parameters: primary drained pore volume (compartment volume), barrier transmissibility, and net thickness. Stratton–Agua Dulce fluvial reservoirs have been divided into three classes according to these functional parameters. These statistics from middle Frio reservoirs at Stratton–Agua Dulce are unique and provide a quantitative basis for comparison between reservoirs, fields, and plays for reserve appreciation from infield development.

G-WIZ Study Description

In the G-WIZ compartmented gas reservoir simulator described by Lord and Collins (1991), the reservoir is seen as being composed of one or more porous, permeable compartments with flow between compartments through low-permeability barriers or baffles. The G-WIZ model is a functional, as opposed to anatomical, model that requires a minimum of reservoir description. Typically, certain compartments are produced while other compartments are unproduced except by flow through compartment baffles. The G-WIZ compartmented gas reservoir simulator calculates the average pressure response of each compartment for any assigned rate or pressure drawdown history. The model does not represent near-well transient behavior and is limited to applications in conventional permeability reservoirs where transient behavior lasts
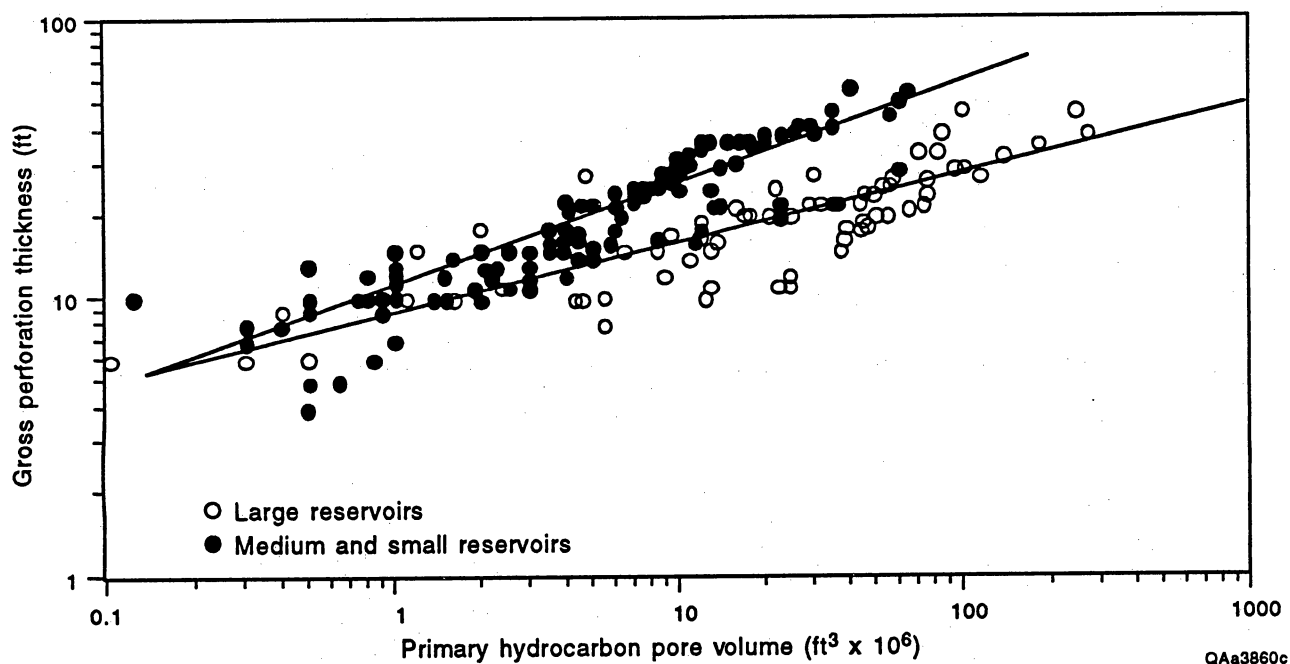
Figure 30. Graph of primary hydrocarbon pore volume versus gross perforation thickness in Stratton field.

several days or less. Under these conditions, monthly production data and conventional 24-hr shut-in pressure measurements are suitable for analysis by the G-WIZ model.

Field data (production rate and static pressure) can be history-matched by adjusting model parameters of compartment pore volumes and barrier transmissibilities until the model response agrees with the reported production and pressure data. Typically a simulation is performed with a two-compartment description of the reservoir surrounding a well, one being directly drained and the other being a supporting volume. The actual supporting volume may consist of multiple compartments that may not have similar pressures. These noncontiguous compartments can affect the performance of a single well as if there was only one supporting compartment and intervening flow baffle. Finite-element simulations of example cases have been performed to show that in a multiwell, multicompartment system, treating each well simulation as a two-compartment system yields an excellent estimate for the primary compartment volume and associated barrier transmissibility.

The most favored method of performing a simulation history match is to use the reported monthly production data as input in a single-well, two-compartment model and allow the model to predict the average pressure in each compartment. The pore volume of each compartment and barrier transmissibility are adjusted until the simulation matches the reported shut-in static pressure data with the pressure predicted for the primary compartment. The early decline of pressure with time and cumulative production is controlled by the primary drainage volume. The late-time decline of pressure is affected by the supporting compartment volume and the barrier transmissibility. An extended production history with sufficient static pressure data allows an effective determination of all three parameters.

In the example shown in figure 31, the production rate data were used as input. The compartment pore volumes and barrier transmissibility are changed to match the declining trend of the static pressure. The predicted pressure of the supporting compartment is also matched in this example by a nearby well completed in the same reservoir very late in the life of the first well. Another well was completed near the first well and is indicated to be in the

65
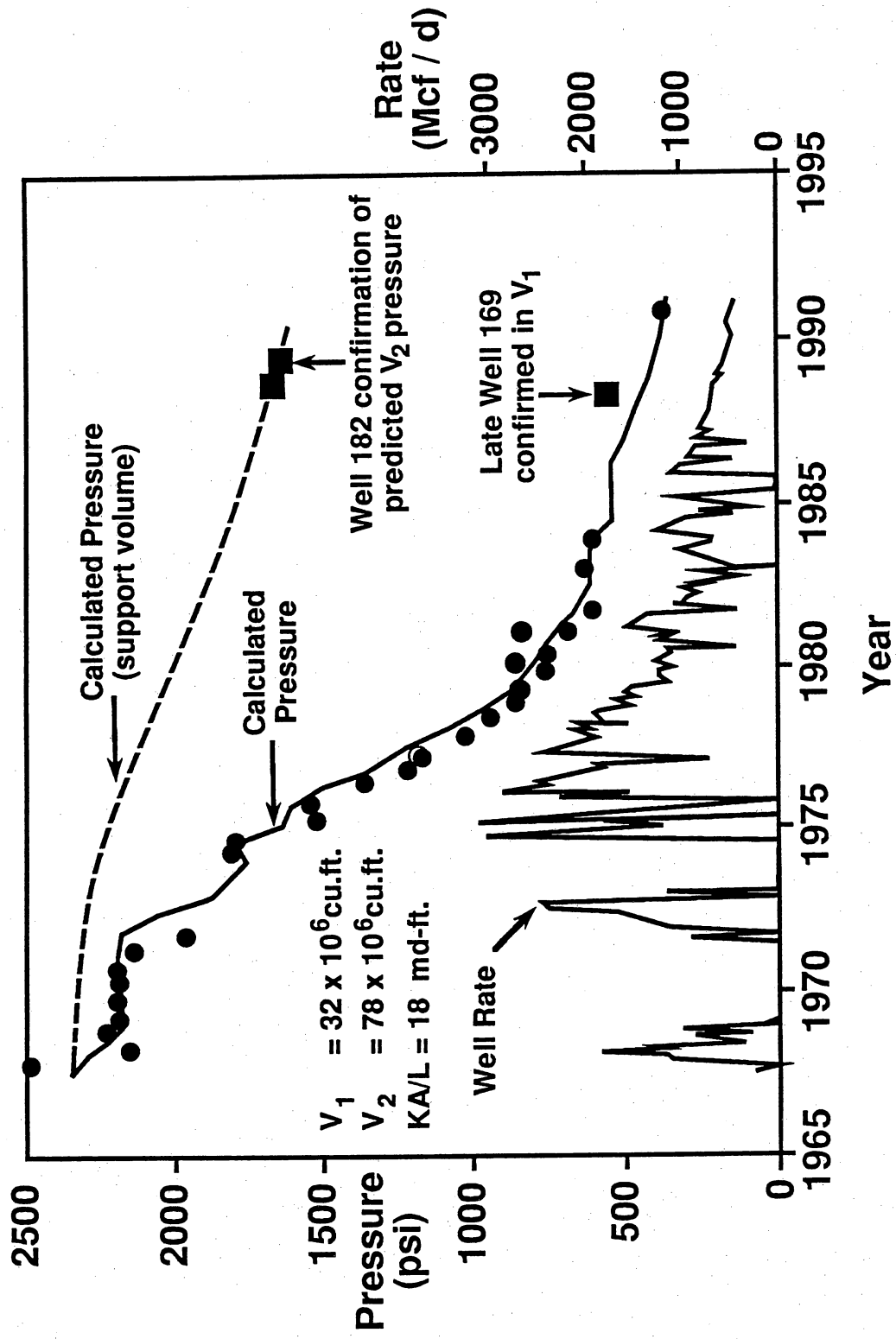
Figure 31. Pressure history match for the Wardner No. 80 in the F-39 reservoir interval using the G-WIZ compartmented gas reservoir simulator.

primary drainage volume of the first well. These two nearby wells are both approximately 0.25 mi from the first well. This two-compartment simulation approach was applied to the 256 completions in the 10 reservoir groups.

CHARACTERISTICS AND EXAMPLES OF LARGE, MEDIUM, AND SMALL FLUVIAL RESERVOIR COMPARTMENT SIZE CLASSES

Large Compartment Size Class Reservoirs

In Stratton field, the B-41 (or Comstock reservoir), E-41 (or Bertram), and F-11 (or Wardner), are categorized as large compartment class reservoirs (fig. 23). The upper bound of the compartment pore volume distributions for 10 reservoir groups is shown in figure 27. These large compartment size class reservoirs were aggressively developed from about 1965 through 1980. Each of these reservoirs was utilized for gas recycling until the early 1970's, prior to the last development phase. These reservoirs exhibit some indications of reservoir heterogeneity on plots of average static shut-in pressures and the maximum shut-in pressures with time, as shown in figures 32 through 34. Investigations to identify additional reserve growth opportunities were performed for of each of these reservoirs by SGR project researchers. No reservoir heterogeneity was found that could have resulted in reserve appreciation after 1979 and at the current well spacing. The large compartment size class reservoirs were not attributed to any reserve appreciation in the Wardner lease reserve growth study from 1979 through 1989.

Future reserve appreciation from large compartment size class reservoirs will probably not be achieved by closer completion spacing to overcome the reservoir heterogeneity that has created incompletely drained portions of the field. The completion density across the field in the large class reservoirs is probably close enough to overcome most channel to channel lithologic and diagenetic heterogeneity that is developed in this class of reservoir. Future reserve appreciation will result from reservoir management and novel methods to lower the average reservoir pressure from current levels of 200 to 300 psi down to less than 100 psi. Completion methods that overcome or prevent serious formation damage in very low pressure reservoirs will be required.
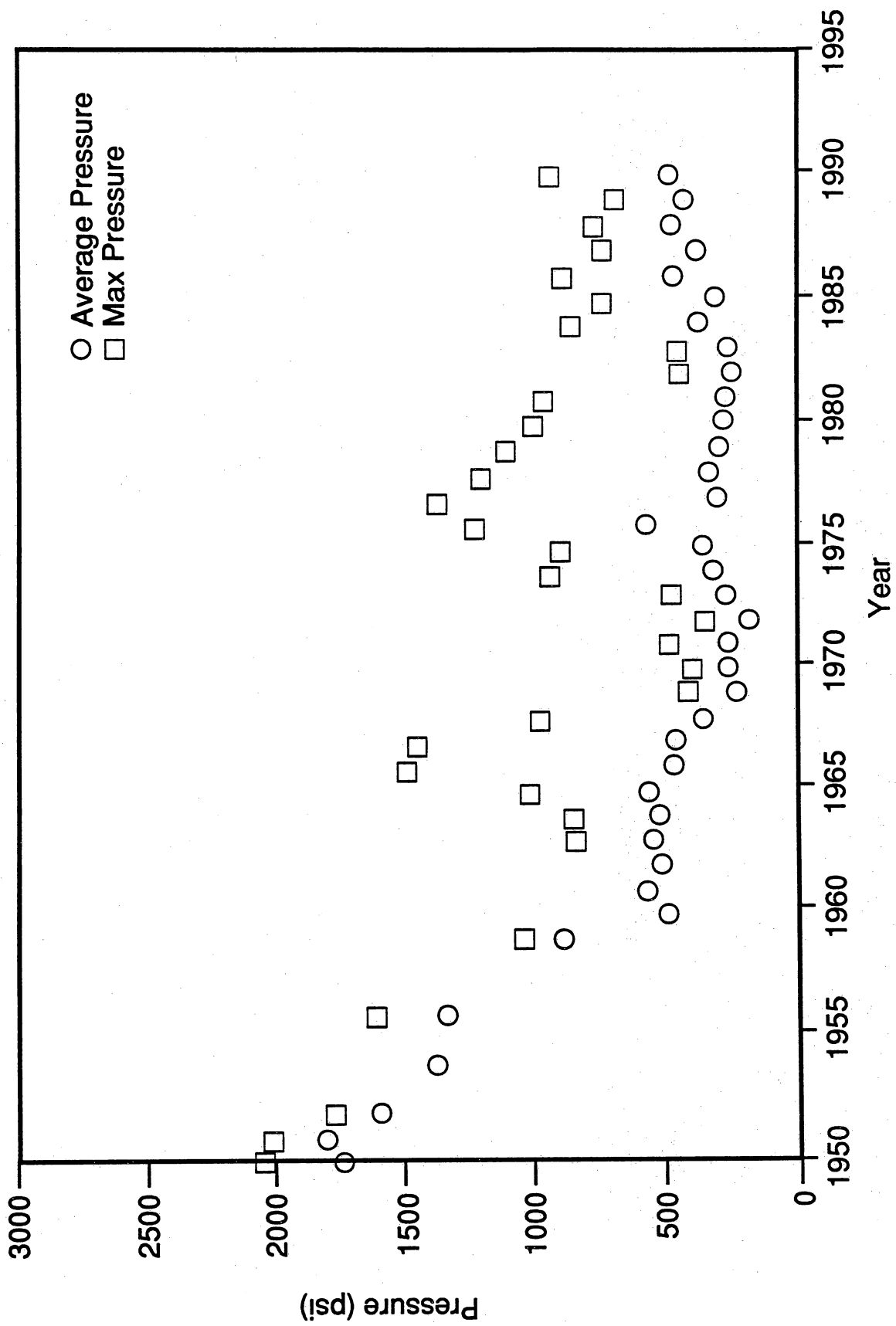
Figure 32. Pressure versus calendar year, Comstock B-41.
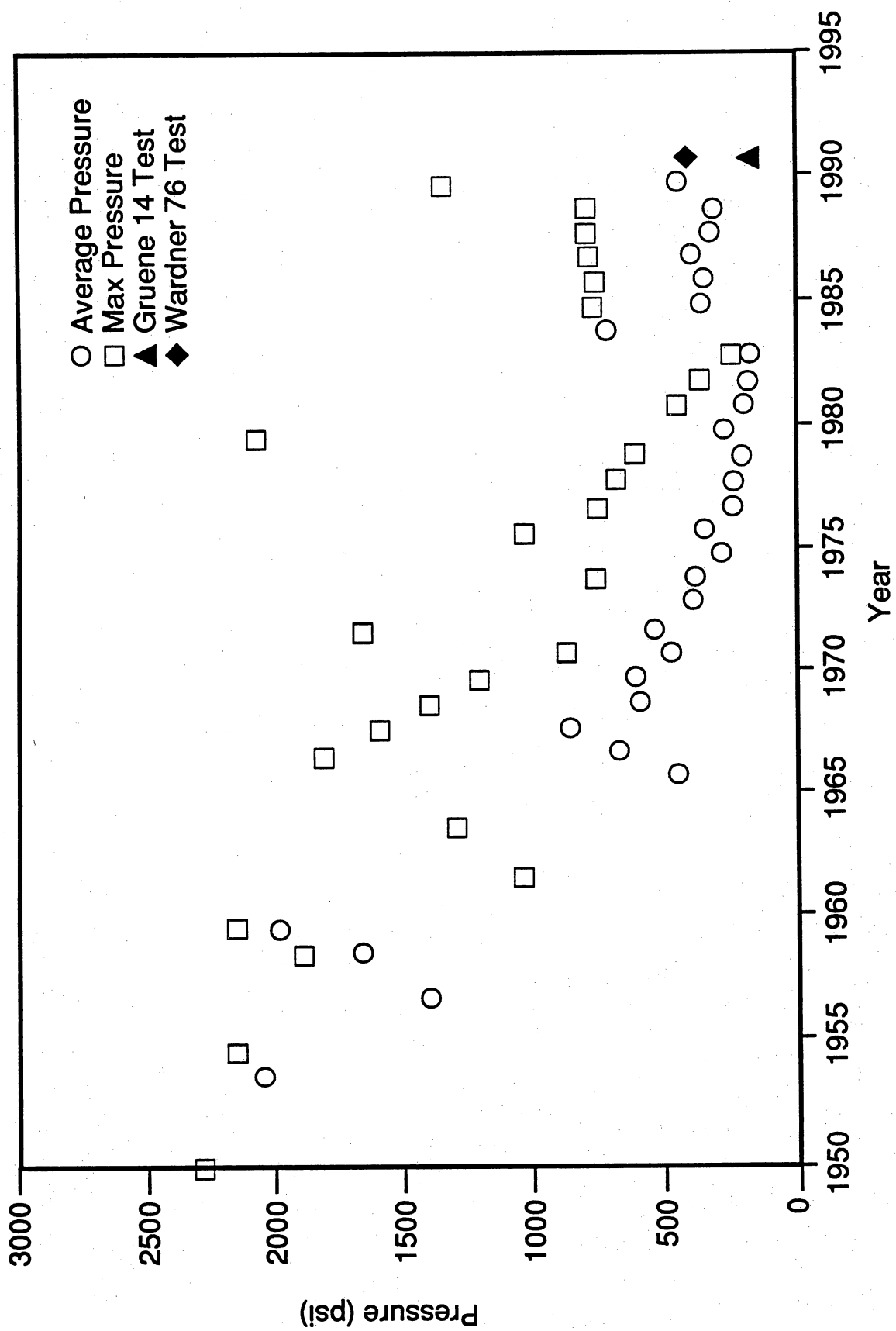
Figure 33. Pressure versus calendar year, Wardner E-41 reservoir.
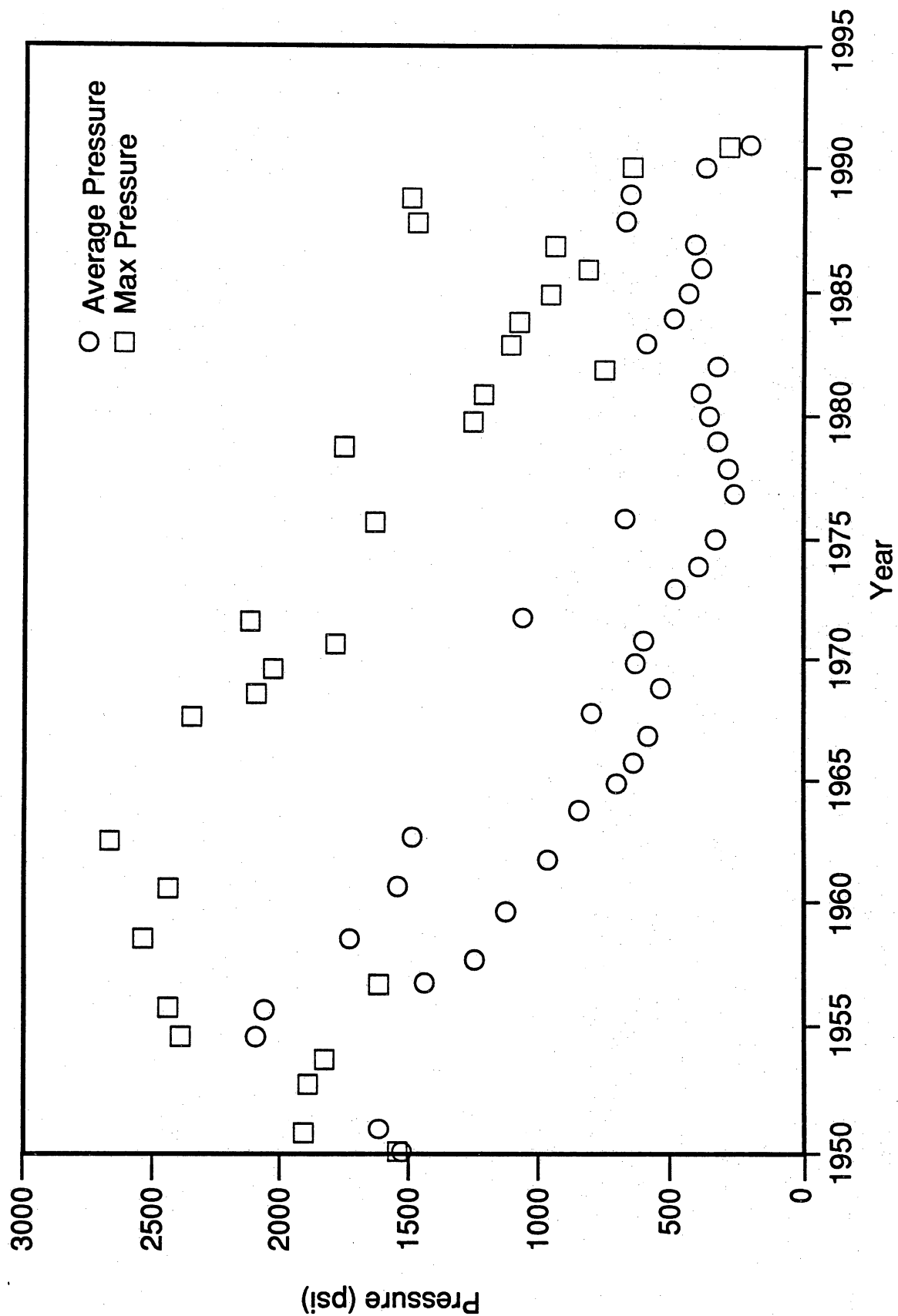
Figure 34. Pressure versus calendar year, Comstock F-11 reservoir.

71

Common characteristics of these large compartment size class reservoirs are

(1) thick, amalgamated channel-fill sandstones and multiple compound splay deposits (15 to 60 ft),

(2) large, continuous productive areas (several mi^2),

(3) high effective permeability (100 md and greater), and

(4) consistent gas-oil or gas-water contacts along the downdip limits of the reservoir.

These amalgamated sandstone reservoirs (B-41, E-41, and F-11) frequently develop gross thicknesses of up to 60 ft or more. Isopach and productive limits maps indicate that these reservoirs are nearly continuous across the greater Stratton–Agua Dulce field complex, approximately 14 mi long and 4 mi wide. In each of these reservoirs, potential test records of the wells completed in the 1940's with near-original pressure show calculated absolute open-flow (CAOF) rates that average 50 MMcf/d, and some rates are 100 MMcf/d, or higher. Hypothetical isochronal tests performed with an analytical reservoir simulator indicate that effective gas permeabilities from 10 to 100 md are necessary to achieve these CAOF rates (without turbulence or skin) for simulated original conditions of the E-41 (Bertram) reservoir. The average cumulative production is 6.0 Bcf per well from 194 completions in these large compartment size class reservoirs. The current completion spacing for wells completed in these three reservoirs averages 113 acres, with 84 percent (mean spacing plus one standard deviation) of completions at a spacing of 230 acres or less in the Stratton–Agua Dulce field area.

Typical reservoir petrophysical parameters were obtained from computed well logs using porosity values greater than 15 percent and formation water saturations lower than 70 percent. The average porosity is 21 percent and is not highly variable. The bulk water volume varies from 10 to greater than 13 percent, and this value is interpreted to be the irreducible bulk volume of water for the E-41 reservoir. Average reservoir sandstone thickness is approximately 22 ft, with net pay values that range from 8 to 13 ft. The sandstone reservoir is slightly shaly with an average bulk volume of shale of 6 percent. Computed petrophysical parameters for individual wells in the Gruene lease SGR project experiment site include porosity, water

72

saturation, volume of shale, net thickness, and bulk volume of water (appendix table 3–4).
Similar petrophysical attributes are indicated for wells penetrating the F-11 reservoir and are
listed in appendix table 3–5.

Large Compartment Size Class Example: E-41 (Bertram)

The distribution of the E-41 gas reservoir across the Stratton–Agua Dulce field area is shown
in figure 35. The area of review covers approximately 20,000 acres. Average completion spacing
in the E-41 reservoir is 108 acres, with 84 percent at a spacing of 190 acres.

Production records of 81 wells completed in the E-41 at Stratton–Agua Dulce indicate a
cumulative gas production of 461.9 Bcf. Some of this gas production is recycled gas. A total of
320 Bcf is reported as recycled injection. The average cumulative production per well for
75 wells with more than 10 MMcf is 6.5 Bcf, and the maximum cumulative production from
several wells was reported to be nearly 35 Bcf per well. Production records indicate CAOF rates
for completions in this reservoir, when the pressure was near original, were on the order of
10 to 100 MMcf/d.

An SGR field experiment was performed in 1991 at the Gruene lease (fig. 14) to
investigate heterogeneity and apparent pressure anomalies in the E-41 reservoir. This reservoir
was penetrated on the Gruene lease by several new wells drilled to deeper pool objectives in
1988. Wireline formation pressure tests taken in the E-41 reservoir found five wells with
relatively high pressures from 620 to 1,749 psi and five wells with expected depleted pressures
from 143 to 235 psi. These wells are within an area of 1 mi^2 (fig. 36). The experiment
investigated potential pressure variation in crosscutting channel sandstones (fig. 37). The
Gruene 14 was selected for testing because this well had a reported pressure of 1,749 psi from a
wireline formation test. After perforation the E-41 interval pressure was measured with a
bottomhole gauge and found to be 183 psi after 72 hr. The anomalously high pressures recorded
by wireline tools in wells drilled in 1988 were concluded to be false and caused by high drilling-
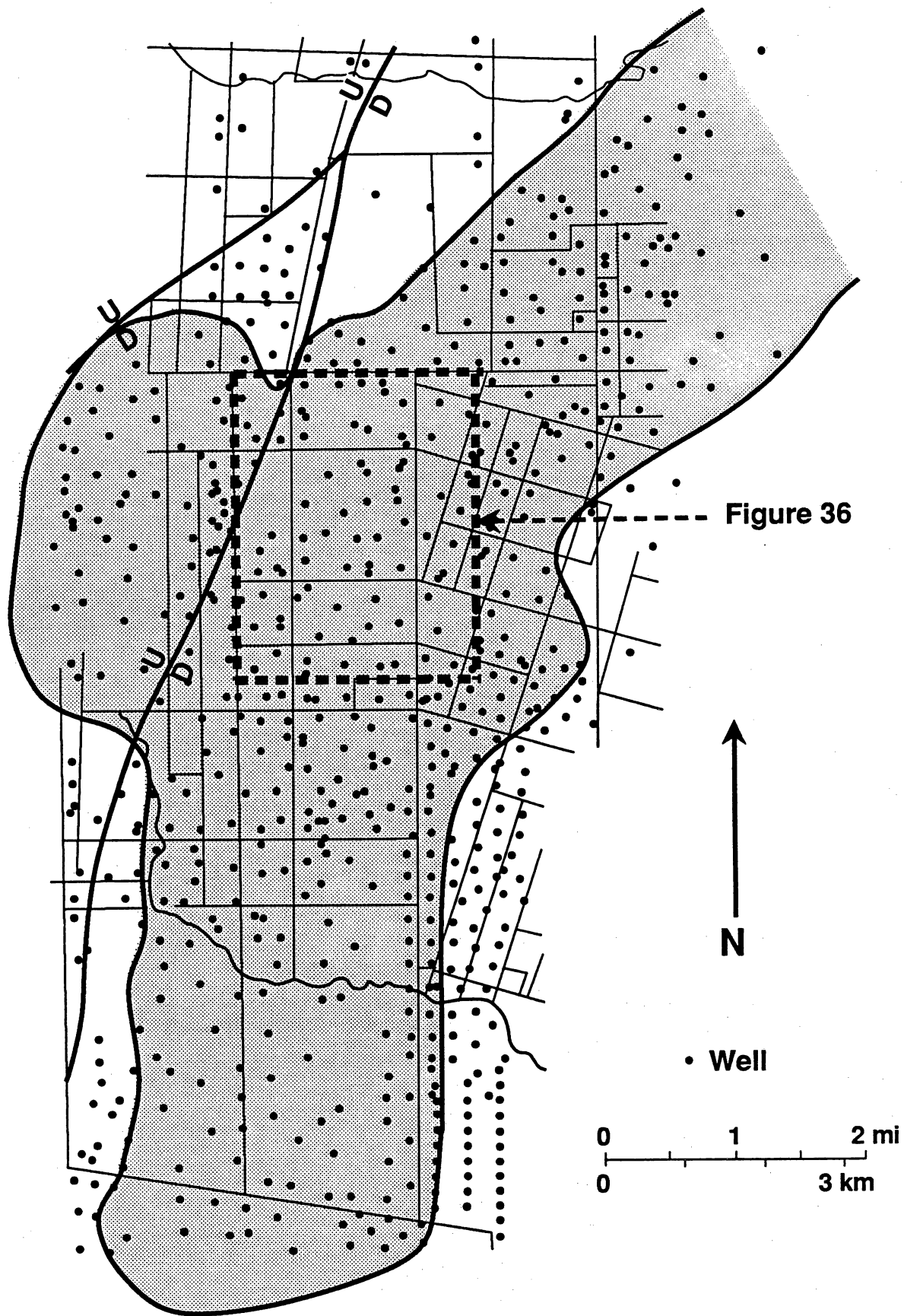
Figure 35. Map distribution of the E-41 reservoir in Stratton-Agua Dulce fields.

A   1985 WPT 200 psi

B   1982 WPT 235 psi

C   1982 WPT 960 psi

D   1988 WPT 275 psi

E   1988 WPT 1057 psi

F   1988 WPT 1749 psi

G   1985 WPT 143 psi

H   1988 WPT 182 psi

I   1988 WPT 620 psi

0   5000 ft

▨ Channel fill   ☀ Completed in reservoir zone

▥ Levee   o Well

▦ Floodplain

BEG/GRI
QA 16280c
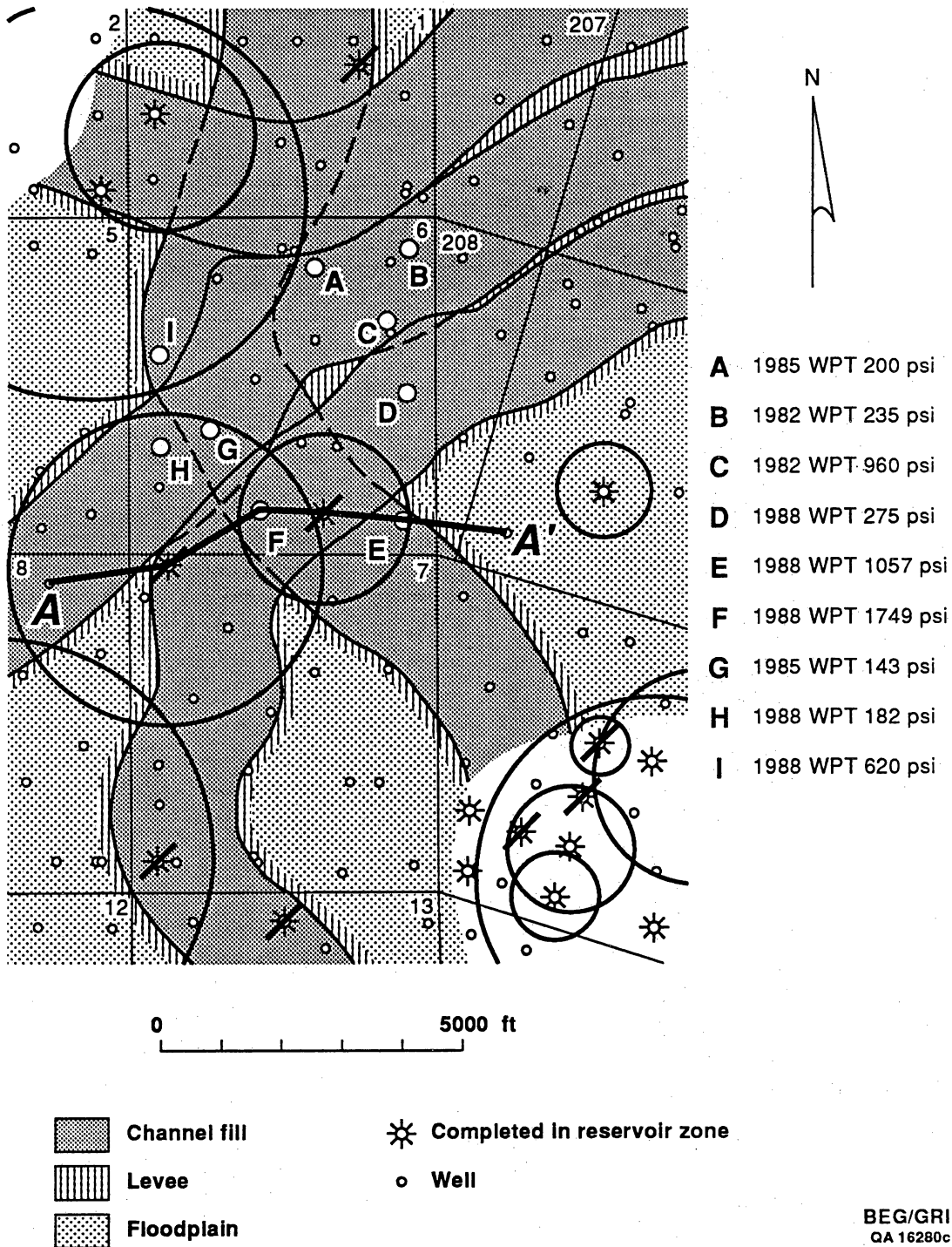
Figure 36. Map of the E-41 reservoir facies in the SGR project experiment site in the Gruene lease.

75
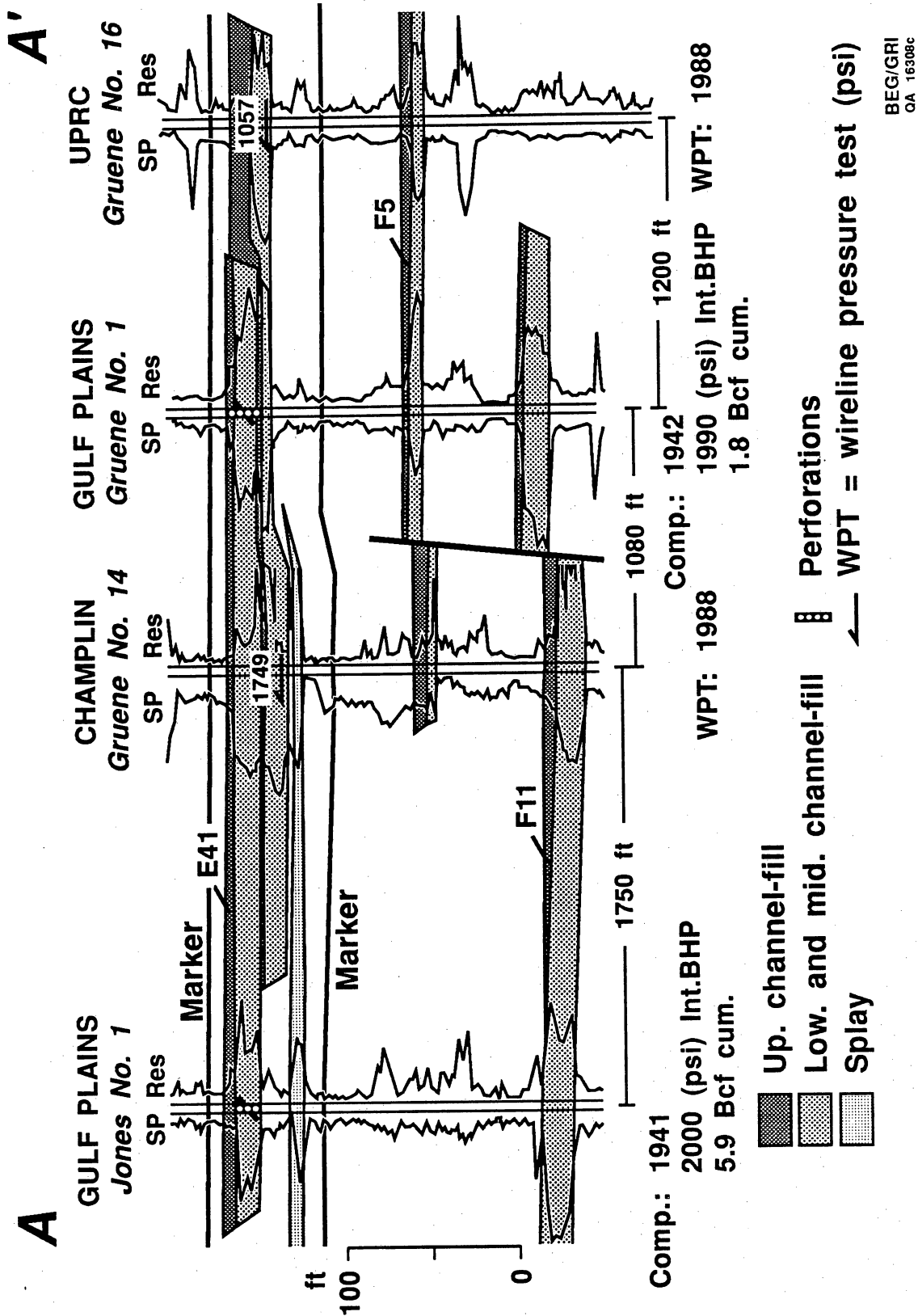
Figure 37. Stratigraphic cross section of the E-41 reservoir facies in the SGR project experiment site in the Gruene lease.

76

mud weights, test tool problems, and inadequate test procedures. The static pressure measured by this test is on trend with average static pressure of the E-41 reservoir (fig. 33).

The E-41 was also tested at the Wardner 76 well to evaluate vertical and lateral reservoir pressure variation. The location of the Wardner 76 well is shown in figure 14, and locations of the perforations tested are shown on the log from the Wardner 76 well in figure 38. The E-41 lower reservoir (6,321 to 6,323 ft) flowed gas at 316 Mcf/d with a flowing well-head pressure of 200 psi. The static reservoir pressure was measured by bottomhole gauge and found to be 412 psi after a 12-hr shut-in. The Wardner No. 76 well was evaluated using the cased-hole interpretation methods described in appendix 3. Gas production without water was evident from the computed results of the E-41 lower reservoir, which showed that the original open-hole water saturation, derived from the electric log, and the water saturation, derived from the thermal decay log (TDL, acquired in 1992), indicated no water encroachment and a minimum bulk volume of water. Gas presence was also inferred from the crossover observed between the sonic and thermal decay neutron porosities. The E-41 middle reservoir was perforated and tested after squeezing the E-41 lower reservoir perforations with cement. The E-41 middle reservoir perforations did not flow gas, and the static pressure measurement of 325 psi from this interval is inconclusive as to whether there was any significant pressure variation between the stacked channel sandstones in the E-41 reservoir. The pressures recorded from the Wardner 76 tests were on trend with the average static pressure of the reservoir (fig. 33).

Medium Compartment Size Class Reservoirs

Medium compartment size class reservoirs (D-29/35, F-39/44, and C-38) are credited with 11.3 Bcf, or 35 percent of the reserve appreciation in the Wardner lease study area from 1979 through 1989. The reserve growth is from completions made in incompletely drained reservoir compartments, even after 40 years of previous production (fig. 9).

SP   Resistivity

6050

6100

6150

6200

6250

⊡ 325 psi
6300

⊡ 412 psi

6350   ⊡ 349 psi

6400

6450

140 psi

6500

6550

E-41
Bertram

F-11
Wardner
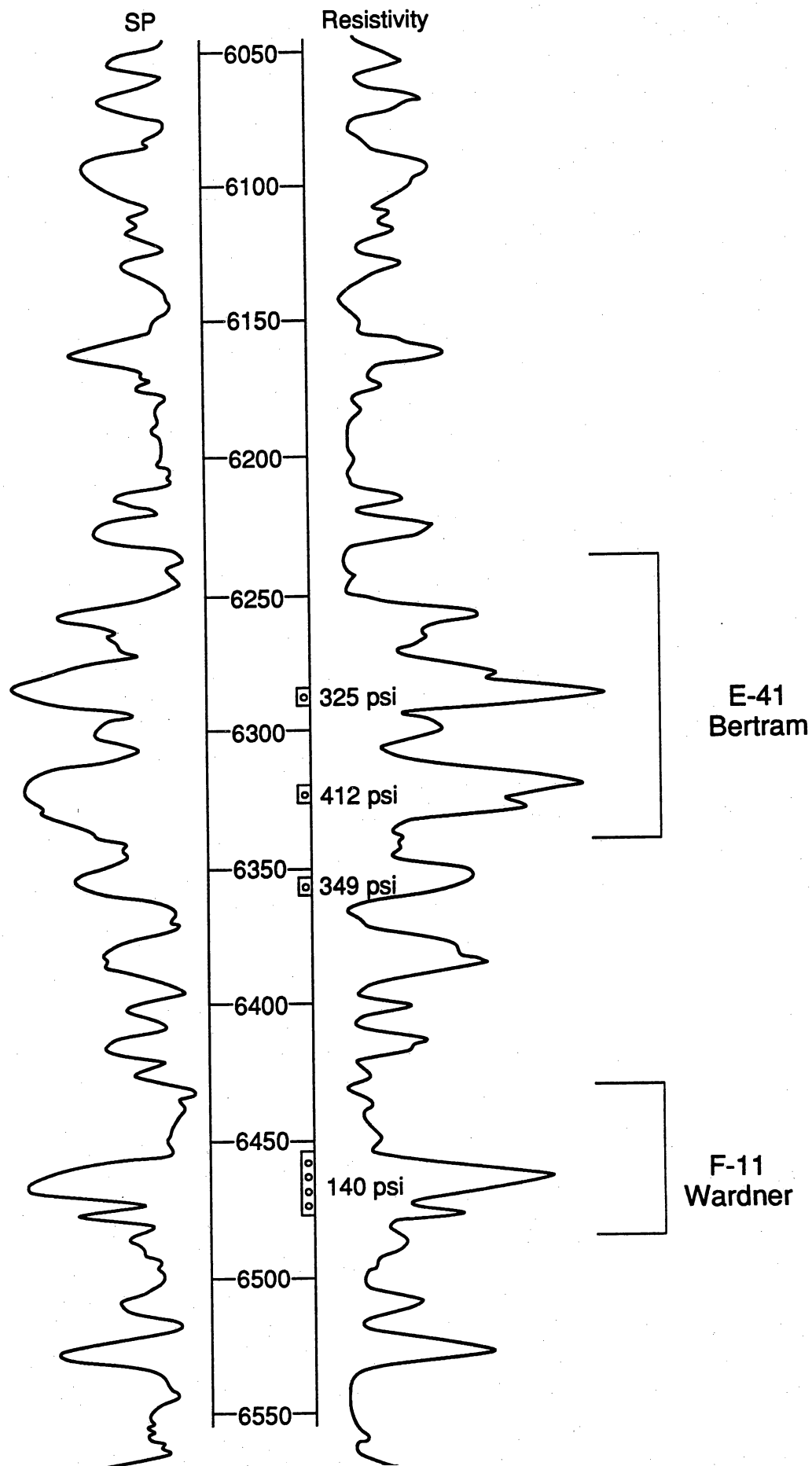
Figure 38. Spontaneous potential and resistivity log for the Wardner No. 76 well.

Permeability in the medium compartment size class reservoirs is variable and creates a condition that accounts for the pressure barriers necessary to produce incompletely drained compartments. Twenty-six transient well tests were performed by SGR project staff in these medium compartment size class reservoirs. Permeability in the better wells ranged from 10 to 100 md. However, in offset locations at distances of 0.25 mi or less, wells with similar log development and thickness were found to have permeabilities of less than 1 md. The gross thickness of medium compartment size class reservoirs is typically about 50 ft, with a net pay thickness of 15 to 20 ft. The general petrophysical characteristics of medium compartment size class reservoirs are listed in appendix table 3–6.

Medium Compartment Size Class Example: F-39 Reservoir

The F-39 reservoir has an average cumulative production of 1,400 MMcf per completion for 80 wells in the Stratton–Agua Dulce field. These 80 wells have an average spacing of 72 acres, with 84 percent spaced at less than 207 acres.

After 60 new wells were drilled in the Wardner lease study area, a significant reserve appreciation was realized in the F-39 reservoir. A reserve growth of about 6.5 Bcf is indicated from eight additional completions made in this discrete reservoir (fig. 39). Initial pressures from these completions are significantly off trend from the older F-39 wells (fig. 40). This reservoir was a target for field investigations to identify compartment barriers, drainage volumes, and shapes from transient well tests (fig. 41).

In 1979, the operator performed an extensive field study of each of the middle Frio reservoirs. From that study, the F-39 reservoir at the Wardner lease was divided into two primary reservoir areas separated by an inferred shale boundary (fig. 42). The new drilling from 1979 through 1989 increased the well control in the area of the inferred shale boundary, and F-39 sandstone was found to exist where shales were previously mapped. From 1988 through 1990, six completions were made in the area previously interpreted as nonreservoir, and
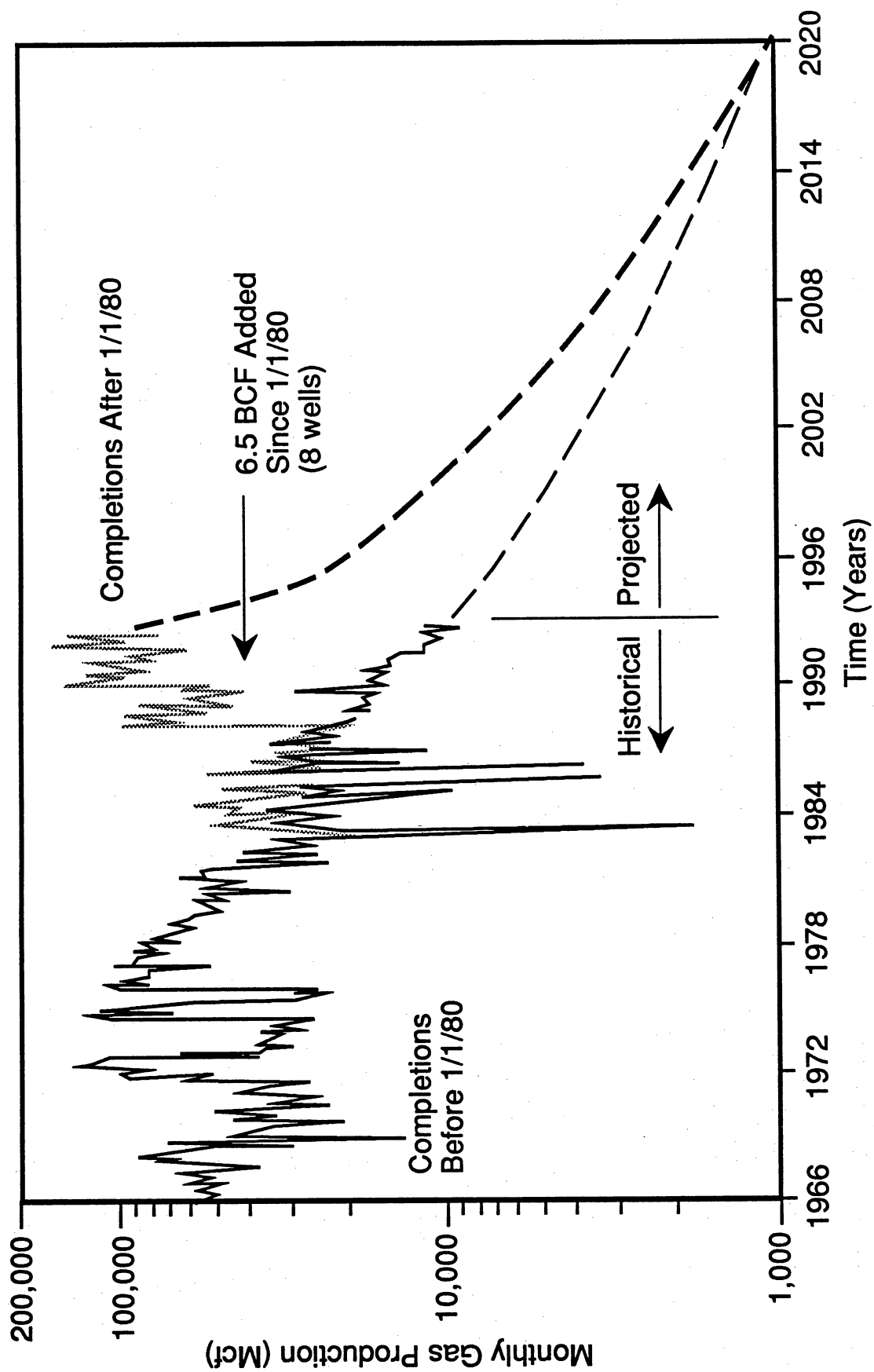
Figure 39. Graph of gas production versus time shows a reserve growth of 6.5 Bcf in the F-39 reservoir.

80
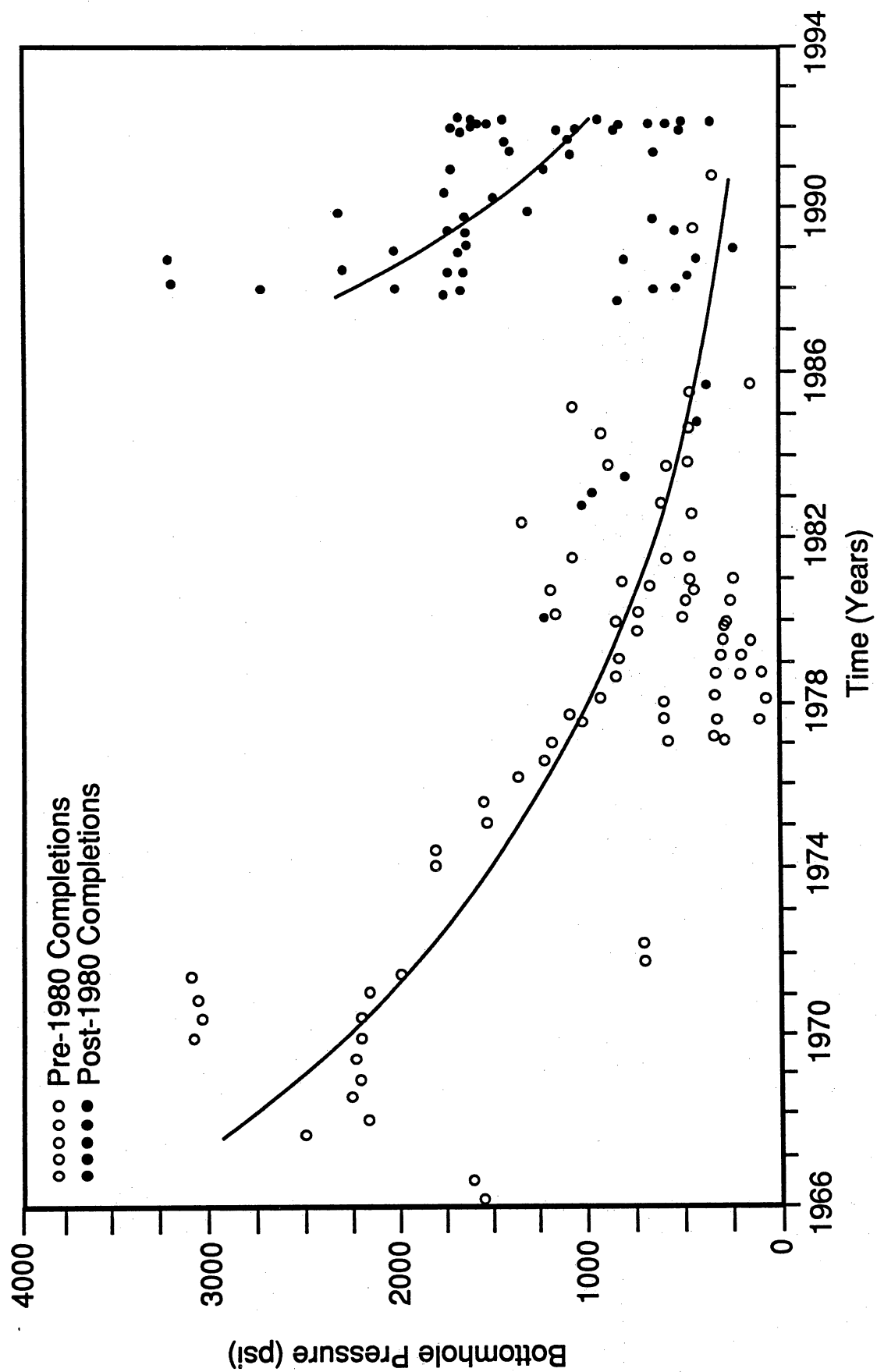
Figure 40. Bottomhole pressure versus time for completions in the F-39 reservoir.

JIM WELLS
NUECES

172

177

74

135

180 157

212 △ 175
202

KLEBERG CO 191 199 187

198 76

204

83

80

W175
△ VSP control well

◉ Project well test

— - — 3-D seismic grid

N

0   5000 ft

0   1500 m

QAa2195c
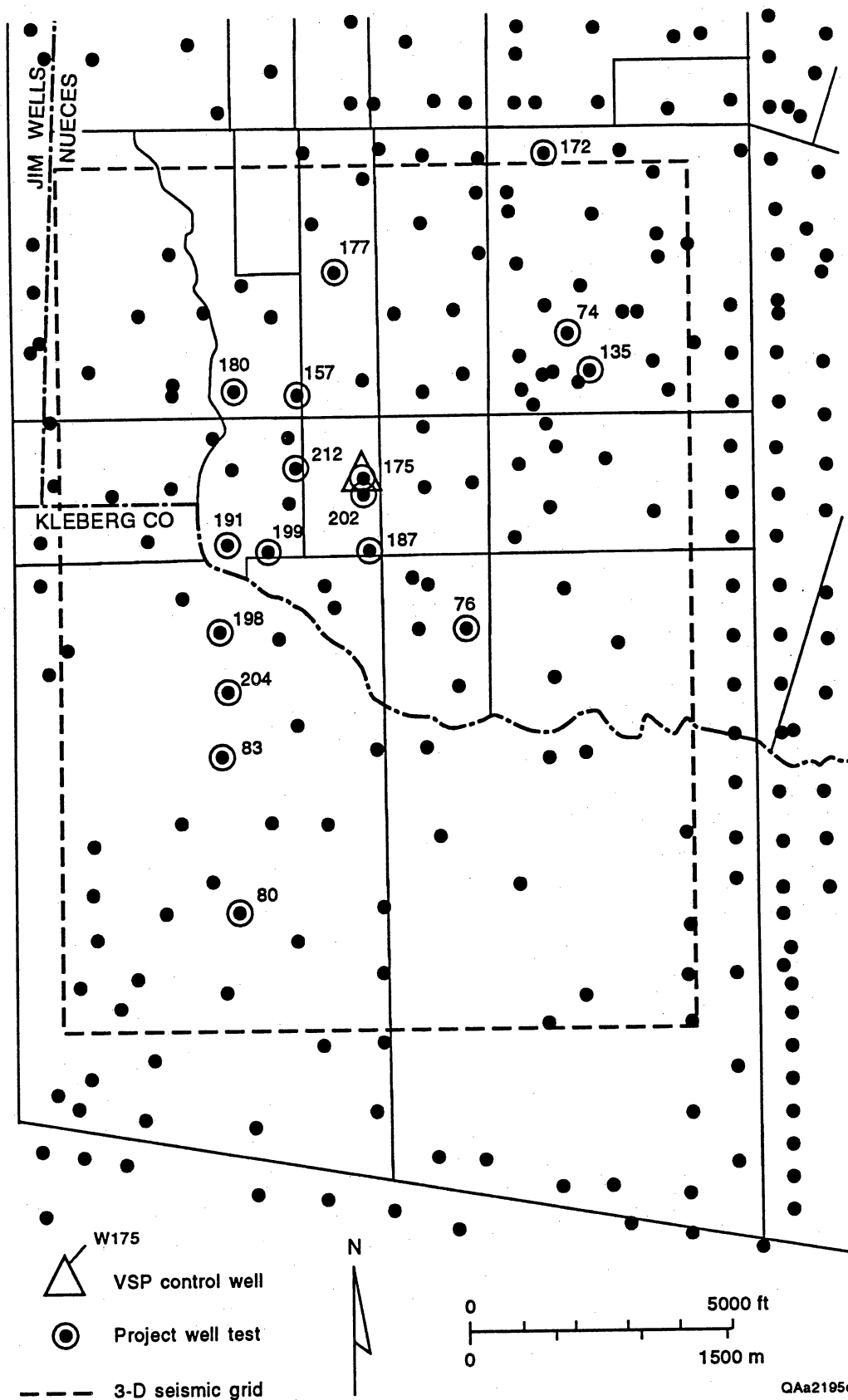
Figure 41. Map showing location of completions in the F-39 reservoir in 1990.
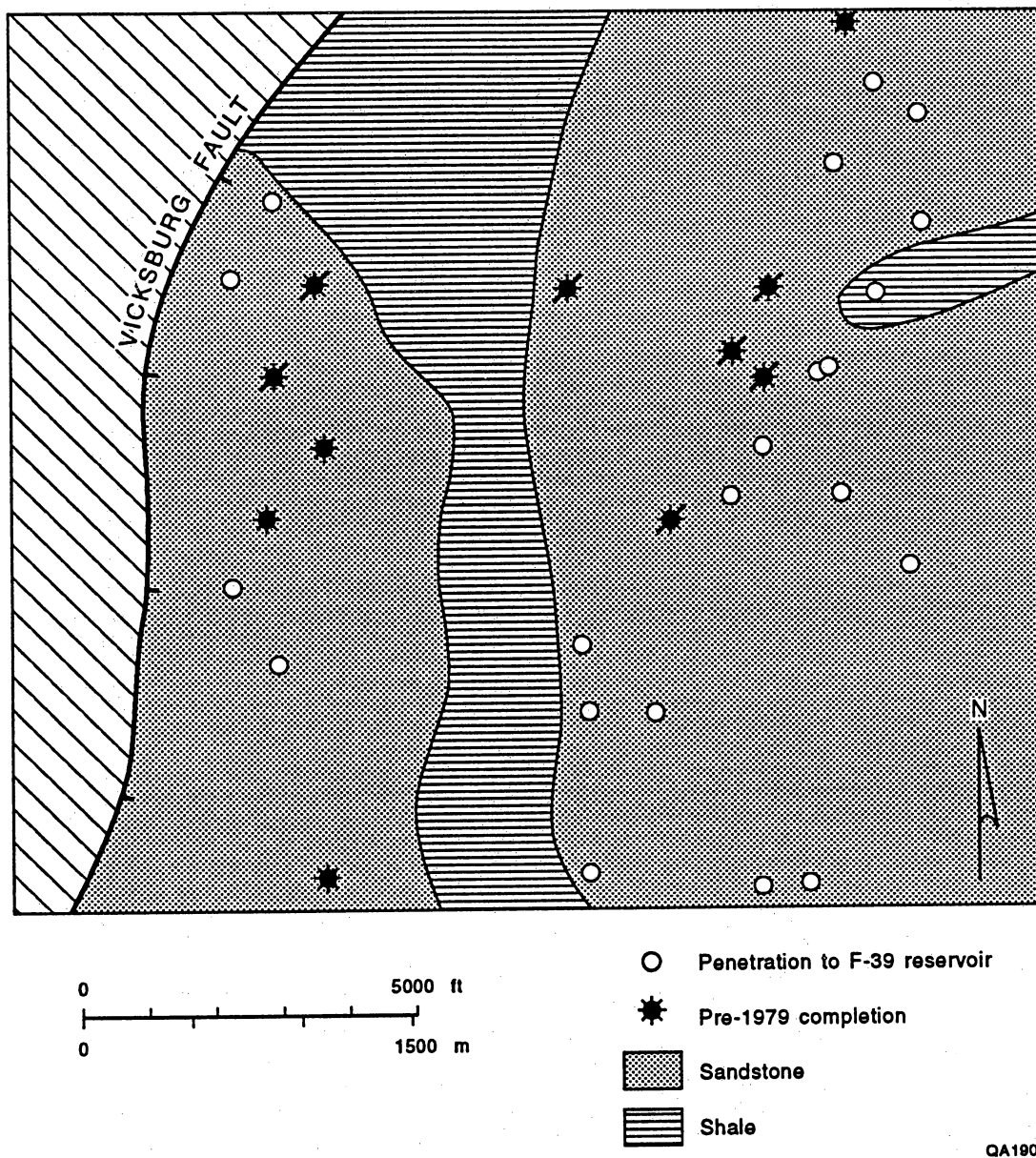
Figure 42. Map showing location of completions in the F-39 reservoir in 1979.

subsequently 5.6 Bcf of untapped and incompletely drained reserves were developed (table 4).

The offsetting wells in the west and east areas had been previously abandoned with

bottomhole pressures of 300 to 500 psi. A reconstructed isobaric map of the area shows the

inferred static pressures across the area in 1988, before the new F-39 completions were made

(fig. 43). Pressures in the previously interpreted nonreservoir area were over 2,000 psi in 1988.

This is slightly greater than 60 percent of the original reservoir pressure of 3,100 psi. The F-39

reservoir had been producing for more than 30 years in the adjacent areas, with wells depleted

to less than 500 psi.

Reserves Per Completion

Six reservoir compartments are identified in the new area. These compartments vary in

size from 67 to 185 acres, and each is produced by one or two wells. The average gas-in-place in

the compartments at the time of completion of these new wells was 941 MMcf and ranged

from 394 to 1,435 MMcf. These gas volumes and areas were estimated from the decline of

pressure (P/Z) with cumulative production and drawdown tests.

Permeability

Gross thickness of the F-39 in the Wardner lease averages 47 ft; average net pay thickness

is 14 ft. Transient well tests were performed in eight wells to establish the pressure and

permeability variation between wells. Average permeability was found to be 30 md, for an

average net pay thickness of 14 ft. Permeability ranged from 1 to 83 md (table 5).

Dominant characteristics of most well tests were barrier effects and channellike (bilinear)

flow. Five well tests in the F-39 reservoir indicated barriers from 40 to 300 ft from the well. The

Horner and type-curve plots of the pressure data have shapes that indicate linear and bilinear

flow in the late-time region, which are interpreted as flow in a long, narrow drainage shape.

Using the methods described by Economides and Economides (1985) for pressure transient

Table 4. Compartment analysis summary, F-39 reservoir, Wardner lease, Stratton field.

Wells	Test date	FSIP (psi)	P* (psi)	KH (md-ft)	K (md)
187	02/17/92	1646	1651	829	83
175	01/03/92	1633	1678	68	3
202	12/31/91	1713	1723	9	1
157	01/27/92	1109	1132	92	6
197	02/07/92	923	1058	425	8
199	03/03/92	781	838	948	35
204	01/24/92	808	1098	209	22
80	11/05/90	385	392	975	38
172	03/13/92	606*	NA	NA	NA
177	02/24/92	813*	NA	NA	NA
180	03/04/92	554*	NA	NA	NA
191	02/04/92	639*	NA	NA	NA
198	04/20/92	1655*	NA	NA	NA

*Static gradient tests only.

Table 5. Summary of test results, F-39 reservoir, Wardner lease, Stratton field.

Wells	First production	Initial pressure	IGIP (MMcf)	Area (acres)
172	01/29/88	1790	1227	114
177	03/19/88	2052	394	67
187	06/14/88	3216	953	83
175				
202				
204	02/28/89	2053	888	191
197	07/11/90	1790	1435	185
157				
199	12/11/90	1773	751	122
Average			941	127

ESTIMATED RESERVOIR PRESSURE (psi)

≥3000

2500 – 3000

1500 – 2500

500 - 1500

<500

0   5000   ft

0   1500   m

Contour interval variable (psi)

Nonreservoir

Control point

Penetration to F-39 reservoir
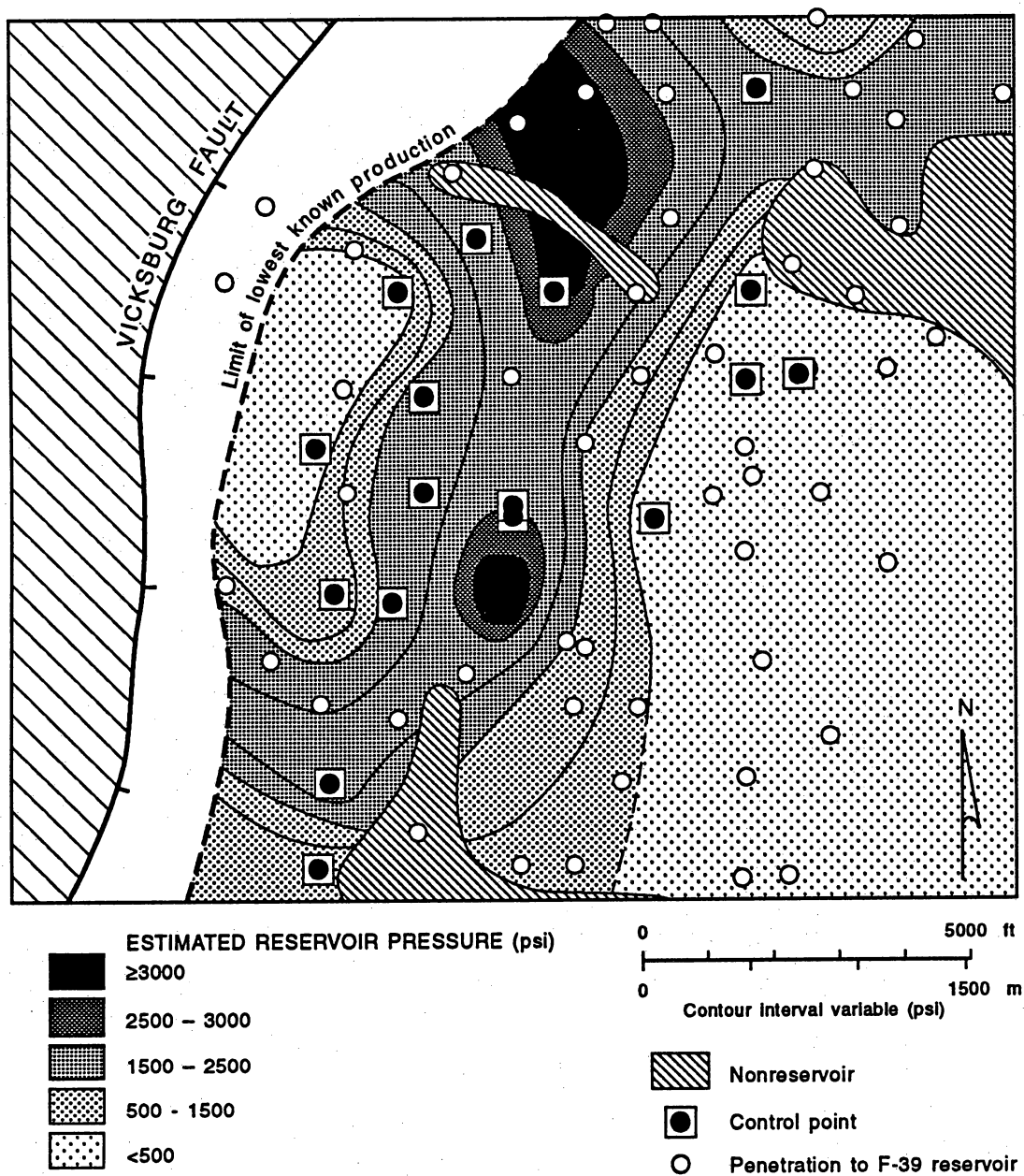
QA19013c

Figure 43. Interpretation of F-39 reservoir pressure in 1988.

analysis in elongated linear flow systems, and history-matching the transient test with an analytical simulator, the widths of the drainage areas were found to average 280 ft, with a range from 100 to 600 ft. These dimensions are consistent with VSP-calibrated 3-D seismic images that show meandering channels as narrow as 200 ft and only 10 ft thick.

Prediction of a Support Volume: G-WIZ Example Wardner 80

The largest volume F-39 well in the Wardner lease is the Wardner 80 (fig. 41). This well has a reported cumulative production of 14 Bcf since completion in 1954. The production and pressure history for this well was appropriate for analysis with the G-WIZ compartmented gas reservoir simulator (fig. 31). The simulator predicts a potentially large and poorly drained supporting reservoir compartment with a pressure of over 1,600 psi and containing 7.8 Bcf in 1991 (fig. 44). This support volume and incompletely drained resource volume is interpreted to be probably the reserves developed by the six new F-39 completions made after 1988. These wells are located 1 to 2 mi north of the Wardner No. 80 well.

Seismic Imaging of a Pressure-Documented Compartment Boundary

Compartmented drainage areas and barriers identified by deterministic well tests can be compared to images obtained from 3-D seismic horizon slices at the F-39 reservoir (fig. 45). A long, narrow shape bounds the Wardner 175, 202, and 187 wells. These wells are interpreted to be in a common reservoir compartment with an area of about 80 acres, according to estimations from pressure and cumulative production data. A flowing drawdown test performed in March 1992 at the Wardner 187 well indicates a minimum area of the primary drainage volume to be about 60 acres.

A stratigraphic cross section of the F39 reservoir near Wardner wells 175 and 202 is illustrated in figure 46. These wells are spaced only 200 ft apart, which is an unusually small well

1967

Primary Volume

Pore Volume = 32×10^6 ft^3

P_i = 2360 psi

IGIP = 4.8 Bcf

Support Volume

Pore Volume = 78×10^6 ft^3

P_i = 2360 psi

IGIP = 11.6 Bcf

1991

Primary Volume

P = 373 psi

GIP = 0.7 Bcf

Support Volume

P = 1612 psi

GIP = 7.8 Bcf

2048

Primary Volume

P = 142 psi

GIP = 0.3 Bcf

Support Volume

P = 918 psi

GIP = 4.3 Bcf
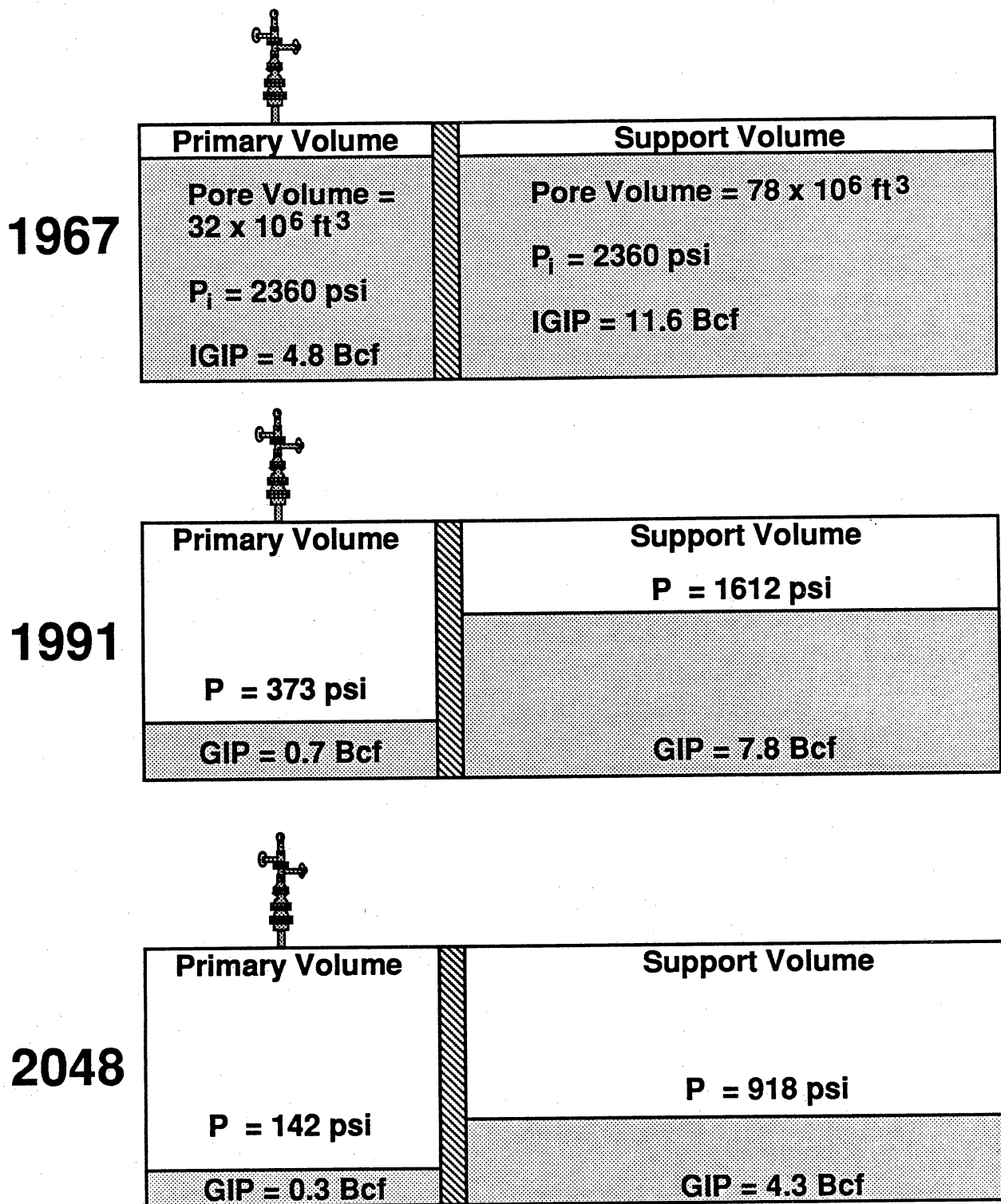
Figure 44. Schematic diagram showing the projected depletion history for the Wardner No. 80 well based on the G-WIZ compartmented gas reservoir simulator.
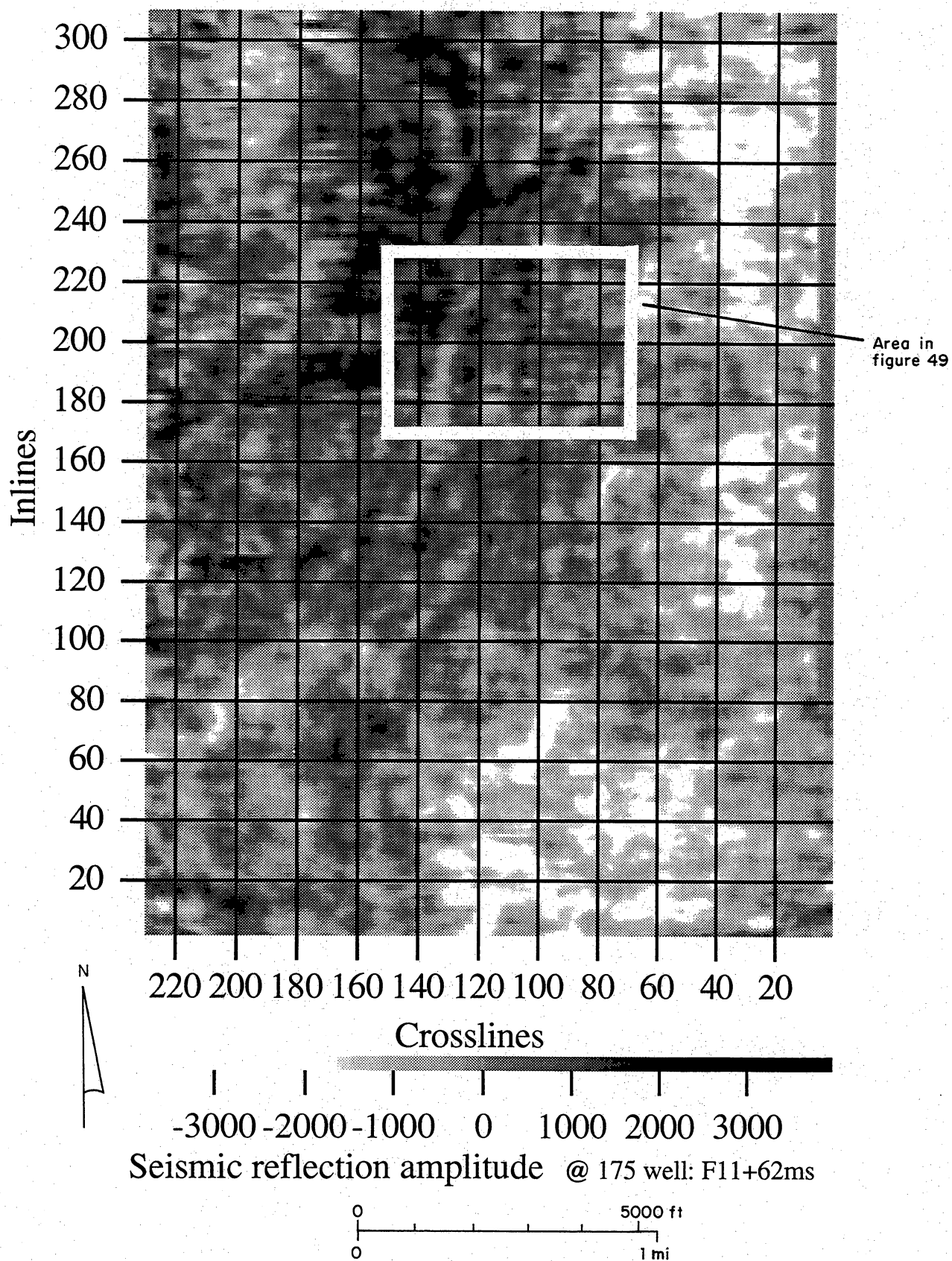
Figure 45. Seismic amplitude slice map of the F-39 reservoir horizon showing the topology of potential compartments.
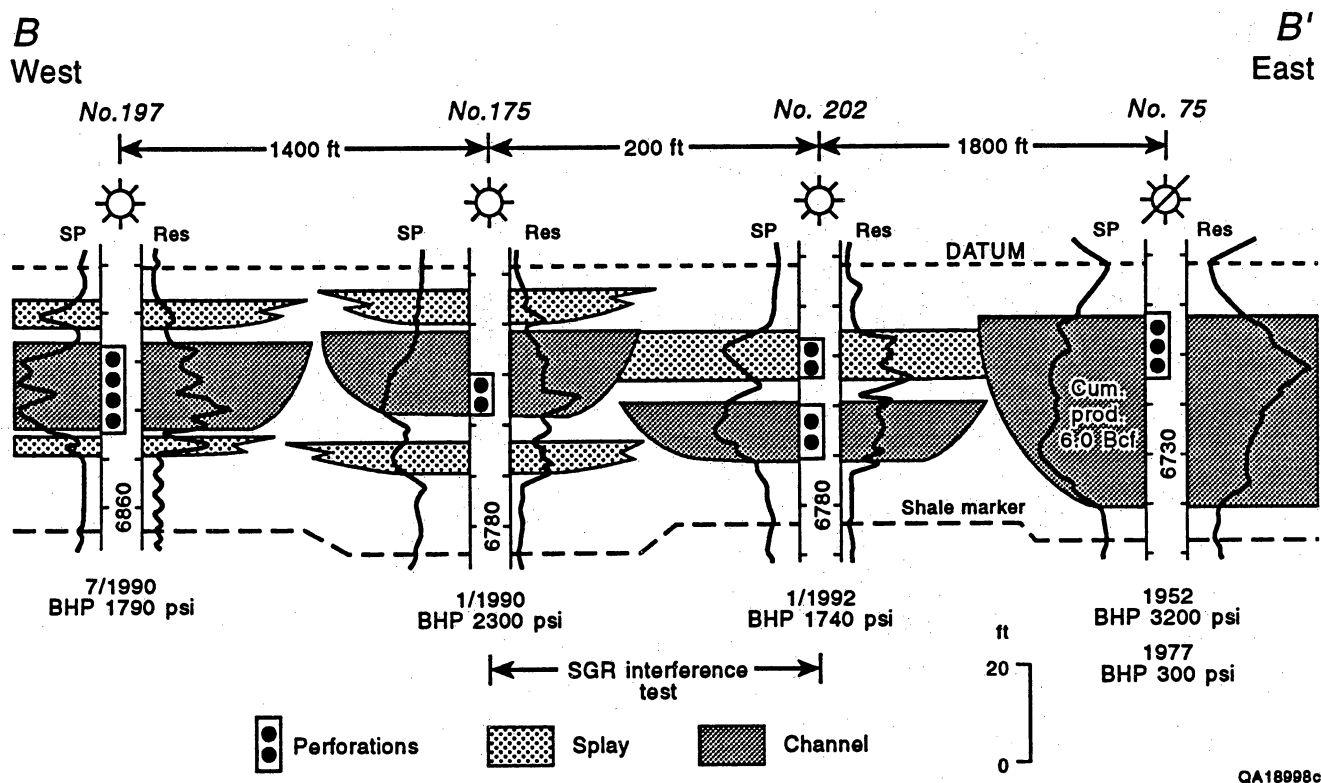
Figure 46. West-east stratigraphic cross section showing F-39 reservoir facies and pressure test data.

separation for gas wells. As shown in the cross section, one zone was perforated in well 202 and two zones were perforated in well 175.

The SGR project conducted a pressure interference test in these two wells (fig. 41). Perforations in well 202 were exposed to a series of strong pressure pulses shown by the bottom curve. The pressure response observed in well 175 (regardless of which perforated zone was isolated) is shown by the relatively flat, no-response curve at the top of the plot in figure 47. To ensure that the pressure measurements were accurately executed, the test was done twice. One definitive conclusion is that there is no line-of-sight pressure communication between the two wells; some type of F-39 compartment boundary exists in the 200-ft interwell space between wells 202 and 175.

The geologic model of the F-39 reservoir was developed prior to the pressure interference testing (fig. 47). The model implies reservoir continuity between the 175 and 202 wells, with a subtle depositional facies change from channel-fill to an adjacent splay sandstone for both the upper and lower part of the F-39 reservoir interval. Analysis of the pressure pulse data indicates there must be a compartment boundary between the two wells. Two seismic images spanning the 175 and 202 wells—a VSP image and a 3-D seismic image—were produced to determine if seismic technology can detect a compartment boundary in this interwell space.

The VSP image is shown in figure 48. The display on the right is the result of applying a vertical seismic profile common depth point (VSPCDP) transform to the upgoing VSP wavefield. The data were recorded in well 202, so the left edge of this VSPCDP image is positioned at the 202 well bore. The VSP geometry allowed stacking bins 25 ft wide to be created, so that well 175 is eight trace spacings (that is, 200 ft) north of well 202. The F-39 reservoir is located within the low-amplitude black peaks at 1.65 s. This sequence of peaks undergoes a measurable waveform change close to the well 175 trace, which implies that some type of stratigraphic discontinuity is located between the two wells and is closer to well 175 than to well 202.

The display on the left side of figure 48 provides additional information about the F-39 stratigraphy. These traces are the upgoing VSP reflection response measured at each
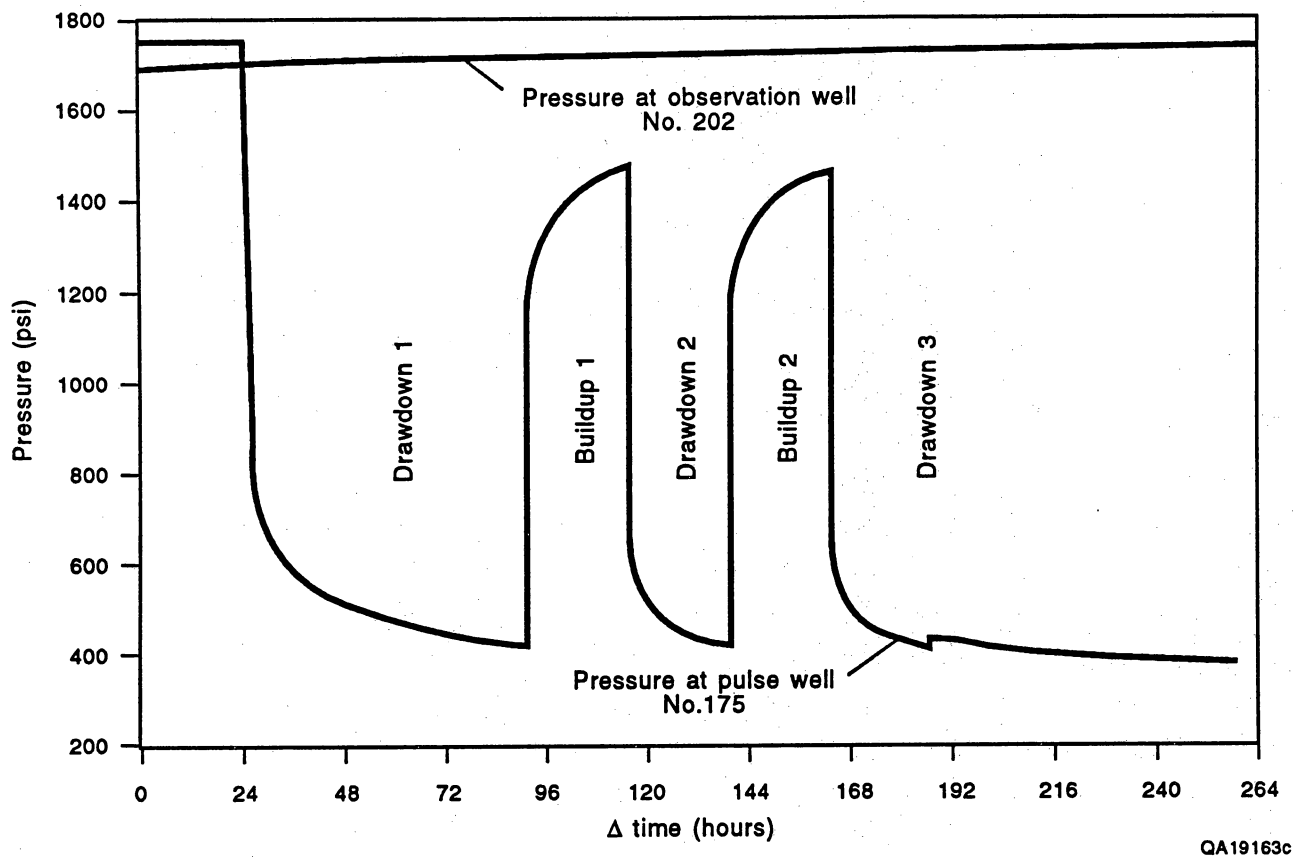
Figure 47. Pressure interference test for pulse well Wardner No. 175 and observation well Wardner No. 202.
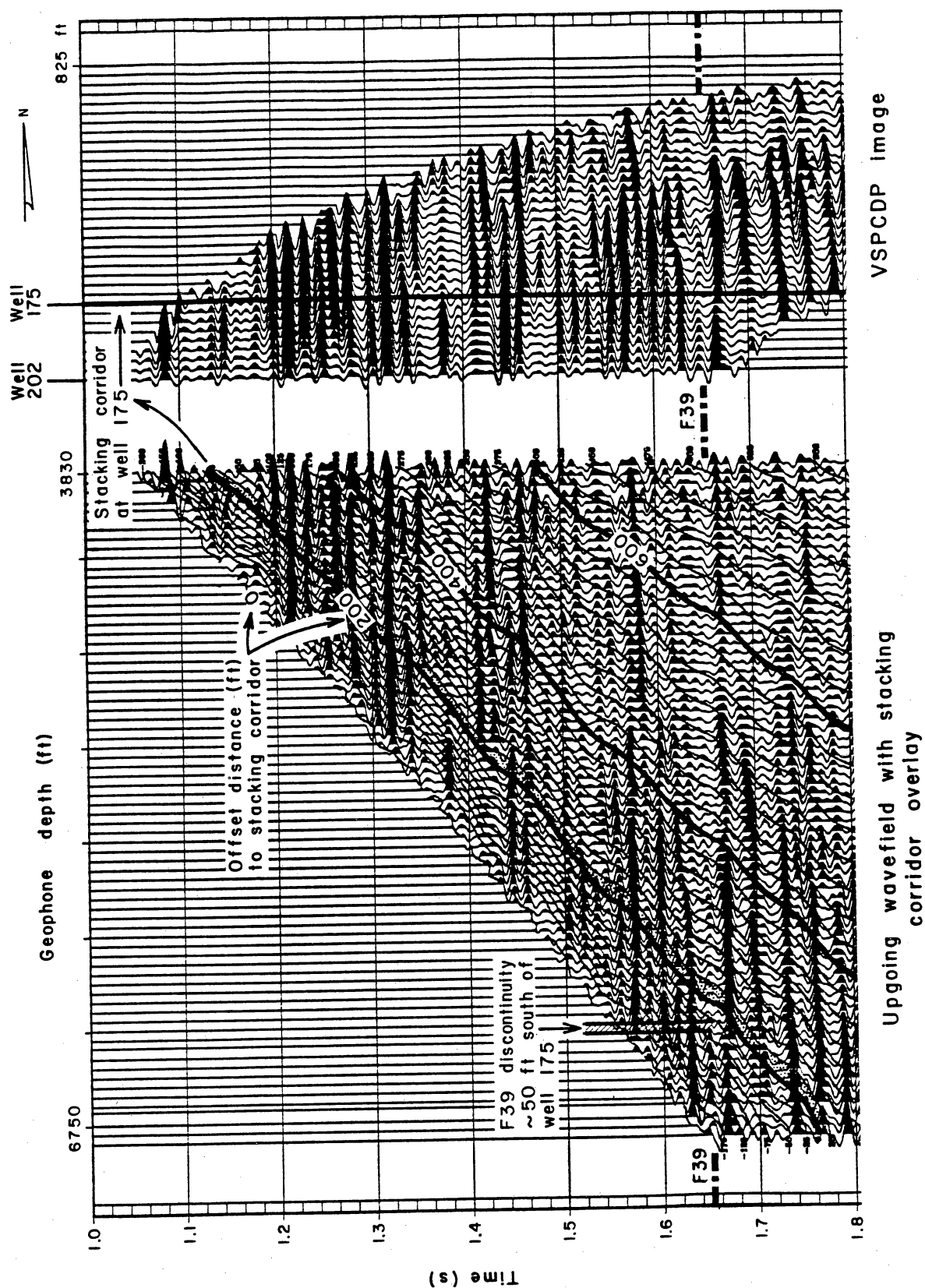
Figure 48. Vertical seismic profile (VSP) for the Wardner No. 202 imaged toward Wardner well No. 175.

94

QAI9598
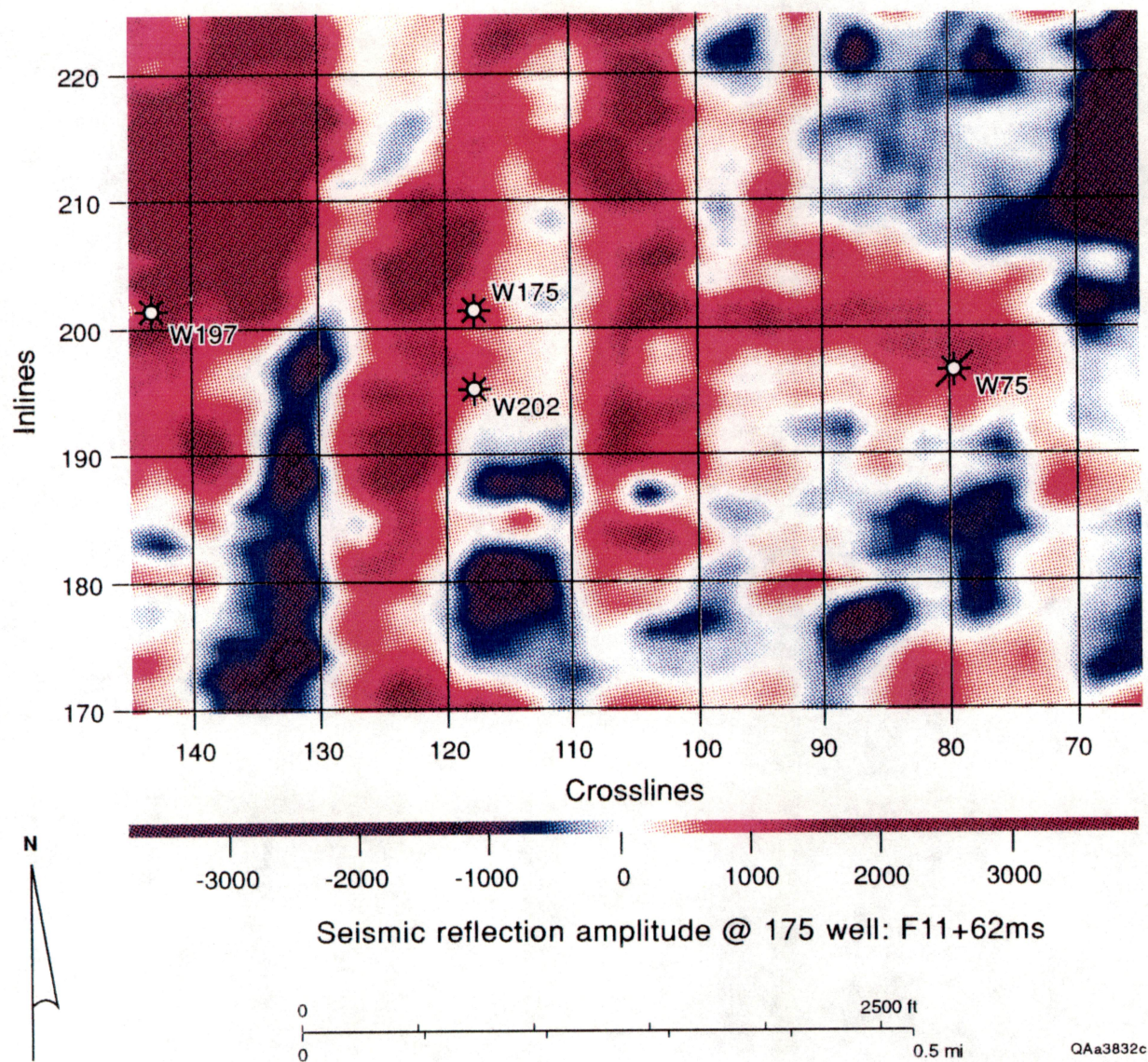
Figure 49. Seiscrop map of the F-39 reservoir in the Wardner lease 3-D data volume.

receiver depth in well 202. The wavy lines crossing this trace from the lower left to the upper right define the stacking corridors created during the VSPCDP image construction. Each stacking corridor spans a horizontal distance of 25 ft. All the trace data inside the leftmost corridor are summed to produce the leftmost trace in the VSPCDP image; that is, the trace at the 202 well bore, and all of the trace data inside corridor 8 are summed to create the VSPCDP trace at well 175, 200 ft north of well 202. The black peaks associated with the F-39 reservoir begin at the left side of this display and continue across stacking corridors 1, 2, 3 . . . until they reach corridor 6, about 50 ft south of well 175. At this point, the F-39 event disappears and does not reappear until stacking corridor 11, about 100 ft north of well 175. One conclusion to be drawn is that the VSP image supports a reservoir model that has a F-39 compartment boundary located about 50 ft south of well 175; that is, at the F-39 reflection discontinuity in stacking corridor 6.

A 3-D image of the F-39 depositional surface (fig. 45) covers the entire 7.5 mi^2 spanned by the Stratton 3-D data volume. Each grid square overlaying the image measures 1,100 ft × 1,100 ft, which imparts a sense of the physical sizes associated with some of the image features. As shown by the color scale, positive reflection amplitudes are red, negative reflection amplitudes are blue, and larger reflection magnitudes are indicated by more intense color shades. The linear north-south features passing immediately by wells 175 and 202 are manifestations of Vicksburg faults extending up into the lower Frio. These faults are clearly visible on the vertical slices through the 3-D data volume. The strong north-south linearity in the seismic amplitude image of the F-39 reservoir may be a partial function of fault-related topographic control on F-39 fluvial deposition from the deeper faulted stratigraphic section in the lower Frio and Vicksburg. Wells 175 and 202 are apparently located near the edge of one of these fault-influenced fluvial channel systems.

A magnified view of this same depositional surface is shown in figure 49. In this display, each grid square measures 550 ft × 550 ft, so rather small topological changes can be measured. A key feature revealed in this image is the light-gray notch that intrudes into the dark-gray, north-south stream channel at the position of well 175. This subtle feature would probably not

be given any consideration in constructing a model of the F-39 reservoir except for the fact that VSP imaging reveals stratigraphic breaks in the F-39 reservoir immediately north and south of well 175. This notchlike feature in the 3-D image supports the idea that the F-39 stratigraphy undergoes a change between wells 175 and 202 and that the change is quite close to the 175 well.

Small Compartment Size Class Reservoirs

Small compartment size reservoirs in the Stratton field include the F-15/F-29, D-11/D-18, and F-31–F-37 reservoir groups (fig. 23). The lower boundary of the compartment pore volume distributions for 10 reservoir groups, shown in figure 27, is primarily composed of small compartment size class reservoirs that account for 21.4 Bcf, or 65 percent of the reserve appreciation in the Wardner lease study area from 1979 through 1989. Reserve growth in the small-compartment reservoir class is primarily from new infield wells drilled into new infield reservoirs or from untapped reservoir compartments in previously established reservoir intervals that were not depleted by adjacent completion into the equivalent reservoir horizon (fig. 9). Geophysical techniques, including 3-D surface seismic data, are one of the best ways to identify reservoirs that contain this resource potential.

Common characteristics of these small compartment size class reservoirs include

(1) thin, dispersed channel-fill sandstones and associated splay deposits,

(2) relatively small and limited areal distribution (<1 mi^2), and

(3) moderate to high effective permeabilities (10–100 md).

Petrophysical characteristics of the small compartment size class reservoirs indicate that they have less porosity development than the medium and large compartment size class reservoirs. Porosities range from 16 to 20 percent. Water saturations range from 44 to 66 percent, and thickness averages 8 ft. Small class reservoirs are more shaly than the large and medium class reservoirs, with a volume of shale generally greater than 13 percent. A bulk

volume of water less than 11 percent is indicative of gas with water-free production. General petrophysical characteristics of small reservoirs are listed in appendix table 3–7.

Geophysical Techniques Applied to Seismic Thin Beds: VSP Calibration Procedure

Frio reservoirs at Stratton field are thin beds in a seismic sense; that is, the reservoirs are thinner than one-fourth of the dominant wavelength in the illuminating seismic wavefield. Not only are some reservoirs only 5 to 15 ft thick, but often two or more of these thin reservoirs are vertically separated only 10 to 20 ft. In this type of stratigraphy, a given thin bed can be positioned anywhere in the seismic reflection wavelet, and the top and base of the reservoir must be accurately defined in terms of seismic travel time to determine where the reservoir window occurs in the reflection waveform. Vertical seismic profiling (VSP) is the most rigorous procedure by which this seismic thin-bed calibration can be achieved because VSP data are recorded both as a function of stratigraphic depth and as a function of seismic travel time.

To facilitate seismic thin-bed interpretation at Stratton field, VSP calibration data were recorded in wells 175, 202, and 153 inside the 3-D seismic grid. An example of these VSP data being used for thin-bed interpretation is shown in figure 50. The thin-bed reservoirs in the center column are accurately positioned by the VSP measurements made in well 175, which establish a precise relationship between stratigraphic depth and VSP travel time at that control well. Note that the zero-offset VSP image plotted beside the reservoirs contains a much wider frequency spectrum (that is, a much narrower reflection wavelet) than does the 3-D seismic image extending away from well 175 and resolves thin beds that cannot be resolved in the 3-D image. When VSP data are properly recorded and processed, they should provide a better vertical resolution of stratigraphic units than do surface-recorded seismic data, as exemplified in this data comparison.

The interpretational procedure used to extract thin-bed images from the Stratton 3-D data volume requires that this VSP image, together with the reservoir time windows that are defined
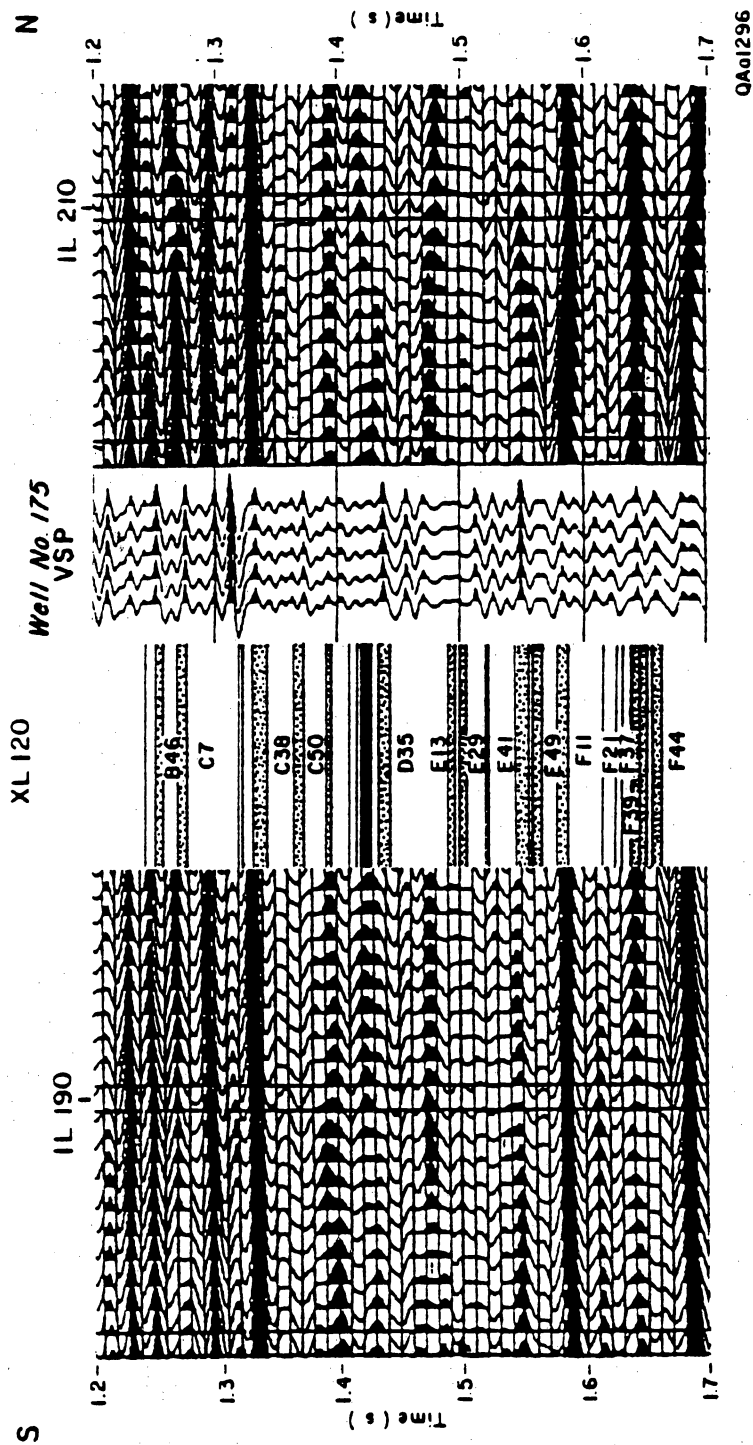
Figure 50. Calibration of thin-bed reservoirs using the vertical seismic profile (VSP) in Wardner well No. 175 tied to crosslines and inlines from the 3-D data volume in the Wardner lease.

in terms of VSP travel time, be time shifted until the zero-offset VSP trace is an optimum match with the 3-D data traces at well 175. Once the optimum time alignment between the VSP and the 3-D traces is found, the reservoir time windows can then be inserted into the 3-D data volume at the stacking bin containing well 175 and each thin bed is then precisely positioned within its associated surface-recorded reflection waveform. The optimum VSP-to-3-D trace alignment at well 175 requires no time shift, as is shown in figure 50.

Some reservoirs in this display are so thin that they can be represented by only a single, narrow, horizontal line, and sometimes 3, 4, or 5 of these reservoirs may be stacked so closely that the entire family of reservoirs comprises a single seismic thin bed positioned within a single reflection peak or trough. An example of such an ensemble of thin, closely stacked reservoirs is the F-20 to F-25 series occurring within a time window spanning only 10 ms or so across the 3-D grid. Only the F-21 reservoir was penetrated by well 175, and that reservoir is depicted as a single, narrow horizontal line in figure 50. Even in this closely clustered thin bed group, the VSP calibration procedure described above accurately positions each member of this thin bed family in the 3-D data volume. This interpretational technique for transferring reservoir depth to VSP travel time and then to 3-D seismic image time was used to define the specific time surface spanning the 3-D volume from which each thin-bed image was extracted. Using the interpretational procedures and VSP thin-bed calibration technique, we extracted several viewing surfaces corresponding to thin-bed reservoir depositional surfaces from the Stratton 3-D data volume.

Geophysical Techniques Applied to Seismic Thin Beds: Seiscrop Mapping

The F-20 to F-25 reservoirs are thin, each one typically less than 10 ft thick, and all numbers of this reservoir series can be vertically stacked within a few tens of feet. In fact, the complete F-20 to F-25 interval is a seismic thin bed. Consequently, a logical way to interpret a 3-D seiscrop image of the F-20 to F-25 reservoirs is to assume that the composite sandstone

101

thickness of all of these closely stacked reservoirs is the dominant factor influencing the image features seen on the F-20 to F-25 seismic depositional surface.

Sandstone thickness of the individual F-20, F-21, F-23, and F-25 reservoirs (as determined from well data inside and surrounding the 3-D seismic grid) is mapped in figures 51 through 54. Only in rare instances does the thickness of any individual reservoir exceed 10 ft. A map showing where these reservoirs overlay each other is depicted in figure 55. This composite F-20 to F-25 sandstone map was made by tracing only the 5-ft contours of the individual reservoir maps. The resulting composite map is qualitative, not quantitative, since it shows only where each reservoir thickness exceeds 5 ft and where the reservoirs tend to stack vertically.

The interpreted F-20 to F-25 seiscrop, determined by using the previously described VSP calibration procedure, is shown in figure 56. On close inspection, several narrow meander features, mostly in the red color shades, can be seen traversing the image in various directions, but no specific depositional pattern is particularly obvious. However, there is a strong correlation between the major features of the seiscrop and the composite sandstone map, as can be seen by overlaying the geological model (fig. 55) and the seiscrop image (fig. 56).

In general, the red seiscrop areas correspond to the presence of sandstone, and the red color tends to intensify whenever several reservoirs stack vertically. An example of this behavior is the color intensity increase near the intersection of inline 230 and crossline 60 where the F-20, F-23, and F-25 reservoirs are stacked in vertical sequences. Because of the strong correlation between the color distribution in the F-20 to F-25 seiscrop and the composite sandstone thickness in the F-20 to F-25 thin-bed interval, the seismic seiscrop image appears to be one of the more reliable indicators of where new infield reservoirs could most likely be found in seismic thin-bed reservoirs similar to the F-20 to F-25 series.

The next section of this report provides three examples from the Wardner lease study area (figs. 14 and 57) of geologic, engineering, and geophysical investigations in Stratton field from the F-series reservoirs (F-21, F-20, and F-37) for identifying and quantifying infield reserve growth. All three examples illustrate depositional setting and resource evaluation of these small
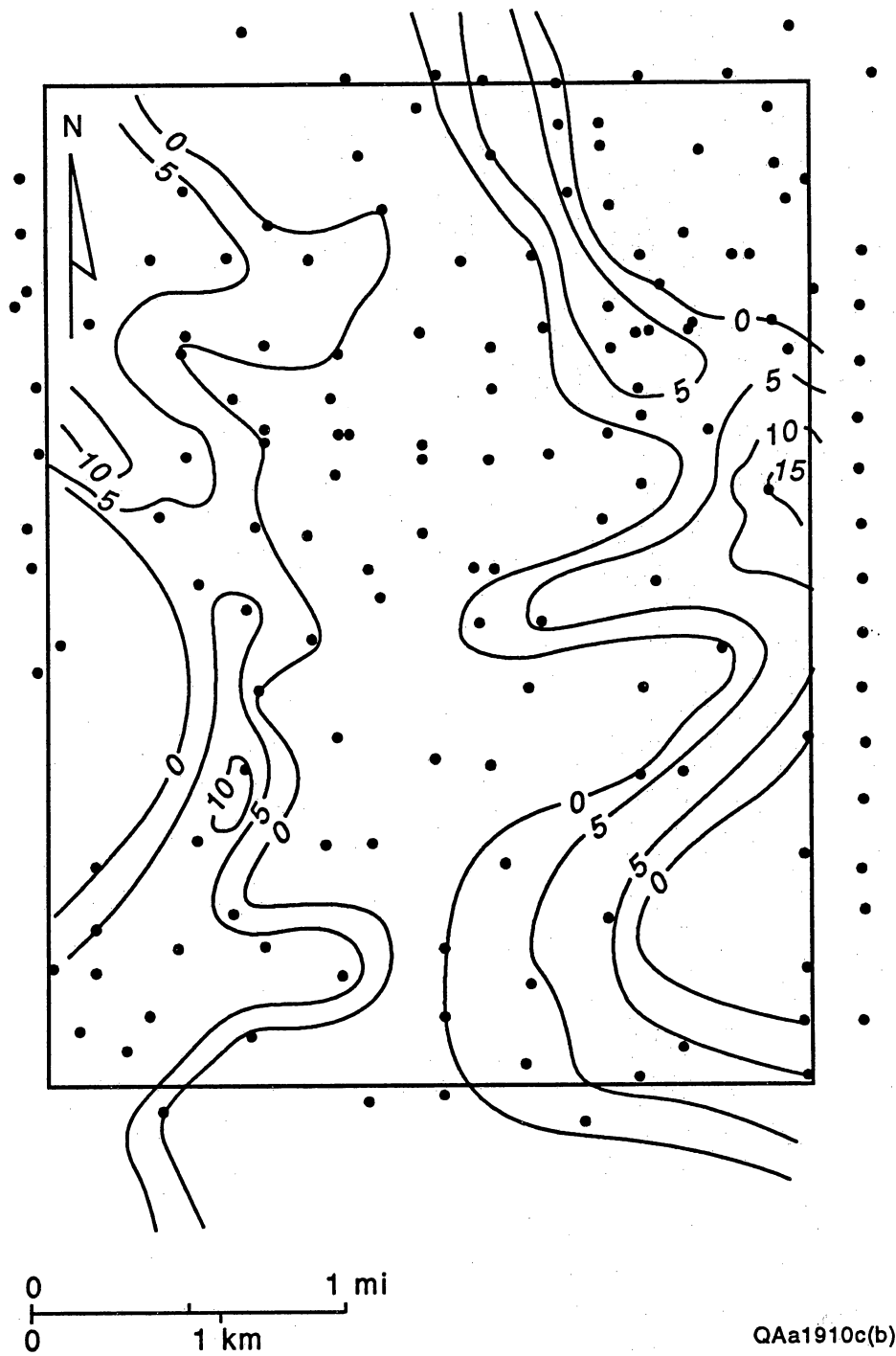
Figure 51. Net sandstone isopach of the F-20 reservoir in the Wardner lease study area.

QAa1910c(b)
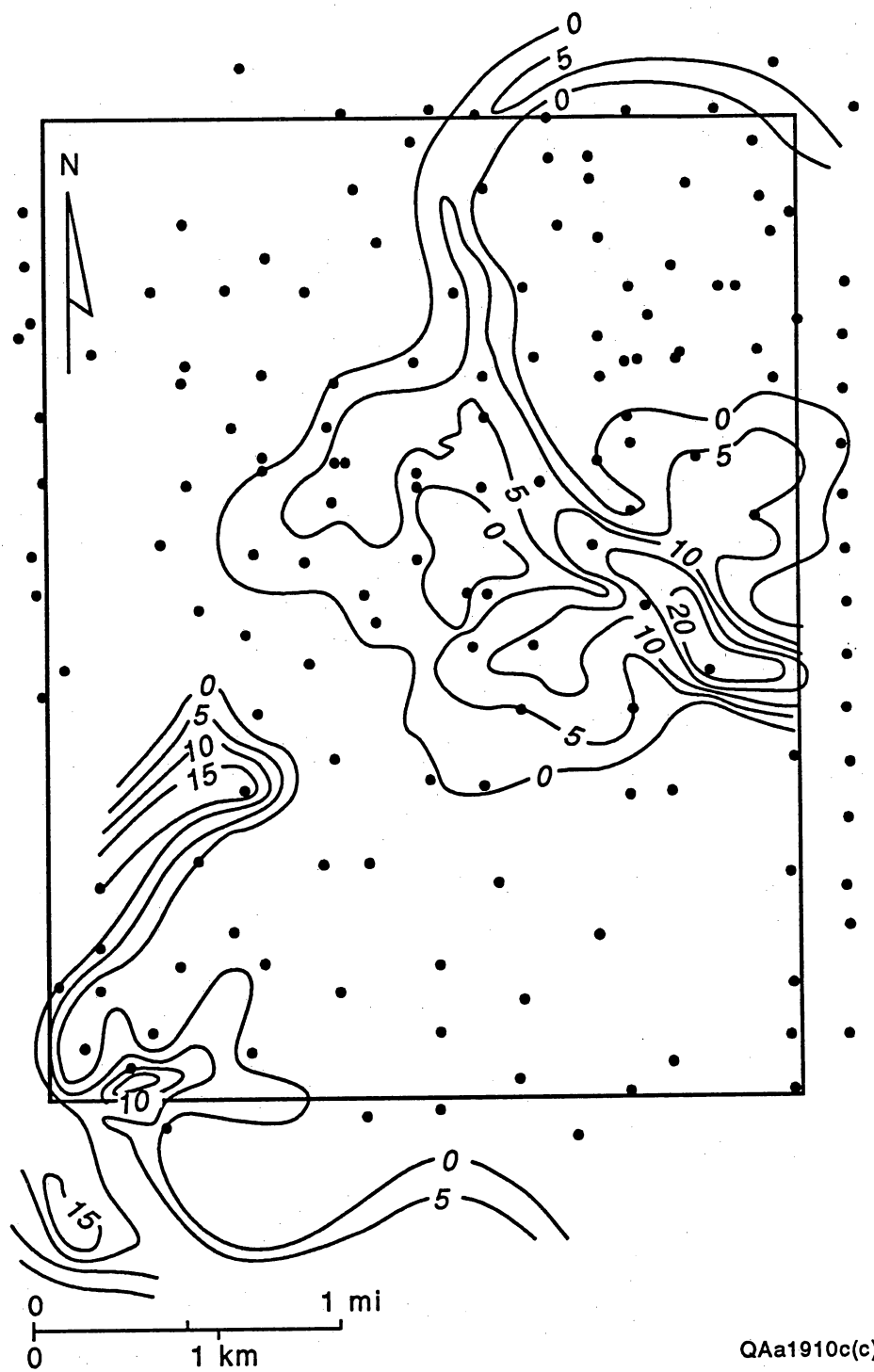
Figure 52. Net sandstone isopach of the F-21 reservoir in the Wardner lease study area.

QAa1910c(c)
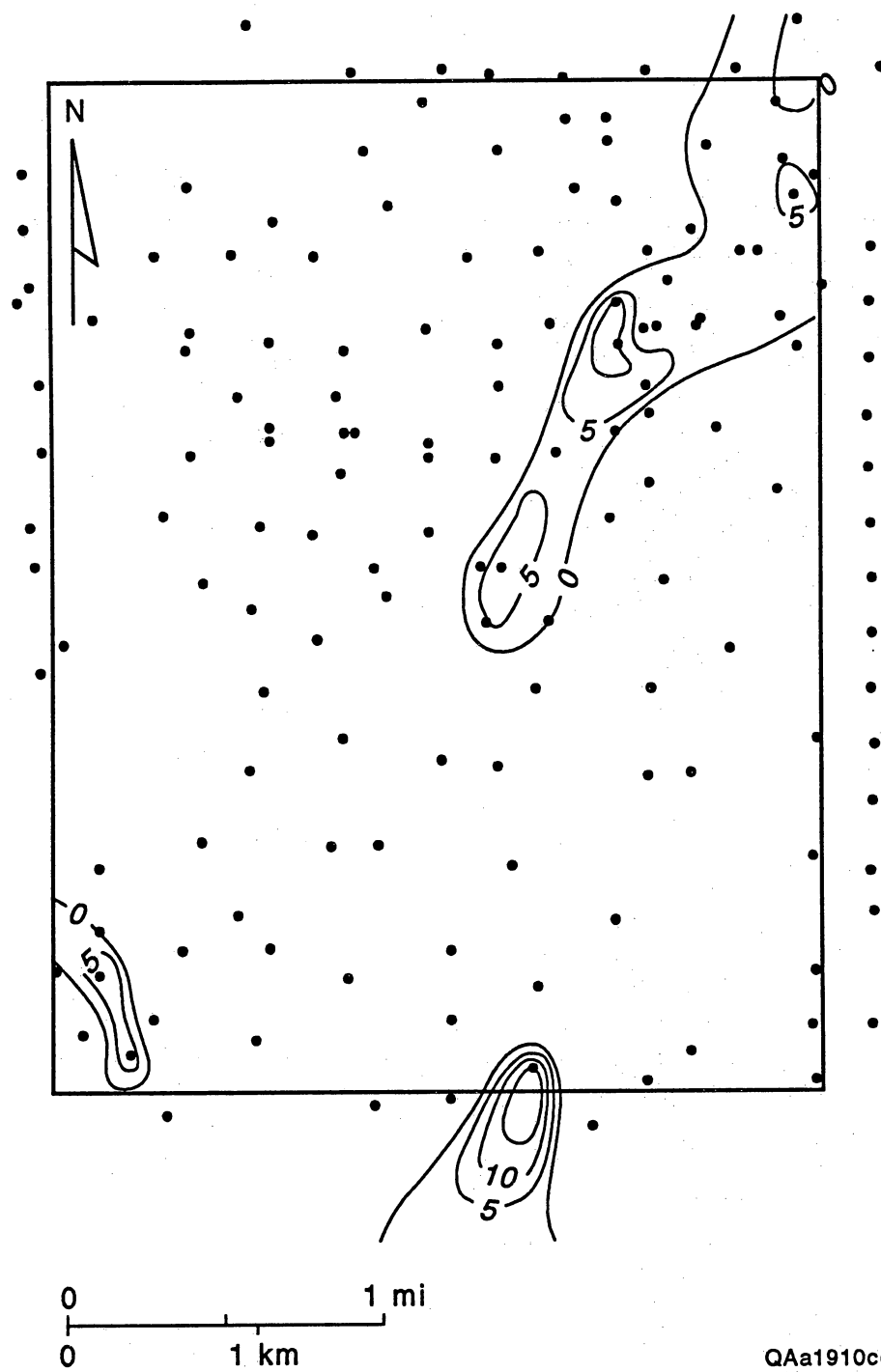
Figure 53. Net sandstone isopach of the F-23 reservoir in the Wardner lease study area.
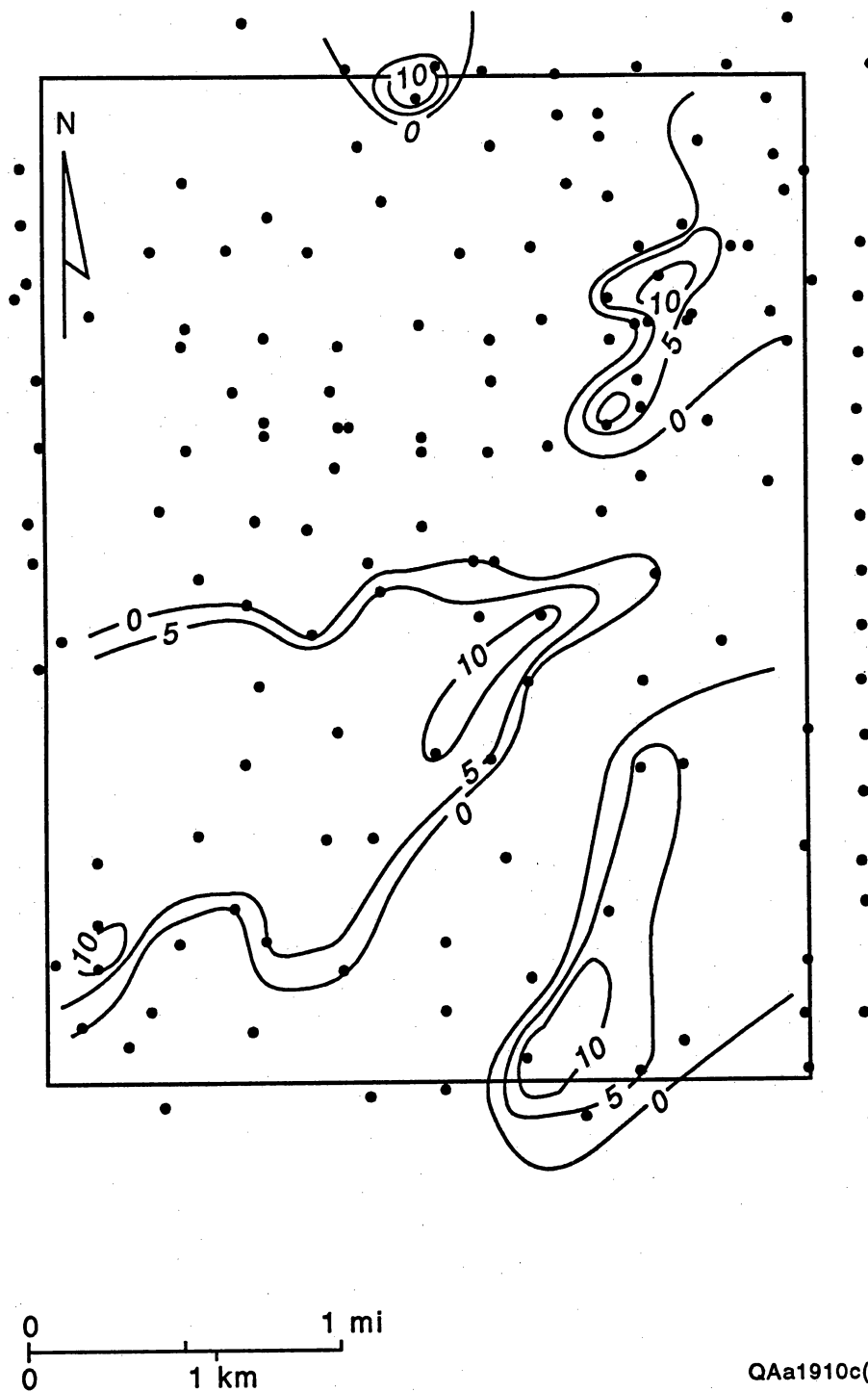
Figure 54. Net sandstone isopach of the F-25 reservoir in the Wardner lease study area.

QAa1910c(d)

Five-foot isopachs

F20   F23
F21   F25

0 ——————— 1 mi

0 ——————— 1 km

QAa1910c(f)
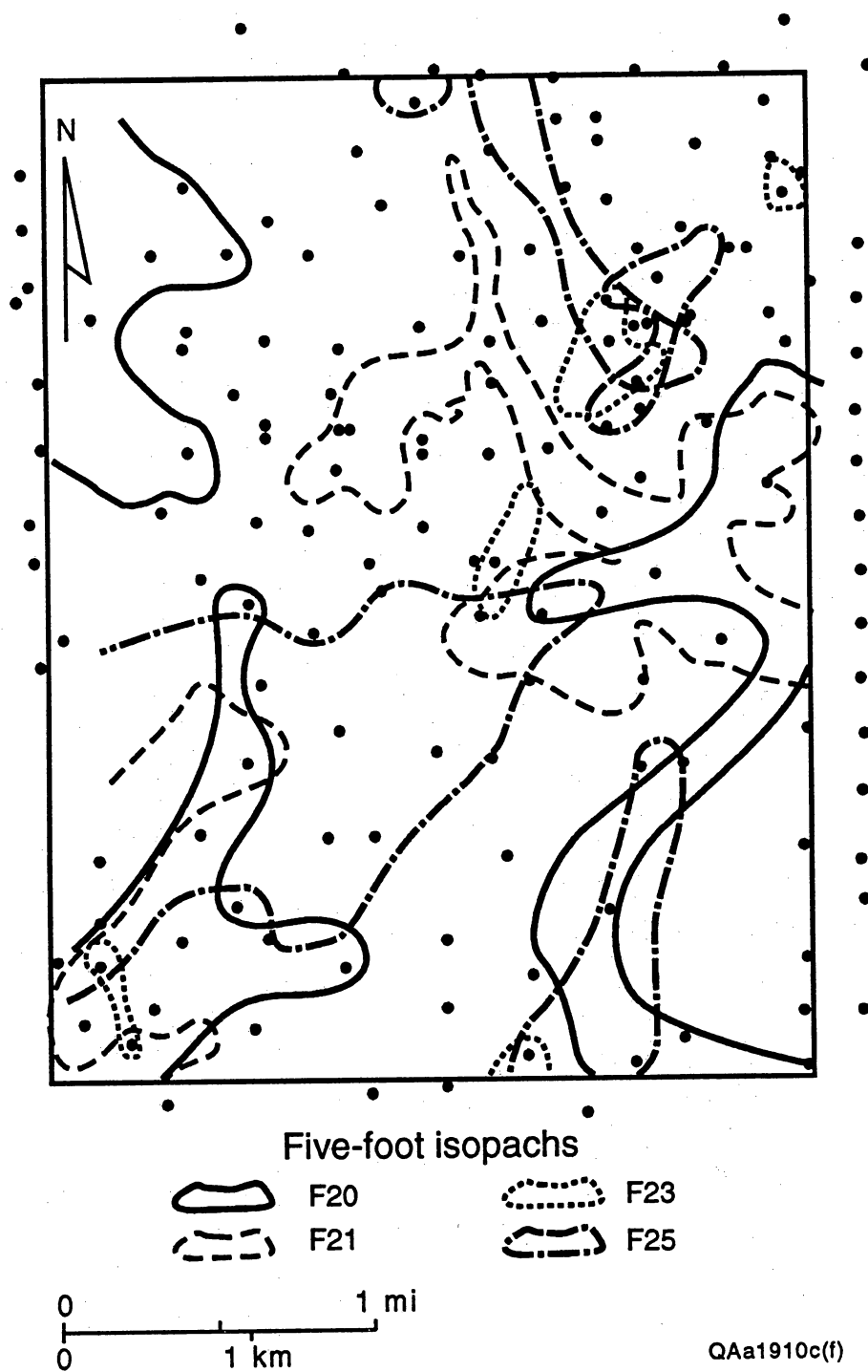
Figure 55. Composite of net sandstone isopachs for the F-20, F-21, F-23, and F-25 reservoirs in the Wardner lease study area.
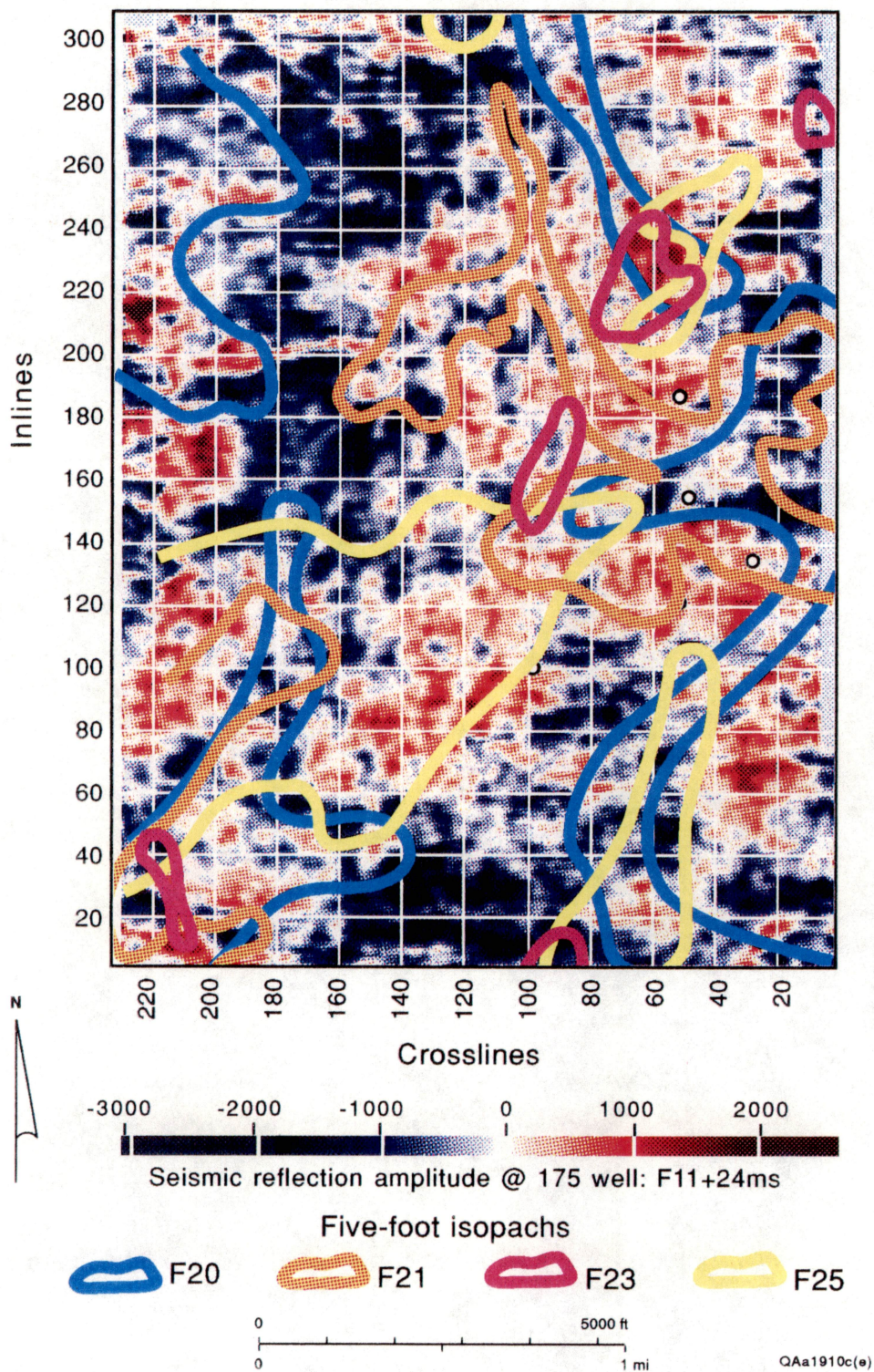
Figure 56. Seiscrop map of thin-bed reservoirs in the F-20 series reservoirs in the Wardner lease study area.
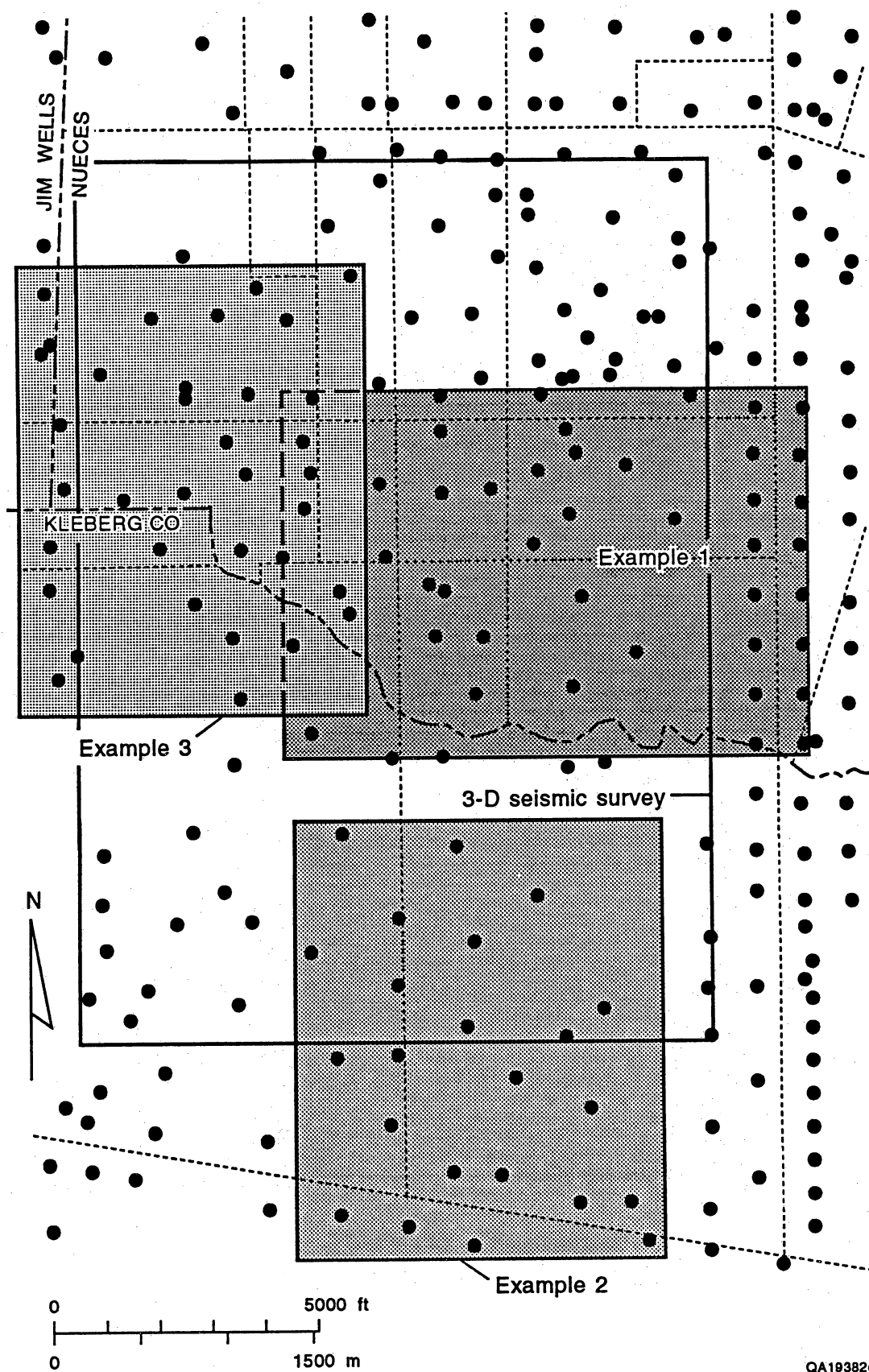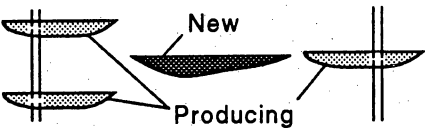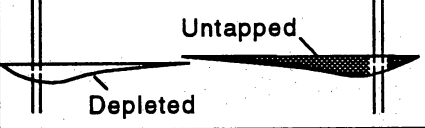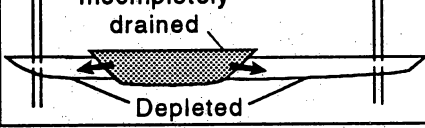
Figure 57. Location of the three examples for small compartment size class reservoirs documenting infield reserve growth.

111

compartment size class reservoirs using both existing data, and in two of the three examples, supplemental data acquired and analyzed by the SGR project. The examples document the importance of reservoir geometry and depositional heterogeneity in creating a secondary gas resource in this mature gas field.

In the first two examples, SGR project staff have conducted extensive field testing that documents the incremental gas resource. Example one demonstrates that new reservoirs may exist between the current well-bore spacing. In example two, untapped reservoir compartments are identified by integrated geologic and engineering evaluation. The third example illustrates the concept of incompletely drained reservoir compartments and is based on a historical analysis of completions spanning 28 years of gas production. Starting with example one, the three examples are presented in an order that reflects a progression from easy to recognize to harder to identify secondary gas resources (fig. 58). These examples support the broader based results described previously in this report and elsewhere as a historical hindcast approach to understanding reserve growth across a larger area of the field (Levey and others, 1991; Sippel and Levey, 1991).

Small Compartment Size Class Example: F-21 Reservoir

In this example, a projected incremental gas resource of 2.6 Bcf of recoverable reserves was determined from pressure data obtained by the operator and additional testing by the SGR project. The lithostratigraphic interval containing the F-21 reservoir was productive in the southwestern and northeastern parts of the Wardner lease study area. After 50 years of development history in the field, more than 15 pre-1988 wells had penetrated nonreservoir facies (fig. 59a) in the study area. In 1988 an area of approximately 320 acres without any well penetrations was the site of a deeper pool target (Wardner No. 176) in the Vicksburg Formation that was drilled at approximately 8,000 ft. Formation evaluation of the open-hole log from this well bore indicated a potential gas zone in the lower part of the middle Frio, which penetrated

Ease of recognition	Reservoir/compartment terminology		Diagram	Incremental resource (Bcf)
Simple ↓ Complex	Example 1	New infield reservoir	New / Producing	2.6
	Example 2	Multiple untapped reservoir/compartments	Untapped / Depleted	1.0
	Example 3	Incompletely drained reservoir/compartment	Incompletely drained / Depleted	2.0

QA19381c

Figure 58. Illustration of three reservoir-compartment types, and estimated volumes of incremental resource calculated for the three examples.

(a)

Window
in production

1 sq. mi.

-6425
-6450
-6475
-6500
-6550
-6475
-6500

0 ——— 2000 ft
0 ——— 600 m

Structure contour
interval 25 ft

(b)

FLOODPLAIN

CHANNEL

SPLAY

Well 176
comp. A
(1988)

Well 195
comp. B
(1988)

Well 201
comp. C
(1990)

0 ——— 2000 ft
0 ——— 600 m

Net sandstone
contour interval 5 ft

N

• Well not deep enough   ✳ New infield reservoir completion

• Well penetrates horizon   △ SGR engineering test

– – – Cross section

QA19383c

Figure 59. Part of Stratton field (a) before the 1988 discovery of the new infield reservoir and (b) in 1991.

114

close to original reservoir pressure at 6,550 ft (the initial completion pressure was 2,856 psi).
Measurement of near-original reservoir pressure (calculated at 97 percent of initial pressure
assuming a gradient of 0.45 psi/ft) in this completion demonstrates that a new infield reservoir
was penetrated.

Three infield wells (Wardner wells 176, 195, and 201) were drilled within 24 months and
completed in this same reservoir at an approximate distance of 0.25 mile between wells
(fig. 59b). Previous research indicated that fluvial channel systems (<30 ft thick) are common
throughout a large part of the middle Frio Formation (Kerr, 1990; Kerr and Jirik, 1990).
Similarity of the spontaneous potential log shapes from the three infield completions suggests
that a single genetic stratigraphic unit was penetrated. The unit comprises channel-fill and
splay sandstones that are laterally adjacent to floodplain mudstones within a fluvial depositional
environment (fig. 60).

Pressure Tests

In mid-1990 the SGR project staff conducted pressure testing in three wells with F-21 gas
completions to determine reservoir permeability, identify the presence of barriers near the
well bore, and quantify the effective reservoir compartment size. Two of the three wells were
tested by pressure buildup under stable-flowing conditions; a static-gradient survey was run on a
third well after a 3-week shut-in period. Original gas in place for this reservoir was calculated at
2.6 Bcf of gas (fig. 61) within an effective reservoir area of 250 acres when an average thickness
of 14 ft is used. The pressure data, adjusted for gas deviation factor (z), were plotted versus
cumulative production to determine the recoverable gas resource.

Evaluation of porosity from neutron-density well logs indicates that porosities of
20 percent occur in both the channel and splay facies of the F-21 reservoir. Engineering
evaluation of the conventional buildup test data indicates that permeability ranges from 40 to
95 md for thicknesses of 24 and 14 ft, respectively. Conventional permeability and porosity are
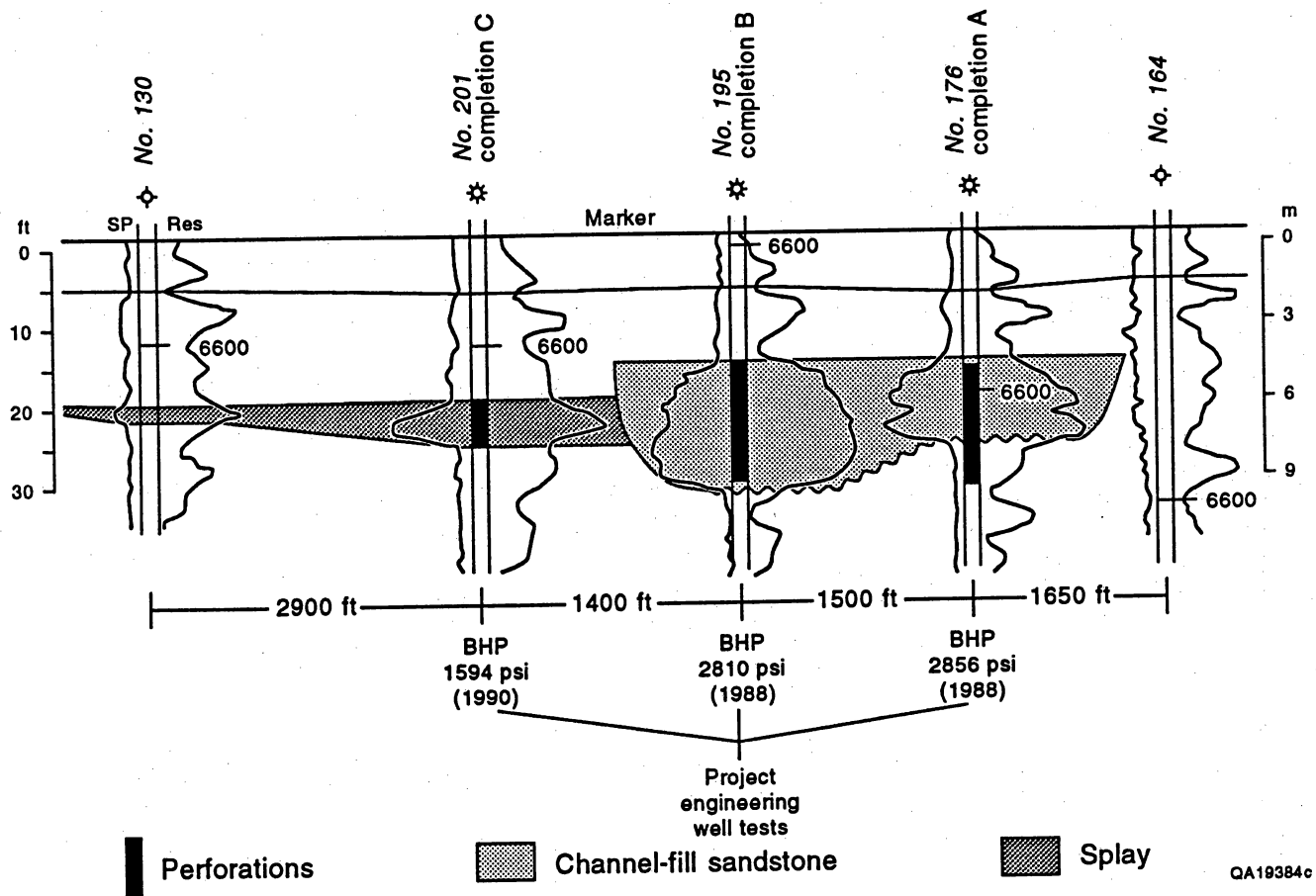
Figure 60. Stratigraphic cross section of example 1, a new infield reservoir. BHP indicates bottom-hole pressure. (See fig. 59 for location.)
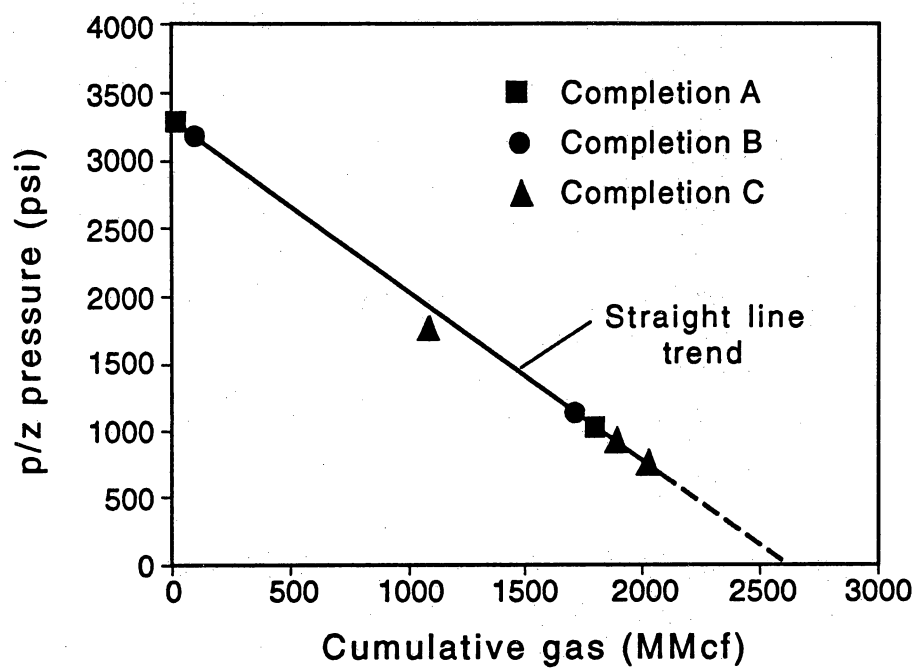
Figure 61. Pressure versus cumulative gas for three completions in example 1 of a new infield reservoir.

typical of this reservoir interval, which is characterized as a high-permeability (type I) reservoir using the classification of Grigsby and Kerr (1991).

The F-21 reservoir was initially encountered during a deeper pool test of reservoirs within the deltaic-dominated Vicksburg Formation. Analysis of well logs clearly indicated gas within the middle Frio Formation at a shallower horizon. Previous drilling in this portion of the field had indicated only minor shows of hydrocarbons, and maps of net sandstone indicated primarily nonreservoir facies in this portion of the field. Original reservoir pressure was discovered in the first completion in a new infield reservoir, and it indicated the need for a revised geologic interpretation to explain the gas production in this lithostratigraphic interval. Pressure and production information from the completions were collected by well testing. Engineering evaluation was incorporated into the revised geologic interpretation. The revised geologic interpretation and engineering data were critical for evaluating the effective utilization of well bores penetrating the reservoir. By matching the volumetric behavior with the mapped areal distribution of this reservoir, an operator can determine if the completions are achieving adequate contact with the resource target.

Magnitude of Secondary Gas Resource

The total secondary natural gas resource in this example (F-21 reservoir) is estimated at 2.6 Bcf. Cumulative production since the discovery of this new infield reservoir is 2.1 Bcf as of August 1, 1991. Categorizing these completions as penetrating a new infield reservoir is based on both geologic and engineering data. Recognition of new infield reservoirs is relatively simple compared with recognition of untapped reservoir compartments or of incompletely drained reservoirs that are productive in adjacent well bores. This new infield reservoir is interpreted as a single reservoir compartment, separate from equivalent prior production within the same lithostratigraphic interval or zone (Williams and Meyers, 1976). The flow-unit boundaries are defined by the transition from floodplain mudstone to channel and splay sandstones within a

118

single genetic stratigraphic unit. This example illustrates the effect of developing a gap in the well spacing to effectively exploit potential resources in a mature gas field.

3-D Imaging of New Infield Reservoirs

Analysis of the 3-D data volume in Stratton field indicate that high quality seismic can image subtle stratigraphic features in the fluvially deposited small compartment size reservoir groups. Using the previously described VSP thin-bed calibration procedure, 3-D imaging of closely spaced thin beds was produced to determine reservoir boundaries and topology in the interwell space. A 3-D amplitude map for the near F-21 reservoir (fig. 62) indicates that narrow (<300 ft wide) fluvial channel systems are mappable at 6,500 ft. These subtle features are identifiable between Wardner wells 201 and 176 (fig. 62).

Small Compartment Size Class Example: F-37 Reservoir

The second example (fig. 58) documents the impact of closely spaced completions (approximately 40-acre spacing) that have defined incremental gas resources in multiple-reservoir compartments. The F-37 reservoir interval is stratigraphically complex and after production was established in 1954, 1.65 Bcf of gas was produced in less than 2 years. Adjacent well bores in this region of the field were drilled to depths that either were slightly shallower than the productive interval or did not penetrate reservoir facies. Initial identification was based on new completions—part of an infield drilling program in the 1980's to deeper pool objectives in the Vicksburg Formation—that showed higher than expected pressures within an interval of previous production from middle Frio gas reservoirs. Six completions (completions A–F) were established by additional drilling (fig. 63). Analysis of the composite pressure history data for four of the completions made between 1977 and 1989 indicated that at least three separate untapped reservoir compartments exist within a 1-mi^2 area. Initial reservoir pressure of the first completion in 1954 was only 75 percent of original pressure (using a 0.45 psi/ft
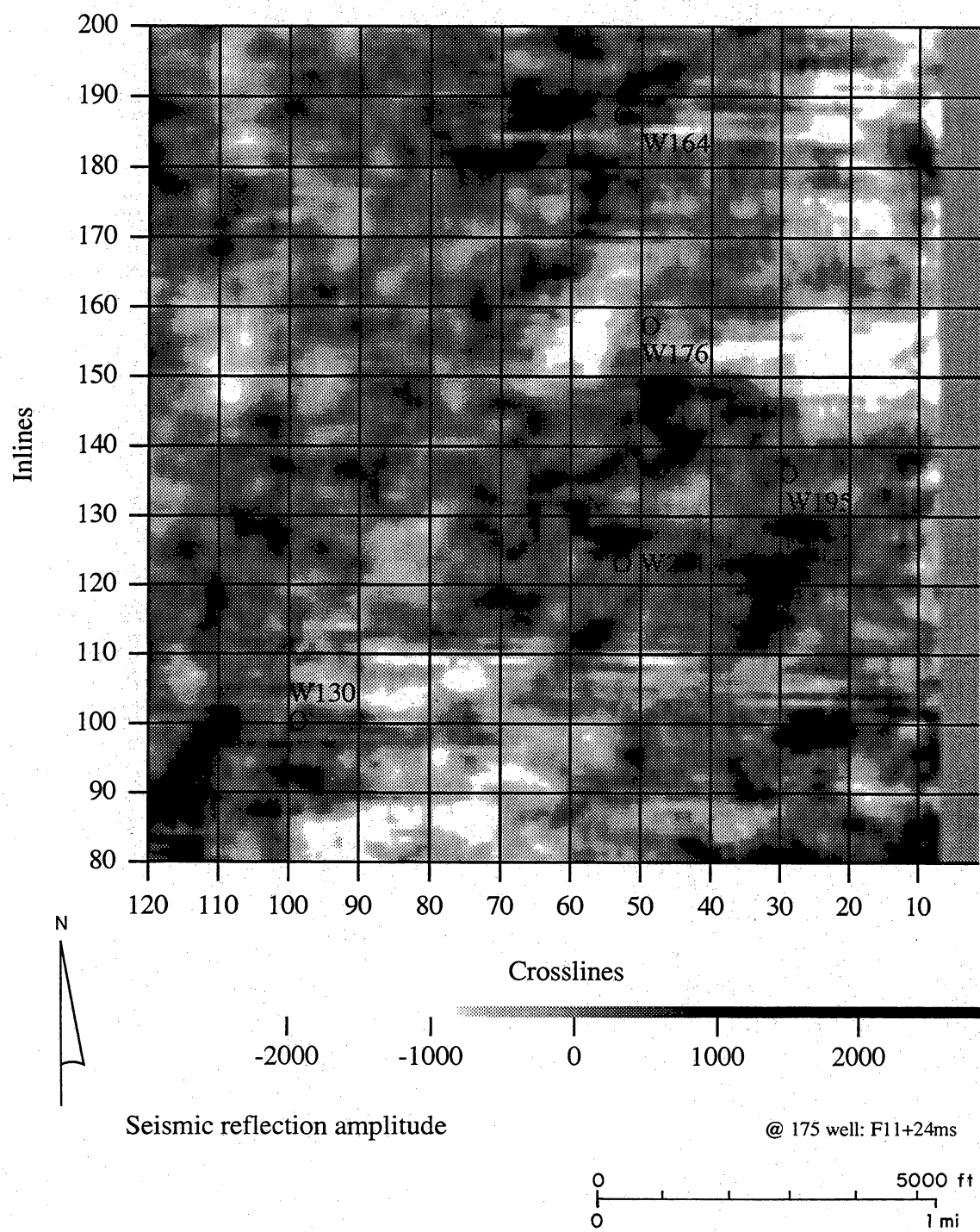
Figure 62. Seiscrop map of the F-21 reservoir in the Wardner lease 3-D data volume.
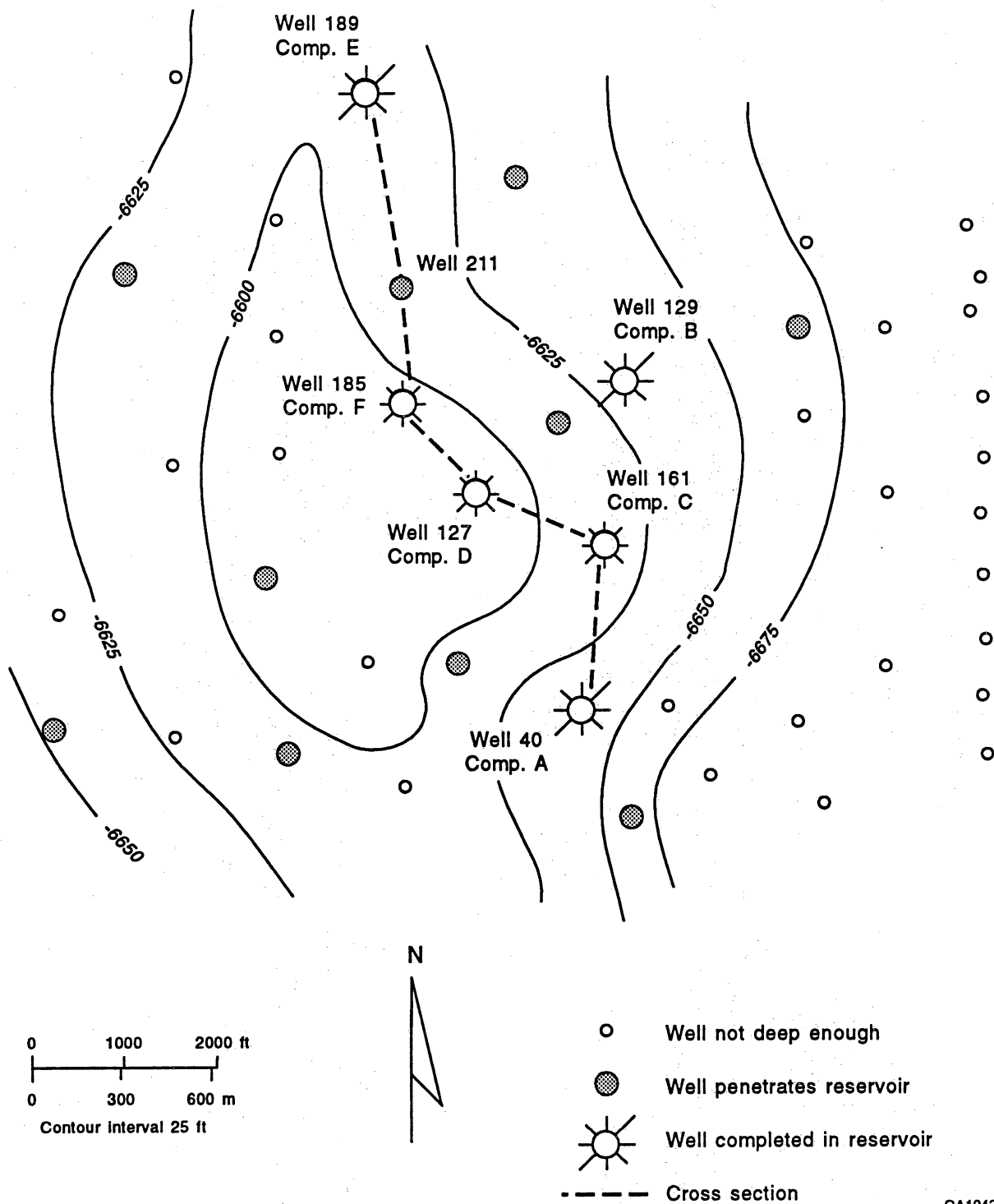
Figure 63. Map view of example 2 showing well-bore penetrations, completions, and structural horizon for multiple reservoir compartments.

gradient). Proximity to long-term established production on the adjacent Stratton field King Ranch lease block to the south raises the possibility of production from this lithostratigraphic interval by previously drilled nearby wells.

Between 1983 and 1989 the bottom-hole pressures of the completions ranged from 1,950 psi to 3,178 psi within a 50-ft vertical interval (fig. 64). Evaluation of engineering and geologic data indicated that narrow fluvial channel systems within a group of closely spaced completions showed a high degree of stratigraphic and reservoir pressure variability. Well log evaluation indicates sandstone reservoir porosities of 20 to 25 percent. In situ reservoir permeability determined from SGR project well tests ranged from 10 to 92 md for reservoir thicknesses of 5 to 11 ft. Conventional permeability and porosity are characteristic of this reservoir interval and indicate a high-permeability reservoir (type I of Grigsby and Kerr, 1991). Multiple completions spaced between 40 to 80 acres apart in the same reservoir exhibit independent pressure (fig. 65) and drainage volumes (fig. 66). Integrated geologic and engineering analysis is required to explain the observed stratigraphic and pressure behavior of these multiple-reservoir compartments. Identifying untapped reservoir compartments within a currently or previously producing zone usually requires detailed correlation of the perforated intervals with well test pressure measurements. Pressure measurements permit comparison of the reservoir pressure in previously producing reservoir intervals with that of later completions.

Magnitude of Secondary Gas Resource

This example documents the impact of closely spaced completions that have contacted incremental resources estimated at approximately 1.5 Bcf per recompletion. Initial interpretation indicated that two reservoir sandstones within a 50-ft vertical interval could be correlated fairly continuously across the area. Six completions have been successful in an area of 640 acres (fig. 63). Analysis of the composite pressure history data for five of the
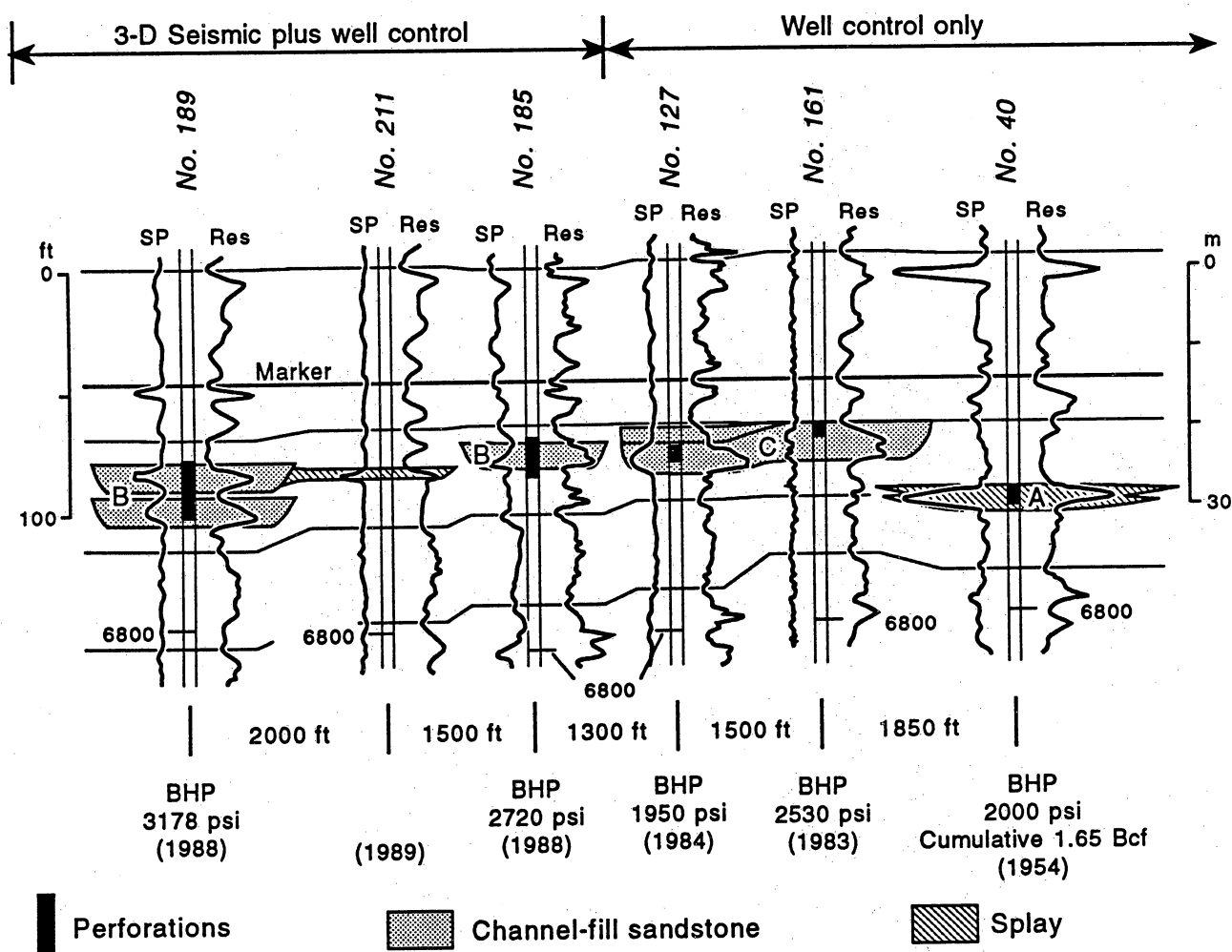
Figure 64. Stratigraphic cross section of example 2 showing multiple reservoir compartments. (See fig. 63 for location.)

125

Figure 65. Composite pressure versus time for multiple reservoir compartments (example 2).
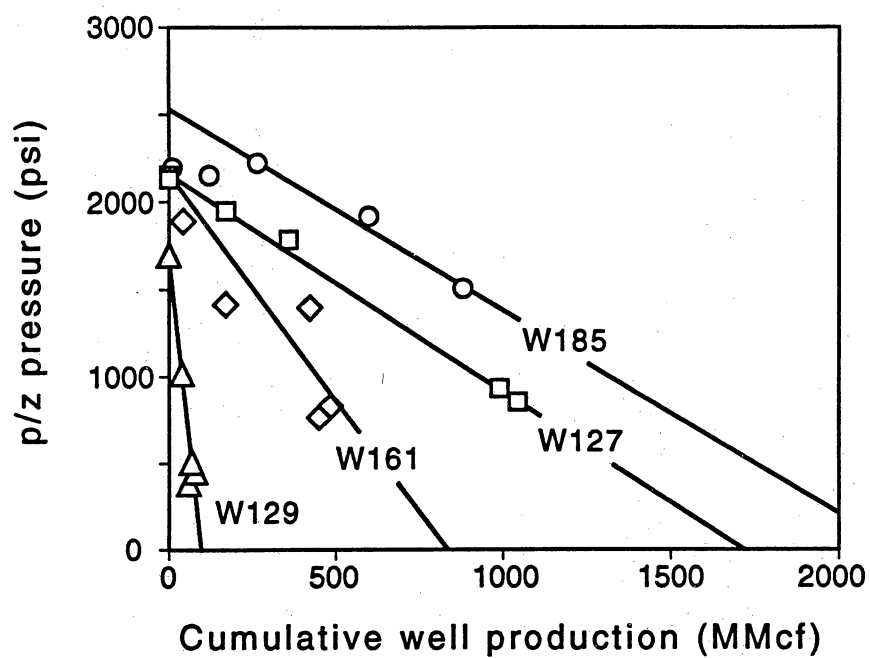
QA19390c

Figure 66. Pressure versus composite cumulative gas for multiple reservoir compartments (example 2).

recompletions made between 1977 and 1989 indicated that at least three separate reservoir compartments have been encountered in these five recompletions. Several reservoir compartments are interpreted to be composed of multiple isolated fluvial channels that are less than 10 ft thick. Infield development indicates that close completion spacing (about 40-acre spacing) can access reserve additions that would not otherwise be captured with wider well spacing.

3-D Imaging of Untapped Reservoir Compartments

In the northern half of the 3-D grid, seismic images constructed in a short vertical interval containing the lower F reservoirs have several similarities. However, an obvious meandering channel labeled as A-B-C (fig. 67) is present in the southern part of the seismic image but is not identifiable in a seismic image less than 10 ms deeper in the data volume (fig. 45). This channel feature illustrates a most important point regarding seismic thin-bed interpretation: subtle, thin-bed fluvial features can be present in one 3-D viewing surface and absent in a second surface that is separated from the first by an extremely small time interval of the order of 10 ms or less. This key observation again stresses the importance of precisely calibrating stratigraphic depth to seismic travel time when interpreting thin beds. The log-based geological model of the F-37 stratigraphy was developed before the 3-D seismic data were recorded. Some of the wells used in this model construction are located in the southern portion of the 3-D seismic grid, as indicated in the expanded view of the seismic image in figure 68. There is a reasonably good correspondence between this geological model and the seismic image in that both the model and the image indicate that wells 185 and 189 are in a fluvial channel-fill environment at the reservoir level but that Wardner well 211 is in a crevasse splay. Of even greater importance is the comparison with the pressure information summarized in figure 65. Only Wardner wells 129 and 185 included in this analysis are inside the 3-D grid, but these two wells show a much different pressure behavior, which requires that a compartment boundary be located in the
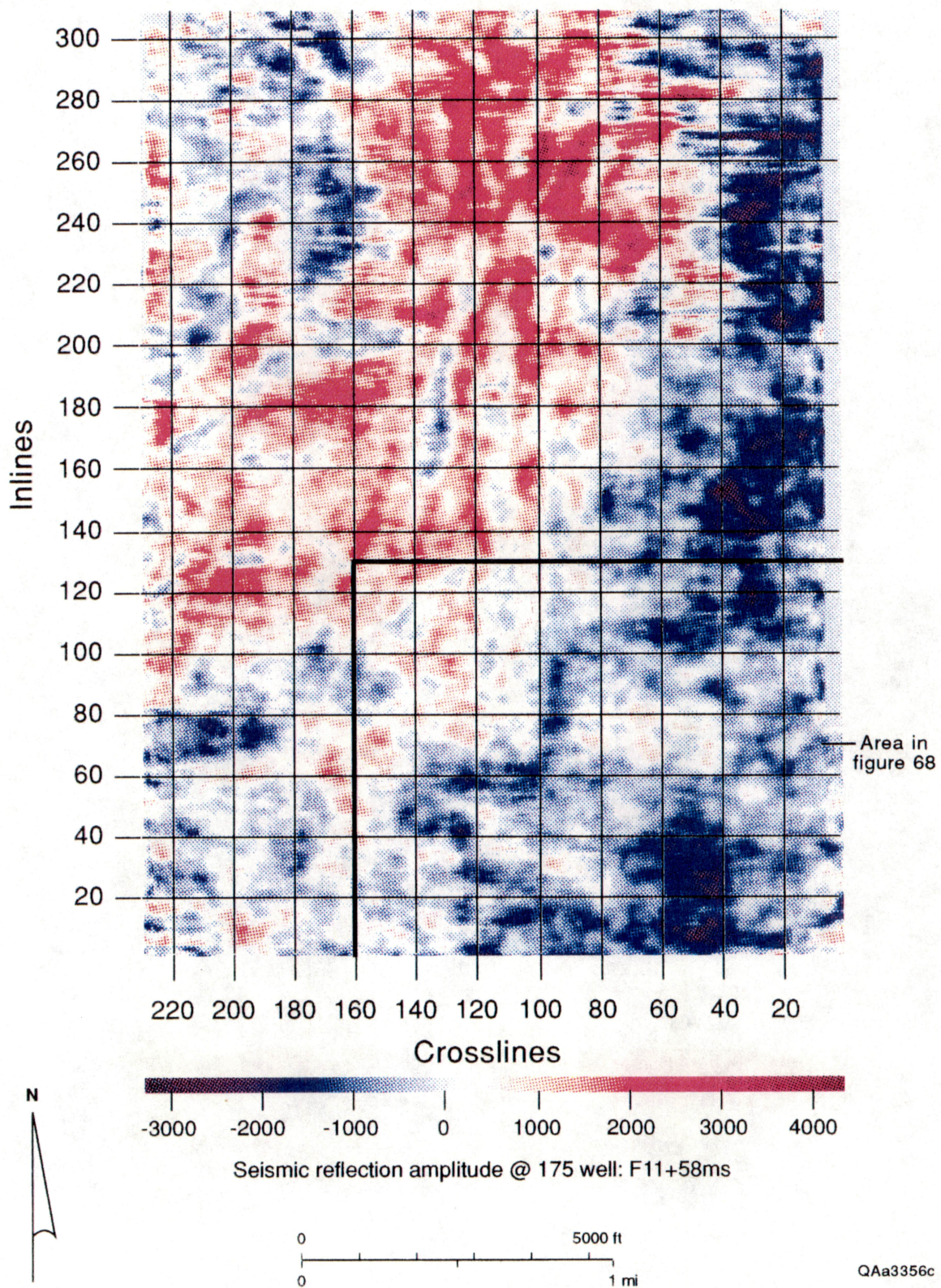
Figure 67. Seiscrop map of the F-37 reservoir in the Wardner lease 3-D data volume.
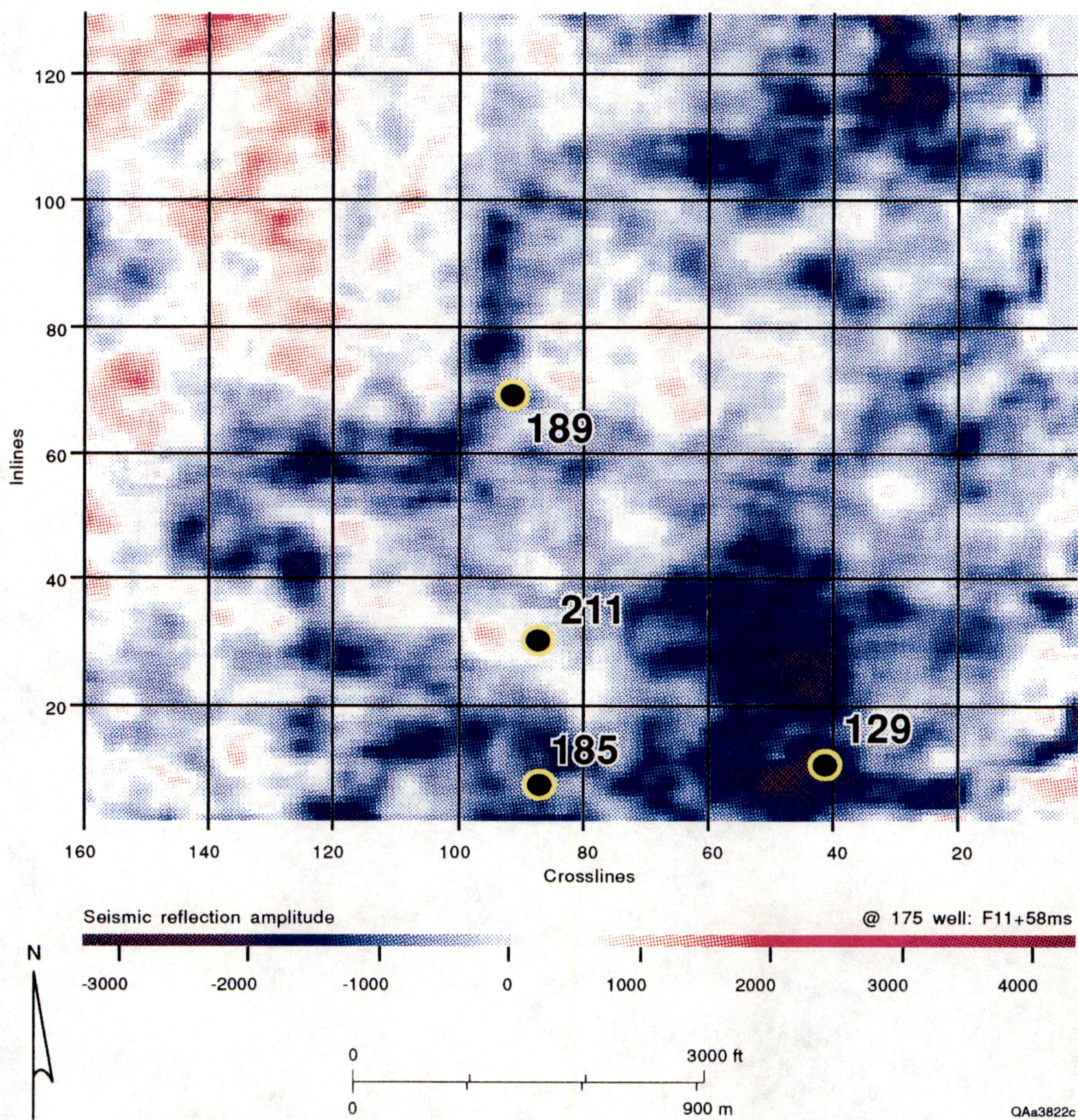
Figure 68. Expanded seiscrop map of the F-37 reservoir in the south part of the Wardner lease 3-D data volume.

interwell space between wells 129 and 185. The combined well log and 3-D seismic image interpretation shown in figure 69 confirms this concept of two distinct reservoir compartments, because the channel labeled C cuts between wells 129 and 185. In this case, the important contributions of the 3-D image are (1) defining what type of stratigraphic feature most likely produced the compartment boundary (that is, a channel cut), and (2) specifying the precise location of the suspected boundary so that future infield drilling can be optimally located.

Small Compartment Size Class Example: F-20 Reservoir

The F-20 reservoir, an example of an incompletely drained reservoir compartment (fig. 9), documents the addition of significant reserves even when initial reservoir pressure of a new completion is only one-third of the original reservoir pressure. Historical analysis of production data, combined with geologic mapping, demonstrates that an approximately 40-acre offset location from previous production with depleted reservoir pressure is contacting additional gas from the same zone (fig. 58). In 1962 two infield development wells were drilled in the southwestern part of the field to deeper pool objectives (>7,000 ft). The first well in 1962 did not test the F-20 reservoir and was abandoned as a dry hole. The second well in 1962 was completed in the middle Frio Formation in a gas sandstone interpreted as a fluvial channel fill (fig. 70). An initial completion pressure of 3,113 psi was measured from the bottom-hole pressure survey. Completion A produced 1.6 Bcf of gas from 1962 to 1980, prior to abandonment. In 1980 an offset well (1,100 ft to the northwest) was drilled that penetrated the equivalent stratigraphic reservoir interval in a structurally lower position (fig. 71). The initial bottom-hole pressure of completion B (18 years later) was measured at 995 psi, which is substantially lower than the original reservoir pressure of 3,130 psi (using a 0.45 psi/ft gradient). Permeability of this reservoir at the second completion was calculated at 10 md on the basis of a backpressure test. Permeability of completion A is believed to be similar in magnitude to that of completion B.

N

3-D seismic plus well control

Well control only

Seismic imaged
intra-channel
barrier ?

189
211
185
129
127
161
40
C
B
A

0   3000 ft
0   900 m

○——○ Cross section   Splay   A   B   C

Fluvial-channel

QAa3359c
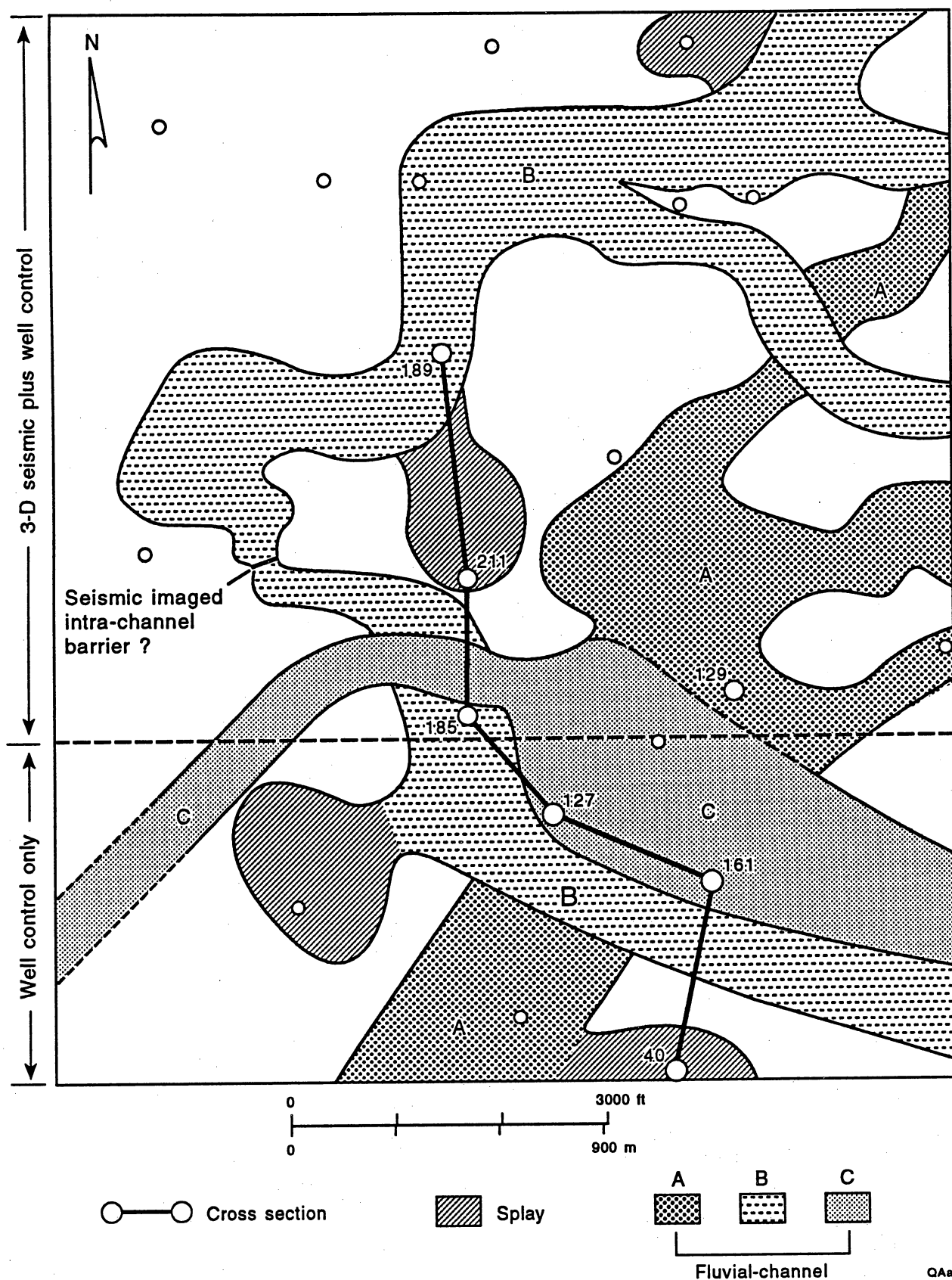
Figure 69. Interpretation using well control and 3-D seismic data volume in the south part of the Wardner lease 3-D data volume.

134
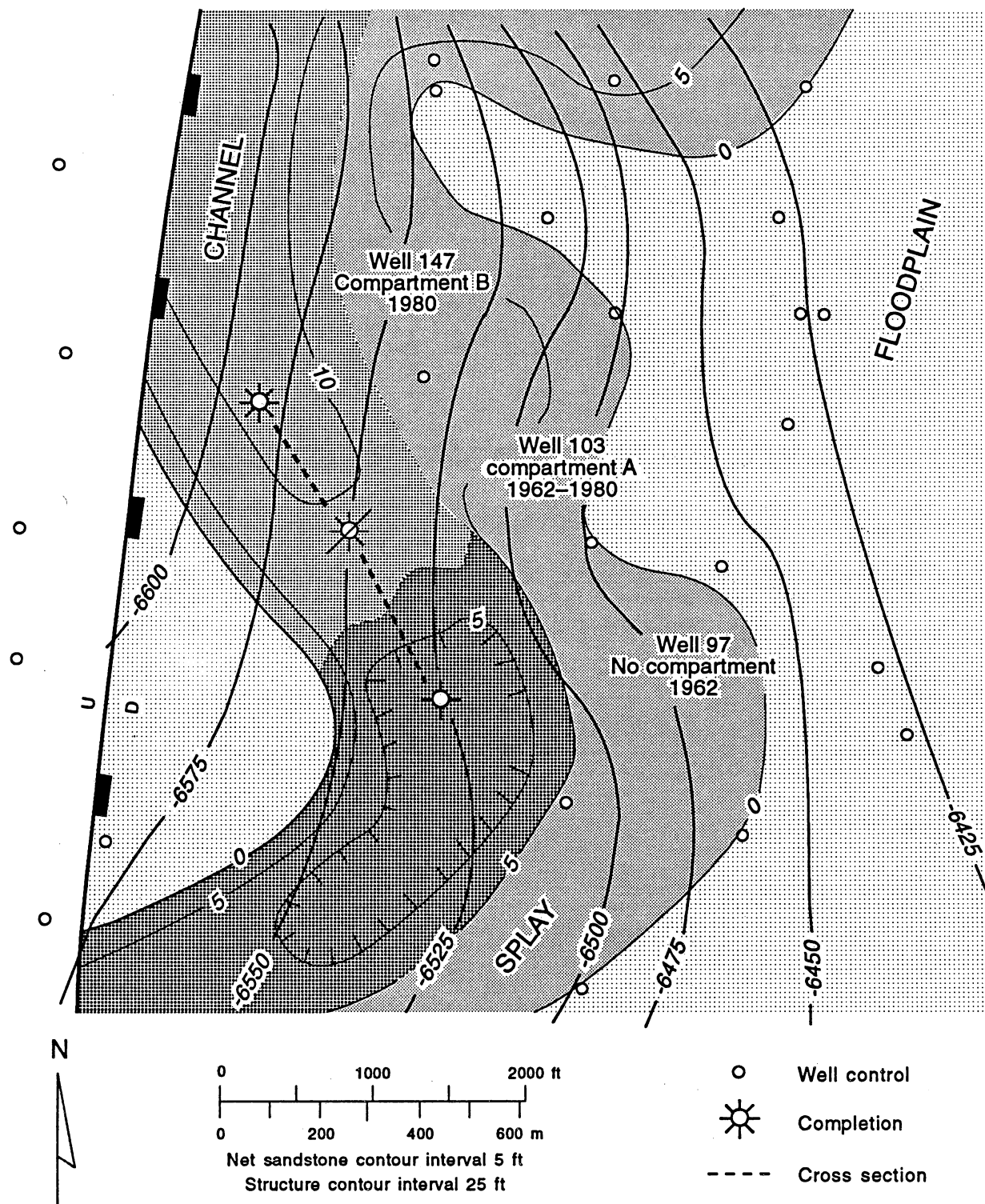
Figure 70. Map view of example 3 showing well-bore penetrations, completions, and structure horizon for an incompletely drained reservoir compartment.

No. 147
completion B

No. 103
completion A

No. 97

1980 – 1990
Cum. 2.0 Bcf
EUR 2.6 Bcf

1962 – 1980
Cum. 1.6 Bcf
EUR 1.6 Bcf

1962

SP   Res

Marker

ft

m

0

0

1

2

50

15

—— 1100 ft ——

—— 1300 ft ——

Initial BHP
995 psi
(1980)

Initial BHP
3113 psi
(1962)

█ Perforations

----- Barrier

1 Reservoir compartment 1
2 Reservoir compartment 2
░ Channel-fill sandstone
▓ Shaly sandstone channel fill
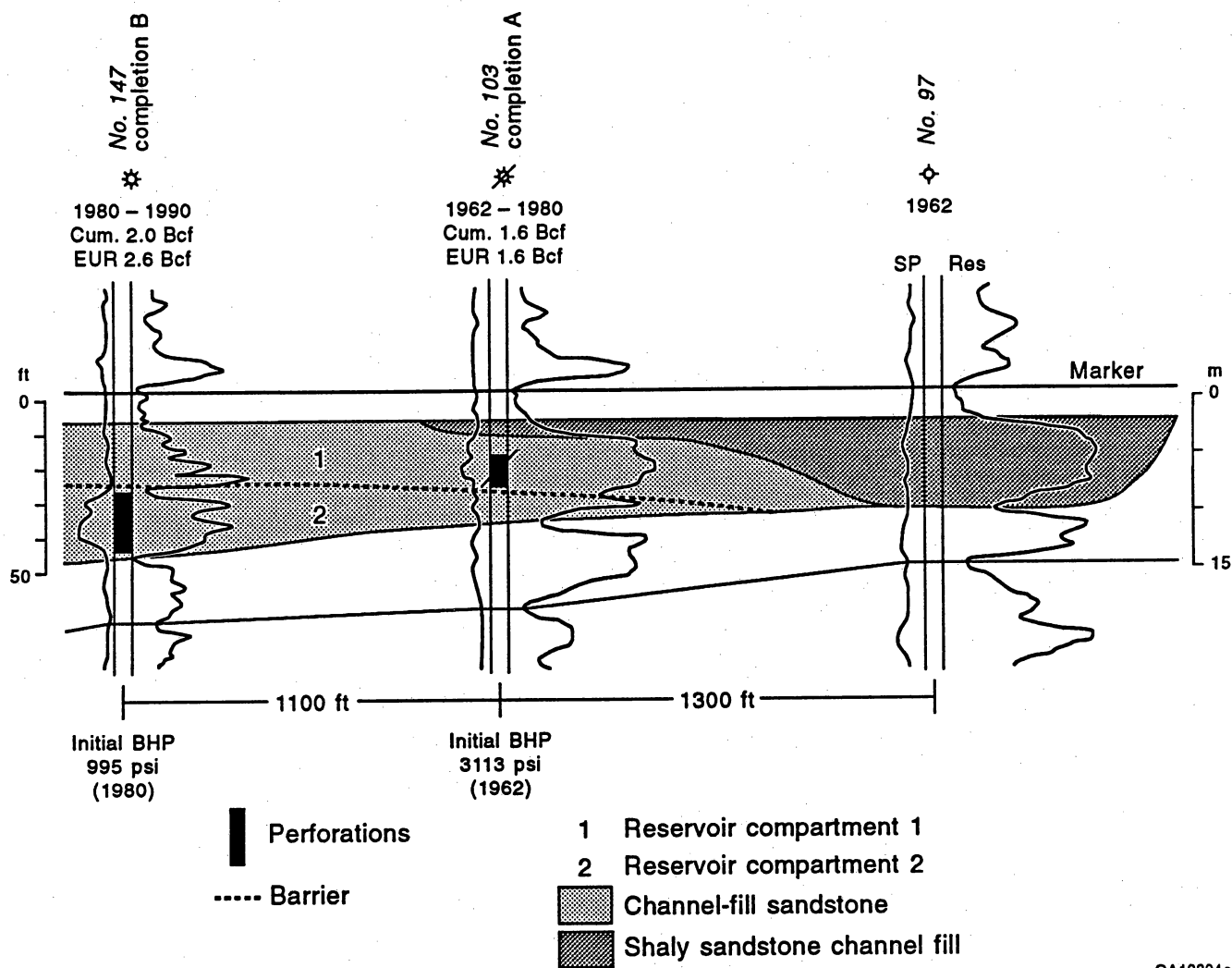
QA19394c

Figure 71. Stratigraphic cross section of example 3, an incompletely drained reservoir compartment (cum. refers to cumulative production; EUR refers to estimated ultimate recovery). (See fig. 70 for location.)

Magnitude of Secondary Gas Resource

Detailed stratigraphic correlation indicates that a thin (<3 ft) intrareservoir marker within this same lithostratigraphic interval may be a clue to the existence of two gas flow units separated into compartments by a partial permeability barrier. Analysis of the production-rate data for the first completion (well 103) indicated a linear trend with no evidence for pressure support, and rate data alone are not adequate to identify volumetric or compartmentalized reservoir behavior. Static reservoir pressure information indicated an elevated pressure for the second completion (well 147), relative to the abandonment pressure of the first completion (fig. 72). A nonlinear decline of reservoir pressure with cumulative production in the same zone or reservoir interval (fig. 39) indicates an incremental resource is being accessed by the second completion, across a barrier or baffle to gas flow, and from an incompletely drained reservoir. The first completion also showed the potential effects of pressure recharge following a 1-year shut-in period (fig. 73). This pressure recharge into the partially depleted gas compartment of the first completion is interpreted as leakage of gas across the intrareservoir barrier identified on well logs. It is an indication of internal compartmentalization of the reservoir into two separate flow units. In this example the recovered incremental resource is 2 Bcf of gas. This is the volume of secondary gas obtained after the abandonment of well 103. Detailed correlation of SP and resistivity logs shows that these flow units represent compartmentalization within the same lithostratigraphic interval, interpreted to reflect lateral accretion in a multistory fluvial channel system. Because of the reduced reservoir pressure, incompletely drained reservoir compartments are difficult to recognize when contrasted with new infield reservoirs or untapped reservoir compartments that often have original or near-original reservoir pressures.
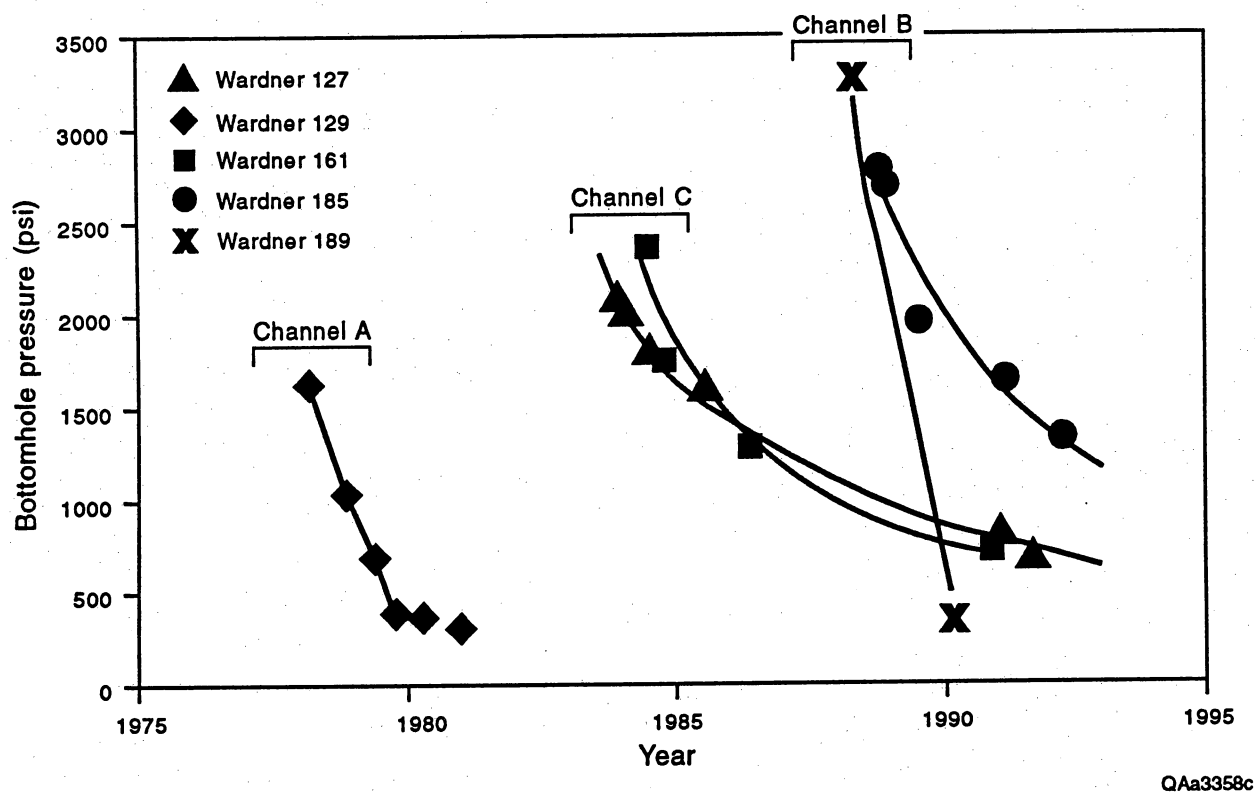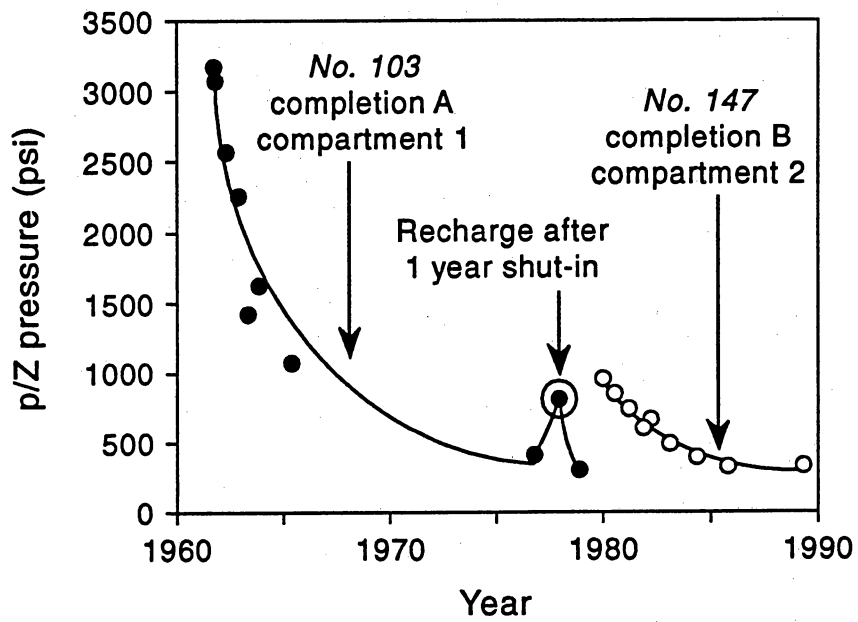
Figure 72. Composite pressure versus time for an incompletely drained reservoir compartment (example 3).
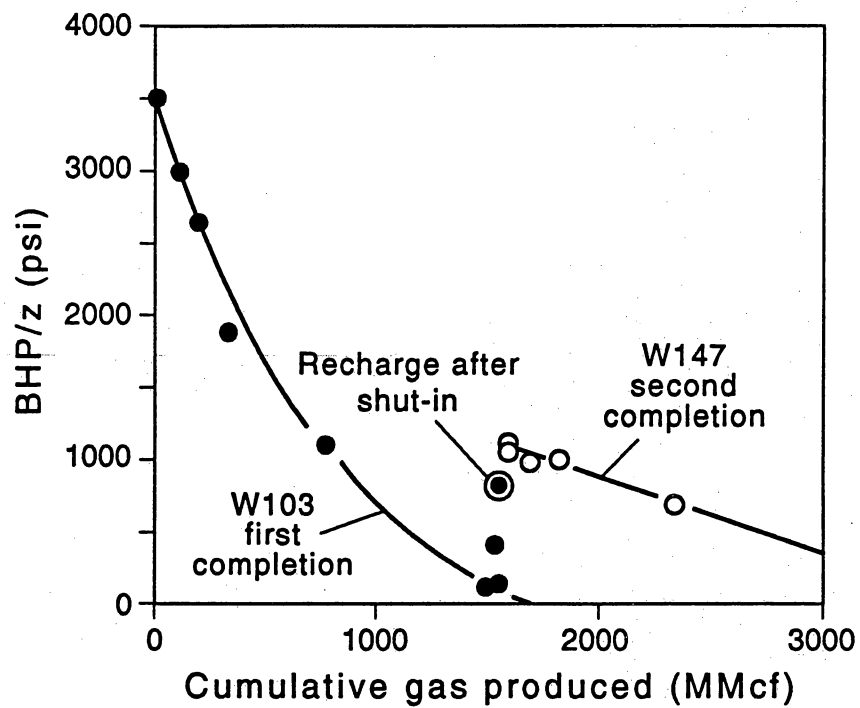
QA19396c

Figure 73. Pressure versus composite cumulative gas for an incompletely drained reservoir compartment (example 3).

Seismic Imaging of Incompletely Drained Reservoir Compartments

Incompletely drained reservoir compartments caused by internal heterogeneity of the reservoir containing barriers or baffles to gas flow are difficult to image seismically. Intrareservoir compartmentalization within a depositional genetic unit caused by shale drapes or diagenetic cements that affect reservoir properties are beyond surface seismic resolution even in areas where VSP thin-bed calibration techniques are effective for delineating thin-bed reservoir depositional surfaces similar to those extracted from the Stratton field 3-D data volume. The high-resolution, low-noise conditions needed for imaging these intrareservoir heterogeneities will probably require cross-well seismic reflection imaging for delineation and characterization of gas reservoirs. Future high-resolution cross-well profiling may provide the improved spatial resolution needed for this type of reservoir delineation.

FORWARD STOCHASTIC MODELING: IMPACT ON INFIELD DEVELOPMENT STRATEGIES

The G-WIZ compartmented gas reservoir simulator was used to build a stochastic model and define an approach to understanding effective well spacing in different compartment size classes. The stochastic technique generates realizations of fluvial reservoirs having internal compartments with intervening barriers. Simulations of multiple reservoir realizations honoring statistical distributions determined from reservoir and field production data yield a unique probability distribution of expected gas recovery for various well spacings and different temporal development scenarios. Gas recovery for the three reservoir classes are evaluated at four well spacings, from 640 acres to 80 acres. By this method, statistical predictions of recovery are generated for each of the three reservoir classes. The technique is generic and can be used with different depositional systems to analytically define optimal well spacing relative to recovery factor and real compartment size distributions. For example, in the small compartment size class, an incremental recovery potential of 24 percent is predicted by decreasing completion spacing from 320 acres to 160 acres.

Identifying Reservoir Compartment Size

Identifying the compartment size class of a reservoir is best accomplished by using the G-WIZ reservoir simulator and developing statistics of primary pore volume and barrier transmissibility from production histories of wells completed in the reservoir. The G-WIZ model is applied as a two-compartment system for each of several wells. An evaluation of 10 or more wells should be sufficient for identifying the appropriate compartment size class to which the group of wells belongs. The statistical distributions of the data from the G-WIZ analyses can be compared with the plots in figures 28 and 29 to determine which compartment size class is appropriate. Another approach to identifying the reservoir compartment size is by analogy of the depositional facies and reservoir architecture. By comparing the spatial framework of fluvial reservoirs from other fields with that of reservoirs in the Stratton–Agua Dulce field study, the compartment size class of an analogous reservoir can be estimated.

Monte Carlo Reservoir Generation

The Monte Carlo technique used to generate the reservoir realizations is based on the construction of reservoir compartments with the form of an isosceles triangle. This shape was selected because it encloses an area with the minimum number of sides. These compartments are distributed in a slightly meandering linear pattern, as shown in figure 74. The stochastic generation of this fluvial channel reservoir model is shown in figure 75. Figure 75a shows that compartments 1 through 4 have been generated. The next compartment to be generated can be attached to either the left or right face of compartment 4, as shown in figure 75b. The attaching face is determined by random selection, or computer simulation of a coin toss. The selection is biased by the geologic model of the reservoir. A fluvial channel has a predominantly linear direction as the river flows downdip to the sea, and a directional bias creates a realistic reservoir shape of channel growth in a downdip direction. The left and right faces are assigned probabilities (P left and P right) that sum to unity and that have values that depend on the
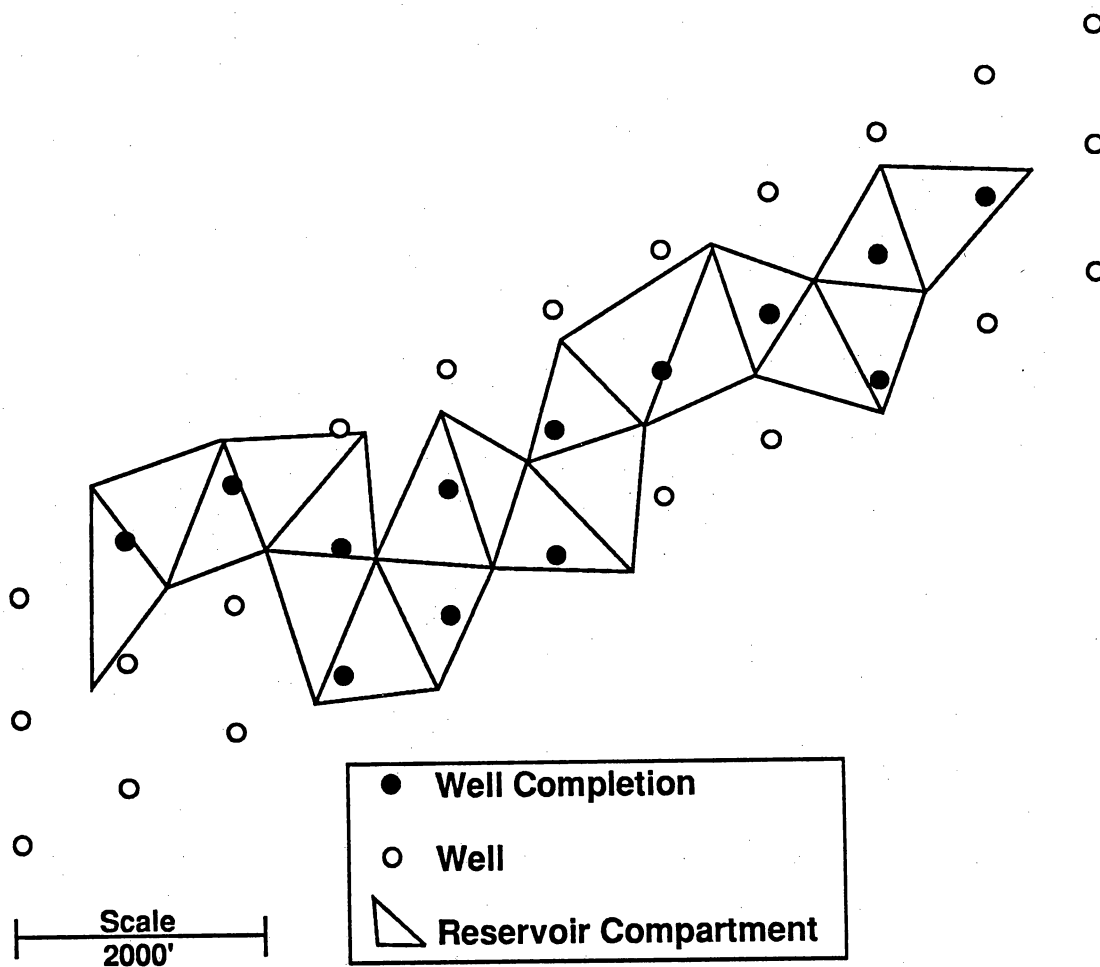
Figure 74. Plane view of Monte Carlo reservoir compartment generation.
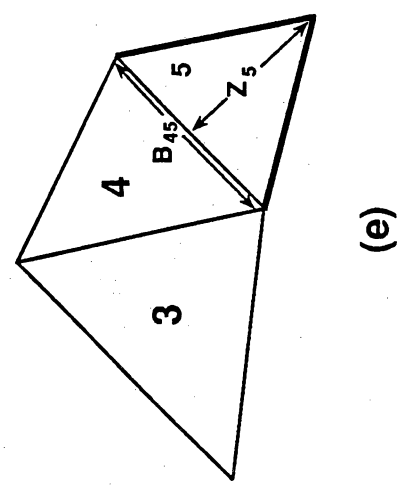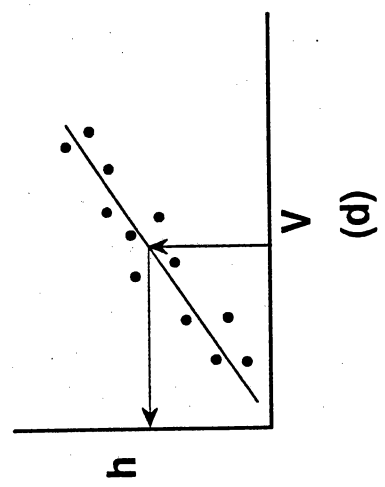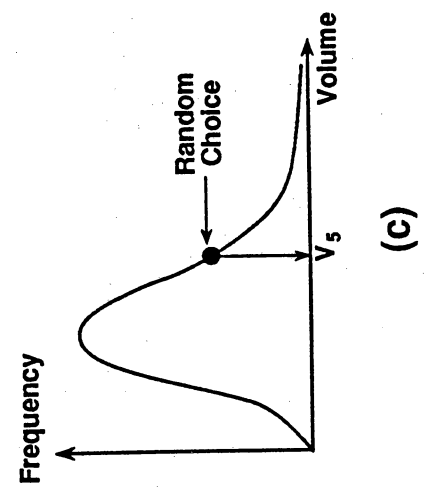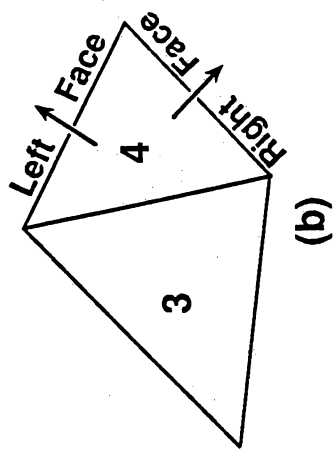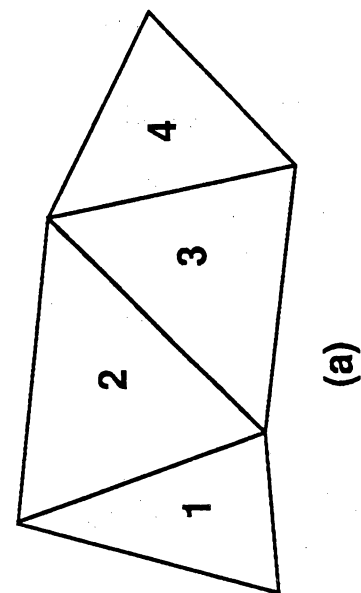
Figure 75. Diagrammatic sketch of methodology showing how compartments are added to create a reservoir realization.

143

angle between the dip direction and the normal to the face. The downdip face acquires the greater probability. A triangle addition is not allowed if it causes the meandering channel to intersect itself. After the face for growth direction is determined, a compartment volume is obtained by random selection from a population generated with a mean and variance appropriate for the statistical distribution of the reservoir class to be evaluated. The selection process for the volume of the compartment (V_5) is shown in figure 75c. An average thickness (h_5) is assigned to the compartment volume from the correlation of net thickness and compartment pore volume characteristic of this compartment size class, as shown in figures 30 and 75d. The gas-saturated porosity (fS_g) is assigned a constant value in all compartments across the reservoir. The area for triangle 5 is then computed by dividing the pore volume by the thickness and gas-saturated porosity. Since the base side for this new triangle is fixed as the appropriate side of triangle 4 (B_{45}), the height (Z_5) of the new triangle is computed from the familiar formula for the area of a triangle where the base and height are known. With the height of the new triangle determined, the generation of the fifth compartment is completed, as shown in figure 75e. This process is repeated until a specified number of compartments have been generated. Figure 76 shows the variability of three reservoir realizations generated with the same population of compartment volume and thickness correlation for a small compartment size class reservoir.

After the geometry for a reservoir realization is generated, the transmissibilities for the interfaces between compartments are generated also by a Monte Carlo technique. Transmissibility between compartments is generated from a population of transmissibilities created using the geometric mean transmissibility and variance of the log value of transmissibility about this mean from the appropriate compartment-class statistics. Transmissibility between compartments is treated as a parameter independent from compartment volume. Simulated gas recoveries can be generated for each reservoir realization using the G-WIZ model after assigning reservoir parameters, gas properties, and well production
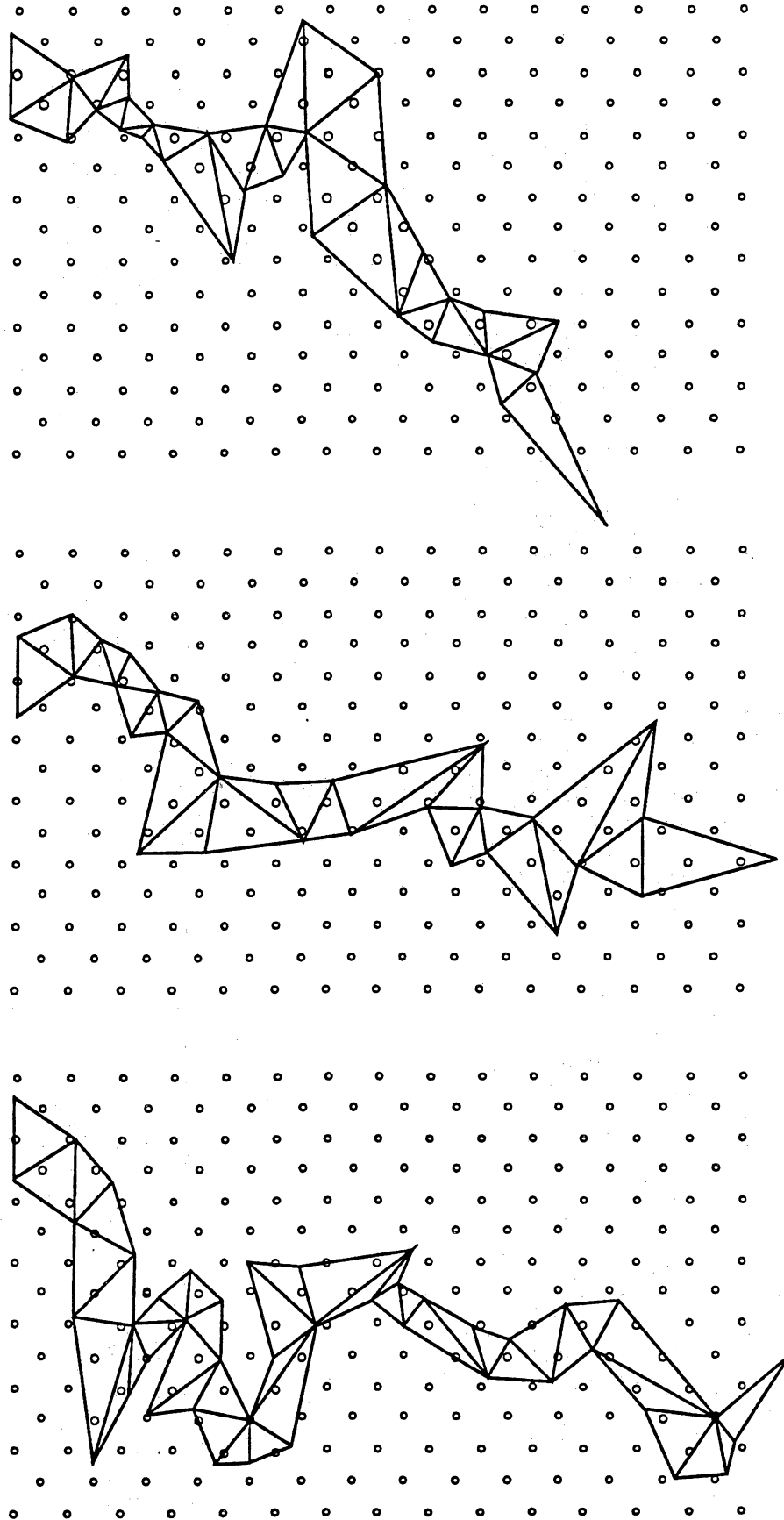
Figure 76. Plane view showing variability in reservoir realizations for small compartment size class.

parameters that honor the operational conditions that are most common in the reservoir being evaluated.

Stochastic Simulations

Stochastic simulations of recovery for each compartment size class from the spectrum of fluvial reservoirs in Stratton–Agua Dulce field were generated. These simulations are used to evaluate the relationship between recovery and well spacing where Monte Carlo techniques were used to generate functional reservoir parameters used as input in the G-WIZ compartmented gas reservoir simulator. The reservoir parameters are based on actual field production data from 10 reservoir groups (figs. 28 and 29). This analysis provides a template for evaluating the infield development potential of a field or reservoir in a quantitative manner. The stochastic simulations were performed with the G-WIZ compartmented gas simulator modified to allow more than 100 compartments and wells and direct input of the compartment and well data generated by the separate Monte Carlo computer program.

The stochastic simulations were performed by performing these three tasks:

(1) Generate 100 reservoir realizations by Monte Carlo processes consistent with the statistics of compartment volume and transmissibility for the reservoir class to be evaluated.

(2) Overlay each reservoir realization with a uniform grid of well locations at a fixed spacing and identify those wells which contact the reservoir.

(3) Evaluate gas recovery at well spacings of 640, 320, 160, and 80 acres per well.

Reservoir properties of temperature and pressure were based on the average values from the 10 reservoir groups evaluated in the compartment size study. An initial reservoir pressure of 2,500 psi and a temperature of 175°F were used in the reservoir realizations with a gas gravity of 0.65 to generate gas PVT and fluid properties. All wells were assigned an inflow Darcy coefficient typical of the values determined from the evaluation of the 256 completions in the Stratton–Agua Dulce compartment size study. The simulations were pressure specified with

146

wells flowing at a bottomhole pressure of 250 psi, and abandonment conditions were assigned at 50 Mcf/d.

Optimum Number of Reservoir Realizations Needed to Simulate Gas Recovery

The first investigation performed was to determine the number of reservoir realizations required to adequately define the frequency distribution (mean and standard deviation) of gas recovery. Figure 77 shows the simulation results for the case of the medium compartment size class on 640-acre well spacing in which all wells were completed at the same time. Frequency distributions of recovery for 10, 20, 40, 60, 80, and 100 realizations are shown. The examples show that the standard deviation is adequately defined when more than 80 realizations are simulated. To assure good statistical results from the simulations, 100 realizations were performed for each gas recovery case evaluated.

Effect of Infield Development Timing on Gas Recovery

An assessment of the variability of recovery from the temporal sequence of completions was assessed and a standard development sequence was used for all subsequent runs. Four development sequences were compared to evaluate the effect of timing of infill development on recovery:

Case 1. Primary wells are all completed at the same date. Infill wells are completed on the same date 10 years after primary well development.

Case 2. Primary well development is completed uniformly over a 5-year period. Infill well development starts 10 years after primary well development and is completed uniformly over a 5-year period.

Case 3. Primary wells are all completed on the same date. Infill wells are completed on the same date when the average pressure of producing compartments is 50 percent of the original pressure.
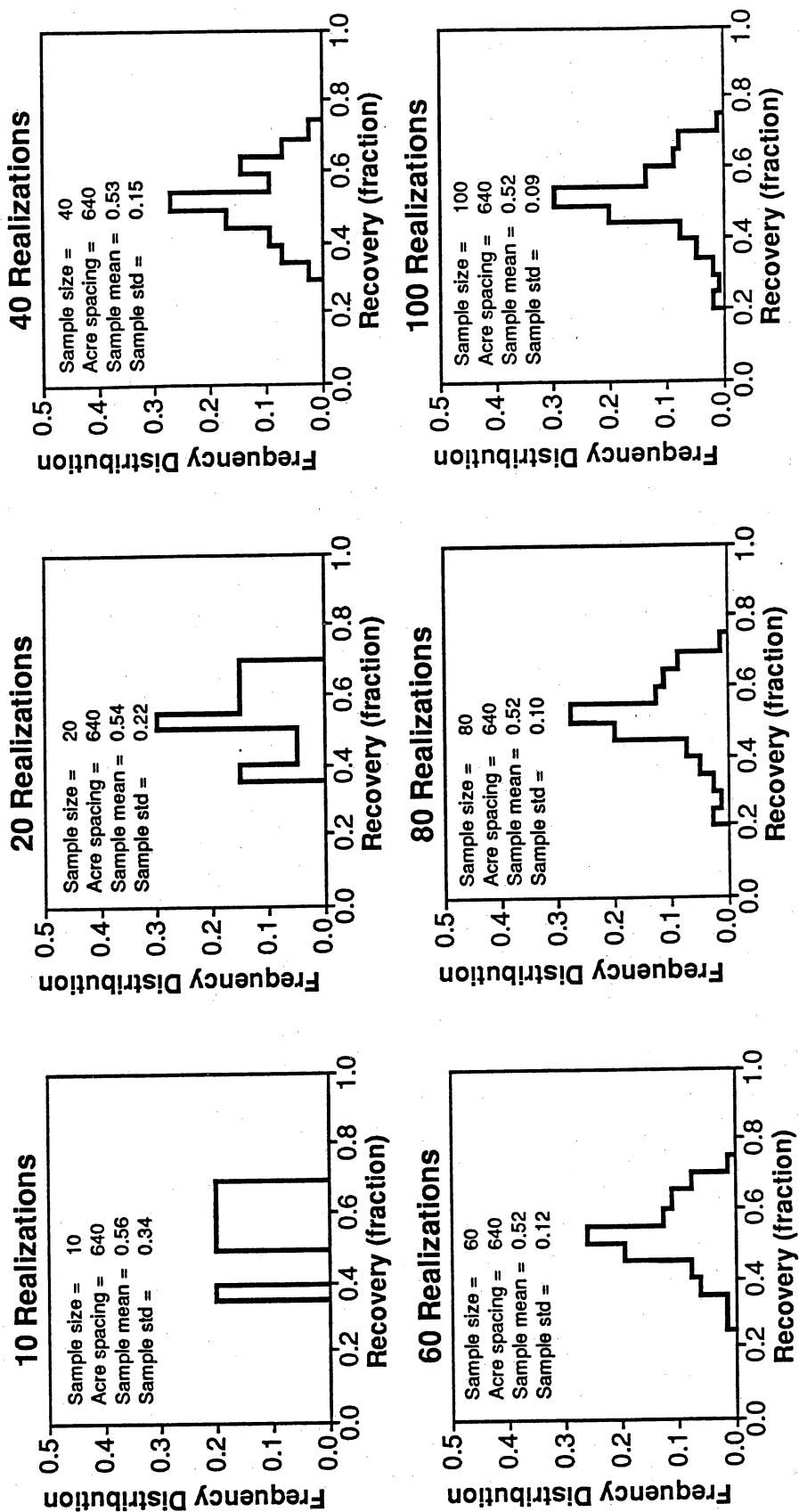
Figure 77. Frequency distribution illustrating sample size effects on gas recovery using 10, 20, 40, 60, 80, and 100 reservoir realizations for a medium compartment size class.

148

Case 4. Primary wells are completed on the same date. Infill wells are completed on the same date when the producing rate from 50 percent of primary wells have declined to 50 Mcf/d and are subsequently abandoned.

Example simulation results from the medium compartment size class reservoirs for 640-acre spacing infilled to 320-acre spacing are shown for these four cases in figure 78. Infill cases 1, 2, and 3 yield essentially the same recovery results. Case 4 yields a slightly smaller recovery where half of the wells are abandoned before infill development. Generally it was found that using any of infill completion cases 1, 2, or 3 would yield the same recovery factor after infill was completed if the initial spacing was the same as the final infill spacing. The timing of primary and infill development is determined not to be a significant factor affecting recovery. Case 2 was selected for studies of incremental recovery.

Effect of Infield Development Spacing on Gas Recovery

With the issues of sufficient realizations and development timing determined, recoveries from the three compartment size classes were evaluated at four well spacings in a simulation study using the G-WIZ simulator. A frequency distribution of 100 realizations for recovery factor was obtained at each well spacing for each reservoir class. The mean recovery factor and the standard deviation were determined from the frequency distribution obtained for each well spacing. The recovery factor for each realization was computed from the original gas in place (OGIP) and the cumulative gas produced by the wells in the model to an abandonment rate of 50 Mcf/d per well.

Figures 79 and 80 exhibit frequency distributions of recovery from 100 reservoir realizations using the case 2 development schedule for small and medium compartment size class reservoirs. Note the difference in the variance (a larger standard deviation) in recovery from these two reservoir classes. Greater variability is evident in the small compartment size class reservoir and is an attribute of the statistical character of the reservoir class.

149
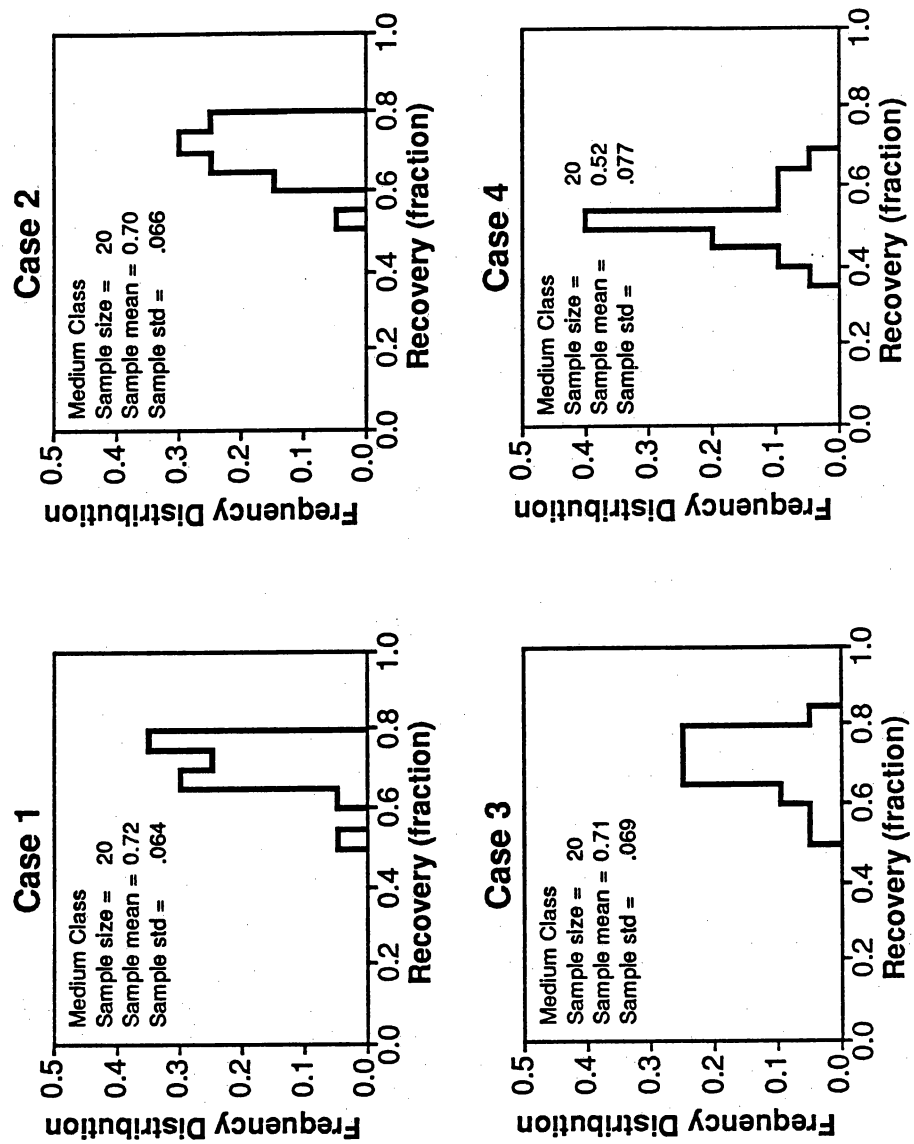
Figure 78. Frequency distribution illustrating effect of completion schedule of infill wells on ultimate gas recovery for the medium compartment size class.
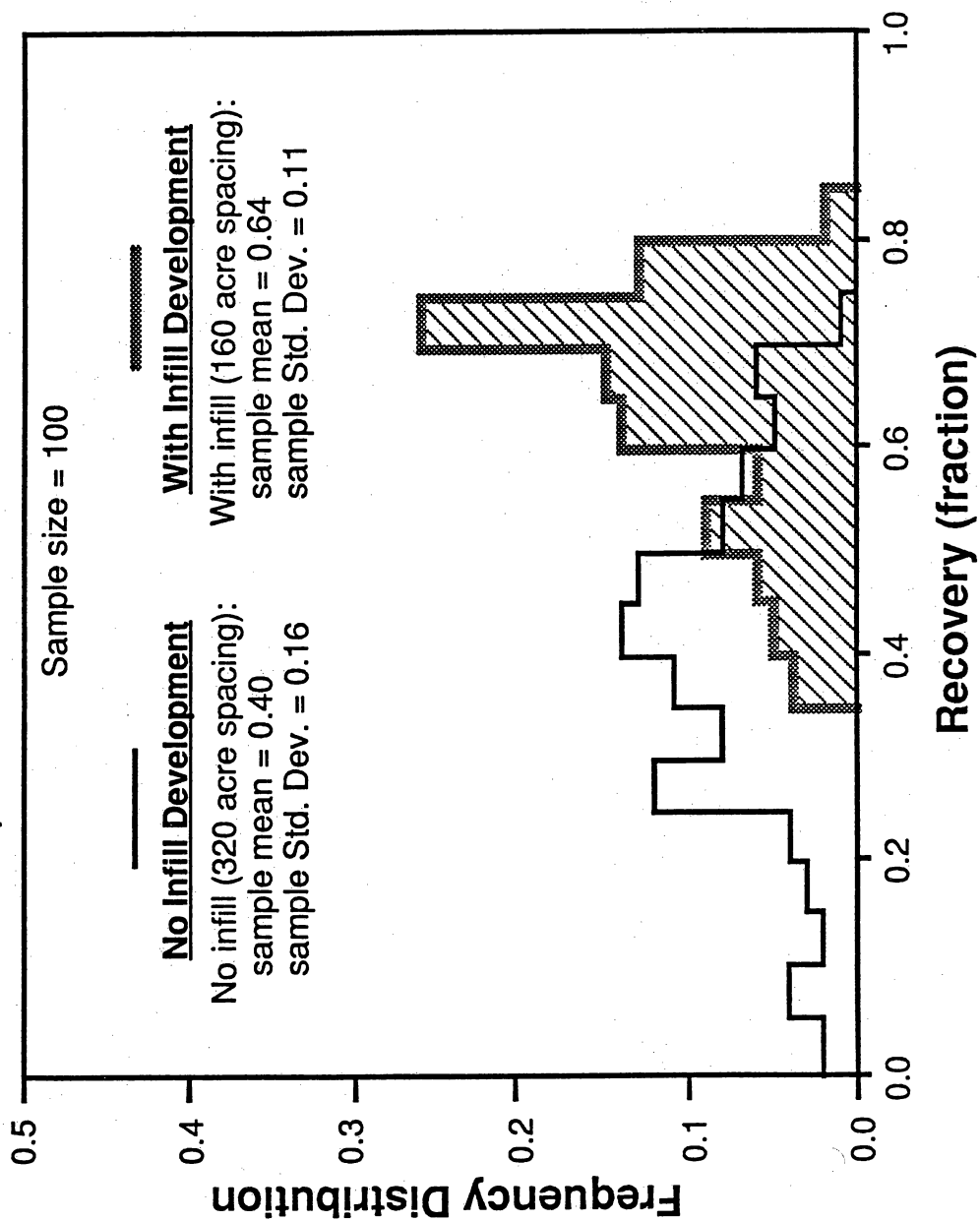
Figure 79. Frequency distribution illustrating effect of case 2 completion schedule on gas recovery for the medium compartment size class.
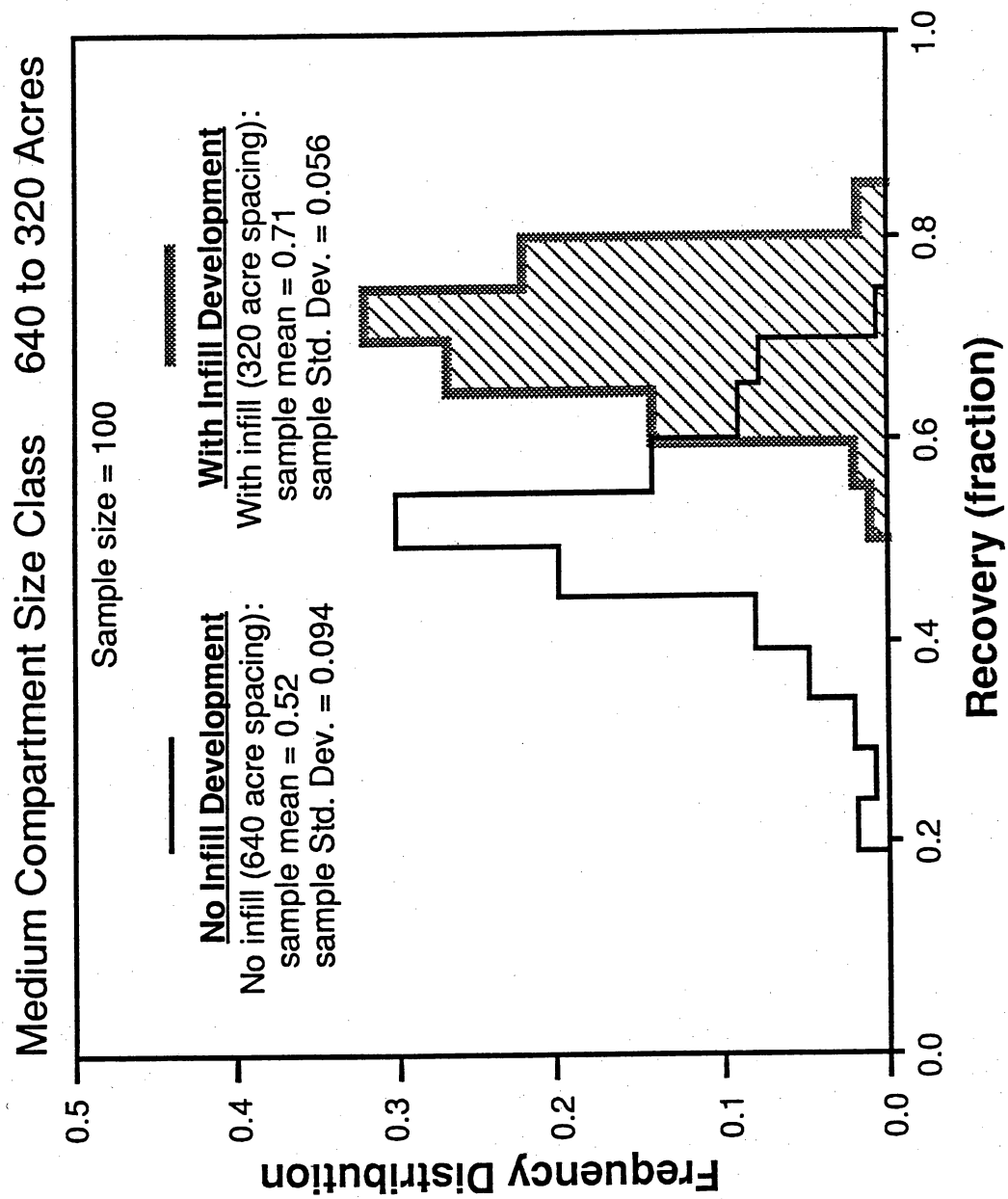
Figure 80. Frequency distribution illustrating effect of case 2 completion schedule on gas recovery for the small compartment size class.

The impact of infill development on recovery is demonstrated in the graph of recovery factor versus well spacing shown in figure 81. The increase in recoverable reserves that can be achieved by infill development is computed by the increment in recovery factor (as the difference in values at two spacings on this graph) multiplied by the OGIP. The incremental gas obtained from infill development can be significant. In table 6, the mean recovery factor and the one standard deviation uncertainty in this value for the three compartment size classes are listed from the data points used to construct the graph in figure 81. The small compartment size class is predicted to have an incremental recovery potential of 24 percent of OGIP by decreasing the completion spacing from 320 to 160 acres. For the large compartment size class, the potential for incremental recovery is indicated to be only 4 percent of the OGIP when the spacing is reduced from 320 acres to 160 acres per well. The total volume of incremental gas resulting from infill development of a large-class reservoir could be more significant where the total OGIP is much greater than for the small-class reservoir. Determination of OGIP must be made in conjunction with the assessment of incremental recovery factor when an economic evaluation is prepared for infill development.

Effective Well Spacing

From figure 81 it is possible to qualitatively determine the most effective well spacing for each of the compartment size classes on the basis of recovery of OGIP. The reservoir and production parameters used in the simulations result in a technical recovery factor of about 90 percent on an acre-foot or unit reservoir basis. This is shown by extrapolating the predicted recoveries for each compartment size class to a well spacing of zero. Figure 82 shows the predicted recoveries from figure 81 with a target recovery factor of 80 percent of total OGIP drawn for all well spacings. The intercept of this recovery factor and the recovery curve for each compartment size class yields a range of spacings most likely to produce this recovery. Results from forward stochastic modeling indicate the most likely well spacings to achieve a

153
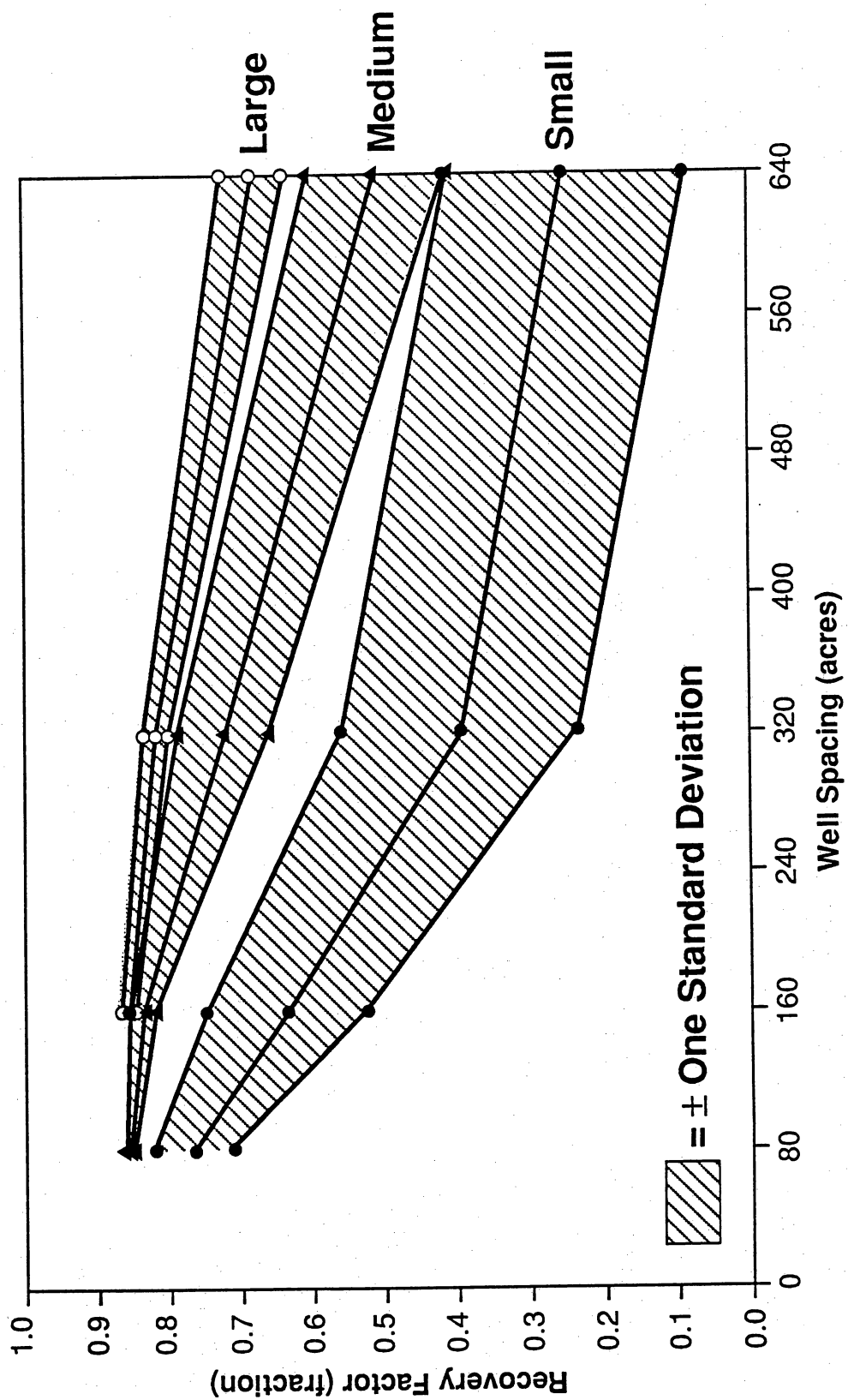
Figure 81. Recovery factor versus well spacing for large, medium, and small compartment size classes. The hatched band indicates plus or minus one standard deviation; 68 percent of all realizations fall within this band.

Table 6. Recovery factor versus spacing.

Compartment size class	640 acre	320 acre	160 acre	80 acre
Large	69 ± 5%	82 ± 2%	86 ± 1%	87 ± 1%
Medium	52 ± 10%	73 ± 6%	84 ± 2%	85 ± 1%
Small	26 ± 16%	40 ± 16%	64 ± 11%	76 ± 7%
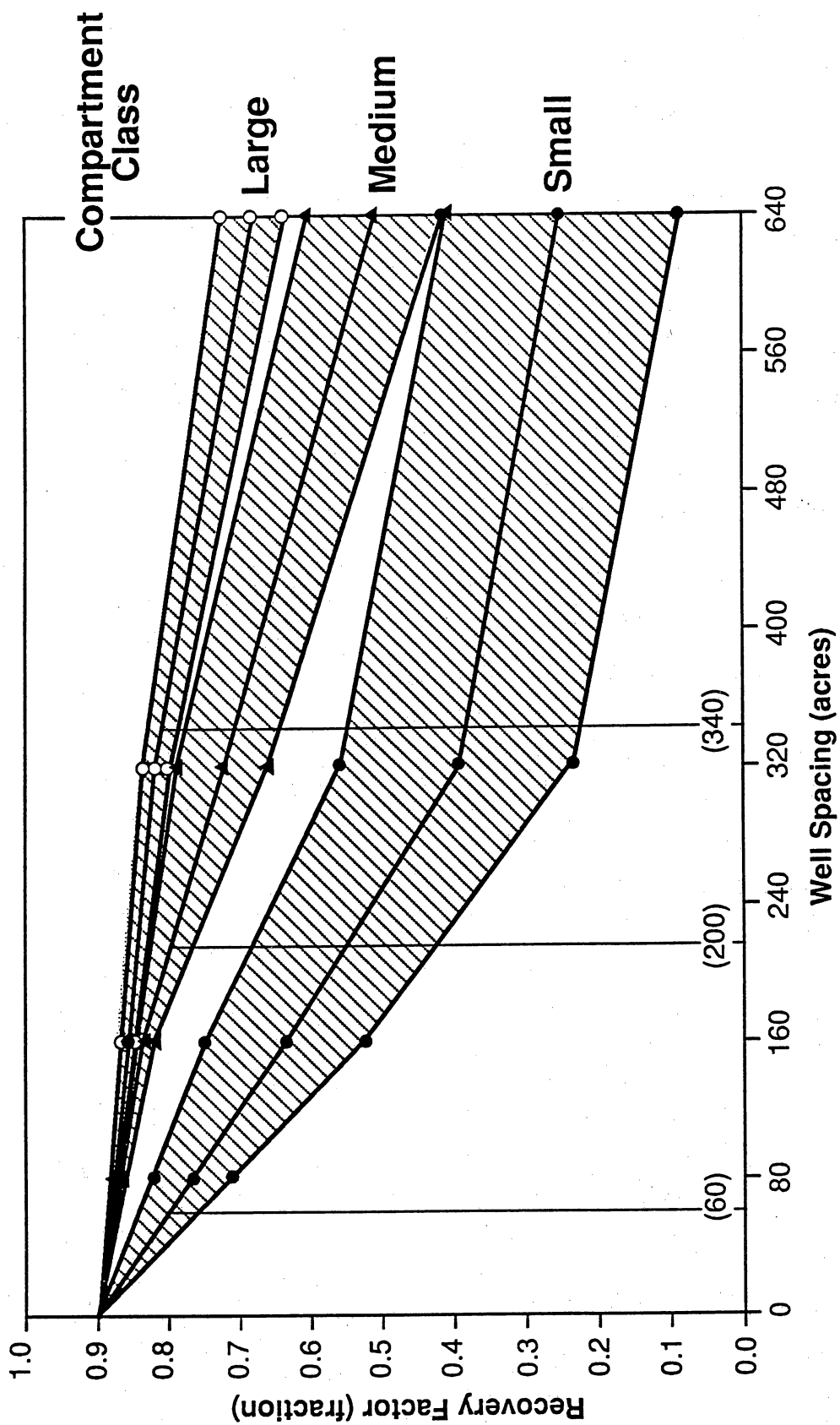
Figure 82. Predicted gas recoveries with well spacing for large, medium, and small compartment size classes.

recovery factor of 80 percent of OGIP are 340, 200, and 60 acres, or less, for the large, medium, and small compartment size class reservoirs, respectively. This procedure can be valuable in assessing the economics and risk for infield development in a reservoir or field.

These results and methods are transferable to other reservoirs, fields, and plays when enough production and pressure data exist to apply the G-WIZ model as a two-compartment system for each of several wells. An estimate can then be made of the distribution of compartment size and transmissibility by comparison with the distributions shown in figures 28 and 29 from the Stratton–Agua Dulce study. Assessment of the proper compartment size class allows the identification of the proper curve from figure 82, or an interpolated curve, which is applicable to the reservoir, and an estimate of the potential incremental recovery can be made.

A Field Application

An example of application of this process is provided by the mini-evaluation study of the 640-acre H. W. Gee lease in Agua Dulce field. Evaluation of 10 wells in the H. W. Gee lease with the G-WIZ compartmented gas reservoir simulator provided sufficient statistics of primary compartment size and barrier transmissibility to compare with the general results of the general stochastic modeling study. Reservoirs at the H. W. Gee lease were found to have characteristics of the small compartment size reservoir class at Stratton–Agua Dulce, as shown in figure 83. This evaluation laid a framework for a development strategy at the Gee lease and confirmed the geologic interpretation of a fluvial depositional system segmented by faulting that creates a potential for small compartments. The stochastic modeling study shows that for this compartment size class, a well spacing of 60 acres or less at each prospective reservoir interval would be required to recover 80 percent of the OGIP. From this evaluation, numbers of additional wells and completions were assessed for the recovery of the remaining gas resources, and the corresponding economics were determined for this additional development.

157
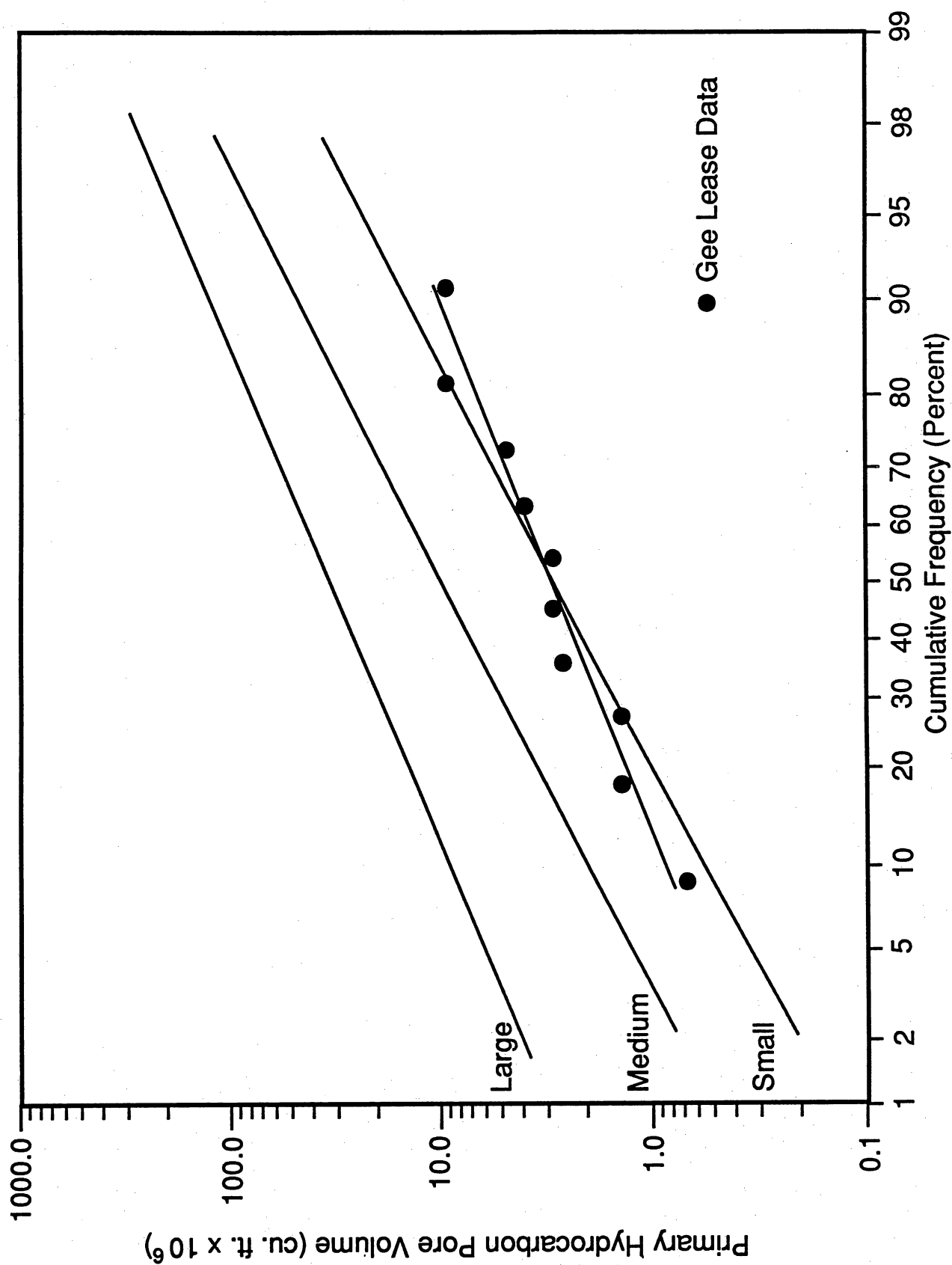
Figure 83. Comparison of Gee lease primary compartment pore volumes with three reservoir classes.

Application of the G-WIZ model and stochastic modeling results are demonstrated to be cost-effective tools to develop strategies necessary for incremental gas recovery.

CONCLUSIONS

Multidisciplinary research in middle Frio fluvial reservoirs of Stratton field has clearly advanced the understanding of gas reservoir flow units and the controls on SGR for reserve appreciation in the largest onshore gas play in the Texas Gulf Coast, the Frio Fluvial-Deltaic Sandstone along the Vicksburg Fault Zone (FR-4). Major conclusions of this research are the following:

1. Well log correlations through the middle Frio stratigraphic interval of the FR-4 gas play in South Texas indicate that the gas reservoirs in Stratton, Seeligson, and Agua Dulce fields are characterized primarily by sandstone bodies of channel-fill and splay deposits bounded by nonreservoir siltstones and mudstones in floodplain, levee, and abandoned channel deposits. A spectrum of fluvial facies architecture exists in a 2,000-ft section of the middle Frio Formation at Stratton–Agua Dulce field. This spectrum varies from laterally continuous amalgamated channel-fill sandstones that have few intrareservoir gas-flow barriers to vertically and laterally separated stacked channel sandstones that create isolated reservoir flow units.

2. Aggressive infield development by the drilling of new wells and recompletions into these Frio and Vicksburg fluvial-deltaic reservoirs achieved reserve appreciation of 100 percent in reservoirs in a large contiguous area (Wardner lease study area) in Stratton field after 40 years of prior development.

3. A comparison of cumulative production analysis with volumetric analysis in the Wardner lease study area indicates that as much as an additional gas resource of 48 Bcf is technically recoverable. However, part of that gas resource is found in the middle Frio interval where reservoir permeability is often degraded by diagenetic alteration of volcanic glass shards affecting permeability and creating reservoir compartmentalization and may currently be assessed by hydraulic stimulation.

159

4. Using the G-WIZ compartmented reservoir simulator, three classes of reservoir compartment size distribution (large, medium, and small) were delineated from the spectrum of fluvial reservoirs. Forward stochastic modeling of gas recovery from the three compartment size classes indicates that well spacing of 340, 200, and 60 acres (or less) provides maximum gas contact efficiency. The correlations developed should be transferable to other fields with similar fluvial facies architecture.

5. Analysis of 3-D seismic imagery in a 7.5-mi^2 grid, coincident with multiple well tests in Stratton field, revealed fluvial channels as narrow as 200 ft and as thin as 10 ft that are visible at depths as deep as 6,800 ft. Reservoir compartment boundaries are imaged within or adjacent to these channels. 3-D seismic imagery provides a cost-effective tool for imaging interwell space.

The results of this research are transportable to other areas in this play and similar gas plays in the lower 48 states. Application of the concepts, approach, and tools developed by the SGR project and tested at Stratton field will help gas operators to develop these infield gas resources.

ACKNOWLEDGMENTS

REFERENCES

Ambrose, W. A., Grigsby, J. D., Hardage, B. A., Langford, R. P., Jirik, L. E., Levey, R. A., Collins, R. E., Sippel, M. A., Howard, W. E., and Vidal, J. M., 1992, Secondary gas recovery: targeted technology applications for infield reserve growth in fluvial reservoirs in the Frio Formation, Seeligson field, South Texas: The University of Texas at Austin, Bureau of Economic Geology, topical report prepared for Gas Research Institute, GRI-92/0244, 200 p.

Bebout, D. G., Weise, B. R., Gregory, R. A., and Edwards, M. B., 1982, Wilcox sandstone reservoirs in the deep subsurface along the Texas Gulf Coast; their potential for production of geopressured geothermal energy: The University of Texas at Austin, Bureau of Economic Geology Report of Investigations No. 117, 125 p.

Dodge, M. M., and Posey, J. S., 1981, Structural cross sections, Tertiary formations, Texas Gulf Coast: The University of Texas at Austin, Bureau of Economic Geology, cross sections.

Economides, C., and Economides, M. J., 1985, Pressure transient analysis in an elongated linear flow system: Society of Petroleum Engineers Journal, p. 839–847.

Finley, R. J., Guevara, E. H., Jirik, L. A., Kerr, D. R., Langford, R. P., Wermund, E. G., Zinke, S. G., Collins, R. E., Hower, T., Lord, Michael, and Ballard, J. R., 1990, Secondary natural gas recovery: targeted technology applications for infield reserve growth: The University of Texas at Austin, Bureau of Economic Geology, annual report prepared for the Gas Research Institute under contract no. 5088-212-1718, GRI Report No. 89/0297, 194 p.

Galloway, W. E., 1977, Catahoula Formation of Texas Coastal Plain: origin, geochemical evolution, and characteristics of uranium deposition: The University of Texas at Austin, Bureau of Economic Geology Report of Investigations No. 87, 59 p.

Galloway, W. E., 1989, Genetic stratigraphic sequences in basin analysis II: application to northwest Gulf of Mexico Cenozoic Basin: American Association of Petroleum Geologists Bulletin, v. 73, no. 2, p. 143–154.

Galloway, W. E., Hobday, D. K., and Magara, Kinji, 1982, Frio Formation of the Texas Gulf Coast Basin—depositional systems, structural framework, and hydrocarbon origin, migration, distribution, and exploration potential: The University of Texas at Austin, Bureau of Economic Geology Report of Investigations No. 122, 78 p.

Grigsby, J. D., and Kerr, D. R., 1991, Diagenetic variability in middle Frio Formation gas reservoirs (Oligocene), Seeligson and Stratton fields, South Texas: Gulf Coast Association of Geological Societies Transactions, v. 41, p. 308–319.

Han, J. H., 1981, Genetic stratigraphy and associated growth structures of the Vicksburg Formation, South Texas: The University of Texas at Austin, Ph.D. dissertation, 162 p.

Han, J. H., and Scott, A. J., 1981, Relationship of syndepositional structures and deltas, Vicksburg Formation (Oligocene), South Texas: Society of Economic Paleontologists and Mineralogists, Gulf Coast Section, Second Annual Research Conference, Program and Abstracts, p. 33–40.

Jirik, L. A., 1990, Reservoir heterogeneity in middle Frio fluvial sandstones: case studies in Seeligson field, Jim Wells County, Texas: Gulf Coast Association of Geological Societies Transactions, v. 40, p. 335–352.

Kerr, D. R., 1990, Reservoir heterogeneity in the Middle Frio Formation: case studies in Stratton and Agua Dulce Fields, Nueces County, Texas: Gulf Coast Association of Geological Societies Transactions, v. 40, p. 363–372.

Kerr, D. R., and Jirik, L. A., 1990, Fluvial architecture and reservoir compartmentalization in the Oligocene middle Frio Formation, South Texas: Gulf Coast Association of Geological Societies Transactions, v. 40, p. 373–380.

Kling, D., 1972, Type field logs in South Texas: volume I; Frio trend: Corpus Christi Geological Society, p. 92.

Kosters, E. C., Bebout, D. G., Seni, S. J., Garrett, C. M., Jr., Brown, L. F., Jr., Hamlin, H. S., Dutton, S. P., Ruppel, S. C., Finley, R. J., and Tyler, Noel, 1989, Atlas of major Texas gas reservoirs: The University of Texas at Austin, Bureau of Economic Geology, 161 p.

Langford, R. P., Wermund, E. G., Grigsby, J. D., Guevara, E. H., and Zinke, S. K., 1992, Reservoir heterogeneity and potential for reserve growth through infield drilling: an example from McAllen Ranch field, Hidalgo County, Texas: The University of Texas at Austin, Bureau of Economic Geology, topical report prepared for Gas Research Institute, GRI-92/0112, 289 p.

Levey, R. A., Finley, R. J., Grigsby, J. D., Guevara, E. H., Hardage, B. A., Langford, R. P., Collins, R. E., Lord, M. E., Sippel, M. A., Howard, W. E., and Vidal, J. M., 1992, Infield gas reserve growth potential: Gulf Coast sandstone reservoirs (Frio, Vicksburg, Wilcox): The University of Texas at Austin, Bureau of Economic Geology, short course notes prepared for Gas Research Institute, U.S. Department of Energy, and State of Texas, 392 p.

Levey, R. A., Sippel, M. A., Langford, R. P., and Finley, R. J., 1991, Natural gas reserve replacement through infield reserve growth: an example from Stratton field, onshore Texas Gulf Coast Basin: Third International Reservoir Characterization Technical Conference, v. 2, paper 3RC-62, unpaginated.

Levey, R. A., Sippel, M. A., Langford, R. P., and Finley, R. J., 1992, Stratigraphic compartmentalization within gas reservoirs: examples from fluvial-deltaic reservoirs of the Texas Gulf Coast: Gulf Coast Association of Geological Societies Transactions, v. 42, p. 227–235.

Lord, M. E., and Collins, R. E., 1991, Detecting compartmented gas reservoirs through production performance: Society of Petroleum Engineers, paper SPE 22941, p. 575–581.

Morton, R. A., and Galloway, W. E., 1991, Depositional, tectonic and eustatic controls on hydrocarbon distribution in divergent basins: Cenozoic Gulf of Mexico case history: Marine Geology, v. 102, p. 239–263.

National Petroleum Council, 1992, NPC natural gas study, v. 2, Supply availability: Washington, D.C., variously paginated.

Nehring, R., 1991, Oil and gas resources, in Salvador, Amos, ed.: The Geology of North America, v. J, The Gulf of Mexico: Geological Society of America, p. 445–494.

Sippel, M. A., and Levey, R. A., 1991, Gas reserve growth analysis of fluvial-deltaic reservoirs in the Frio and Vicksburg Formations located in the Stratton field, onshore Texas Gulf Coast Basin: Society of Petroleum Engineers, paper SPE 22919, p. 337–344.

Williams, H. R., and Meyers, C. J., 1976, Manual of oil and gas terms: New York, Matthew Bender, 657 p.

Xue, L., and Galloway, W. E., 1990, High resolution, log-derived, genetic stratigraphic sequence profile of the Paleogene section, central Texas Gulf Coast; sequence stratigraphy as an exploration tool: concepts and practices in the Gulf Coast: 11th Annual Research Conference, Society of Economic Paleontologists and Mineralogists Foundation, Gulf Coast Section, p. 399–408.

APPENDIX 1. VERTICAL SEISMIC PROFILING AND 3-D SEISMIC DATA ACQUISITION

Introduction

Because no seismic velocity control existed inside the planned 3-D seismic grid, vertical seismic profiles (VSPs) were recorded in wells 175, 202, and 153 before initiating the 3-D seismic acquisition. All three VSP wells were positioned where high fold areas of the 3-D image space were to be created. Wells 175 and 202 were only 200 ft apart, so in an areal sense the VSP data recorded in these two wells represent a single velocity control point. The 175 and 202 VSP data were recorded and processed by Schlumberger, and the 153 VSP data were recorded and processed by Halliburton.

These VSP data demonstrated that the velocity down to the top of the Vicksburg exhibited almost no lateral variation across the central part of the 3-D survey grid. This laterally uniform velocity behavior is illustrated in appendix figure 1-1, which shows depth-vs-travel time curves measured in wells 153 and 175. On the basis of this areally consistent velocity, the travel time curve measured in well 175 was assumed to represent velocity check shot information that could be used to make accurately timed synthetic seismograms at any well within the 3-D grid.

In addition to providing the velocity control needed for synthetic seismogram calculations, a more important use of the VSP data was to produce an independent reflection image of the stratigraphy near each VSP well. Because the VSP measurement creates a precise relationship between seismic travel time and stratigraphic depth, these VSP images were used to define exactly which wavelet feature in the 3-D data volume corresponds to the narrow time window of each thin-bed Frio reservoir. This VSP calibration technique is most important when the reflection events being interpreted are created by closely spaced thin-bed reservoirs.
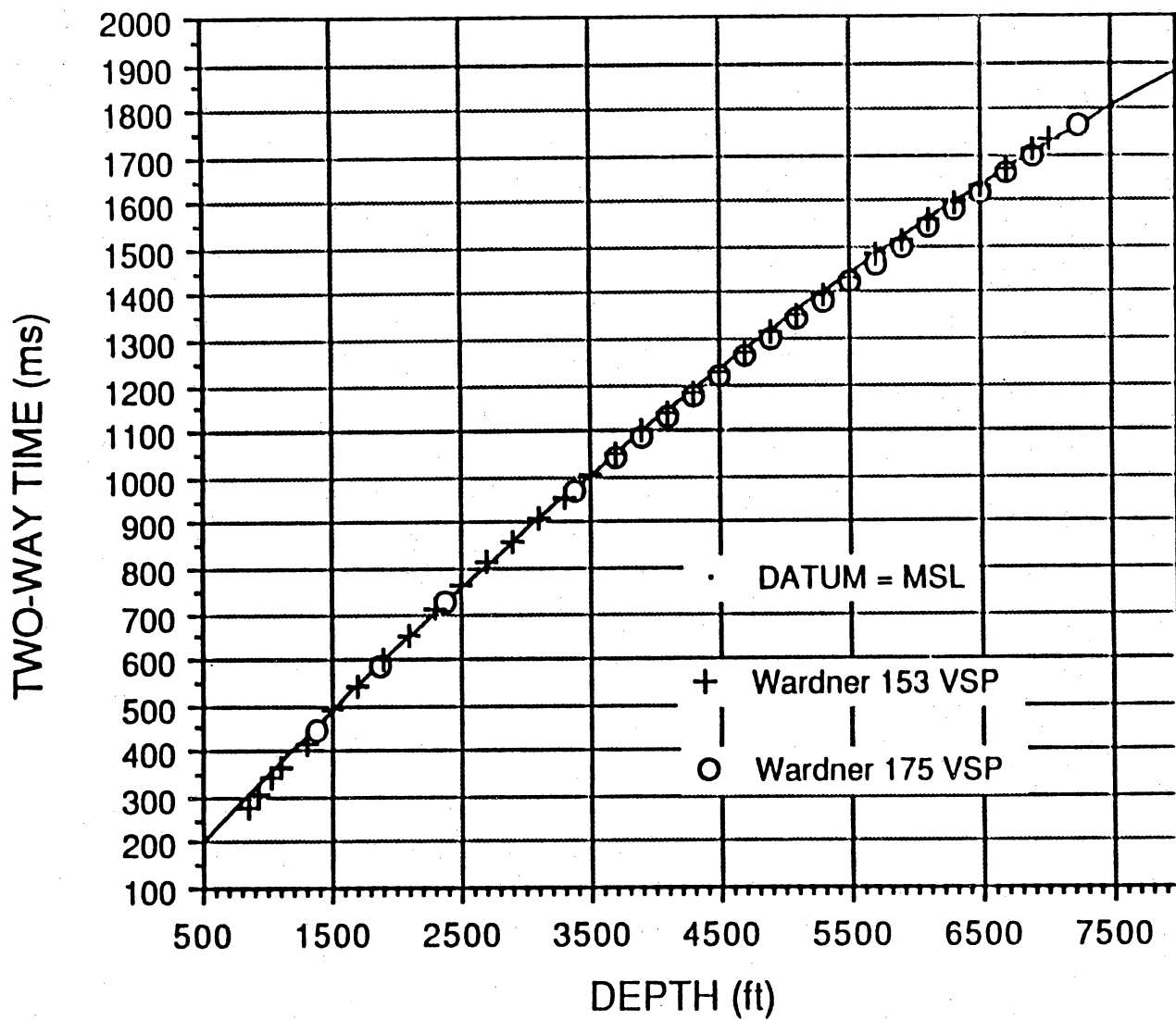
Figure 1-1. Seismic travel time versus depth behavior determined by VSP measurements at two separate locations (well 153 and well 175) within the Stratton 3-D seismic grid.

Wavetesting

Before commencing the 3-D data recording, wavetesting was done to determine which vibrator sweep parameters would create the most desirable seismic wavefield. The wavetest geometry is diagrammed in appendix figure 1–2. Four vibrators were positioned inline with successive vibrator pads separated 35 ft to form a source array covering 105 ft in the north-south direction. Two receiver lines extended away from this source array; one line oriented north-south and the other east-west. Each triangle in appendix figure 1–2 represents a group of 12 geophones planted inline at regular intervals to form a receiver array covering 110 ft. Forty of these receiver groups were laid out in all four directions away from the source array to create a maximum receiver offset of 4,400 ft at the end points of the receiver lines.

Sweep parameters that were tested are listed in appendix table 1–1. For completeness of this wavetest documentation, wavetest records generated by each of the six combinations of parameters given in the table are shown as appendix figures 1–3 through 1–8. The particular vibrator parameters used to produce each record are designated in the label at the bottom of each wavefield display.

The base of the Frio, which is the deepest stratigraphic level to be studied, is located a little above 2.0 s at the shorter offset distances in these displays. Thus, in the wavetest analysis, attention was focused primarily on the reflection character between 1.0 and 2.0 s, and secondarily on the Vicksburg reflections below 2.0 s because Vicksburg faulting could extend upward into the lower Frio and affect reservoir compartmentalization in the deeper F-series of reservoirs. In evaluating the wavetest records, consideration was given to the following questions:

A. Is there robust energy in the frequency range below 30 Hz? Since low frequencies are not severely attenuated by the low-velocity rocks existing in Stratton field, these frequencies should always be retrievable for velocity analysis purposes.

+4400 ft

N

Four inline vibrators
comprising 105 ft array
oriented north-south

-4400 ft

+4400 ft

Receiver groups
spanning 110 ft

-4400 ft
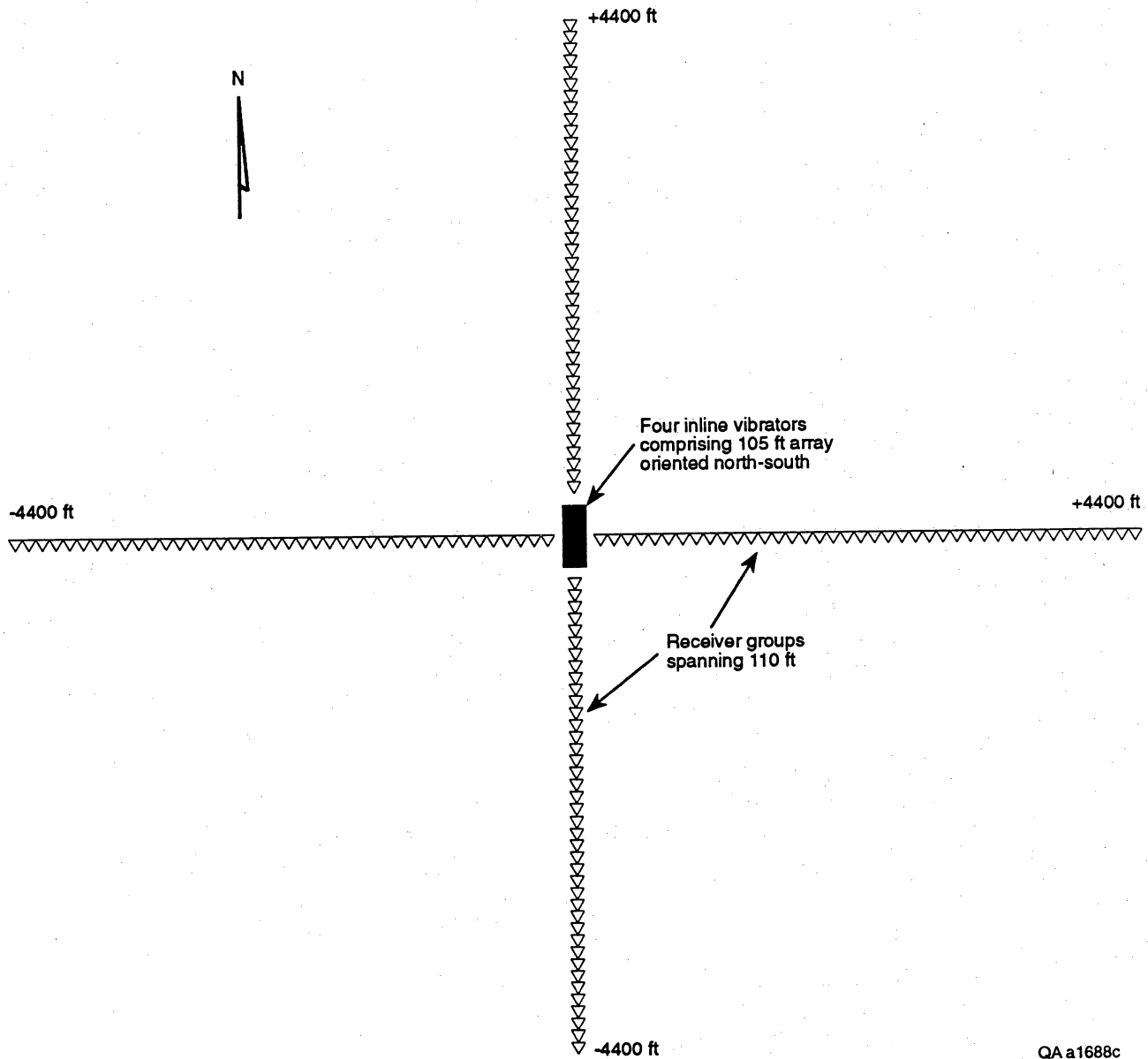
QA a1688c

Figure 1-2. Surface wavetest geometry used to determine which vibrator sweep parameters produced the optimum illumination of the Frio reservoir interval.

Table 1–1. Vibrator parameters used in wavetesting program.

Sweep Range	Sweep Length	Sweep Rate	Vibrator Movement
8-80 Hz	14 s	Linear	Stationary
8-100 Hz	14 s	Linear	Stationary
8-120 Hz	14 s	Linear	Stationary
8-120 Hz	14 s	Linear	30 ft
8-120 Hz	14 s	3dB/octave	Stationary
8-140 Hz	14 s	Linear	Stationary
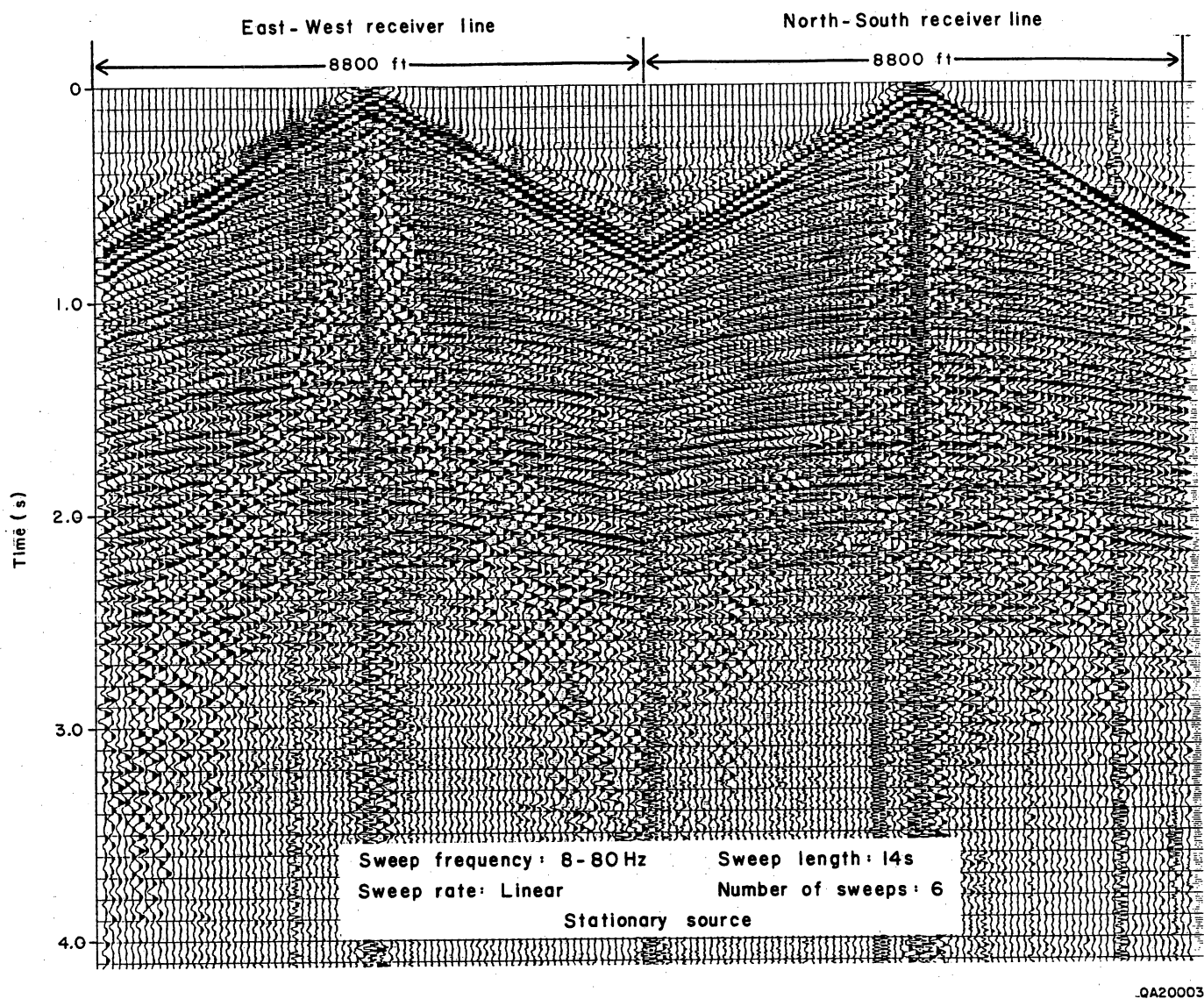
Figure 1-3. Wavetest record generated using the vibrator sweep parameters described in bottom part of the traces.
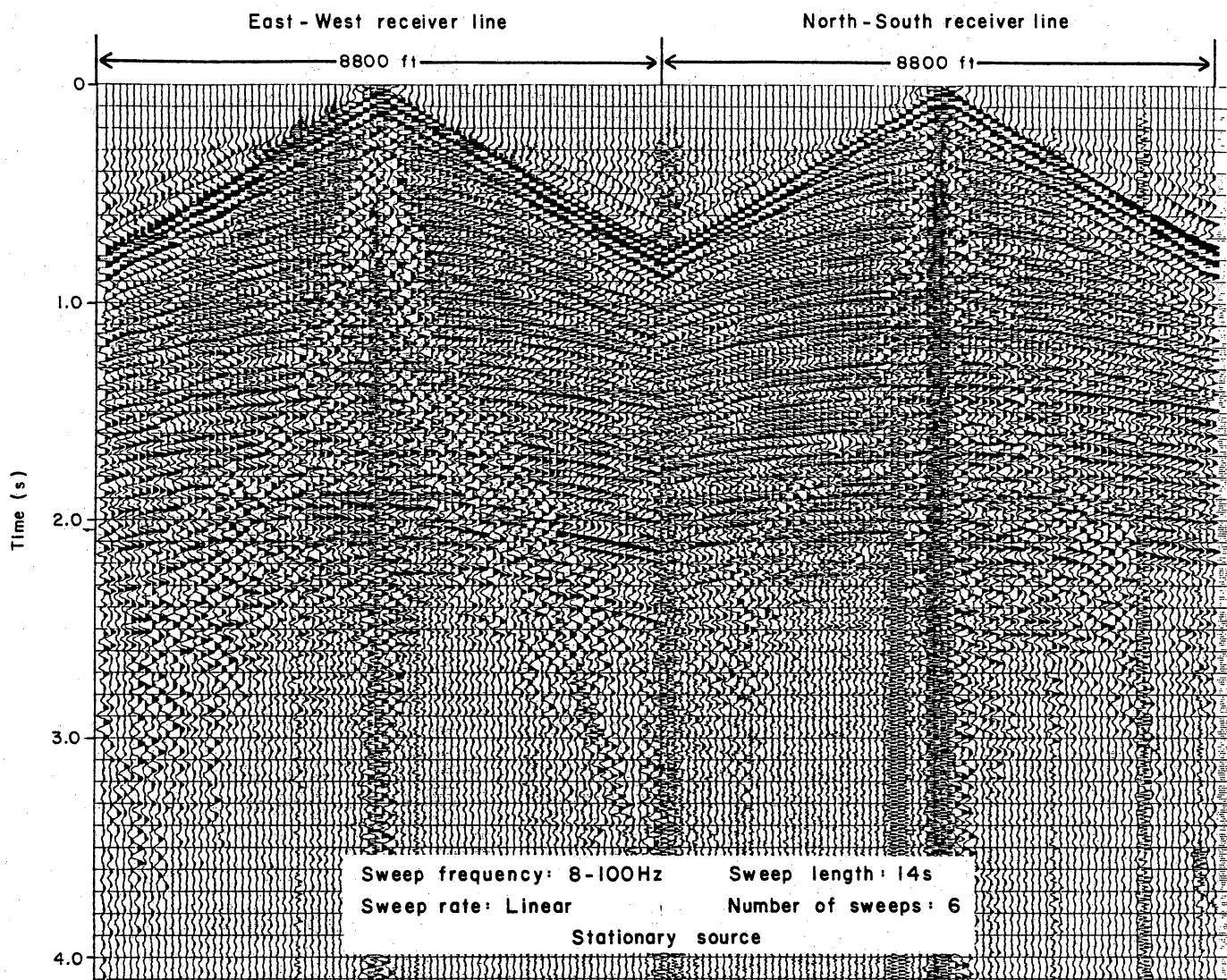
Figure 1–4. Wavetest record generated using the vibrator sweep parameters described in bottom part of the traces.
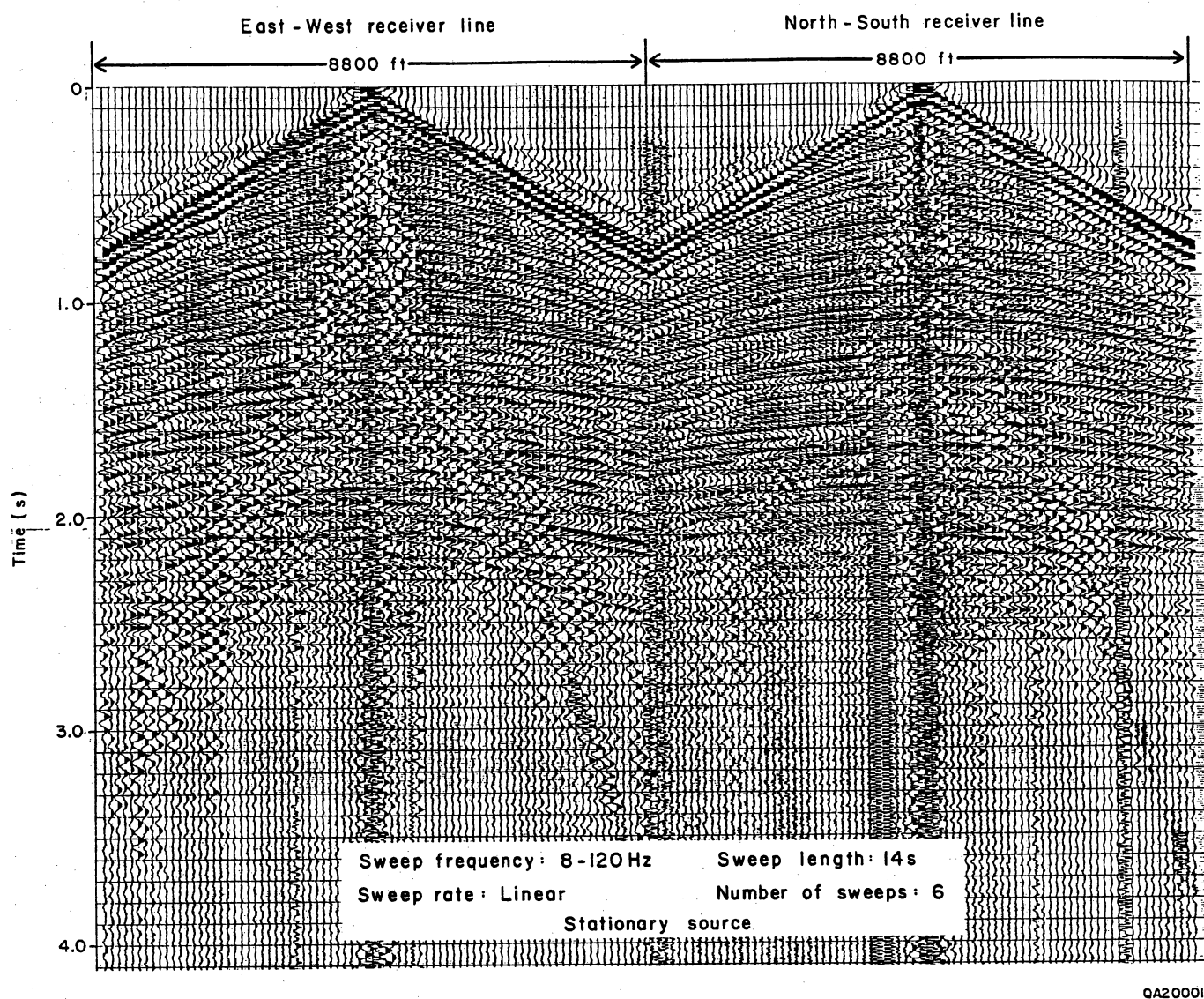
Figure 1–5. Wavetest record generated using the vibrator sweep parameters described in bottom part of the traces.

172
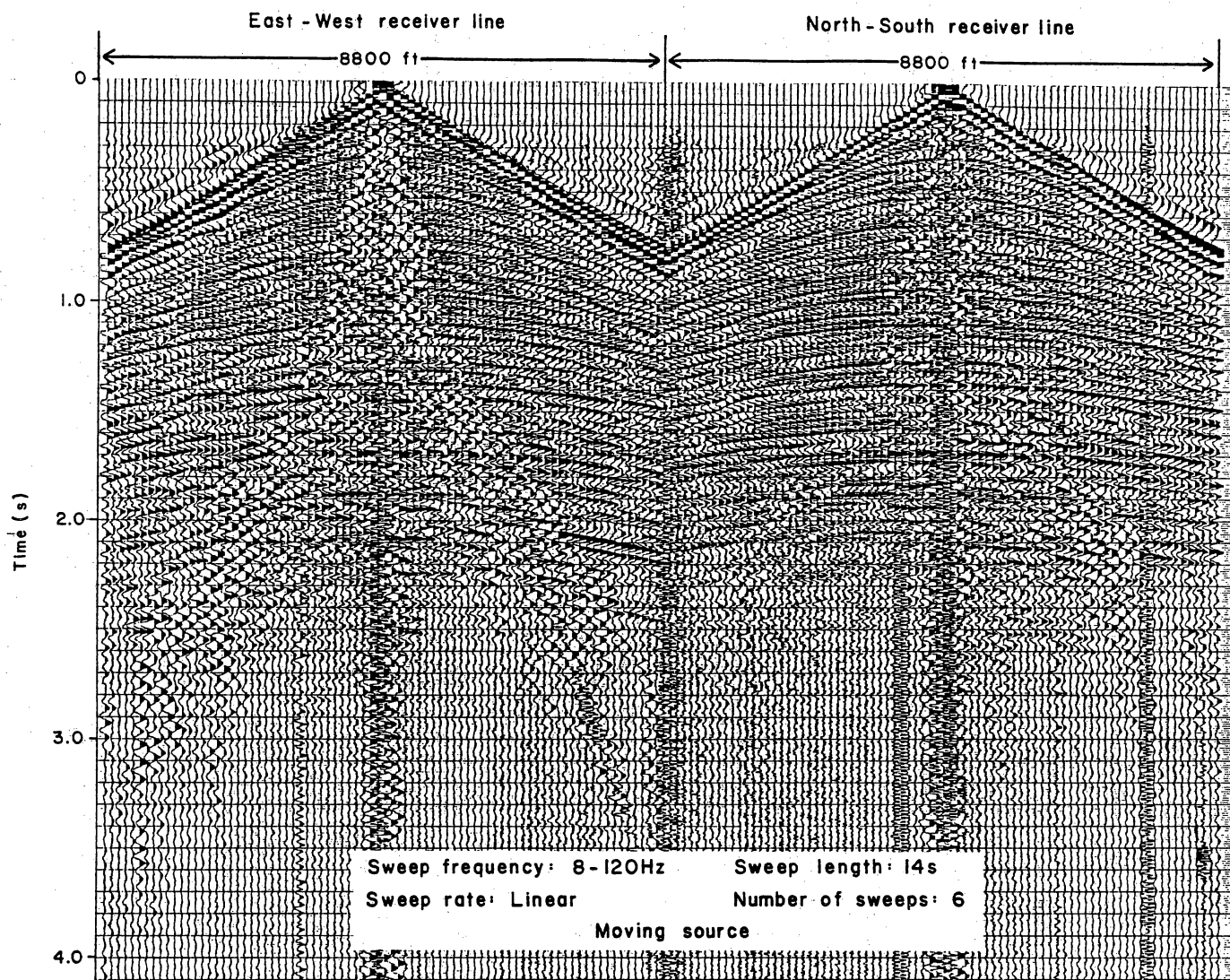
Figure 1–6. Wavetest record generated using the vibrator sweep parameters described in bottom part of the traces.

East - West receiver line North-South receiver line

8800 ft 8800 ft

Time (s)

Sweep frequency: 8-120 Hz   Sweep length: 14s
Sweep rate: 3dB/octave   Number of sweeps: 6
Stationary source
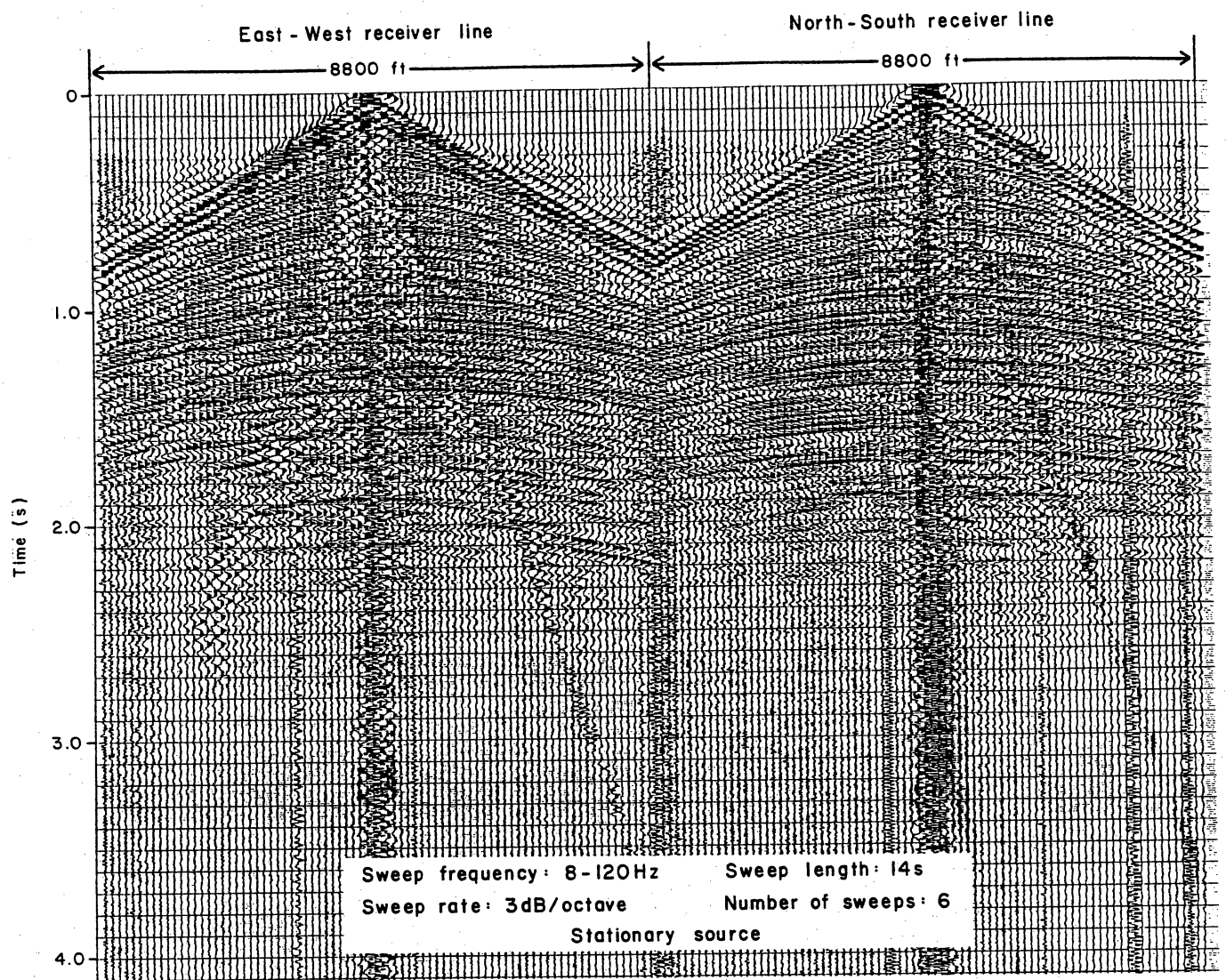
QA20000

Figure 1–7. Wavetest record generated using the vibrator sweep parameters described in bottom part of the traces.

174

East-West receiver line   North-South receiver line

8800 ft   8800 ft

Sweep frequency: 8-140Hz   Sweep length: 14s
Sweep rate: Linear   Number of sweeps: 6
Stationary source
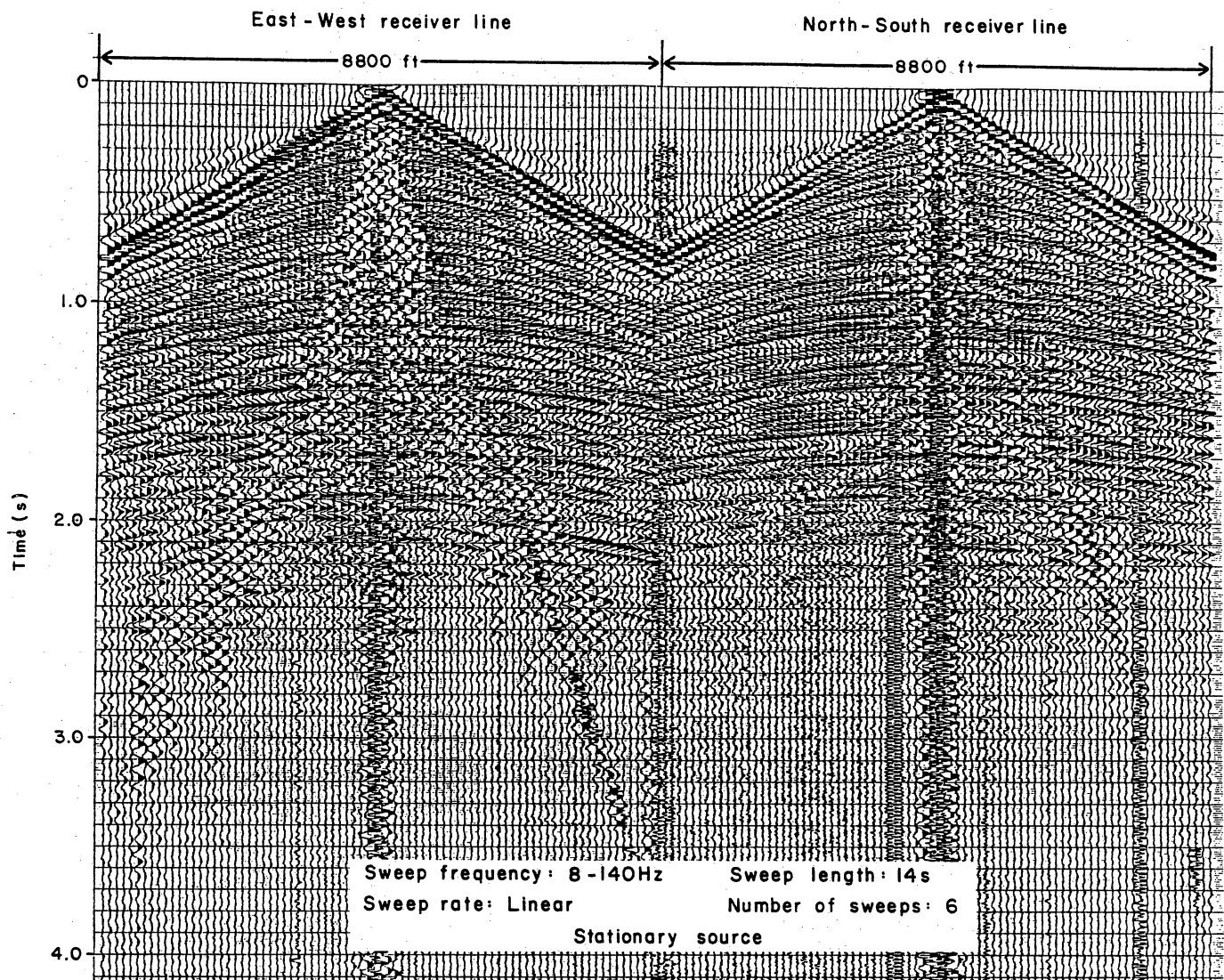
QAI9999

Figure 1–8. Wavetest record generated using the vibrator sweep parameters described in bottom part of the traces.

175

Consequently, the optimum wavefield should contain a large amount of low-frequency energy.

B.   When sufficient low-frequency energy is observed, is there also measurable reflection signal above 60, 70, or even 80 Hz that will allow thin beds to be detected?

C.   Can deep Vicksburg reflections be seen so that accurate fault imaging can be done to allow fault systems to be projected upward into the Frio?

Some subjective judgment is involved in deciding which vibrator parameters produced the most desirable data. After analyzing these wavetests, we decided that the parameters specified in appendix figure 1–6 had created the best field record. The linear, 8–120 Hz sweep produced strong, low-frequency reflection signals and also contained a considerable amount of high-frequency reflection energy. In contrast, the 8–80 Hz and 8–100 Hz sweeps (app. figs. 1–3 and 1–4) did not create as much high-frequency energy, so thin bed detection would suffer if these choices were used for the data recording. The nonlinear, 3dB/octave sweep (app. fig. 1–7) and the 8–140 Hz sweep (app. fig. 1–8) desirable because they did not produce as much low-frequency signal, and consequently, the Vicksburg might not be adequately imaged. A moving source technique was selected rather than the stationary source option so that less surface damage would be done.

One note of interest revealed by these wavetest records is that the north-south receiver line in each figure contains less ground roll than does the east-west receiver line. This ground roll manifests itself as a low-frequency noise wavefield, which starts at the apex of each east-west field record and spreads outward to form a triangular-shaped area in which the reflection signal is significantly deteriorated. The difference in the ground roll noise on the east-west and north-south receiver lines results because the vibrators were oriented inline to form a north-south array 105 ft long, which tended to attenuate ground roll traveling in the north and south directions. Because the source array had no east-west dimension, there was no ground roll attenuation in either the east or west direction. These

records thus document the value of an inline source array, in comparison with a crossline array in attenuating ground roll.

3-D Seismic Acquisition

The Stratton 3-D seismic data were recorded between July 28 and August 5, 1992, by Halliburton Geophysical Services. The source and receiver geometry used for the data collection is illustrated in appendix figures 1–9 through 1–12. The survey area extended 18,480 ft (3.5 mi) north-south and 12,320 ft (2.33 mi) east-west and had to be shot as four overlapping swaths of data.

Each swath consisted of six parallel east-west receiver lines spaced 1,320 ft (0.25 mi) apart. Receiver groups were positioned at regular intervals of 110 ft, so each receiver line required 112 data recording channels. The MDS-18A recording system used by Halliburton easily accommodated the 672 data channels needed for each six-line swath.

Data recording began at the extreme southeast corner of swath 1 (app. fig. 1–9). Vibration points (VP's) were flagged at intervals of 220 ft along north-south source lines, and these source lines crossed perpendicular to the receiver lines at intervals of 880 ft (1/6 mi). The vibrators worked northward on source line 1, then moved west to source line 2 and worked southward, then moved west to source line 3 and worked northward, and continued this back-and-forth movement until all of the VP's in swath 1 were recorded.

The recording spread was then rolled northward to incorporate three more receiver lines (swath 2 of app. fig. 1–10), and the three southernmost receiver lines of swath 1 were retrieved. Similar north-south back-and-forth vibrator movements and northward rolling of the receiver grid were used to record swaths 2 (app. fig. 1–10), 3 (app. fig. 1–11), and 4 (app. fig. 1–12).

In the southern portion of the recording grid, ground conditions allowed source and receiver lines to be cleared through the mesquite pastures and agricultural crops to create

18,480 ft

15 14 13 12 11 10 9 8 7 6 5 4 3 2 1

880 ft

1320 ft

12,320 ft

● Well   ········ Receiver   - - - Source   —— Road   QA19850c
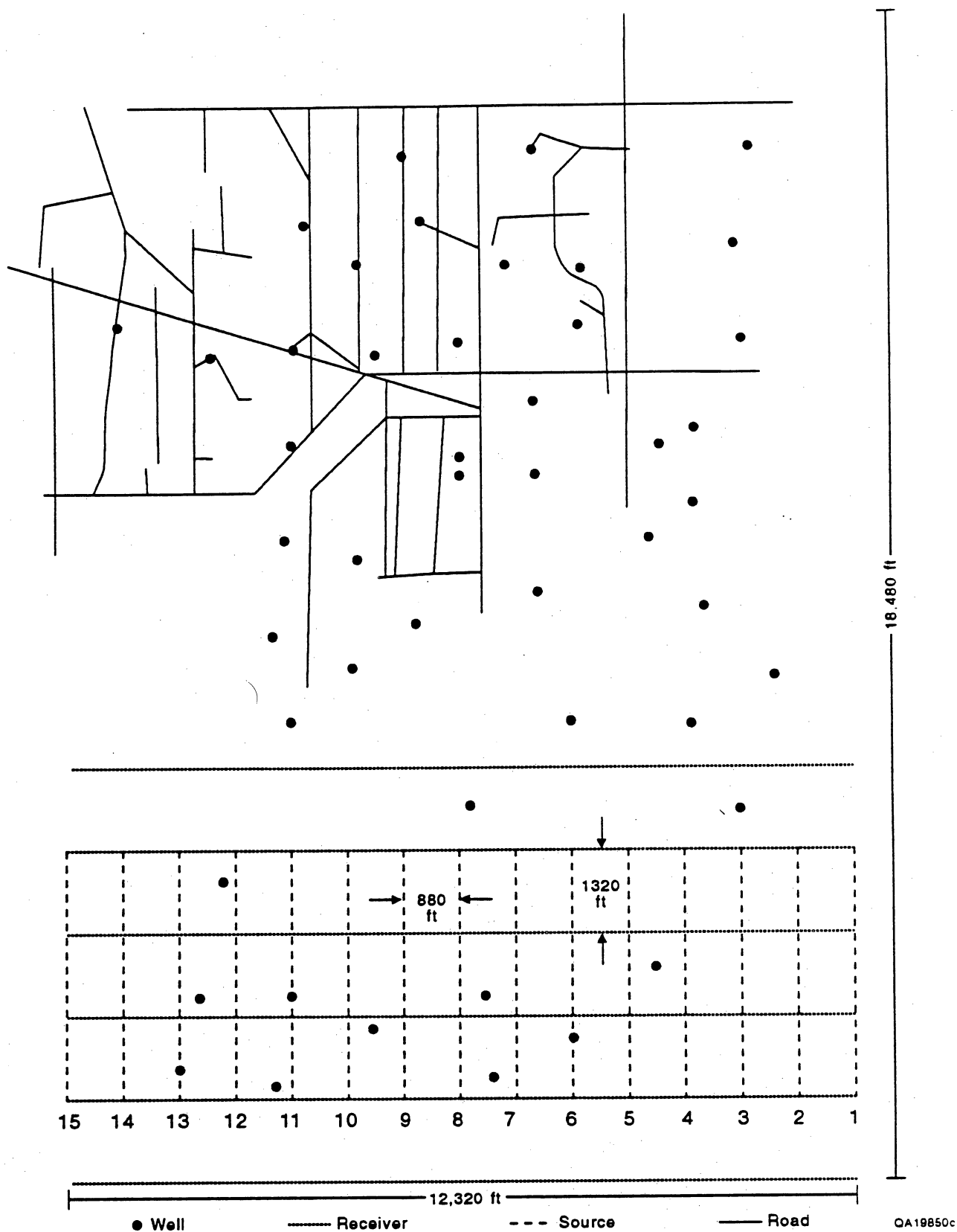
Figure 1–9. Source-receiver geometry used to record swath 1 of the 3-D seismic grid. Dashes used to identify source; receiver lines indicate only the line positions, not individual source and receiver flags.
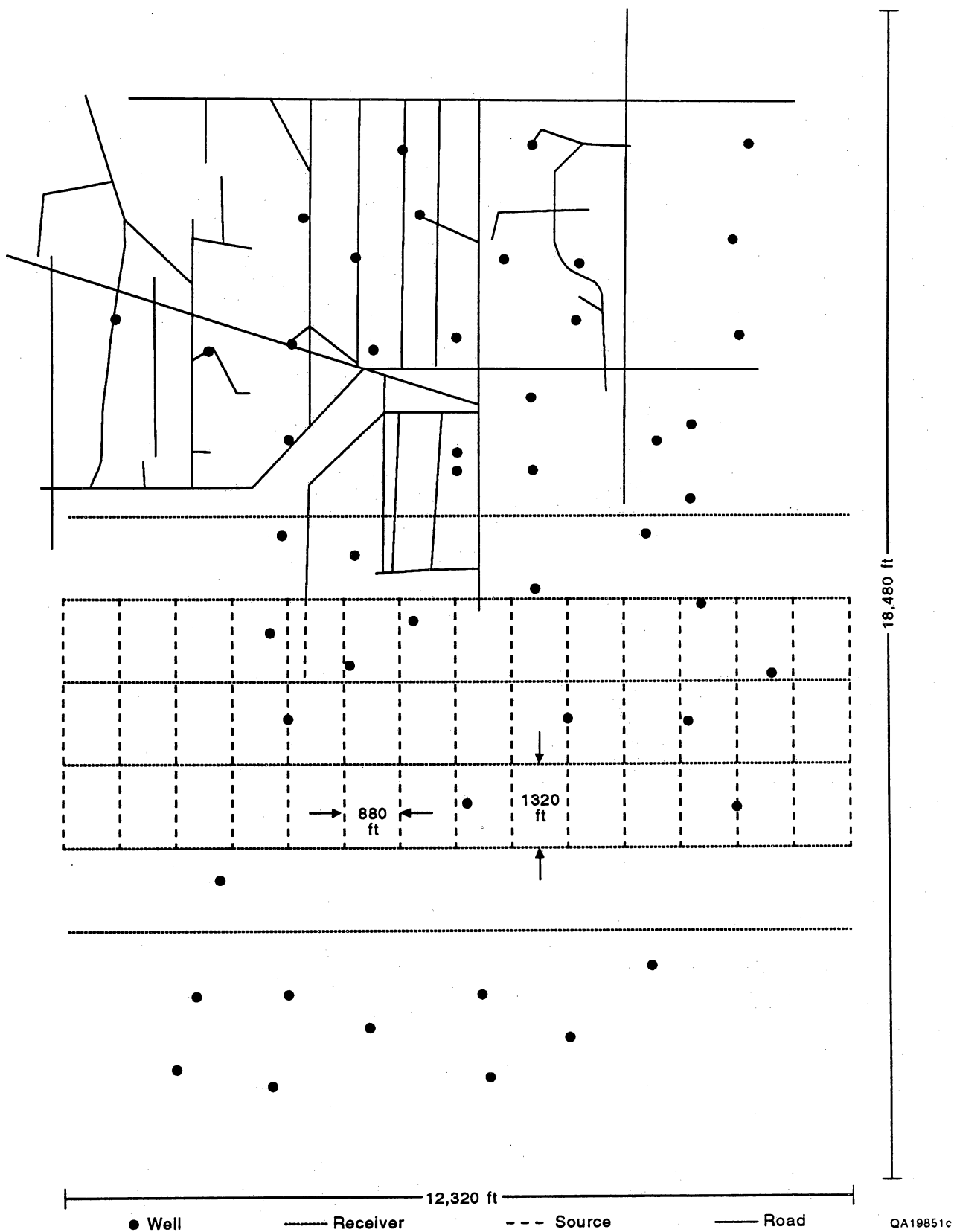
Figure 1-10. Source-receiver geometry used to record swath 2 of the 3-D seismic grid. Dashes used to identify source; receiver lines indicate only the line positions, not individual source and receiver flags.
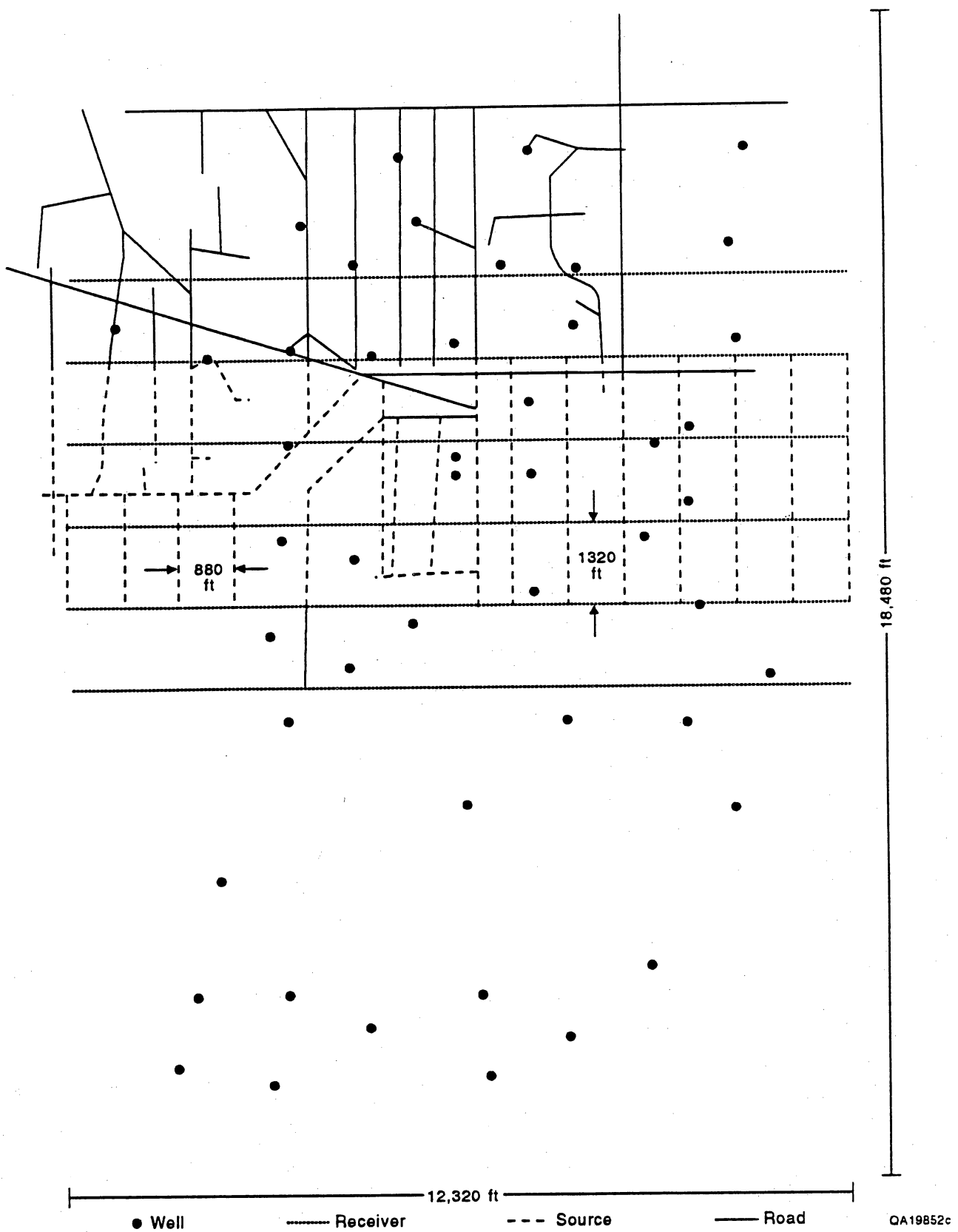
Figure 1–11. Source-receiver geometry used to record swath 3 of the 3-D seismic grid. Dashes used to identify source; receiver lines indicate only the line positions, not individual source and receiver flags.

180
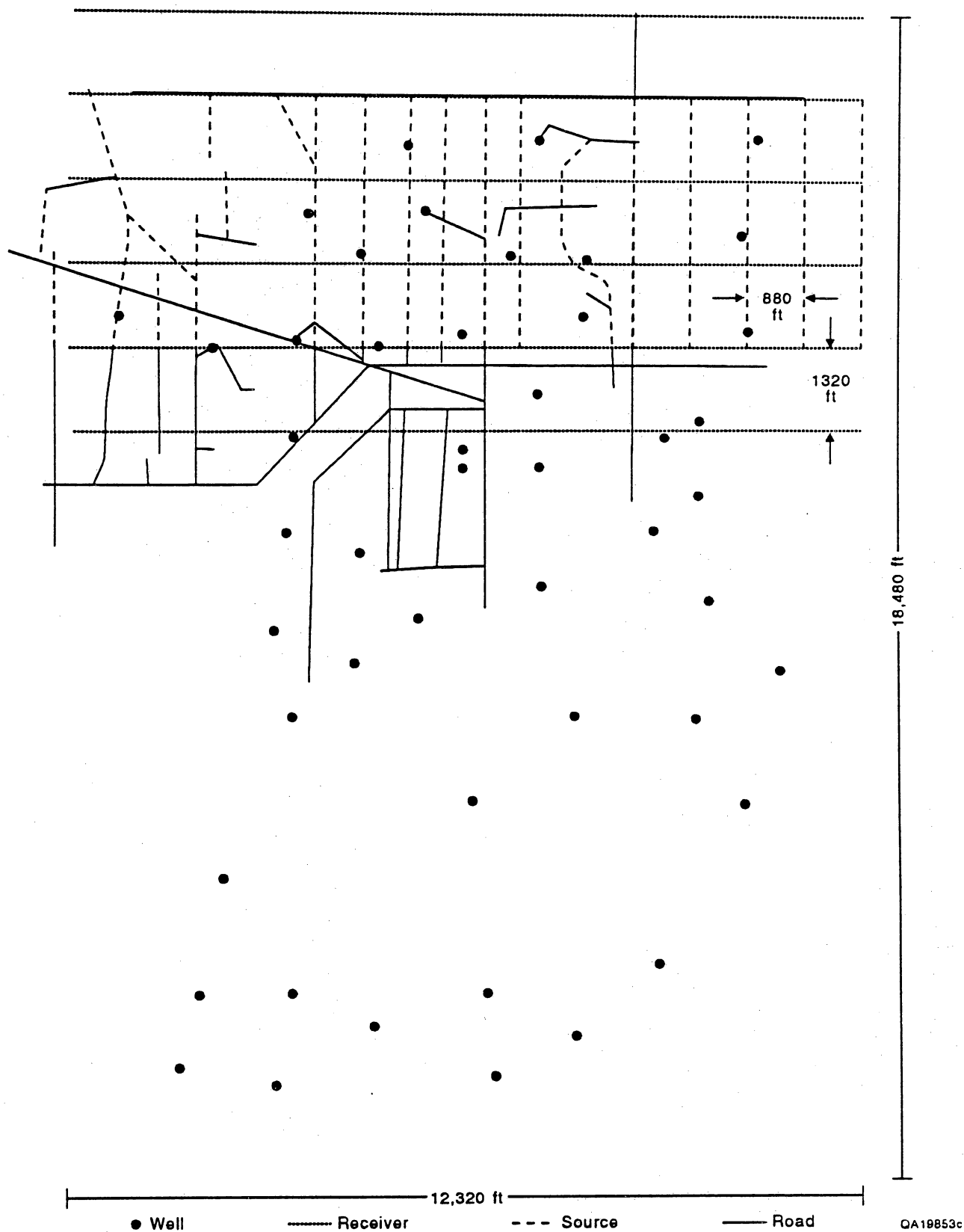
Figure 1–12. Source-receiver geometry used to record swath 4 of the 3-D seismic grid. Dashes used to identify source; receiver lines indicate only the line positions, not individual source and receiver flags.

the regular line spacing shown for swaths 1 and 2. However, in the northern portion, the landowner asked that the vibrators stay on existing roads, and an irregularly spaced source grid had to be used in swaths 3 and 4. This irregular source line spacing did not affect data quality; in fact, the highest stacking fold occurred in swaths 3 and 4.

Stacking Bins

The receiver spacing of 110 ft and source spacing of 220 ft used to record the data created acquisition bins measuring 55 ft east-west and 110 ft north-south. After the data were stacked, a data interpolation was done to reduce the north-south trace spacing to 55 ft. The data were then migrated, and all workstation data interpretation was done using these migrated data bins of 55×55 ft. A total of 69,548 stacking bins were required to cover the total image space of 7.6 mi^2.

Stacking Fold

Field geometry was designed to produce a minimum stacking fold of 20 over most of the image space. Actual stacking fold maps generated during data processing showed that this design objective was accomplished and that approximately 70 percent of the image space was composed of 20- to 30-fold data.

Receiver Arrays

Receiver flags were surveyed at intervals of 110 ft along all receiver lines. Each receiver group consisted of 12 inline, 10-Hz geophones planted 9.2 ft apart, with the 12-element array centered about the receiver flag, as shown in appendix figure 1–13. This array design produced a uniform ground coverage with no gaps between receiver groups.
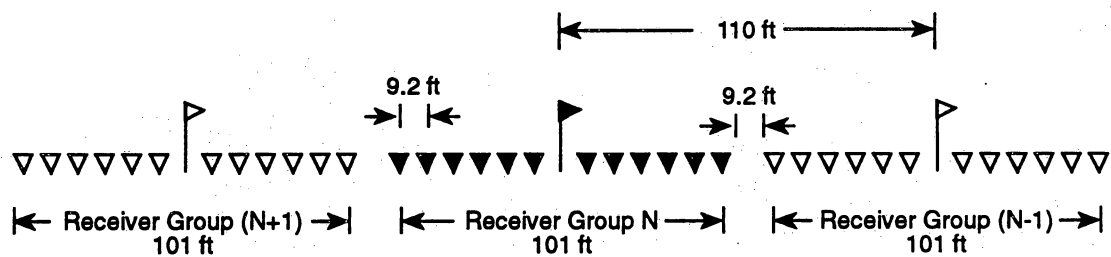
Figure 1–13. Receiver array geometry used to create uniform ground coverage along each receiver line.

Source Arrays

Four Failing Y-2400 vibrators were used to form the source array. The pre-survey wavetesting indicated that a summation of six sweeps from a four-vibrator array produced good illumination of the Frio and Vicksburg, so the vibrator movement between successive sweeps was designed to conform to the geometry illustrated in appendix figure 1–14. The four vibrators were positioned inline with their pads separated 35 ft, and the rear edge of the pad of vibrator 2 was aligned with the source flag. After each sweep, all four vibrators moved forward 5.8 ft. After six sweeps, the front edge of the pad of vibrator 3 was at the source flag, which produced a source array equivalent to 24 vibrators symmetrically distributed about the flag, as shown in panel (b) of appendix figure 1–14.

Because a Failing Y-2400 vibrator can generate approximately 40,000 lb of peak force, this 24-element source array is equivalent to 960,000 lb (480 tons) of force being applied at each VP to produce the downgoing seismic wavefields. Good signal-to-noise field records were created because of this robust energy input.

Ground-Force Phase Locking

A stringent phase lock requirement was set for the vibrators used in the Stratton recording. This requirement was that all four vibrators in the array must exhibit less than 10° of phase error, relative to each other and also relative to the master sweep signal. All of Halliburton's vibrators had good ground-force phase-locking electronics, and the performance of the vibrators was regularly checked from phase displays generated in the recording cab. As a result, all four vibrator pads stayed synchronized during each complete 14-s sweep from 10 to 120 Hz. Without ground-force phase locking, vibrator pad movements can get so badly out of phase relative to each other that arrayed vibrators can actually cancel some frequency components in the seismic wavefield, particularly the higher

(a)

105 ft

vib 1   vib 2   vib 3   vib 4

Back edge of pad of
vibrator 2 aligned with
flag for sweep 1

vib 1   vib 2   vib 3   vib 4

Vibrators moving
between sweeps
3 and 4

vib 1   vib 2   vib 3   vib 4

Front edge of pad of
vibrator 3 aligned with
flag for sweep 6

135 ft

(b)

Source flag

35 ft   35 ft   35 ft

1   2   3   4   Sweep 1

1 1   2 2   3 3   4 4   Sweeps 1 and 2

Ground positions
of vibrator pads

1 1 1 1 1 1 2 2 2 2 2 2 3 3 3 3 3 3 4 4 4 4 4 4   Sweeps 1 through 6

135 ft

OAa1164

Figure 1-14. (a) A side view of the positioning and movement of the four-vibrator source array relative to the source flag as six sweeps were recorded to create the field record at each source point. (b) A map view showing the pad positions of vibrators 1, 2, 3, and 4 relative to the source flag as six sweeps were recorded.

frequencies needed to detect thin beds. This careful attention to ground-force phase locking

of the vibrators is one reason high-quality, broadband data were recorded at Stratton field.

Data Processing

The Stratton 3-D data were processed by Halliburton Geophysical Services following

the numerical procedure given in appendix table 1–2. Seismic velocity analysis of the field

records confirmed the VSP measurements, which showed the velocity from the surface to

the lower Frio did not exhibit significant lateral variation across the recording grid. This

uniform lateral velocity behavior, coupled with the good signal-to-noise character of the

seismic data, produced high-quality stacks with minimal multiple contamination.

Particular attention was given to precise static adjustments of the field traces summed

in each stacking bin. As a result, the final binned data revealed numerous subtle Frio

reflections having laterally varying waveshapes, as would be expected in a good-quality

seismic image of a heterogeneous, fluvially deposited section.

Even though no appreciable structure exists in the Frio, the 3-D seismic data volume

was still carefully migrated. Migration is as important in an area of flat, subtle,

heterogeneous stratigraphy as it is in areas of severe structure because migration improves

horizontal resolution and produces improved images of channel edges, pinch-outs and

reflection terminations. All interpretation results illustrated in this report were produced

using the final migrated data volume.

Table 1–2. Data processing sequence.

Zero Phase Correlation
    Minimum Phase Conversion

Data Initialization
    Generation of Spatial Attributes

Prestack Q Compensation

Mute

Ramp Offsets:	110	6545	Ft
Ramp Times:	0	1300	Ms

Surface Consistent Wavelet Deconvolution
    Source Domain
    Receiver Domain

Time Invariant Equalization

Ramp Offsets:	110	6545			Ft
Ramp Times:	0	1300			Ms
Gate Lengths:	1000	1000	1000	1000	Ms

Velocity Analysis

High Spatial Frequency Statics Estimation
    Surface Consistent
    Gate 1:   400 Ms wide, cdps 1–230, Times 1050–1050 Ms

Velocity Analysis

High Spatial Frequency Statics Estimation
    Surface Consistent
    Gate 1:   400 Ms wide, cdps 1–230, Times 1050–1050 Ms

Normal Moveout Correction

Mute

Ramp Offsets:	110	6545	Ft
Ramp Times:	0	1100	Ms

Common Depth Point Stack

Stack Mode:	Diversity Amplitude
Maximum Fold:	35

Spectral Whitening

FX Filter

2:1   Post Stack Interpolation (to 55 ft line interval)

3-D   Wave Equation Migration
    One Pass

Time Invariant Filter
    8–105 Hz. 0–4 Sec

Time Invariant Equalization

Start Time:	100				Ms
Gate Lengths:	1000	1000	1000	2000	Ms

APPENDIX 2. SEISMIC INTERPRETATION PROCEDURE

The east-west vertical seismic section shown in appendix figure 2–1 is positioned approximately in the center of the Stratton 3-D image space. It illustrates features of the seismic response that influenced the 3-D data interpretation process. This seismic interpretation is restricted to the Frio portion of the stratigraphic section, which is a time window extending from about 1.0 s to about 2.5 s on this seismic line. The severely faulted section below 1.7 s is the Vicksburg, and some Vicksburg-age faults extend upward into the lower Frio and affect the deposition and compartmentalization of deeper Frio reservoirs. Several middle Frio reservoirs occur in the time window between 1.35 s and 1.65 s, where the seismic reflections are laterally discontinuous and have widely ranging amplitudes. Much of the seismic interpretation and imaging concentrated on this interval, in which the seismic reflection character is highly variable. One property of the Frio reflections that aids interpretation is the generally flat and conformable stratigraphy. If the Frio was highly faulted or exhibited great structural relief, it would be more difficult to follow the laterally variable reflection character of these fluvially deposited reservoirs.

Interpreting the Stratton 3-D data volume consisted of the following steps:

(1) Interpret one reliable, good-quality, continuous Frio reflection completely across the entire 3-D grid.

(2) Use VSP control to define exactly which stratigraphic level in the Frio corresponds to this reflector.

(3) Flatten this interpreted horizon over the complete data volume to represent the typical, zero-dip condition that existed for a distance of 2 to 3 mi in the low-energy, meandering-stream environment in which the Frio sediments were deposited.

(4) Horizontally slice the complete flattened 3-D data volume along constant time planes below this flattened reference datum to simulate a layer stripping of the

previously deposited sediments. Use VSP control to specify the correct stratigraphic depth for each time surface.

(5) Continue this layer stripping to deeper levels until the seismic reflections are no longer flat (no longer conformable to the flattened reference datum).

(6) Select a new seismic horizon immediately below the last valid horizontal time slice and repeat steps 1 through 5.

Because the Frio reflections inside the Stratton 3-D grid were so flat and conformable throughout a large vertical range, only two reference surfaces had to be interpreted and flattened to produce valid time slices from the top to the base of the Frio.

The upper reference surface is shown as a green line and the lower reference surface as a blue line extending completely across the seismic line in appendix figure 2–1. The upper reference surface (near 1.3 s) corresponds to the C-38 reservoir level, and the lower reference surface (near 1.6 s) corresponds to the F-11 reservoir. Neither reference surface is shown as a flattened datum. The deepest Frio interpretation was done at the F-39 reservoir level, and the time surface where F-39 deposition occurs is shown as the yellow line near 1.65 s. Note that this yellow line (F-39) is conformable to the lower blue reference surface (F-11) and exhibits a modest amount of unconformity relative to the upper green reference surface (C-38).
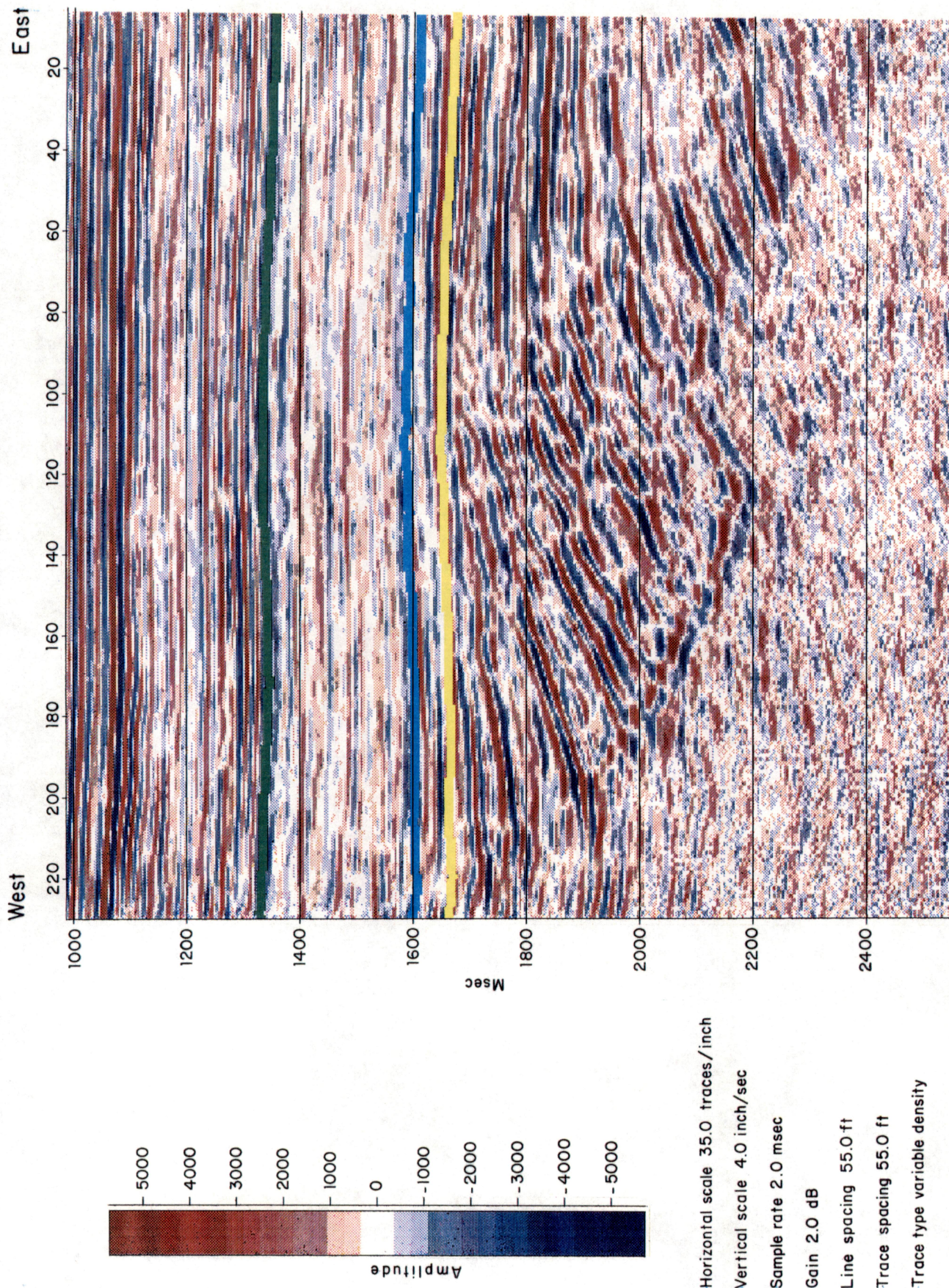
Figure 2–1. An east-west seismic section, 2 1/3 mi long, passing through well 175 where VSP control data were recorded. The green and blue lines mark the two Frio reflections that were flattened and used as reference surfaces for layer stripping. The deepest Frio seismic interpretation done in this study, the F-39 reservoir, is indicated by the yellow line.

APPENDIX 3. PETROPHYSICS

Introduction

The integrated petrophysical model obtained by combining core analysis results with calibrated log-derived parameters from the Elliff 40 and 36 and Wardner 184 wells was used in Stratton field for a complete petrophysical evaluation of clean and shaly sandstones.

Several problems were addressed by this model. Shaly sandstones in the Wardner lease contain variable amounts of shale and clays with large amounts of bound water. Therefore, the porosity logs must be corrected for shale content to obtain the effective porosity. High clay conductivity also affects the resistivity readings, so a special shaly sandstone equation must be used to calculate water saturation. Clay and shale content also causes an increase of the irreducible water saturation and a reduction of the effective permeability; this was accounted for in the log interpretation model.

The following sections discuss the open-hole and cased-hole interpretation techniques developed in Stratton field to find additional gas resources by computing lithology, porosity, water saturation, and permeability. Estimation of formation pressures by indirect methods using log measurements is also discussed.

Open-Hole Interpretation Techniques

This section describes the open-hole interpretation methods applied in Stratton field to improve the evaluation of gas reservoirs, identify potential pay zones, and derive petrophysical parameters necessary for the calculation of secondary gas resources. Also included is a review of some "quick-look" techniques that prove useful in many Frio reservoirs for determination of pay zones.

Data Acquisition

The Elliff No. 40 well, drilled by Union Pacific Resources Company (UPRC) in May 1990, was chosen for the Secondary Gas Project as the cooperative well for acquisition of high-quality open-hole data through the Frio reservoirs. The logging program consisted of cores and dual induction, formation density, compensated neutron, gamma-ray, formation microscanner, and sequential formation tester logs. After the well was cased, a thermal decay log was run for pressure prediction from cased-hole logs. The objective of the open-hole data acquisition was to develop a log interpretation method based on a shaly sandstone model to be used for the remaining wells in Stratton field for identification of potential gas-producing zones.

Logs from the Wardner and Elliff lease were also obtained from UPRC, digitized, borehole corrected, standardized, and processed with the petrophysical model developed. Most of these wells had recent triple-combo logs and wireline formation tester pressures available. The formation pressures were analyzed, and only those deemed to be representative were presented in the computed results.

Log Editing

Because log responses differ among service companies and logging runs, corrections are required before proceeding with the interpretation method. These corrections consisted of depth matching, borehole corrections, log reconstruction in extreme borehole conditions (washouts), SP baseline, standardization of gamma-ray and porosity logs, and correction to the deep induction for invasion and thin-bed effects.

Appendix figure 3–1 shows the standardization of a density log. Notice that a correction is required in order to match the fieldwide standard. A bulk shift of +.04 g/cc was applied in this particular case. Similar standardization procedures were performed on the compensated neutron and gamma-ray logs. Appendix figure 3–2 shows results before and after log editing with corresponding computed results of porosity and water saturation. Notice the false pay
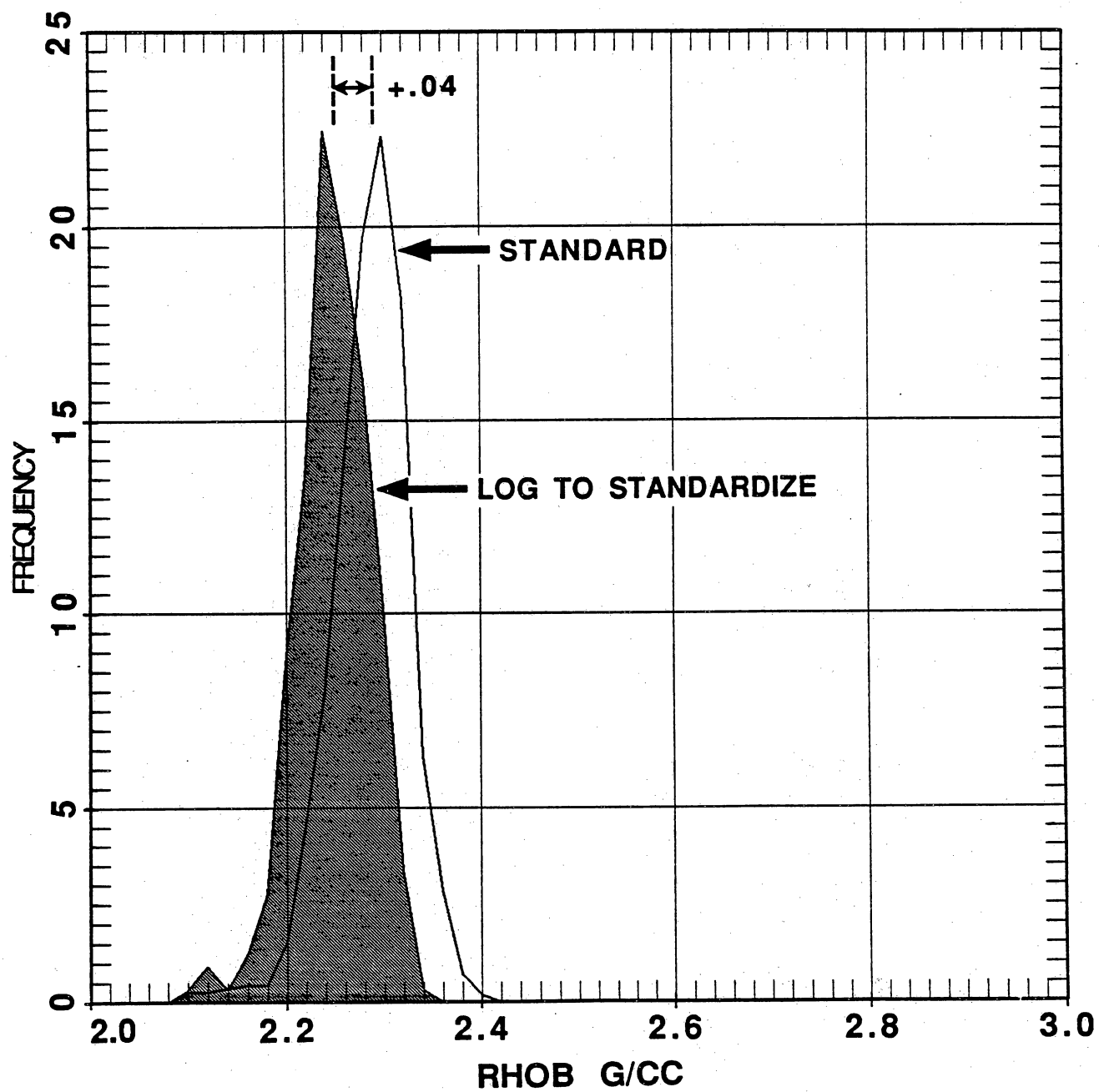
Figure 3–1. Standardization of a density log to fieldwide norm in Stratton field.
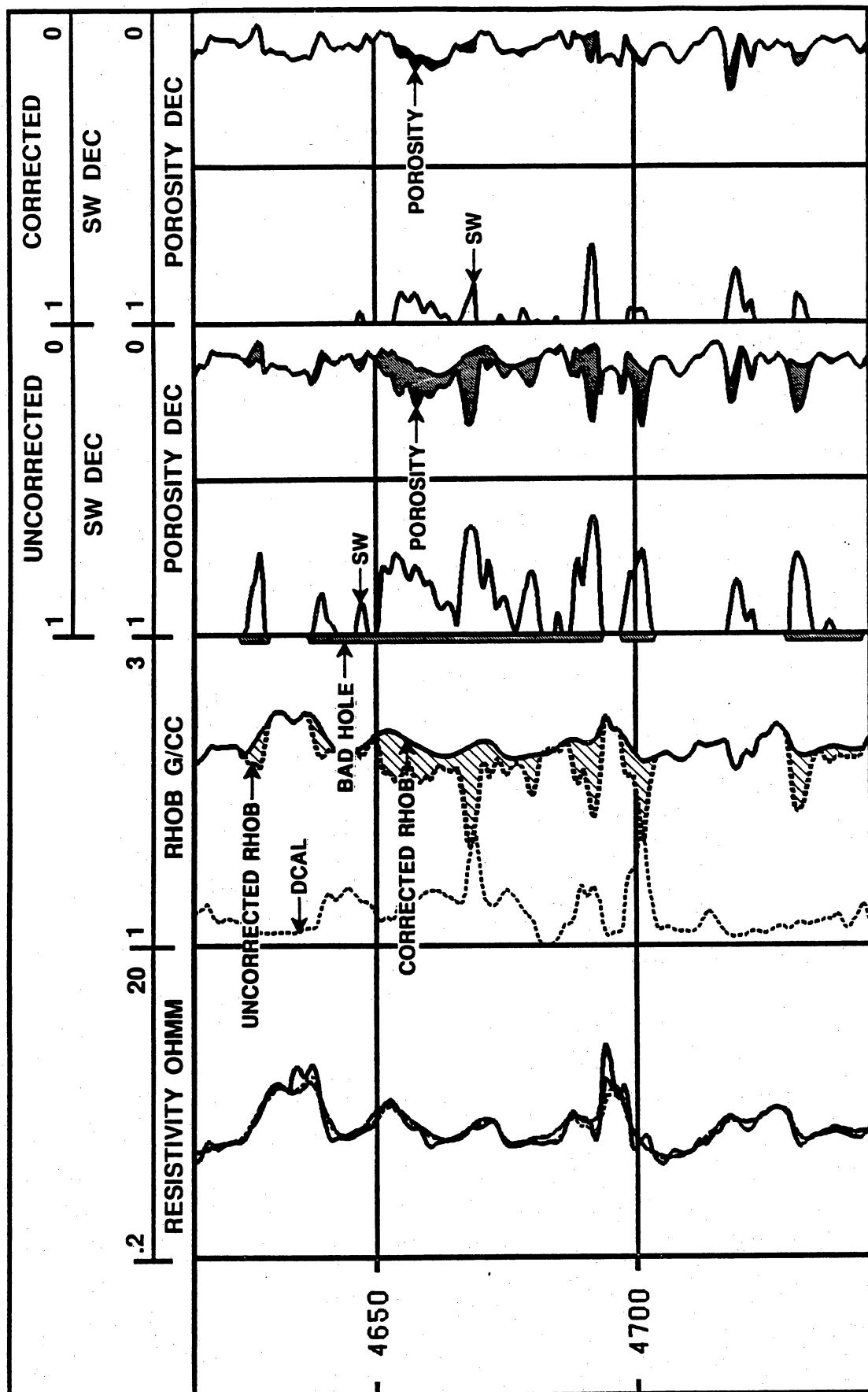
Figure 3–2. Example of density log reconstruction in zones of bad hole and washouts.

196

zones found in the low-resistivity zones (shale) when the porosity logs are not corrected for borehole washouts.

Thin-Bed Corrections to Deep Resistivity Logs

In the Frio reservoirs, sandstones vary in thickness from 0 to more than 40 ft. For thin sandstones, a correction for thin-bed effects to the deep resistivity measurement is needed in order to obtain an accurate value for resistivity at the center of the sandstone. The correction method used in this study consists of using the additional information provided by the shallow focused log and the SP log. The relationship for this correction is

$$R_{corr} = \frac{(Rild / R_{fl}) \, sh \quad {}^{*}R_{fl}}{10^{\, SP/-K}}$$

where

R_{corr}	= minimum value of the corrected formation resistivity,
$(Rild/R_{fl}) \, sh$	= average value of the ratio of the deep resistivity to the focused log resistivity in the shales,
R_{fl}	= focused log resistivity,
SP	= maximum SP deflection in the sand, and
K	= temperature coefficient.

The relationship is simply an application of the rule (Doll and others, 1960) that the minimum expected resistivity in the formation is equal to (Rw/Rmf) *Rxo. This enhancement works particularly well in thin-bed zones such as the D-15 to D-34 sandstone reservoirs.

Determination of Formation Water Salinity

To obtain reliable water saturations, an accurate value of formation water salinity is essential. Formation water salinity is related to resistivity at a specific temperature. In Stratton field, formation water resistivities were found to vary from 0.17 to 0.32 ohm-m at 75°F,

depending on well location and depth of the formation. These values were determined from log-derived resistivity values in water-bearing sands and from measurement of water salinity and resistivity of 14 formation water samples collected from different wells in Stratton field. For the samples recovered from gas-producing intervals, the measured salinities were corrected for the dilution problem associated with gas production. The value of formation water resistivity of 0.17 ohm-m at 75°F was found to be representative of the Frio Formation in Stratton field. Average measured chloride was 23,700 ppm at this resistivity value. Appendix table 3–1 shows the range of recovered water salinities with estimated formation water resistivities after corrections for dilution effects.

Use of Core Data to Verify the Model

Core data analysis results were used to calibrate the log-derived petrophysical values and to validate the interpretation model (Truman and others, 1986). Conventional whole-core analyses were available from three wells in the field, the Elliff 40 and 36 and Wardner 184 wells. In addition, thin section point count, porosity, permeability at stressed conditions, and capillary pressure measurements were also performed and utilized to validate the petrophysical model. The following text illustrates how the core analysis data were used to calibrate the petrophysical model.

Porosity Determination

Comparison of core porosities versus log-derived porosities indicates that the density-neutron combination provides the best log porosity indicator in the Frio Formation. Porosities from core analyses were used to confirm the calculation of log porosities after corrections for shale and gas effects. Core measurements were made at 800 psi and also at net overburden (NOB) stresses. Core porosities were then plotted against the computed porosity results. Good agreement was found using a fixed matrix density of 2.65 g/cc, a fluid density of 1.0 g/cc, and

Table 3–1. Correction of formation water salinity for dilution in Stratton.

Well	Reservoir	Measured -CLPPM	Corrected -CLPPM	Dilution	Estimated Rw @ 75°F
Elliff 28	G9	4120	16480	0.75	.25
Wardner 75	D18	10003	16841	0.40	.24
Gruene 12F	F39	—	—	—	—
Elliff 2J	E31	6948	17678	0.60	.23
Elliff 31F	E31	19190	22700	0.15	.18
Wardner 177F	F44	12019	16780	0.28	.24
UCLI No. 13	D-20	12616	17440	0.27	.23
Elliff 29-D	D-35	18059	20398	0.11	.20
Rivers A2UT	C-46	18478	18665	0.01	.22
Wardner 166	VK	14104	18688	0.24	.22
Wardner 7 UT	C-46	13901	13970	0.0	.28
Wardner 133	M24	5458	11139	0.51	.35

$$R_w @ 75°F = \left(\frac{1}{-cl\,(0.0023 + 0.273) + 0.273} \right)$$

Well	Gas MCFD	Oil BOPD	Water BWPD
Elliff 28	159	0.368	0.077
Wardner 75	204	1.145	1.385
Gruene 12F	581	4.944	3.461
Elliff 2J	59	0.059	0.028
Elliff 31F	218	0.848	2.279
Wardner 177F	239	0.315	13.542
UCLI No. 13	250	6.165	0.047
Elliff 29-D	545	0.433	1.323
Rivers B-5	267	0.47	2.502
ML Rivers A-17	207	0.206	0.766
Rivers A2UT	421	0.755	18.546
Wardner 166	486	6.417	302.321
Wardner 7 UT	118	0.237	2.954
Wardner 133	—	—	—

the sandstones matrix for the neutron porosity. Total and effective porosities were obtained by using the following equations:

$$\varnothing_{DC} = \frac{\rho ma - \rho b}{\rho ma - \rho f} - Vsh \frac{\rho ma - \rho sh}{\rho ma - \rho f}$$

$$\varnothing sc = \varnothing s - \varnothing ssh \ Vsh$$

$$\varnothing_{Nc} = \frac{\varnothing n}{\varnothing nf} - Vsh \frac{\varnothing nsh}{\varnothing nf}$$

where

$\varnothing_{DC}$	=	corrected density porosity
$\varnothing sc$	=	corrected sonic porosity
$\varnothing_{Nc}$	=	corrected neutron porosity
Vsh	=	bulk shale volume
ρb	=	formation density
ρf	=	fluid density
$\varnothing nf$	=	neutron response in fluid
ρma	=	matrix density
ρsh	=	shale density
$\varnothing nsh$	=	neutron porosity in shale
$\varnothing ssh$	=	sonic porosity in shale

Appendix table 3–2 summarizes the parameters used in Stratton field for calculation of porosities, water saturation, and shale volumes.

Use of High-Resolution (1.2-inch) Data

In several zones in the Elliff 40 well, the measured core porosities were different from log-derived porosity. A comparison of core-derived bulk density versus log-derived bulk density measurements revealed that a closer match could be obtained using the high-resolution density (Langford and others, 1992). Appendix figure 3–3 compares bulk density from 6-inch data and 1.2-inch data plotted alongside core bulk density. Core bulk density values were calculated using

Table 3-2. Typical petrophysical parameters, Stratton field.

Shale Determination Parameters

	Clean	Shale
Gamma Ray (API)	60	100
Apparent Grain Density (gm/cc)	2.65	2.90

Water Saturation Parameters

R_w @ 75°F   =   0.17 ohm-m
C_{wb} @ 75°F =   7 mho/m
$a = 1$, $m = 1.89$, $n = 1.79$

Shale Parameters for Porosity Determination

	Wet	Dry
Density (gm/cc)	2.37	2.65
Neutron (PU)	45	38

Matrix Values for Porosity Determination

Density (gm/cc)	2.65
Neutron	sandstone
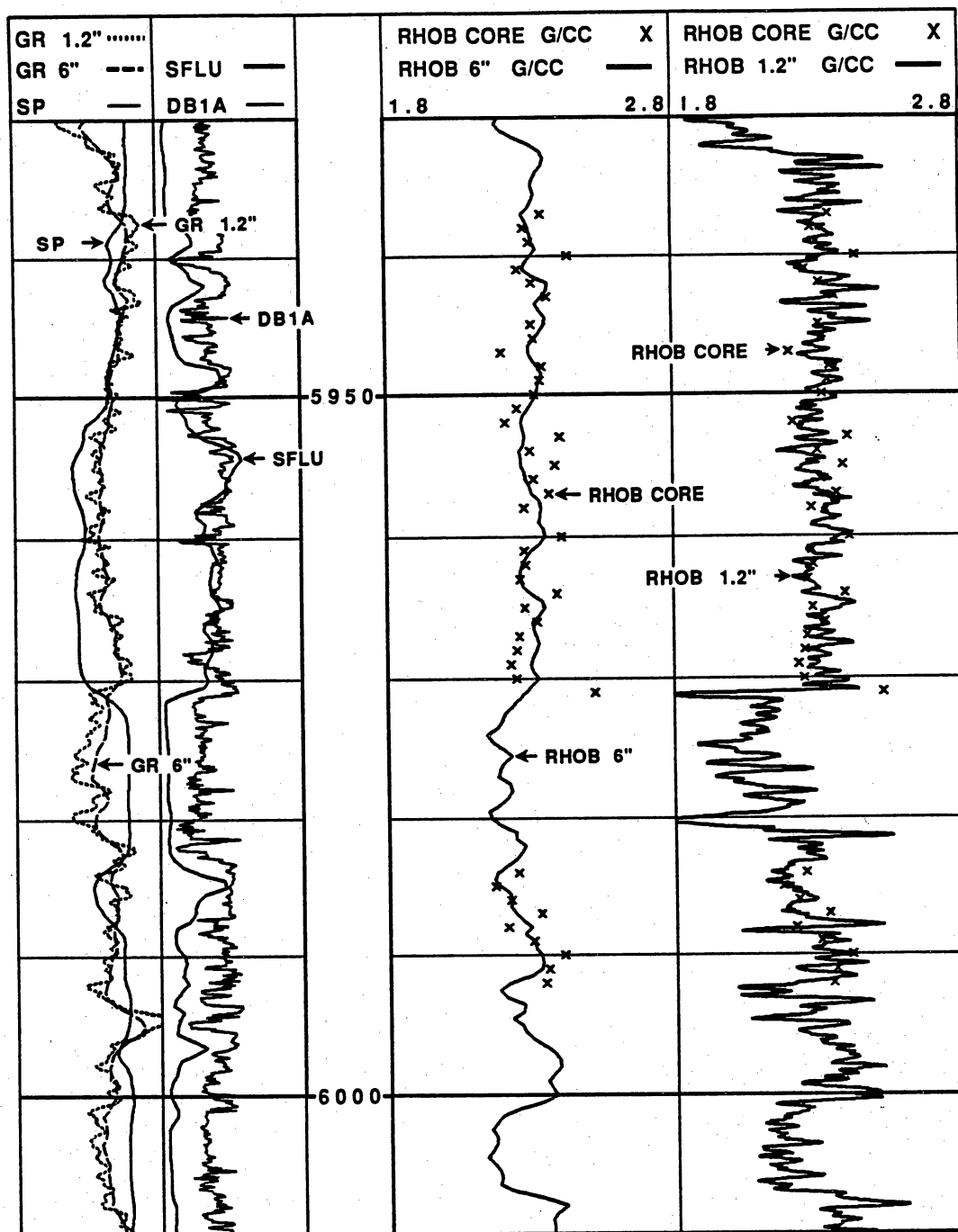
Figure 3–3. High-resolution logs provide a better match with core data.

reported core grain density measurements and a fluid density of 1 g/cc.

In the zones from 5,982 to 5,992 ft, a better match is obtained using the 1.2-inch bulk density as opposed to the 6-inch bulk density, indicating that high-resolution data are better for locating gas in thin-bed zones.

Use of Petrographic Core Data

All petrographic data were evaluated for use in the petrophysical model. Because a shaly sand interpretation model was used (Schlumberger, 1974), most of the emphasis was placed on derivation of bulk volume of shale. A good estimation of the shale volume is needed to compensate for shale effects in the porosity and water saturation calculations. Of the petrographic measurements, thin-section point count (TSPC) analysis yields the best estimate of shale volume. Thin-section analysis provides the fine fraction minerals used to calibrate the log-derived shale indicators. TSPC analysis shale results were compared with several log shale indicators to determine the best correlation (Howard and others, 1986). Apparent grain density (RAPP) values from the neutron-density, gamma-ray, spontaneous potential (SP), and neutron porosity (NPHI) logs were plotted. The SP, RAPP, and NPHI have the best fit (app. fig. 3–4), whereas the gamma ray is not useful as a shale indicator in the Frio Formation because of the presence of radioactive minerals in clean sandstones. Combining all these indicators, their minimum value provides a good fit with TSPC analysis. Appendix figure 3–5 shows the final shale volume computed from logs versus TSPC values. These shale indicators were used for the rest of the wells in the field. Additionally, thin-section analysis also confirmed the permeability reduction of type II reservoirs; shards of volcanic glass were observed in the mudstones. Volcanic glass has been related to permeability reduction in the middle Frio and causes higher gamma-ray responses and an increase in the thorium and potassium readings on the spectral gamma-ray log readings.

203

ELLIFF #36
VSH TSP VS. LOGS
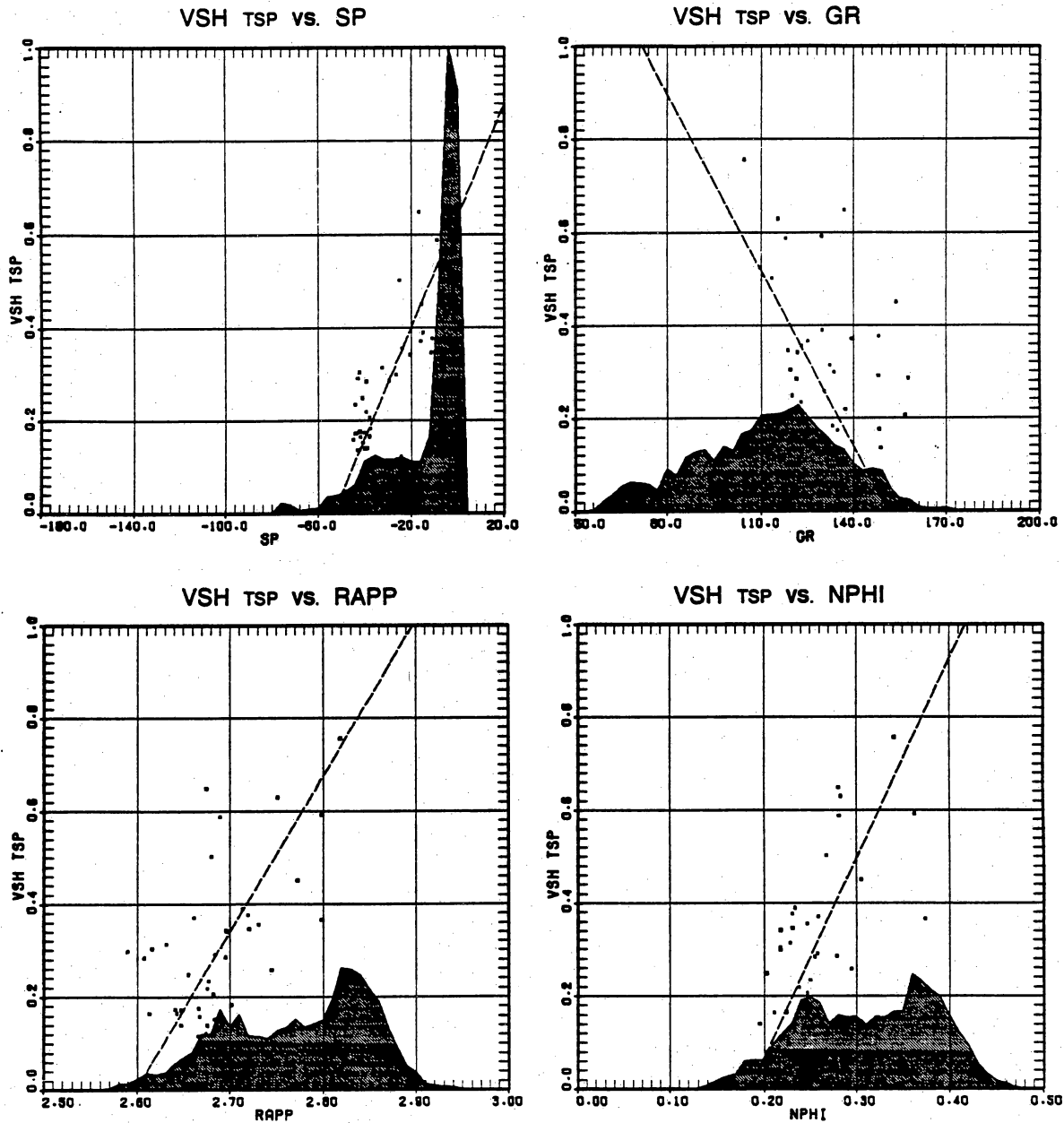
Figure 3–4. SP, RAPP, and NPHI offer the best fit with VSH from thin-section point count.
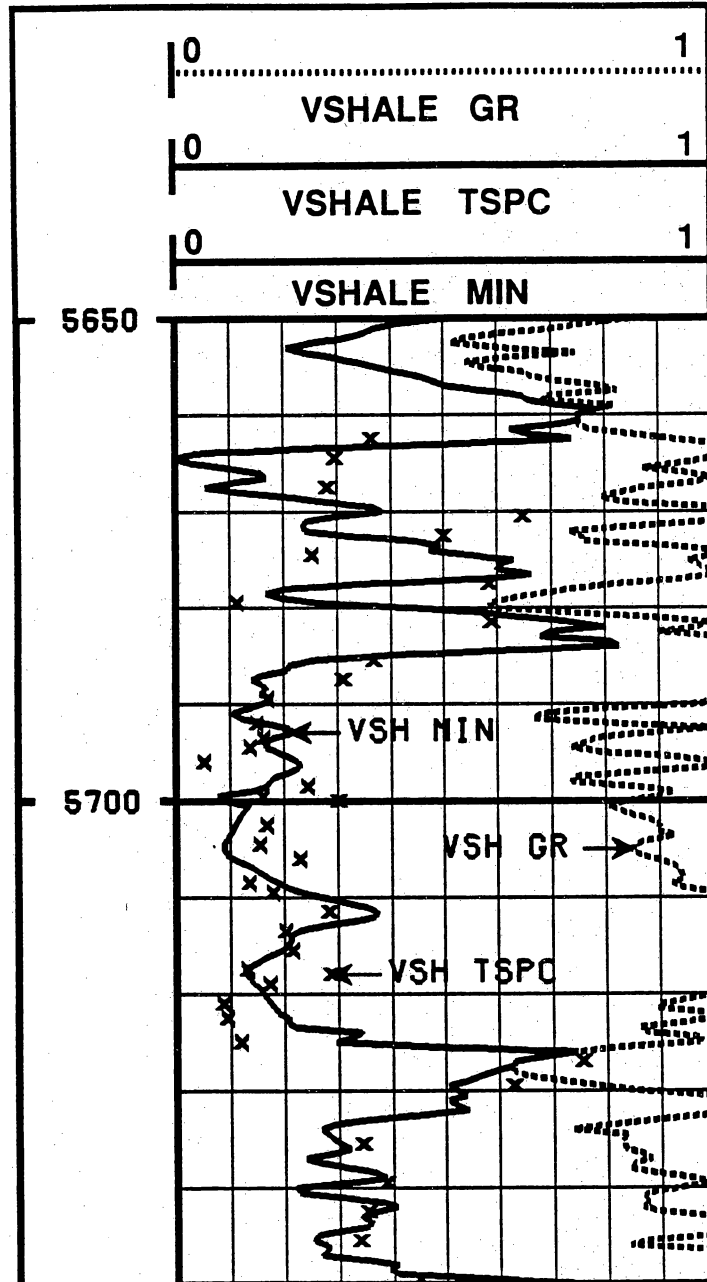
Figure 3-5. Comparison of final log-derived shale volume versus shale volume from thin section.

Cementation Exponent "m" and Saturation Exponent "n"

Another important factor needed to obtain a representative water saturation is the value of the cementation exponent "m" and the saturation exponent "n" at reservoir conditions. The values of m = 1.89 and n = 1.79 were measured in the Frio reservoir in previous BEG research performed by ResTech in Seeligson field. Because these values are very close to recommended parameters in most shale-sand sequences in the Gulf Coast region, they were applied to the saturation equation.

Determination of Formation Water Saturation

The dual water method (Clavier and others, 1977) was found to be the most applicable in Stratton field. This shaly sand model effectively accounts for the high surface area of the shales and clays lining the pores of shaly reservoirs in the Frio Formation. The model also accounts for any additional gas stored in the shale porosity. Using the measured formation water resistivities, electrical factors, and irreducible water saturations obtained from capillary pressures, the method was validated. This model was used for the rest of the wells evaluated.

Log-Derived Versus Core-Derived Results

Appendix figure 3–6 compares log-derived results with core-derived results in the cored interval of the D34 and D35 reservoir. Overall, the results of the log-analysis model are in good agreement with the core-analysis results. Establishment of this match is important to correctly estimate reservoir values in sandstones when core data are unavailable.

Appendix figure 3–7 shows another example of the log and core match for the F-11 reservoir in the Frio. With the electrical factors and formation water resistivity chosen, the formation water saturation equation is validated by comparing it with the irreducible water saturation derived from capillary pressure measurements (Sw-cap). Notice the excellent
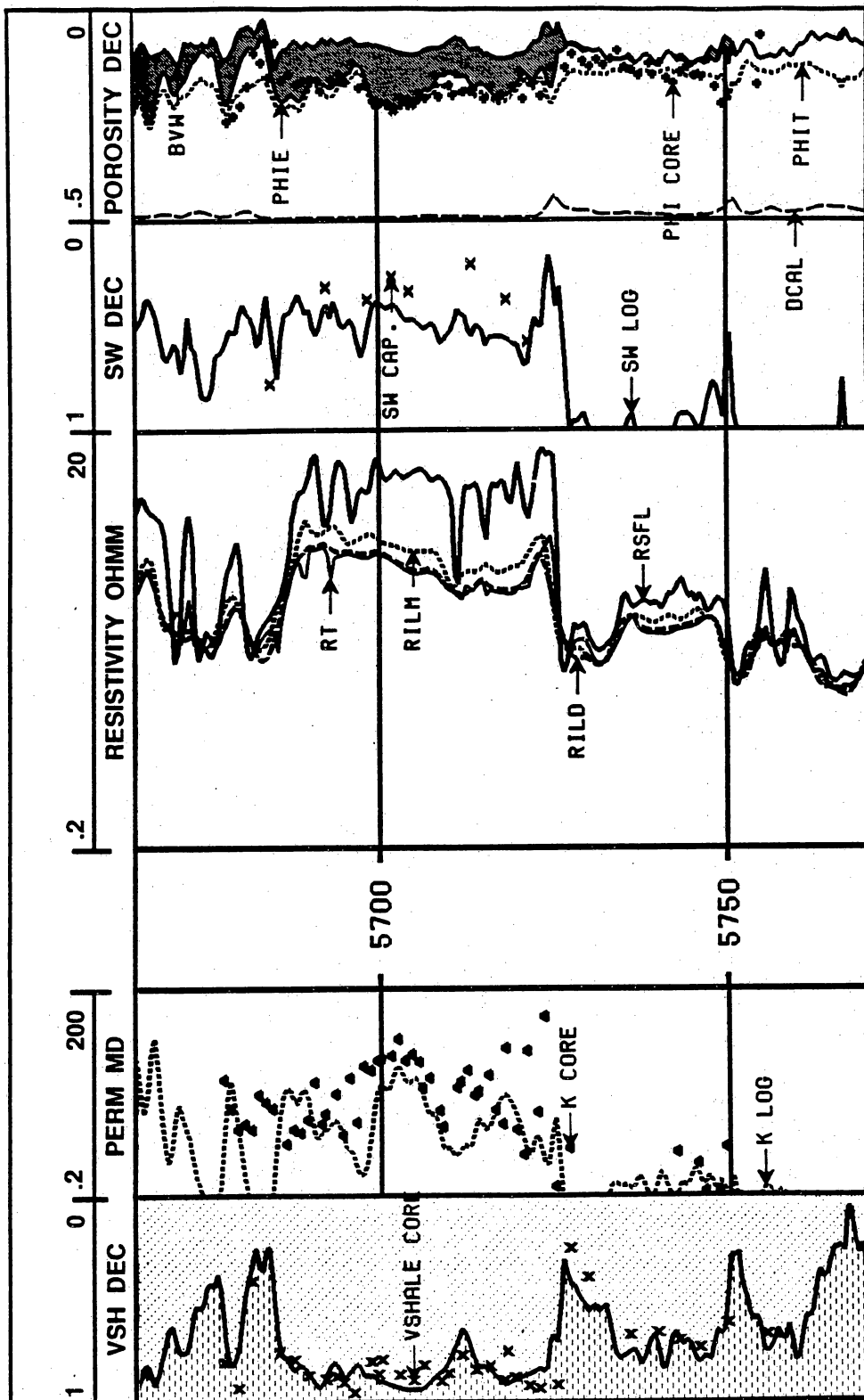
Figure 3–6. Results of log-analysis model are in good agreement with core analysis results.

207
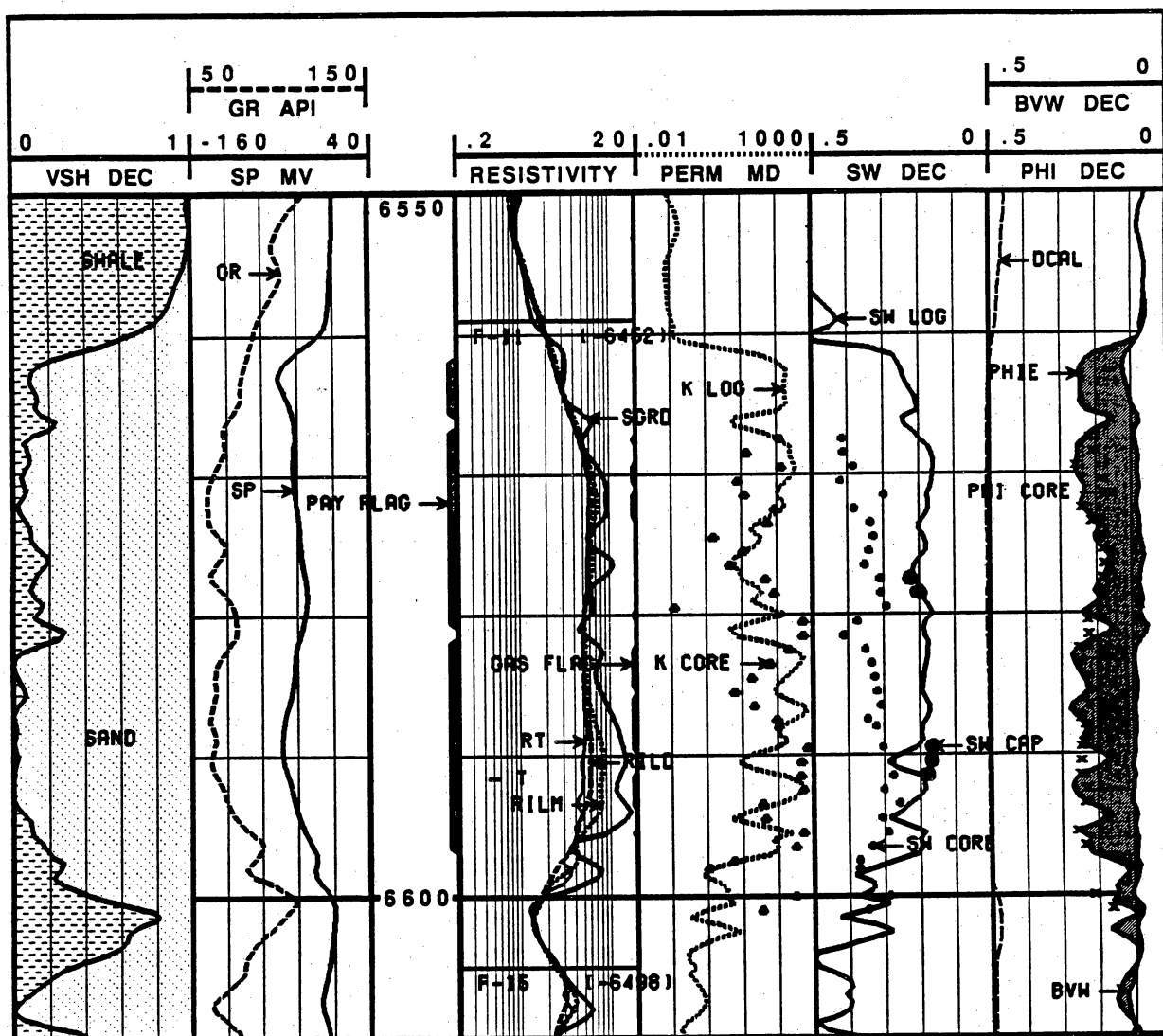
Figure 3–7. Formation water saturation equation results versus capillary pressure saturations.

porosity match between core data and log porosity, as well as the agreement of log-derived water saturation and capillary saturations.

Core-analysis data were also used to obtain a permeability relationship as a function of rock type for both high- (>200 md) and low- (<15 md) permeability sandstones reservoirs. These trends of permeability were also incorporated into the computed log interpretation model. The permeability model is explained in more detail in the permeability prediction section in this report.

Use of Capillary Pressures to Predict the Free Water Level for the D-29, D-34,
    and D-35 Reservoirs

Using capillary pressure measurements on the D-35 reservoir and the advanced capillary pressure model (ADCAP) (Hawkins and others, 1993), free water level projections based on log calculations and capillary pressure data were made for the D-29, D-34, and D-35 sands of the Elliff lease. These free water level projections were predicted as −5,529 ± 30 ft subsea for the D-29, −5,585 ± 27 ft for the D34, and −5,605 ± 7 ft subsea for the D-35 reservoir, in the area near the Elliff 36 well. The method also provided a 95 percent confidence limit (the D-35 is ±7 ft), indicating that the data fit the model very well. These estimates were obtained by fitting core data measurements and log-derived parameters to relate four important reservoir parameters: capillary pressure, porosity, water saturation, and permeability.

These predicted water levels were also verified with isoresistivity maps of each reservoir and by finding the lowest known gas producer. The predicted free water level for the D-35 reservoir was confirmed when we predicted that two proposed recompletions in wells Texon–Royalty 5 and 7 should not be perforated because they would intersect the gas-water contact. Texon–Royalty 5 well was perforated and produced water as predicted.

Quick-Look Methods

Reasonable results can be obtained using some quick-look methods to find gas-bearing zones. Apparent water resistivity, neutron-density and neutron-sonic crossover analysis, comparison of a pseudo-SP (obtained from the Rxo/Rt values) with the real SP, and determination of porosity, Ro, water saturation, and the minimum bulk volume of water that indicates nonmovable water were methods used in this research to pick zones of interest. The modern open-hole logging suite of dual induction, compensated neutron, formation density, borehole compensated sonic, wireline formation tester, and sidewall cores can be used for evaluation of the Stratton wells. These techniques are reviewed in the following sections.

Rwa

The apparent water resistivity (Rwa) is derived from the Archie equation and is usually presented in the triple-combo log, if requested to the wireline company. By defining a Rwa minimum in the water sands and determining the value of the Rwa deflection in the zones of interest, the ratio of Rwa/Rwa min can be used to predict water saturation: a ratio of 1/1 = 100 percent Sw, 2/1 = 71 percent Sw, 3/1 = 58 percent Sw, and 4/1 = 50 percent Sw. Any show better than 3/1 should be productive in the Frio, assuming that reservoirs are not pressure depleted. Any shows better than 2/1 should be evaluated further.

Neutron-Density Crossover

Gas affects neutron and density in opposite ways. Low gas density causes the neutron porosity to read too low, whereas density porosity reads too high. These two porosity logs will cross over in clean sands when gas is present. Sonic and neutron porosities can be used in the same manner. Even in shaly sands, shale affects the neutron, causing the neutron to read too

high and thus masking some shaly gas productive zones. Sonic and neutron curves are affected by shale in the same direction, thus allowing some gas crossover, even in shaly sands.

Comparison of SP with a Pseudo-SP Derived from Rxo/Rt Values (Rxo/Rt QL)

Comparison of the SP with a pseudo-SP derived from the Rxo/Rt ratio (Dumanoir and others, 1972) provides an idea of hydrocarbon mobility. If during the drilling process mud filtrate has invaded the formation and displaced the gas near the well bore, there will be a difference between Sw and Sxo for Rmf >Rw. Whenever Sw = Sxo, the zone will produce water, regardless of the apparent water saturation. Thus, impermeable and water-bearing zones can be eliminated. Using the following equation,

$$\frac{Sw}{Sxo} = \left[\frac{Rxo/Rt}{(Rm/Rw)SP} \right]^{1/2} \text{,}$$

we can compare the Rxo/Rt ratio to the Rmf/Rw value derived from the SP. Whenever the ratio of Rxo/Rt equals Rmf/Rw from the SP, the zone will produce water or be tight. Whenever the Rxo/Rt ratio is less than the Rmf/Rw, the zone should be hydrocarbon productive. A quick-look technique derives a pseudo-SP from Rxo/Rt to be compared with the SP.

Porosity

Porosity can be read directly from the density log, if density porosity is computed using a 2.65 g/cc grain density and a fluid density of 1.0. Additionally, an equivalent wet formation resistivity (Ro) can be computed using the following equation:

$$Ro = Rw/\varnothing_D{}^m$$

In hydrocarbon-bearing zones, Ro will read lower than Rt and can be similarly used with the Rwa curve to pick zones of interest.

Water Saturation

An Archie saturation is adequate for a quick look of cleaner sands, such as in Stratton:

$$Sw^{1.79} = Rw/\varnothing^{1.89} Rt.$$

Use a value of .17 ohm at 75°F for Rw and correct accordingly for formation temperatures. Water saturations less than 60 percent are productive in most cases if the sand is not depleted.

Bulk Volume of Water (BVW)

The product of $\varnothing$ * SW (in decimal units) will provide the bulk volume of water. Values of BVW lower than .11 indicate zones at irreducible water in most cases. If the porosity is higher than 18, the zone should be tested.

Wireline Formation Tester

This tool is indispensable in monitoring pressures in depletion gas drive reservoirs in the Frio Formation and to determine fluid type. Wireline pressures need to be supervised closely at the well site to obtain representative formation pressures. Pressure monitoring may be the most critical evaluation technique to pick out nondepleted zones.

Sidewall Cores

Sidewall cores are useful for porosity and inferred permeability, and to determine hydrocarbon shows. The comparison of critical water saturation reported by core analysis with computed water saturation may also be useful to pick pay zones (Granberry and others, 1977).

Example

Appendix figure 3–8 shows an example of the application of these indicators in a hydrocarbon-bearing zone (F-39) and in a water-bearing zone. In the hydrocarbon-bearing zone at 6,900 ft, notice the increase in Rwa readings, the separation between the SP and the Rxo/Rt QL curve, the separation between the Ro curve and the Rt curve, and the value of BVW fairly constant around .11. All these indicators point to a gas-bearing zone, as confirmed by the production test from 6,902 to 6,910 ft with 565 Mcf/d production. Not all the indicators work all the time, but a combination of these indicators gives more confidence to the interpreter in finding pay zones.

Optimum Logging Suite

For conventional evaluation of Frio reservoirs, the "triple-combo"—the dual induction-laterolog, compensated neutron and formation density, and gamma-ray logs—proves adequate. These logs, combined with sequential wireline formation testing and sidewall coring, will provide optimum information.

For a more detailed analysis and for isolating thin pay zones of less than 6 ft, the new high vertical resolution induction devices are recommended. Several versions are now available from the wireline industry. One in particular, used by the project in McFaddin field, was the array induction log, which enabled resolution of beds to a 1-ft thickness and allowed delineation of several thin gas-bearing zones that would have been missed using conventional logs.

Examples of Open-Hole Interpretation

Computed results can be used to predict potential gas-producing zones and to explain some of the anomalies found during production. For example, appendix figure 3–9 shows a

GAS BEARING ZONE

-80	SP	MV		20
-80	(RXO/RT)	QL		20
0	RWA	OHMM		.5

RESISTIVITY

SW

POROSITY

.2 OHMM 20.   1.0   0   .3   0

6900

RWA →

F-39

565 MCFD
2.6 BCD
2 BWD

← (RXO/RT)QL

→ SP

RT →

RO →

RILD →

← RSFL

← RILM

PHIE →

← BVX

← SWE

BVH →

WATER BEARING ZONE

← RILM

4800

RILD →

← (RXO/RT)QL

← RSFL

← RWA

← SWE

→ SP

RT →

4850

RO →

← BVH
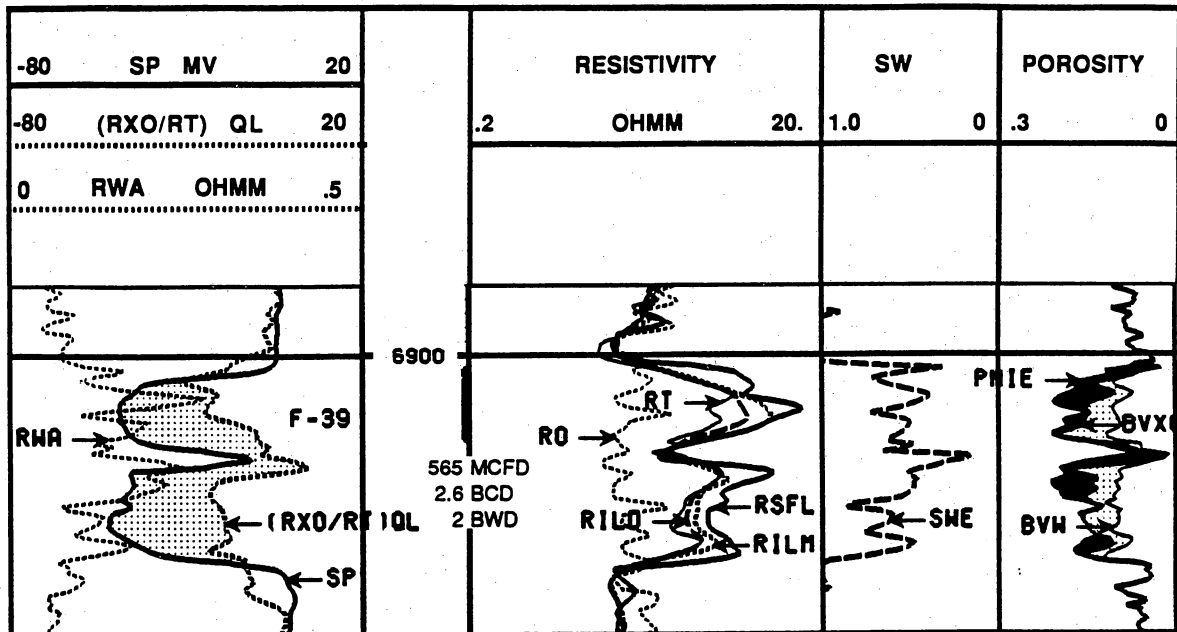
PHIE →
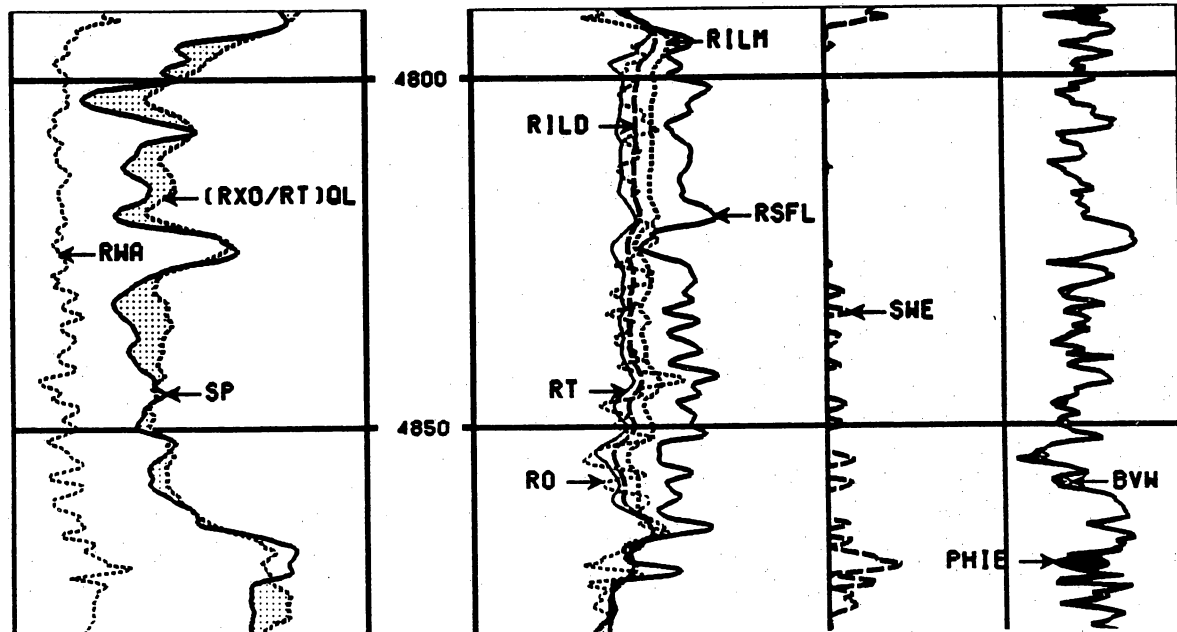
Figure 3–8. Quick-look indicators in gas- and water-bearing zones.

214

Figure 3–9. More representative water saturation values are obtained by using a shaly sandstone model.

shaly sand tested in the Gruene 13 well. With an Archie saturation equation, the zone appears marginal, having saturations above 60 percent. However, using the shaly sandstone model developed, a more representative water saturation of 45 percent is obtained. Unfortunately, the sandstone was depleted and only produced 77 Mcf/d when tested.

Another example of computed results helps explain gas with water production. The Wardner 206 well (app. fig. 3–10) shows the perforated interval in the E-49 reservoir. The test produced 288 Mcf/d with a shut-in pressure of 1,050 psi. However, the water production of 138 BFW per hour rendered this test uneconomical. It is easy to see that the water production is coming from the transition zone from 6,420 to 6,434 ft. The decrease of resistivity and increase in water saturation and bulk volume of water with depth confirms this water production.

Validation of Wireline Pressures

Because many Frio reservoirs are pressure depletion drives, identification of nondepleted zones is critical. Wireline pressure tests in open-hole wells and short-term production tests in cased-hole wells are common techniques used to determine reservoir pressure. Some wireline formation pressures can be misleading due to tool defects, miscalibrations, or incomplete pressure test sets. Validation of wireline pressures and supervision of the testing operation at the well site is indispensable in obtaining representative formation pressures.

One problem encountered obtaining valid formation pressure data is when insufficient setting time is allowed to obtain a stabilized shut-in pressure. For example, in appendix figure 3–11, a 60-sf wireline set produces a low pressure of 139 psi. By contrast, in appendix figure 3–12, the tool was set 0.5 ft higher and for 251 s, yielding a more representative but not quite stabilized pressure of 3,556 psi. A valid test is shown in appendix figure 3–13; here the tool was allowed enough time so that the shut-in pressures stabilized to 4,604 psi after 142 s.
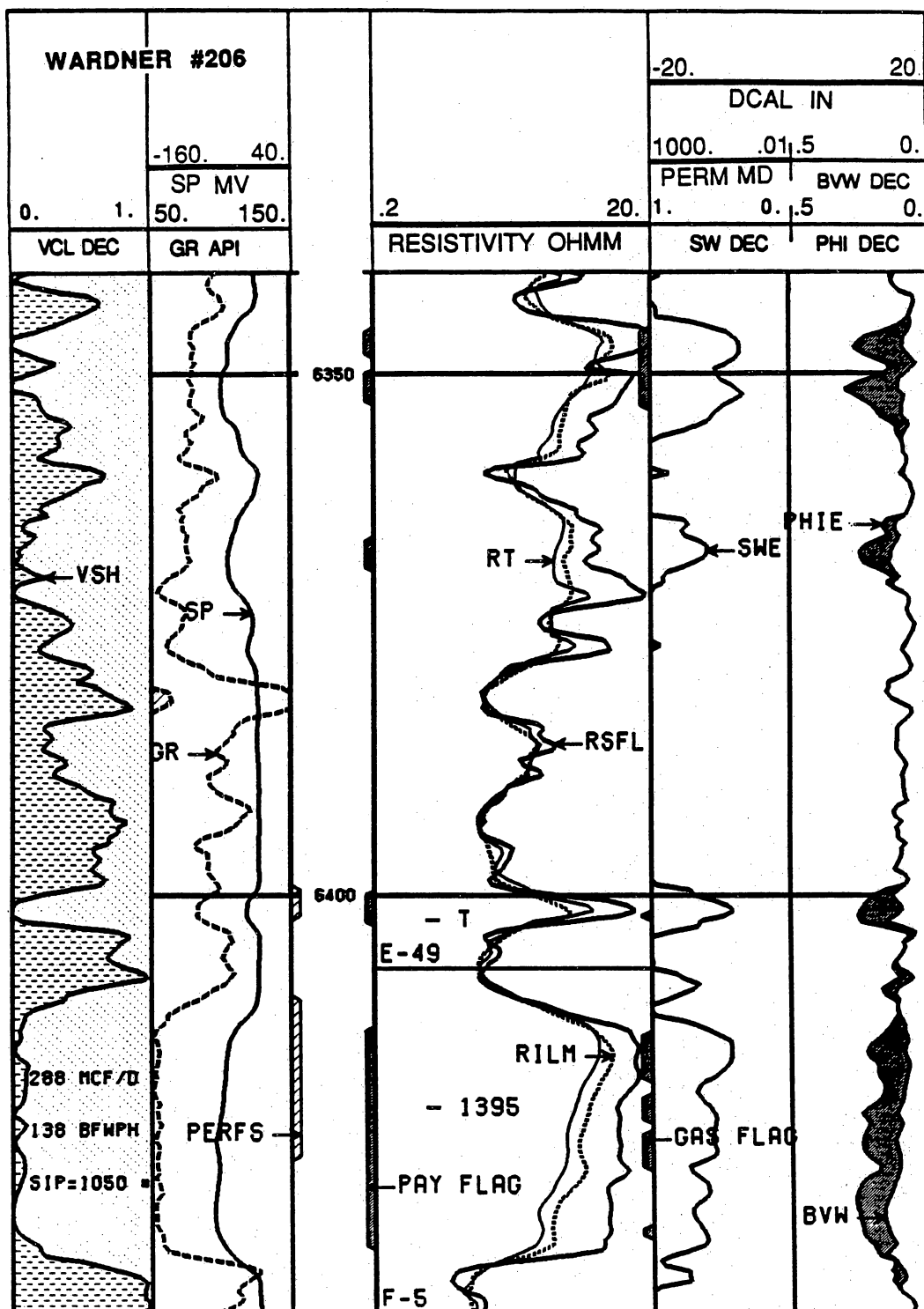
Figure 3–10. Example of a transition zone.

217

WARDNER #185	DATE 5/8/88	REPEAT FORMATION TESTER	

MSPE				TENS		
0	RPS	10000		0	10	20
TESTER SUM			HUNDREDS	UNITS		
0	PSI	10000				
SET # 12			-10 0 10	-10 0 10		

```
4069.    407.5
4069.    475.5
4068.    463.5
3556.    451.5
3546.    439.5
3530.    427.5
3509.    415.5
3474.    403.5
3412.    391.5
3313.    379.5
3162.    367.5
2975.    355.5
2421.    343.5
1901.    331.5
1415.    319.5
1086.    307.5
 832.    295.5
 646.    283.5
 512.    271.5
 399.    259.5
 313.    247.5
 233.    235.5
 252.    223.5
1328.    211.5
4064.    199.5
4074.    187.5
4073.    175.5
4076.    163.5
4082.    151.5
            139.5
```

SET #12

Figure 3-12. Representative wireline pressure of 3,556 psi.

```
4074.    127.5
4075.    115.5
4076.    103.5
4079.     91.5
 139.     79.5
 121.     67.5
  99.     55.5
 281.     43.5
4077.     31.5
 40.7.    19.5
 4076.     7.5
```

1°/MIN
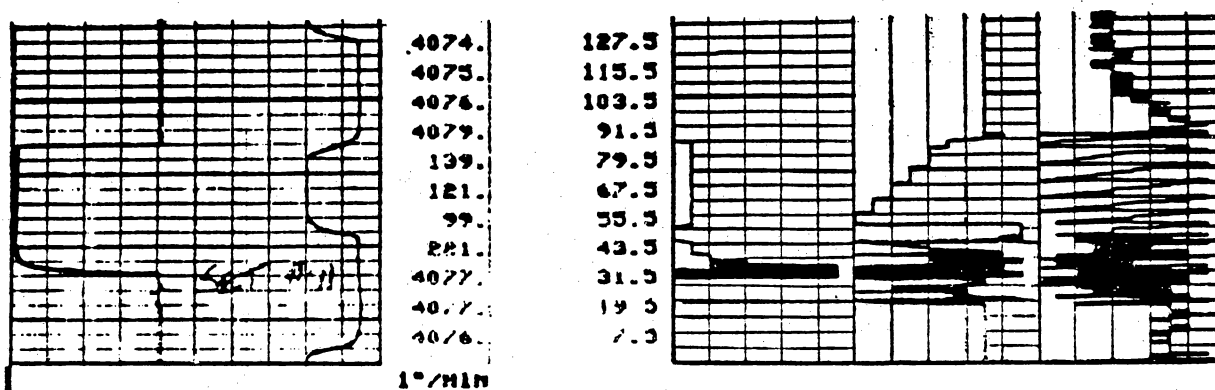
Figure 3-11. False wireline pressure of 139 psi.

218

7341 FT.

THOUSANDS			TENS		
0	10	20	0	10	20

TESTER SUM

	HUNDREDS			UNITS		

PRESS	10000	-10	0	10	-10	0	10

04901 00154
04901 00154
04902 00154
04902 00154
04903 00154   PSD RETRACT
04625 00152
04624 00142
04624 00131
04624 00121
04624 00110
04595 00100

04590 00079
04560 00068
04530 00058
00040 00047
01000 00037   PRETEST
04932 00026   PRETEST
04933 00016
TEST TIME   PSD SET
DEPTH 07341.0
WELEX

THOUSANDS			TENS		
0	10	20	0	10	20

TESTER SUM

	HUNDREDS			UNITS		

PRESS	10000	-10	0	10	-10	0	10

Figure 3–13. Valid wireline formation pressure.

Because of low-permeability streaks found in the Frio sandstones, the set time might be too long to obtain representative pressures. When this happens, move the tool and find a more permeable zone for pressure and fluid testing. Another problem is that in using wireline pressures later in the life of the well during recompletion operations, the target reservoir may already have lower pressures because of depletion from nearby production. Available wireline pressures were studied, and the most representative pressures were used to investigate pressure variations throughout the field for each reservoir. Appendix table 3–3 illustrates the pressure variations found for several reservoirs of interest. These pressure variations suggest compartmentalization in Stratton reservoirs.

Keys to Obtaining Valid Wireline Pressure Readings in Gulf Coast Sandstones

(1) Plan testing operations in advance with the service company so that proper tool modification can be implemented to optimize data acquisition.

(2) Control the size of the pretest chamber (use 5 or 10 cc pretest chamber) in low-permeability sands to minimize pretest time.

(3) Select optimum test depths and choose zones with $\emptyset$ >14 pu and good SP and gamma-ray deflection.

(4) Identify invalid pressure readings by monitoring pressure buildup.

(5) In low-permeability zones, let the tool set long enough to reach stable shut-in pressure.

(6) Repeat pretest measurement 0.5 ft above or below selected depth if test is tight or invalid, to find the most permeable zones.

(7) Verify tool calibration by setting tool in casing to obtain zero pressure and by comparing hydrostatic pressure with mud weight.

Table 3-3. Stratton field, Wardner lease RFT shut-in pressures (psi) (chronological order).

ZONE	144 JAN 1979 PSI	GRAD	169 OCT 1987 PSI	GRAD	184 APRIL 1988 PSI	GRAD	182 MAY 1988 PSI	GRAD	185 MAY 1988 PSI	GRAD	183 JUNE 1988 PSI	GRAD	181 SEPT 1988 PSI	GRAD	200 DEC 1988 PSI	GRAD	206 MAR 1989 PSI	GRAD	208 APRIL 1989 PSI	GRAD
B-41	475	.10					110	.02	634	.13									514	.11
B-46																				
C-7	1948	.40																		
C-18																				
C-28																				
C-35																	T			
C-38	2318	.44																	2829F	.54
C-46			2474	.46													T		1619	.30
C-50	2102	.39					115	.02											T	
D-6															T					
D-11													2214G	.40			2340	.42	1760	.32
D-15																				
D-18																				
D-23																				
D-34											T		2688	.47			T		T	
D-35			832	.14			154	.03			T									
D-44			837	.14			139	.02			T		T							
E-4			858	.15							T						T		2856	.47
E-11					T															
E-13	2671	.45																		
E-18																				
E-25	2762	.45					292	.05	338	.05			T						253	.04
E-29	2065	.34	1012	.16			1641	.27	1715	.28									T	
E-31						—			T											
E-38					T						573	.09	519	.08	442	.07	1395	.22	T	
E-41			871	.14	T				328D	.05			489	.08					T	
E-49			1482	.23					1616	.25										
F-5													2878	.45	2055	.32	2966	.46	T	
F-7									390D	.06	745	.11	519	.08	809	.12	1302	.20	3073	.47
F-11			944	.14	T				2944	.45	3088	.47								
F-15			871	.13	T				2490	.38	2698	.41								
F-21					T						T		T							
F-25					T				2590	.38							940	.14	2518	.38
F-34			1012	.15													1467	.21		
F-37			3443	.51	2767	.40			3554	.52					978	.14	1535	.22	3560	.52
F-39			1070	.16											2064G	.30				
F-44																				
G-1					T		T		1657	.24			T				1784	.25		

D = depleted, t = tight, G = recovers gas, W = recovers water, F = filtrate

Research was also done to investigate relationships between wireline pressures and open-hole log measurements. A relationship was found that related invasion depth, ILM/ILD and $\emptyset d/\emptyset n$ ratios. However, a test in Wardner well 201 yielded inconclusive results. Research was then continued using cased-hole measurements.

Permeability Prediction

Permeability was computed using correlations developed between core porosity and core permeability for type I (high-permeability) and type II (low-permeability) rocks. As shown in appendix figure 3–14, log-derived values of porosity were substituted for core porosity. The following relationships were used:

(a) For type I, higher quality rocks

$$k = .0060643 \left[10^{(0.18294\,\emptyset)} \right]$$

(b) For type II, lower permeability rocks

$$k = .005339 \left[10^{(0.14286\,\emptyset)} \right]$$

where

k = permeability in millidarcys and

$\emptyset$ = log porosity in percentage.

These permeability relationships were derived from core data acquired in the Stratton field from type I and type II reservoirs (fig. 3–14 shows these relationships).

Core analysis also reveals that permeability corrections for Klinkenberg effects are only significant below 0.04 md and that corrections to unstressed porosity to reservoir conditions are less than 1/4 pu. Notice that the lower permeability reservoirs have more dispersion than the one found for higher permeability reservoirs (app. fig. 3–14). These two permeability relationships were incorporated into the model to estimate permeability for each of the two

Higher Permeability Reservoirs

Kair unstress

Phi unstress

$y = 8.0643e{-}3 \cdot 10^{\wedge}(0.18294x)$ $R^{\wedge}2 = 0.794$

Lower Permeability Reservoirs

Kair unstress

Phi unstress

$y = 5.3390e{-}3 \cdot 10^{\wedge}(0.14286x)$ $R^{\wedge}2 = 0.295$
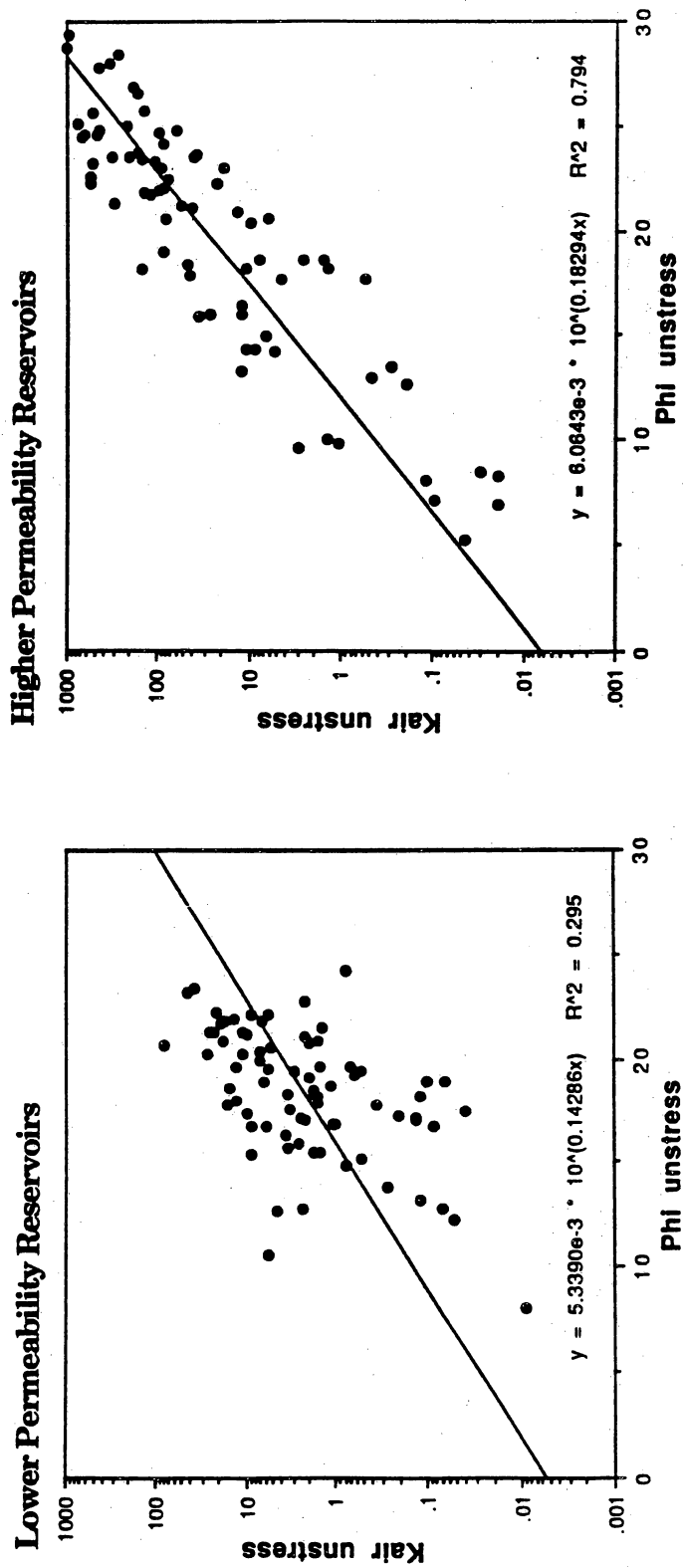
Note: Permeability is relative to air and measured from core plugs at surface conditions.

Figure 3–14. Porosity and permeability of middle Frio reservoirs, Stratton field.

223

rock types. Appendix figure 3–15 illustrates the fit obtained between log and core permeabilities. Rock types could also be predicted from log data as explained below.

Use of Logs to Differentiate Reservoir Types

Our studies of core data revealed that volcanic glass presence indicates low-permeability, type II reservoirs. Volcanic glass causes an increase in gamma-ray values, as shown in appendix figure 3–16, and furthermore, cased-hole spectral gamma-ray measurements revealed that zones containing volcanic glass have a higher count of thorium and potassium than do zones without volcanic glass. Therefore, by observing the gamma ray or newer spectral gamma-ray logs, it is possible to predict if a sandstone contains volcanic glass and therefore is a lower permeability type II reservoir.

Comparison of Microresistivity Readings with Minipermeameter Data

Permeability can also be inferred from microresistivity curves of the formation microscanner or the high-resolution dipmeter log. The C-18 reservoir minipermeameter data measured by BEG staff at the Elliff 40 well showed a good correlation with the dipmeter microresistivity, as observed in appendix figure 3–17. However, the same comparison for the E-13 reservoir produced a poor correlation, indicating that prediction of permeability from microresistivities may at times be misleading.

Cased-Hole Petrophysical Research

Cased-hole evaluation techniques similar to the techniques developed in Seeligson were used to identify and quantify gas-bearing zones in existing well bores by assessing gas presence and determining lithology, porosity and water saturation (original and current) (Jirik and others, 1991). Cased-hole logs were run in three old wells, the Warner 76 and 135 and the Elliff 20
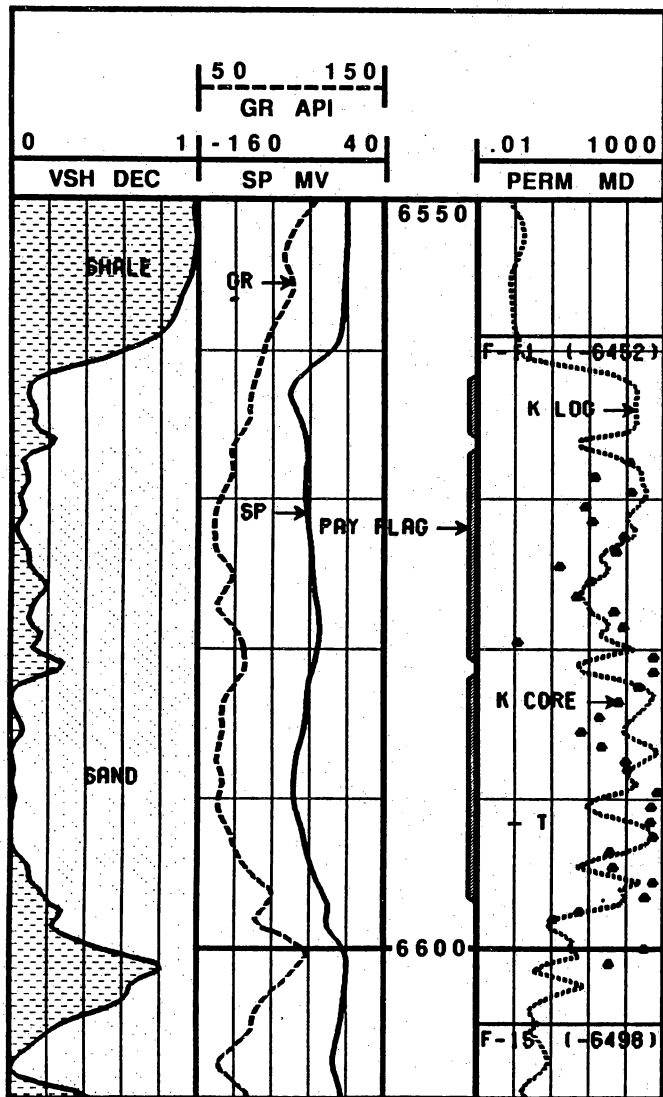
HIGH PERMEABILITY (TYPE I)   LOW PERMEABILITY (TYPE II)
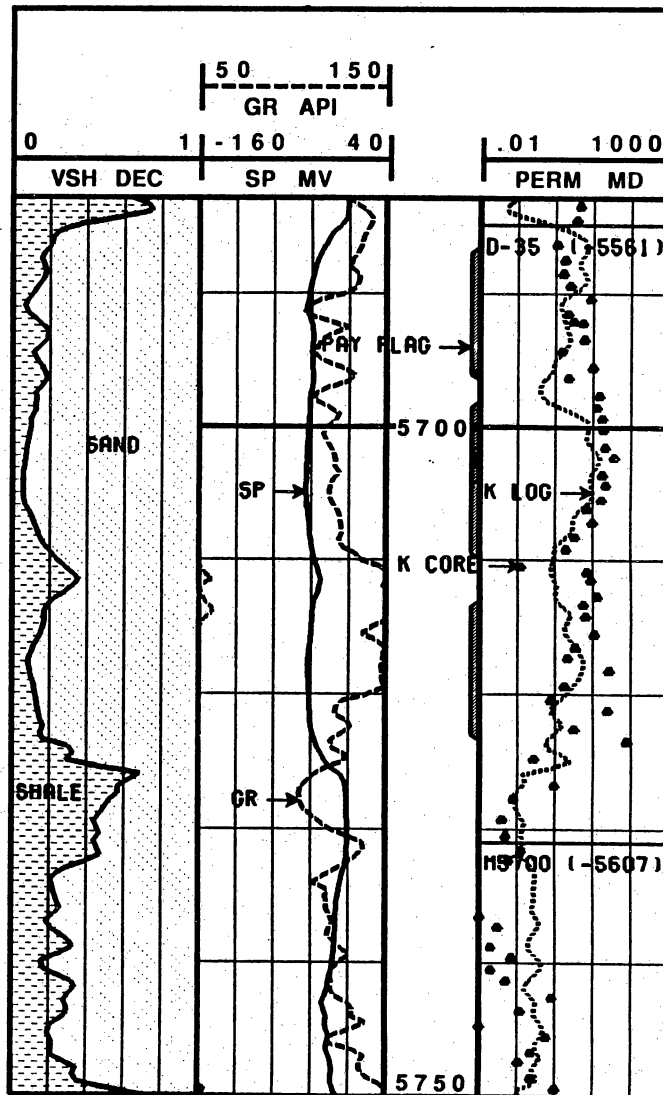
Figure 3–15. Comparison of core and log permeabilities.
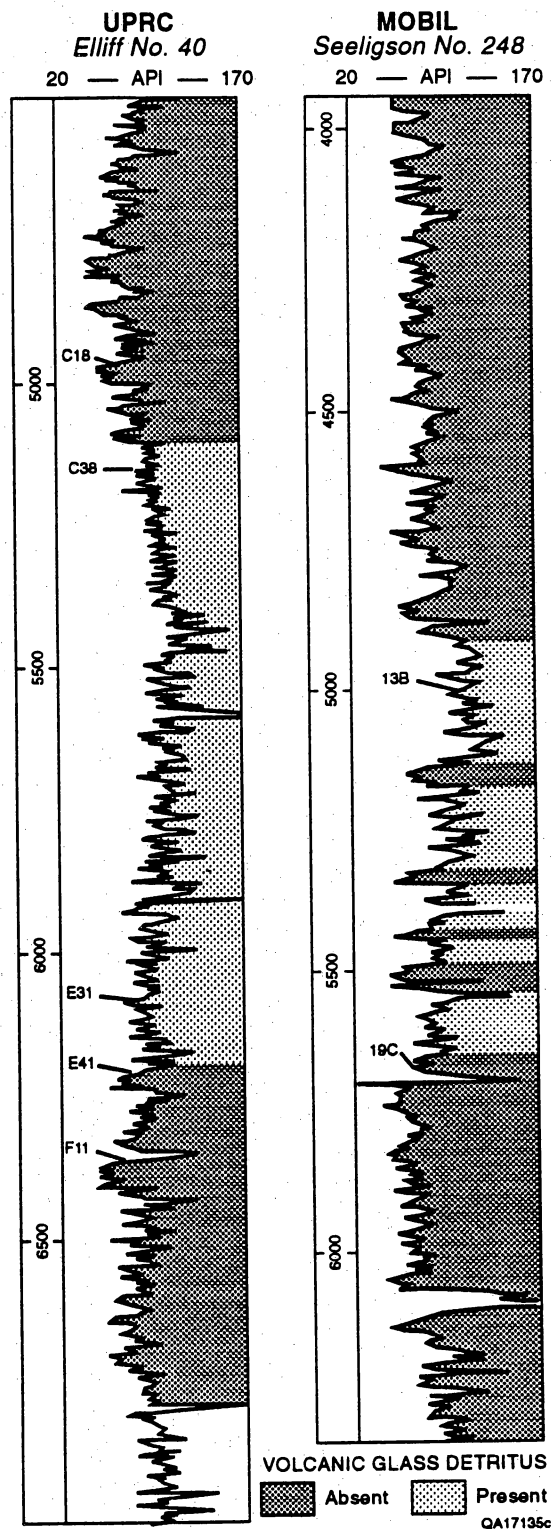
Figure 3–16. Volcanic glass causes an increase in gamma-ray values.
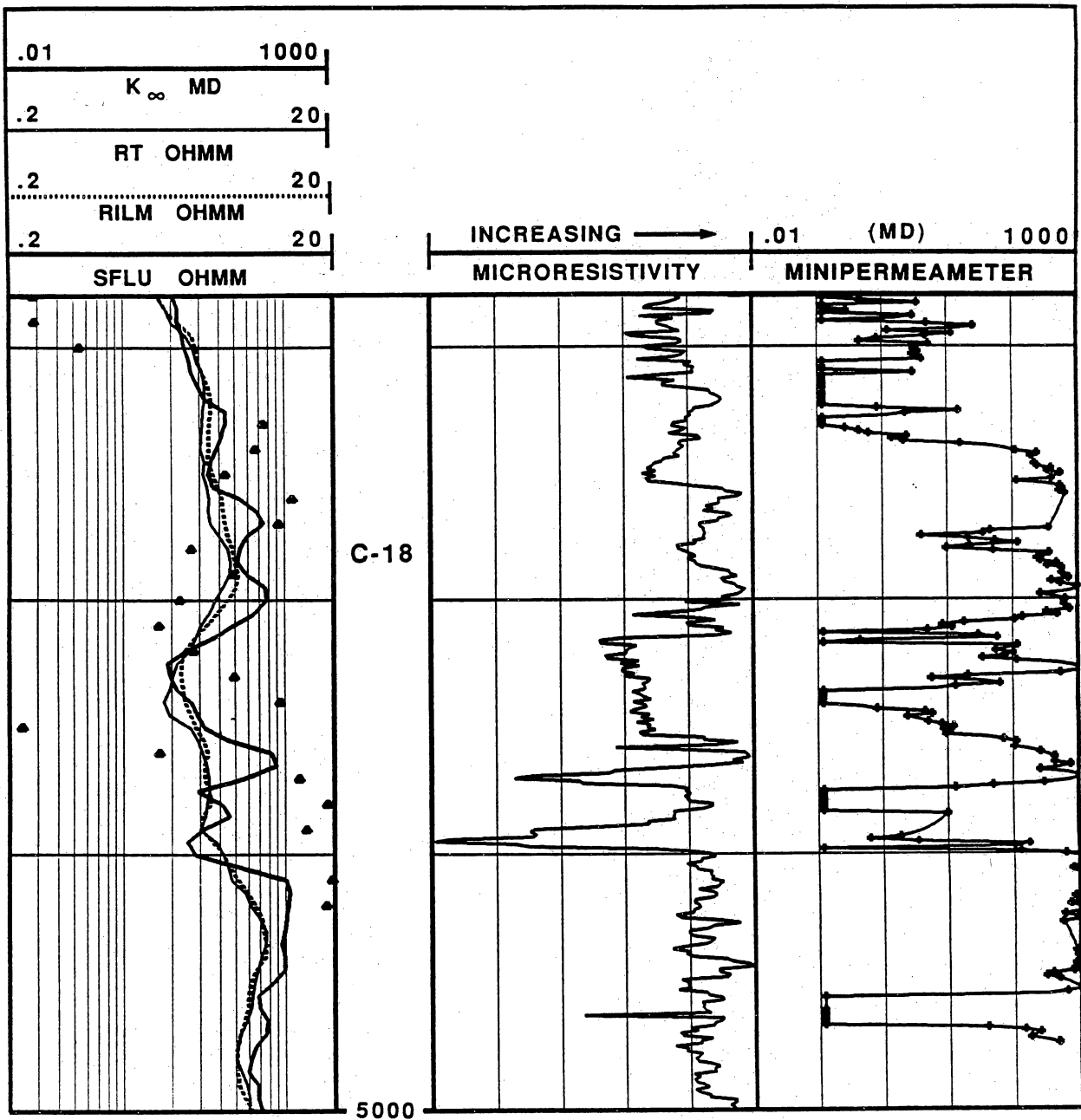
Figure 3–17. A good correlation is observed between microresistivity and minipermeameter measurements in the C-18 reservoir.

227

wells. Subsequent testing revealed that gas zones could be identified. However, our attempt to predict reservoir pressures from logs produced inconclusive results due to the wide range of cased-hole values when compared to recent wireline pressures.

Cased-Hole Logging Program

The original logging program in old cased-hole wells in Stratton consists generally of an electrical survey (Hilchie, 1979) and a few sidewall core samples. A cased-hole logging program was designed to complement the available data and fully evaluate the well. Pulsed-neutron, gamma-ray, and digital or dipole sonic logs were used for petrophysical evaluation to determine porosity, lithology, and water saturation. Diagnostic logs were run to infer the mechanical well conditions and quality of cement bonding. These diagnostic logs consisted of cement bond, noise, and temperature logs. The borehole gravity survey was attempted in the Wardner 135 well, but the tool failed due to temperature limitations.

Cased-Hole Evaluation Model

The cased-hole logs provide the additional information necessary to properly evaluate the formation, shale volume, porosity, and original and current water saturations. These data can effectively be obtained in Stratton field using the cased-hole evaluation program developed in Seeligson field.

Shale Volume

In Stratton field the lithology consists of sandstone shale sequences. As in the open-hole analysis, the lithology determination is based on shale indicators. The volume of shale used to correct the porosity logs and the saturation equation is calculated from the pulsed-neutron sigma measurement.

Porosity

Porosities were derived for the combinations of the compressional sonic porosity and the pulsed neutron porosity. These logs respond in a similar manner in non-gas-bearing zones (oil or water). However, gas affects both logs in opposite ways (porosity sonic > neutron porosity). Gas presence can also be inferred from the characteristic crossover of the normalized near and far pulsed neutron count rates. The acoustic log porosity can be obtained from the compressional travel time. Previous BEG/GRI research in Seeligson field has shown that reliable compressional travel times can be obtained through casing when cement bonding is better than 50 percent, and formation arrivals can be distinguished in the variable density display (VDL). The following Hunt-Raymer equation was used to compute sonic porosities:

$$\emptyset_s = 0.625 \; \frac{t - tma}{t}$$

where

t $\quad$ = compressional travel time

tma = matrix travel time = 55.5 msc/ft.

Using equations similar to the ones presented for open-hole porosity determination, $\emptyset nc$ and $\emptyset sc$ corrected for shale effects are obtained. The two porosities are used to obtain the porosity of the formation. In bonded zones, where the cased-hole sonic porosity is reliable, the weighted average of the $\emptyset nc$ and $\emptyset sc$ is used. However, when cement bond conditions are marginal, the sonic porosity is not reliable, and the neutron porosity alone has to be used.

Water Saturation

Having cased-hole porosity, cased-hole and original open-hole water saturations can be calculated and compared. The cased-hole water saturation is obtained using the pulsed-neutron sigma measurement. Open-hole water saturations are derived from the original electrical logs. The long and short normal devices are used to derive an approximate water saturation using the

229

same shaly sand interpretation model described in the open-hole research section. Comparing the open-hole water saturation with the cased-hole water saturation, potential gas-producing zones are identified.

Example of Cased-Hole Interpretation

Appendix figure 3–18 shows the result of a cased-hole evaluation in the Wardner 76 well. As a result of this experiment, the E-41, considered to be depleted by the operator, was recommended for testing on the basis of petrophysical research results. The zone was tested in the E-41L and produced 316 Mcf/d at 412 psi. Notice the gas crossover in the porosity logs and the separation of the pulsed-neutron count rates, indicating gas presence. The open-hole and cased-hole water saturations are low and produce approximately the same value, indicating that gas is present. The minimum bulk volume of water indicates a reservoir at irreducible water saturation. The E-41M reservoir, on the other hand, shows less porosity and higher water saturations. This zone was tested with no gas show. The E-49 zone at the bottom was also tested but had no gas production.

Temperature Anomalies

The reason the E-41L proved gas productive, when it was considered to be depleted, relates to gas recharging from lower completions. The temperature log shown in appendix figure 3–19 indicates a cooling effect from 6,475 ft up to 6,300 ft. Interpretation of this anomaly indicates that gas from the squeezed zone at 6,475 ft is moving through a channel behind cement and has recharged the most permeable zone directly above, which is the E-41L.
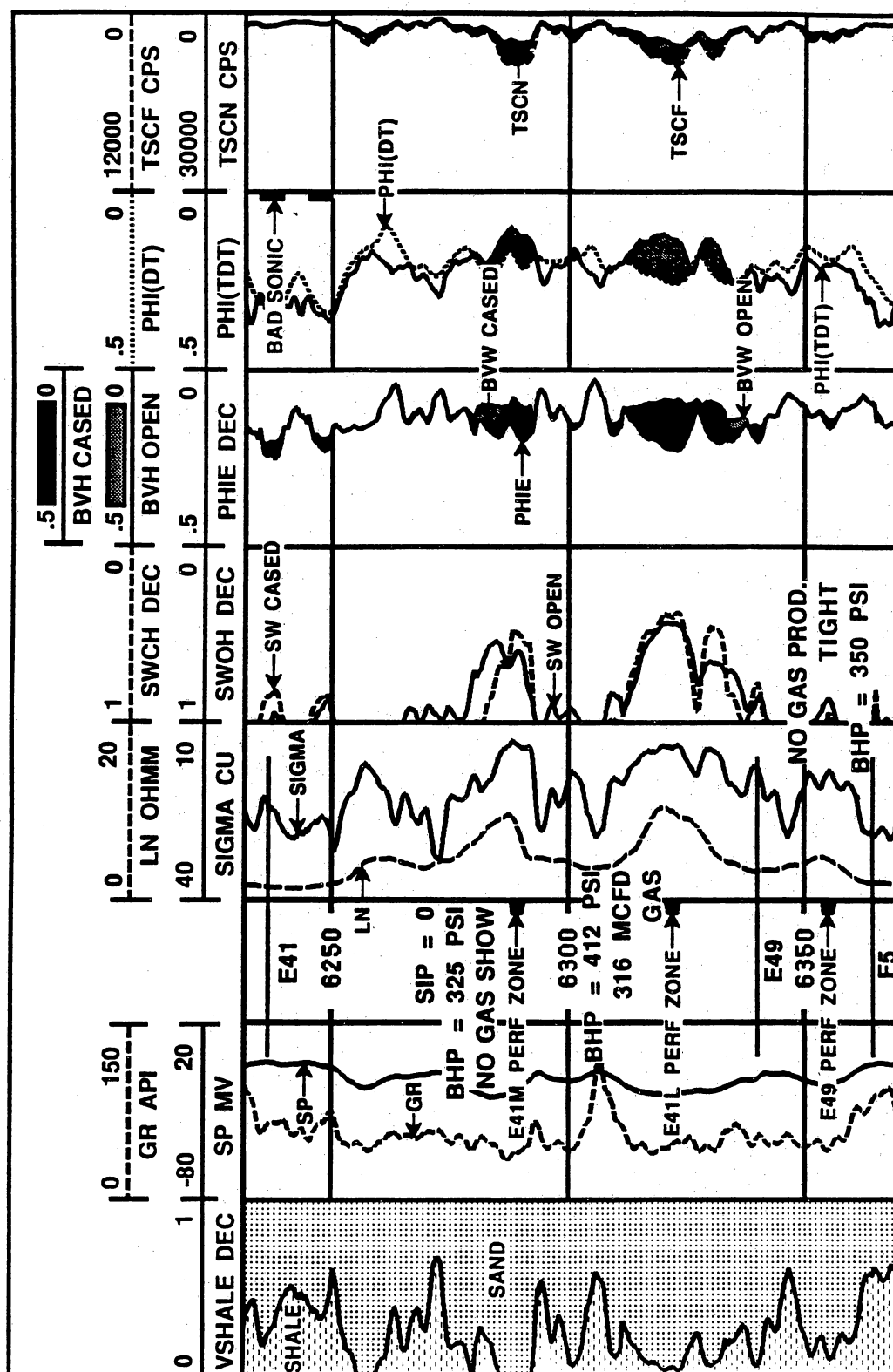
Figure 3–18. The cased-hole program was designed to complement original electrical survey: cased-hole, pulsed-neutron, gamma-ray, dipole sonic, temperature, noise, and cement bond logs.
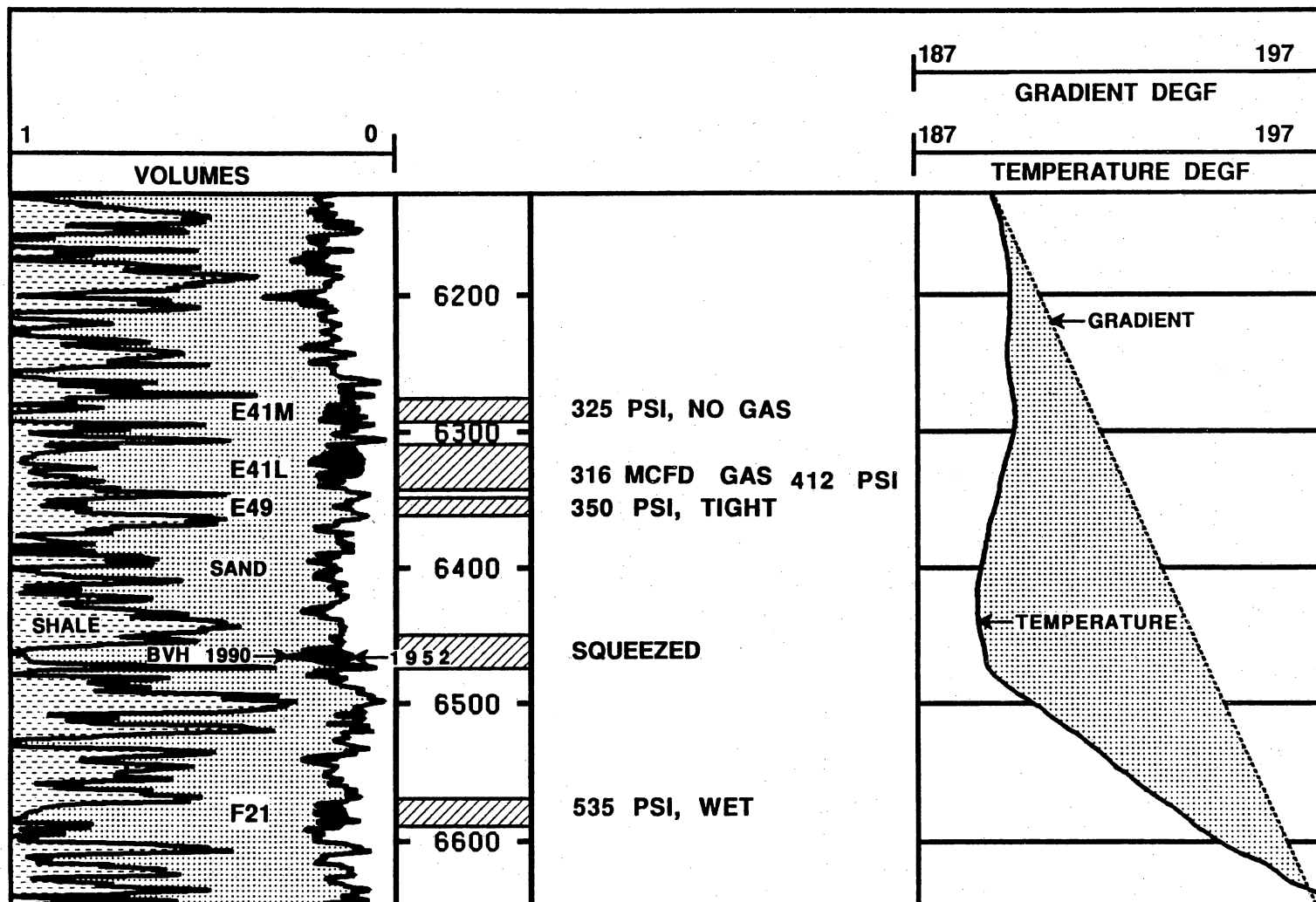
Figure 3–19. Temperature log indicates gas recharging of E-41L reservoir by gas from the squeezed zone at 6,475 ft.

Pressure Estimation from Cased-Hole Logs

Research done in Seeligson field was continued in Stratton field to determine if additional data could improve the results of pressure prediction using cased-hole measurements. Results proved inconclusive because the collected data were variable. In Stratton and Seeligson, wireline formation pressures were correlated with pulsed neutron measurements, standardized, then merged together from data acquired in the Elliff 40 and Seeligson 248 wells. A correlation was found with the pulsed-neutron count ratio. Appendix figure 3–20 shows a plot of wireline pressures versus pulsed-neutron near/far count ratios. Notice the trend found by linear regression but the large divergence in predicted pressures for a given ratio.

The problems are many. First, there is uncertainty in wireline formation pressures when compared with downhole pressure measurements in Stratton. Second, the thermal decay tool is a radioactive measurement and has inherent statistical variations. Third, the pulsed-neutron count rate is also affected by porosity, hydrogen index, volume of shale, gas saturation, and borehole effects. Prediction of formation pressures using indirect methods has been investigated by SGR project staff in Stratton field, who used log data obtained in open- and cased-hole wells; however there are too many unknown factors to consider in quantitative prediction of formation pressures from logs.

Petrophysical Support for Geophysical Applications

The petrophysical input to geophysical applications requires knowledge of the formation velocities and bulk density properties of all lithologies penetrated, including the effects on these measurements of depth, fluid type, pore pressure, and formation type. For amplitude variation with offset (AVO) modeling, it is important to perform fluid replacement modeling on the acoustic and density logs in order to infer equivalent log responses for wet and gas-saturated sandstones. These responses are essential to perform proper interpretation of AVO responses.

233
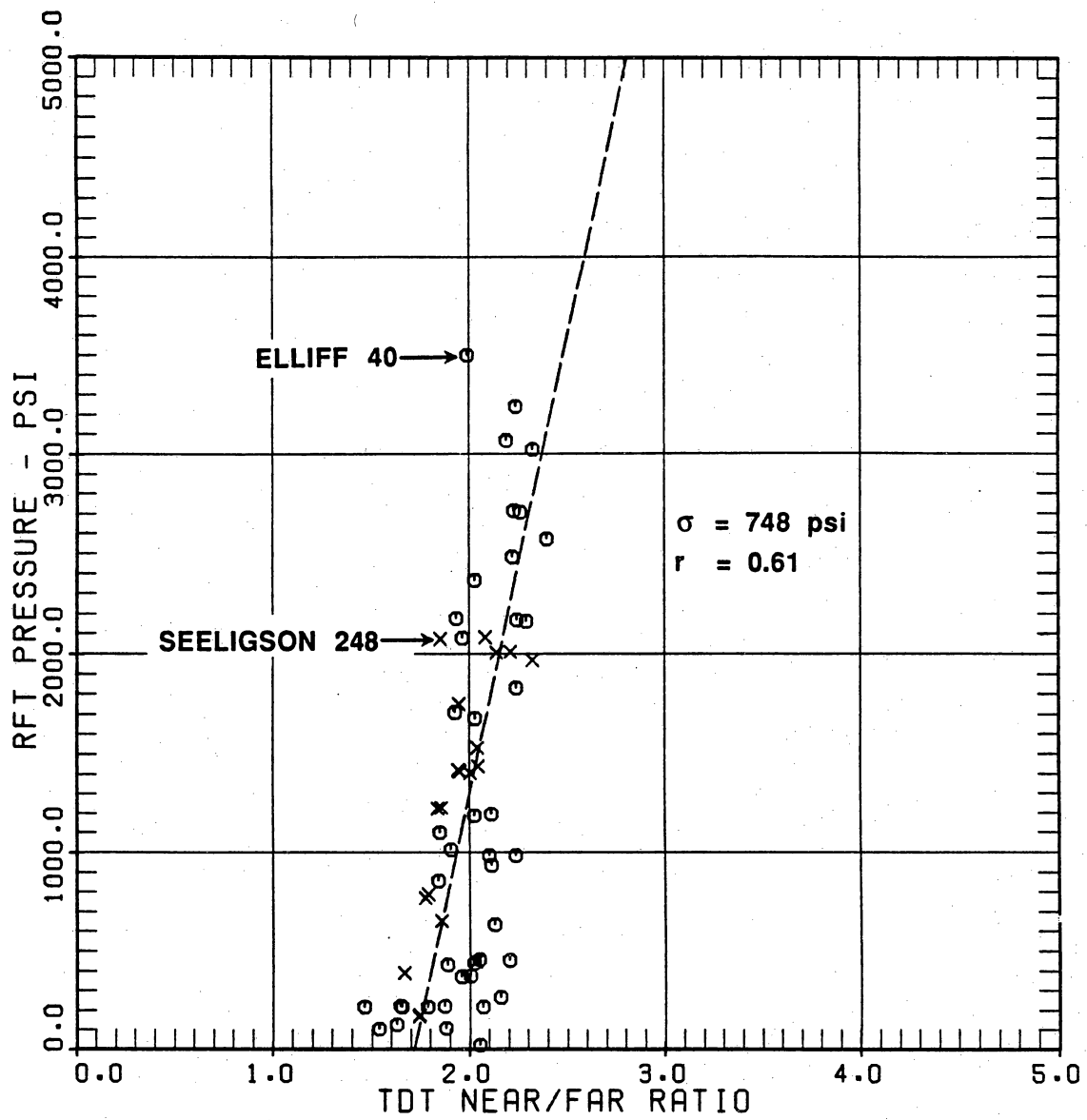
Figure 3–20. Correlation found between wireline pressure and thermal decay tool (TDT) ratios.

In the Wardner 76 well, fluid replacement modeling was done on the compressional and shear velocities and also on a synthetic density log generated from petrophysical modeling. This well was an old cased-hole well from which no density log was available, but it was of interest to the geophysicist because a modern dipole sonic had been acquired by the project for petrophysical research on detecting gas behind casing (utilizing the methods described in the cased-hole section of the petrophysical research discussed in this report).

Generation of a Synthetic Density Log

Using the cased-hole-computed results of porosity, water saturation, and volume of shale, a synthetic density log was created for the Wardner 76 well using the density response equation

$$\rho b = \emptyset \left\lceil Sw\, \rho_f + (1 - Sw)\rho gas \right\rceil + Vsh\, \rho sh + (1 - \emptyset - Vsh)\, \rho ma$$

where

ρb = bulk density

$\emptyset$ = porosity

Sw = water saturation

ρ_f = fluid density

ρgas = gas density

Vsh = volume of shale

ρsh = shale density

ρma = grain density.

Sw was used in the equation instead of Sxo because we were interested in the density response for the zone not affected by filtrate. The validity of this density modeling was verified by testing the equation in a nearby well (Wardner 202) where a real density was available. Appendix figure 3–21 shows the good fit obtained between synthetic and real density.

Figure 3–21. Correlation of synthetic density log to real density log, Wardner 202 well.

Fluid Substitution Modeling

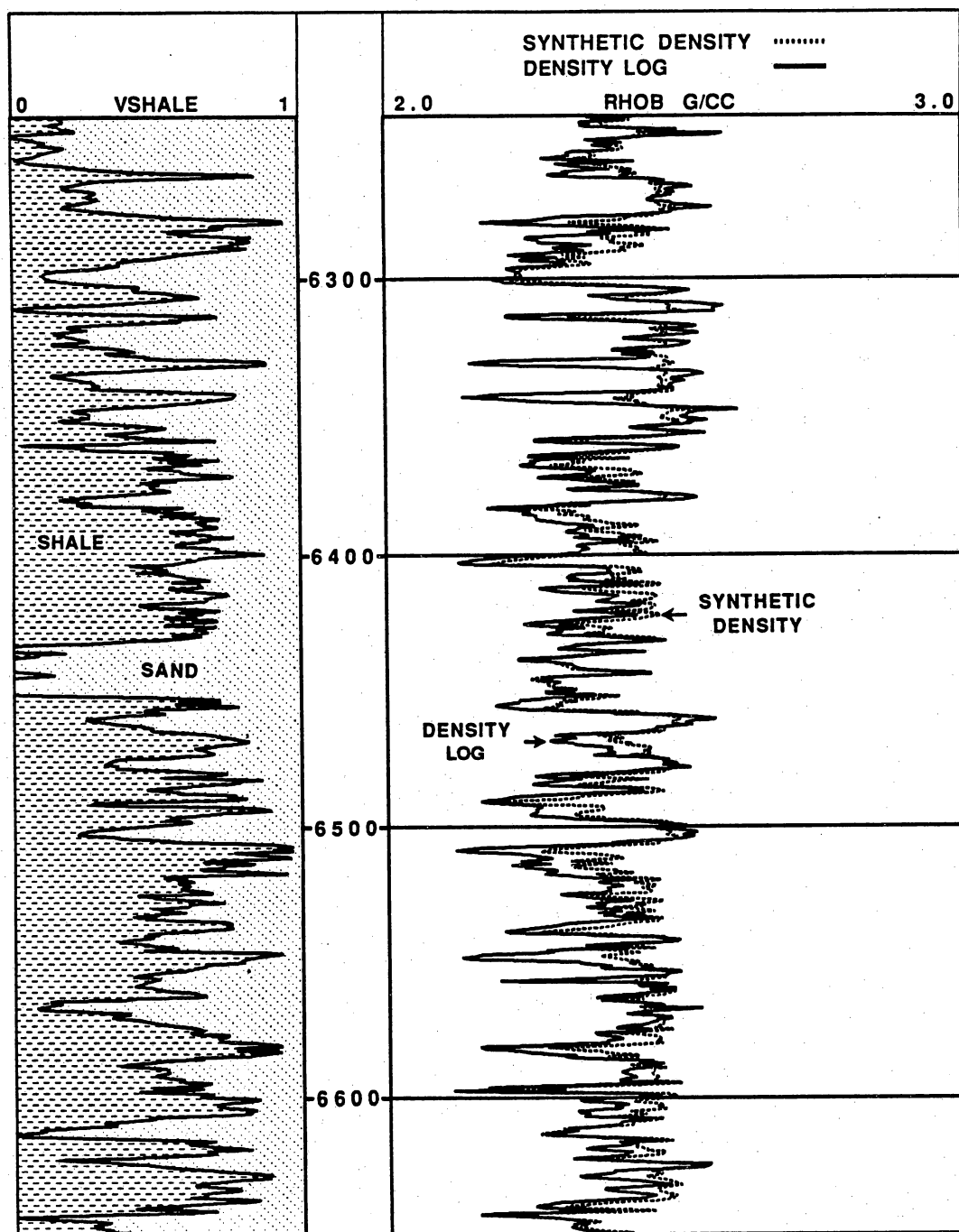Using the measured sonic velocities and the synthetic densities calculated for the Wardner 76 well, response equations for these measurements were solved in the gas-bearing sandstones for their equivalent 100 percent water saturation state.

Appendix figure 3–22 illustrates changes in sonic compressional and shear travel times, and in density values as a function of water saturation. The changes between gas and water are minimum for the shear travel times, but are significant for the compressional travel time and density logs.

Conclusions

A petrophysical model calibrated to core data for Stratton field was used to find gas-bearing zones and to estimate additional gas reserves. Capillary pressures were used to validate the model and to predict the free water levels. Use of high-resolution logs provided a better match with core analysis results. Potential gas-bearing zones could also be identified using quick-look techniques. Logs were used to identify reservoir types, predict permeability trends, and to identify additional gas-bearing zones in old cased-hole wells. Attempts to predict reservoir pressures from logs provided inconclusive results.

- A petrophysical model calibrated to core data was used to find gas-bearing zones and to estimate additional gas reserves. The results also indicated variations in thickness, porosity, and shale content of individual sandstone members.

- Special core measurements of capillary pressures were used to verify the water saturation equation. Capillary pressures were also used with the ADCAP model to predict the free water levels for the D reservoirs.

- A comparison of core-derived formation density with the high-resolution log indicated that a better match is obtained using high-resolution measurements.

- Quick-look techniques were also used to identify gas-bearing zones.
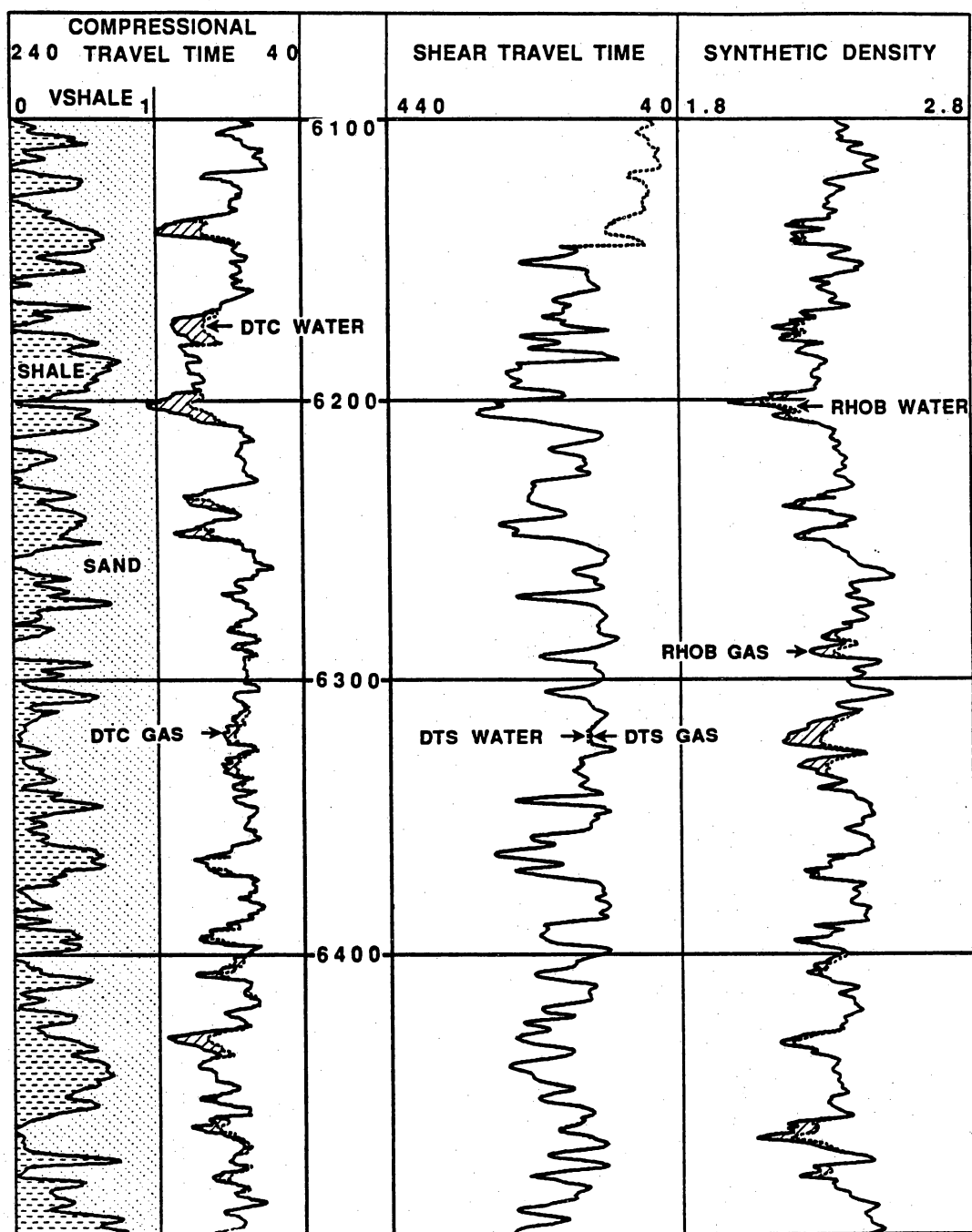
Figure 3–22. Fluid substitution modeling for sonic and density logs, Wardner 76 well.

- Permeability and rock type were also estimated using logs and computed results.

- Additional gas zones were also identified using modern cased-hole logs in old cased-hole wells and methods developed in this project.

- Wireline formation pressures can be misleading. Attempts to predict reservoir pressures by indirect methods using logs and log-derived parameters provided inconclusive results.

Table 3–4. Petrophysical characteristics of large reservoirs in Gruene lease E-41.

Gruene	Net (ft)	Ø (PU)	Sw (%)	Vsh (%)	BVW (PU)
7	34	21	57	4	12
9	27	19	61	8	12
12	13.5	21	57	10	12
13	26.5	21	56	3	12
14	31	21	55	5	11
16	15	23	62	1	14
17	19.5	21	56	6	12
18	34.5	19	52	11	10
19	8.5	21	51	5	10
21	15	21	62	2	13
Avg	22.5	21	57	6	12

PU   Porosity units
BVW Bulk volume water
Vsh Volume of shale

Table 3-5. Petrophysical characteristics of a large-compartment reservoir—Wardner lease.

Wardner	Net (ft)	Ø (PU)	Sw (%)	Vsh (%)	BVW (PU)
126	4.5	17	61	8	10
140	3.5	16.5	48	10	8
153	28.5	20	56	8	11
185	20	21	55	8	11
170	14.5	19	56	2	11
174	6	18.4	59	9	11
175	15.5	17	49.7	11	8
176	30.5	19	40	9	8
181	20.5	20	51	11	10
183	15.5	18	57	8	10
184	37.5	22	42	11	9
185	26.5	20	35	6	7
187	13.5	19	47	09	9
189	27	22	35	09	8
191	22.5	19	56	15	10
193	21.5	19.6	57	6	11
195	20.5	23	36	5	8
	14.5	18.9	49	15	9
198	0	0	—	—	10
200	24.5	20	48	16	8
201	19.5	23	36	7	10
206	23	21	50	11	11
208	18	20	58	10	12
209	33	23	51	11	12

Table 3–6. Petrophysical characteristics of a medium reservoir (F-39, near Wardner 175).

Wardner	Net (ft)	Ø (PU)	Sw (%)	Vsh (%)	BVW (PU)
135	0	—	—	—	—
153	10	18	64	3	12
157	20	18	48	5	8
164	23.5	19	50	3	10
165	18	18	49	6	9
170	4.5	23	67	8	7
172	18.5	24	32	9	8
174	16	20	61	6	12
175	11.5	17	54	11	9
176	9.5	22	58	1	12
180	16	18	52	2	9
183	0	—	—	—	—
184	8.5	22	61	8	13
185	0				
186	21.5	20	42	9	8
187	8	20	52	9	10
189	0	—	—	—	
191	17.5	18	52	7	9
193	.5	17	59	9	10
195	8.5	22	64	4	14
196	15.5	22	58	2	10
197	14.5	20	47	7	9
198	13.5	16	57	12	9
200	27	18	46	9	8
201	7	23	65	3	15
202	15.5	18	45	13	9
203	13.5	19	51	11	10
206	20.5	20	40	14	8
208	0	—	—	—	—
209	15	21	42	6	9

Table 3–7. Petrophysical characteristics of small reservoirs (F-15 to top F-31).

Wardner	Net (ft)	Ø (PU)	Sw (%)	Vsh (%)	BVW (PU)
126	2	18	68	14	12
153	8.5	18	54	10	10
164	6	18	65	21	12
165	2.5	18	67	26	12
170	8	18	63	10	11
172	2	18	56	28	10
174	6	18	60	9	11
175	15.5	19	49	11	9
176	30.5	20	41	9	8
181	4	17	61	13	10
183	4	17	63	11	11
184	4.5	18	61	15	11
185	.5	15.4	64	8	10
186	1.0	17	64	71	11
187	1.0	16	66	30	11
189	3.5	19	67	28	13
191	1.0	16	61	26	10
193	2.0	19	51	10	10
195	28.5	19	44	4	8
196	10.5	19	60	10	11
198	32.5	20	56	7	11
200	5.0	21	59	19	12
201	19.5	20	51	5	10
206	5.5	17	62	17	11
208	5.5	18	56	7	10

APPENDIX 3 REFERENCES

Clavier, C., Coates, G., and Dumanoir, J. L., 1977, The theoretical and experimental basis of the "dual water" model for the interpretation of shaly sands: Society of Petroleum Engineers Transactions Paper 6859.

Doll, H. G., Dumanoir, J. L., and Martin, M., 1960, Suggestions for better electric log combinations and improved interpretations: Geophysics, v. 25, no. 4, p. 854–882.

Dumanoir, J. L., Hall, J. D., and Jones, J. M., 1972, Rxo/Rt methods for wellsite interpretation: SPWLA 13th Annual Logging Symposium, May 7–10.

Granberry, R. J., and Keelan, D. K., 1977, Critical water estimates for Gulf Coast sands, Gulf Coast Association of Geological Societies Transactions, v. 27.

Hawkins, J. M., Luffel, D. L., and Harris, T. G., 1993, Capillary pressure model predicts distance to gas/water, oil/water contact: Oil and Gas Journal, Jan. 18.

Hilchie, D. W., 1979, Old electrical log interpretation: Colorado School of Mines, Department of Petroleum Engineering.

Howard, W. E., and Hunt, E. R., 1986, Travis Peak: an integrated approach to formation evaluation: Unconventional Gas Technology Symposium of the Society of Petroleum Engineers, May 18–21, SPE Paper 15208.

Jirik, L. A., Howard, W. E., and Sadler, D. L., 1991, Identification of bypassed gas reserves through integrated geological and petrophysical techniques: a case study in Seeligson field, Jim Wells County, South Texas: Society of Petroleum Engineers, Gas Technology Symposium, SPE Paper 21483, p. 7–16.

Langford, R. P., Grigsby, J. D., and Howard, W. E., 1992, Use of the enhanced density and microresistivity logs in interpreting diagenetic facies in Tertiary Gulf Coast sandstones: Proceedings, 1992 Society of Petroleum Well Log Analysts Annual Logging Symposium, June 14–17, paper BB.

Schlumberger Well Services, 1974, More complete open hole interpretation: Schlumberger Log Interpretations/Applications.

Truman, R. B., Davies, D. K., Howard, W. E., and Vessell, R. K., 1986, Utilization of rock characterization data to improve well log interpretation: Society of Professional Well Log Analysts 27th Annual Logging Symposium, June 9–13, Paper V, p. 1–10.